European **S**ynchrotron **R**adiation **F**acility
INSTALLATION EUROPEENNE DE RAYONNEMENT SYNCHROTRON

Beamline Review, November 5-6, 2013

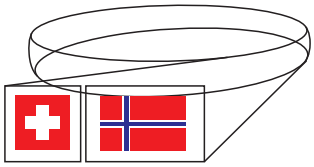

Swiss-**N**orwegian **B**eam **L**ines

●

Multifunctional beam lines for complex in-situ XRD and XAFS experiments

September 2013

The present report provides an overview of the Swiss-Norwegian Beam Lines, its activity during the four-year period 2009-2012 and the options for the future development of the project. These years have completed a very important period in the life of SNBL. Following the report in 2008 of the last ESRF Beamline Review Committee and an internal assessment by the Committee appointed by the SNX Council, several areas for new investment were identified. Where sufficient resources were available, the recommendations have been rapidly implemented during this period. The extensive capability for performing *in-situ* experiments now available at SNBL is a good example of this kind of investment. Where external support was required, the user community (in concert with the in-house staff) has been very successful in raising the necessary funds.

Therefore, both of the beamlines have seen major upgrades over the last few years. These have been aimed both at bringing the beamline infrastructure and controls up to the latest standards, and at installing and commissioning new instrumentation. The largest single investment has been the Pilatus2M detector and associated diffractometry. The necessary additional funding (in excess of €1M) was provided jointly by the research councils of Switzerland and Norway.

In 2012, Swiss and Norwegian administrations considered the renewal of the four-year bi-national agreement for SNBL, and asked for a new budget to be defined which was commensurate with its goals. In this context, a number of questions were addressed. Is the technical status of the beamline and its instrumentation well correlated to the research interests of synchrotron users in general and, more especially, how does it relate to the scientific activities of the Swiss and Norwegian academic communities? What instrumentation is needed in order to keep the facility attractive and competitive, bearing in mind that many new beamlines are under construction both within the ESRF and elsewhere in Europe?

Discussions organized in both countries showed a continued and wide interest within the Swiss and Norwegian synchrotron communities to operate SNBL well beyond the current budget period. Moreover, the SNX Council received a strong commitment from the Norwegian and Swiss administrations for their continuing support. It is therefore a pleasure to be able to report that the SNBL SNX Cooperation Agreement and Memorandum of Understanding for the period 2013-2016, together with a generous funding profile from both Norway (RCN) and Switzerland (SERI), has been approved by both countries. Thus, we can safely claim today that the long-term perspectives of the Swiss-Norwegian CRG are secured until 2017 and look very promising beyond, and we look forward to maintaining and developing the service which we provide to our user community.

V. DMITRIEV, P. PATTISON, H. EMERICH

BEAM LINES REVIEW PANEL 2008:
Recommendations and Actions

The preceding review of SNBL took place in 2008. The recommendations of the Review Committee and the actions taken after review were:

- **The beamline should continue its very successful phase of operation.**

  The steady output of high-ranked scientific articles over the last years proves the ongoing productivity of SNBL. Every round we have numerous ESRF proposals asking specifically for SNBL and its combined approach to address the characterization of dynamic systems.

- **Priority should be given to those areas which really benefit from the simultaneous combination of techniques.**

  A significant fraction of experiments carried out at SNBL now involve simultaneous combination of techniques. In-situ experiments have become routine on both beamlines.

- **Improve the speed of powder and single-crystal diffraction (sub-second) to push the frontiers of chemical crystallography by detector upgrades.**

  Detector upgrades on BM01A have been completed with purchase and installation of Agilent Titan CCD detector and Dectris Pilatus2M pixel detector. Powder diffraction time resolution now reduced to about 1s per pattern for time resolved experiments. Complete single crystal diffraction measurements can be carried out on a timescale of a few minutes.
  We upgraded on BM01B our EXAFS monochromator such that we can now toggle between high speed mode (10-20s per spectra compared to many minutes before) and the old high resolution mode still needed for energies >30keV. The same is true for Powder Diffraction: the acquisition of a 2D detector has brought down measurement times for a full powder pattern to the second range. The recently installed focusing crystal is expected to reduce measurement times to the lower second or even sub-second scale.

- **Preserve the capability of stand-alone powder diffraction after the ESRF upgrade as a strategic resource.**

  Stand-alone powder diffraction continues to be available routinely at SNBL. Even with the recently added 2D CMOS detector the existing high resolution powder set-up has remained untouched. Furthermore, both systems can work in parallel allowing to perform fast measurement with our new 2D detector but also to follow/scan individual peaks in high resolution mode at the same time. Additionally a single high energy channel (without analysers) has been added recently to the HRPD

instrument. This allows to cross-check the calibration of the 2D detector by providing a reference HRPD pattern at any wavelength.

- **Given the outstanding performance achieved at SNBL in extracting maximum information from 2D reconstruction of reciprocal space extra effort should be put into developing software codes to model the non-Bragg contribution.**

  A fruitful collaboration has begun between SNBL and ESRF staff for the development of software aimed at the display and analysis of non-Bragg contributions to the scattered intensity. A very successful joint ESRF/SNBL workshop on diffuse scattering has been organized.

  .

- **The ESRF and SNBL should discuss a strategic and more productive way to accommodate the protein crystallography interests of the member states of SNBL.**

  Swiss and Norwegian protein crystallographers have been successful in obtaining beamtime on ESRF beamlines without the need for special arrangements. In the case of Switzerland, most of the PX experiments have in any case moved to the Swiss Light Source.

- **There is a lot of integrated systems development at the SNBL which could benefit the ESRF especially during its upgrade phase and vice versa.**

  The possibilities for an exchange of information about developments at SNBL and ESRF are in place, and there have been useful collaborations in the field of instrument control (e.g. for in-situ experiments and for the control of the Pilatus detector). SNBL has been very open in sharing information with other ESRF beamlines. Items like our gas delivery system, our combined EXAFS-PD-Raman approach, cell design, our new 2D-detectors etc. have led to many fruitful discussions and exchange of ideas with all concerned ESRF groups. On the other hand with the idea of using our new 2D detector systems for their purposes the ESRF is also putting efforts into software development needed for this system.

- **Continue and expand upon student and post-doc programs especially considering collaborative methods of working and joint appointments with ESRF and SNBL.**

  The student and post-doc programs have been expanded at SNBL, principally via visits from Norwegian scientists. The Norwegian Research Council in now actively supporting visits to SNBL by Norwegian students and post-docs.

- **During the upgrade phase, SNBL should take the opportunity of optimizing off-line and laboratory space.**

  Additional storage and laboratory space in now available close to the beamline.

- **Continue with the very fruitful Memorandum of Understanding with DUBBLE and look for similar opportunities.**

  The MoU between SNBL and DUBBLE continues to provide useful opportunities for the exchange of beamtime and other resources between the two CRGs. A similar MoU has been established between SNBL and MAX LAB.

CONTENTS

I. INTRODUCTION

The mission of the Swiss-Norwegian Beam Lines at ESRF (SNBL) is to provide scientists from both Norway and Switzerland, from both academia and industry, with increased access to synchrotron radiation. A user on SNBL has access to state-of-the-art, custom-designed instrumentation for diffraction and absorption experiments. Both partner countries have relatively large and exceptionally active scientific communities using X-ray diffraction and absorption as their main probes; for these groups the amount of public beamtime offered by ESRF was insufficient from day one, and this is the *raison d'être* of the Swiss-Norwegian Beam Lines at ESRF. To circumvent this potential bottleneck, the Swiss and Norwegian scientists formed in 1990 a consortium and applied for access to a bending magnet port at ESRF.

Strong, long-term financial support was pledged by the Norwegian Research Council and the Swiss National Science Foundation, with substantial contributions coming from universities concerned. On the Swiss side, the foundation's support was intended to raise interest amongst the Swiss scientific community in the benefits of hard synchrotron radiation, with the goal to contribute to the creation of a SR user community and to prepare it for the use of a Swiss Synchrotron Light Source. The realization of this bi-national facility aimed as well at providing scientists from the two partner countries with instruments custom-built for their own specific needs. Initially, the Swiss-Norwegian facility was planned as a single multi-purpose line. However, in the interest of increased operational efficiency and to attract an even wider user community, the consortium soon decided to split this single line into two branch lines: one dedicated to single-crystal diffraction and the other to powder diffraction, EXAFS and topography. The split-beamline design also permitted to optimize the x-ray optical configuration for the two types of experiments, scattering and absorption.

The facility started to operate in the fall of 1994. First on-line was the high-resolution powder diffractometer, and then followed: a single-crystal diffractometer, an image plate system, an EXAFS spectrometer, and, finally, a newly developed high-resolution single-crystal diffractometer, specially conceived to carry heavy loads. Most recently, the image plate detector has been replaced with one of the latest generation of pixel detectors. All of this instrumentation was commissioned with users.

The SNBL currently has four different experimental techniques, which are distributed over two beamlines, and include:

- High-resolution single-crystal diffractometry
- Large-area 2D detector for x-ray diffraction and scattering
- High-resolution powder diffractometry
- XAFS spectrometry.

II. FUNDING and ORGANISATION

II.1 Funding and Governing Bodies

The two funding organisations of the SNBL project are Swiss State Secretariat for Education, Research and Innovation (SERI) and Norwegian Research Council (NSR) who contribute equally to the operation costs. The Norwegian contribution consists of two equal parts providing by NSR itself and by Norwegian universities. Until and including the year 2007, the SNBL budget was considered and approved by the funding agencies on annual base. Since 2008, both funding agencies, SER (SERI from 2012) and NSR, opted for a 4-year budget, and the SNBL budget under the terms of the Swiss-Norwegian contract is €5'400'000 for the four-year period 2009-2012, and €6'400'000 for the current four-year period 2013-2016.

The Cooperation Agreement and Memorandum of Understanding signed by Swiss and Norwegian sides, which is reconsidered and renewed every 4 years, is a legal basis for the existence of SNBL and its funding. The current Agreement is valid for the period 2013-2016. The organisation chart of the bi-national facility is shown in Fig.II.1.

The *Swiss-Norwegian Foundation for Research with X-rays (SNX)* is a federally registered Swiss foundation established in 2004. The foundation is a governing body for SNBL. It also acts as the legal body *vis-à-vis* the ESRF. The SNX affairs are handled by a seven-member council (SNX Council) consisting of three Swiss and three Norwegian members, with one member, the SNBL Director,

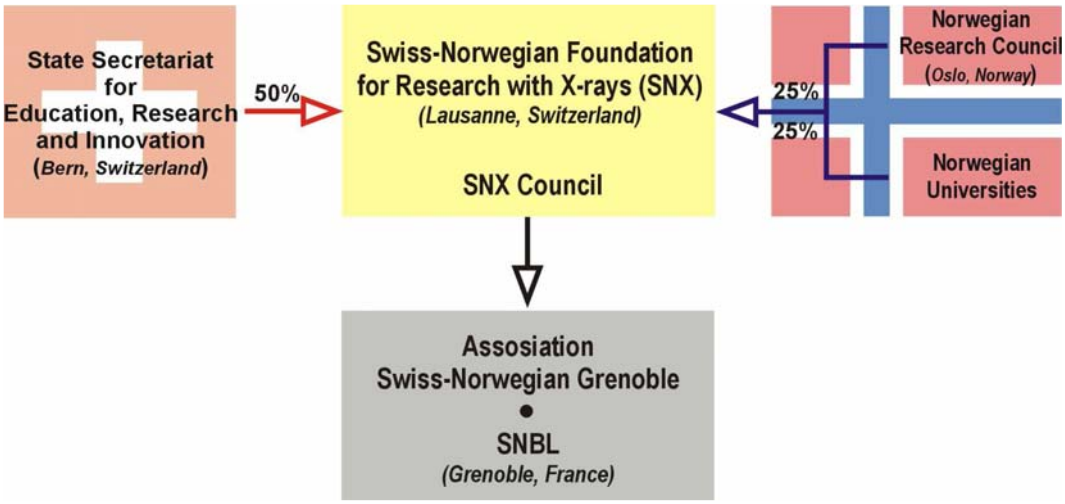

***Figure II.1**. Block diagram of the organisational structure of SNBL.*

functioning as the Executive Director of the foundation but having no voting right. One observer each from SERI and NSR attend the council meetings which take place twice a year.

The *Association Swiss-Norwegian Grenoble* is a French association, which employs all Grenoble-resident staff. It is run by a three-member board, with the SNBL Director as its President, and SNX Chair and Vice-Chair as members.

II.2 Beam time allocation procedure

The SNX Council also acts as a Proposal Review Committee to SNBL. It allocates 2/3 beam time available for users at any run. Decision on a proposal is taken on the basis of two reports communicated by one of the SNX Council members, one of advisors, and a report submitted by an independent anonymous referee (non-Swiss, non-Norwegian), selected by the BL Director. The 1/3 of the beamtime that has, in accordance to the ESRF-SNX contract, to be made available to general ESRF users falls under the remit of the general ESRF beamtime allocation panels and ESRF directors.

The SNX Council established three classes of proposals for SNBL in 2005:

- *Standard Research Proposals*
- *Long Term Project Proposals*
- *Urgent Research Proposals*

In addition to the standard proposals typical for ESRF and other CRGs, SN users may request a long-term commitment from the SNBL to provide beamtime during up to four successive scheduling periods (two years). A given user group cannot operate more than one Long-Term Proposal (LTP) in the same period. The percentage of LTPs is limited to 1/3 of beamtime available for SNBL.

SN users may request as well an urgent commitment to provide beamtime within a maximum of three months of submitting a proposal. The special status of an Urgent Proposal should be clearly justified. Time requested should not exceed 6 shifts. The percentage of Urgent Projects is limited to 5% maximum of the beamtime available for SNBL and is designated as Director's discretionary beamtime. No fixed deadlines are made for such proposals. If approved, beamtime is normally allocated within 2 months of the proposal date. The UP undergoes a two-step appraisal procedure, the first step being performed by the SNBL Director, who makes a preliminary evaluation as to the urgency of the project, and its scientific quality, and the second step carried out by the competent SNX Council member.

III. TECHNICAL DESCRIPTION OF THE BEAM LINES

III.1 General Layout and X-ray Optics

Much of the optical layout of BM01 has remained unchanged since the last review in 2008, particular concerning the beamline BM01A. Therefore part of the general description of the layout is identical to the text in our earlier report. Developments in the optical configuration of BM01B, as well as the many changes in the instrumentation in both of the experimental hutches, will be spelled out in more detail below.

The ESRF delivers a 6mrad wide fan of synchrotron radiation to SNBL from bending magnet BM01. A water-cooled aperture plate at the entrance to the Optics Hutch (26m from the source point) divides this beam into two parts of width 2.5mrad and 1.0mrad, with a gap of 2.5mrad between the two beams. The fan of 2.5mrad width supplies the photons to BM1A, while the 1.0mrad beam provides the synchrotron radiation to BM1B. SNBL has been designed from the onset to allow both lines to operate simultaneously, and with a minimum of interaction between the X-ray optics, vacuum system, shielding and controls for each branch line. There are three leaded hutches in series. The first hutch (Optics) contains the majority of the optical components for both branch lines (Figs.III.1-2). These include two mirrors and a monochromator for BM1A, two separate monochromators for BM1B, as well as various slits, beam position monitors, station shutters, valves and other vacuum components. Although the X-ray optical configurations of both beamlines are fairly conventional, the space restrictions have been a major technical challenge. The available space between the two fans of synchrotron beam which pass through the Optics Hutch is only about 70mm, yet our goal is to operate the two beamlines independently. The two Experimental Hutches are arranged sequentially down the beamline, with the vacuum pipework for BM1A passing through the BM1B Hutch (and through the data acquisition cabin). Two major instruments are positioned in each of the two Experimental Hutches. In BM1A, there is a heavy duty multi-axis single crystal diffractometer followed by a large-area pixel detector. BM1B is equipped with a high resolution powder diffractometer and an EXAFS spectrometer. A detailed description of the instrumentation on each beamline is given below.

The optical configuration of BM1A is a conventional arrangement of vertically collimating mirror, followed by a double crystal Si(111) monochromator and a vertically focusing mirror. The beamline can be configured to operate without mirrors (in order to access higher X-ray photon energies, for example), although some manual realignment of the beamline components is necessary for the changeover. In normal operation, the Rh-coated mirrors provide vertical focusing and harmonic rejection while horizontal focusing is achieved with a sagittally bent second crystal. It is also possible to interchange the second crystal bending mechanism with a flat crystal mount, if a highly parallel beam is required. The first crystal of the monochromator is water-cooled, as is the first mirror. The mirrors both have a fixed radius of curvature, and the optimum focal spot is roughly circular with a FWHM of about 300 microns. The excellent mechanical and thermal stability of the X-ray optics (at least up to the present maximum

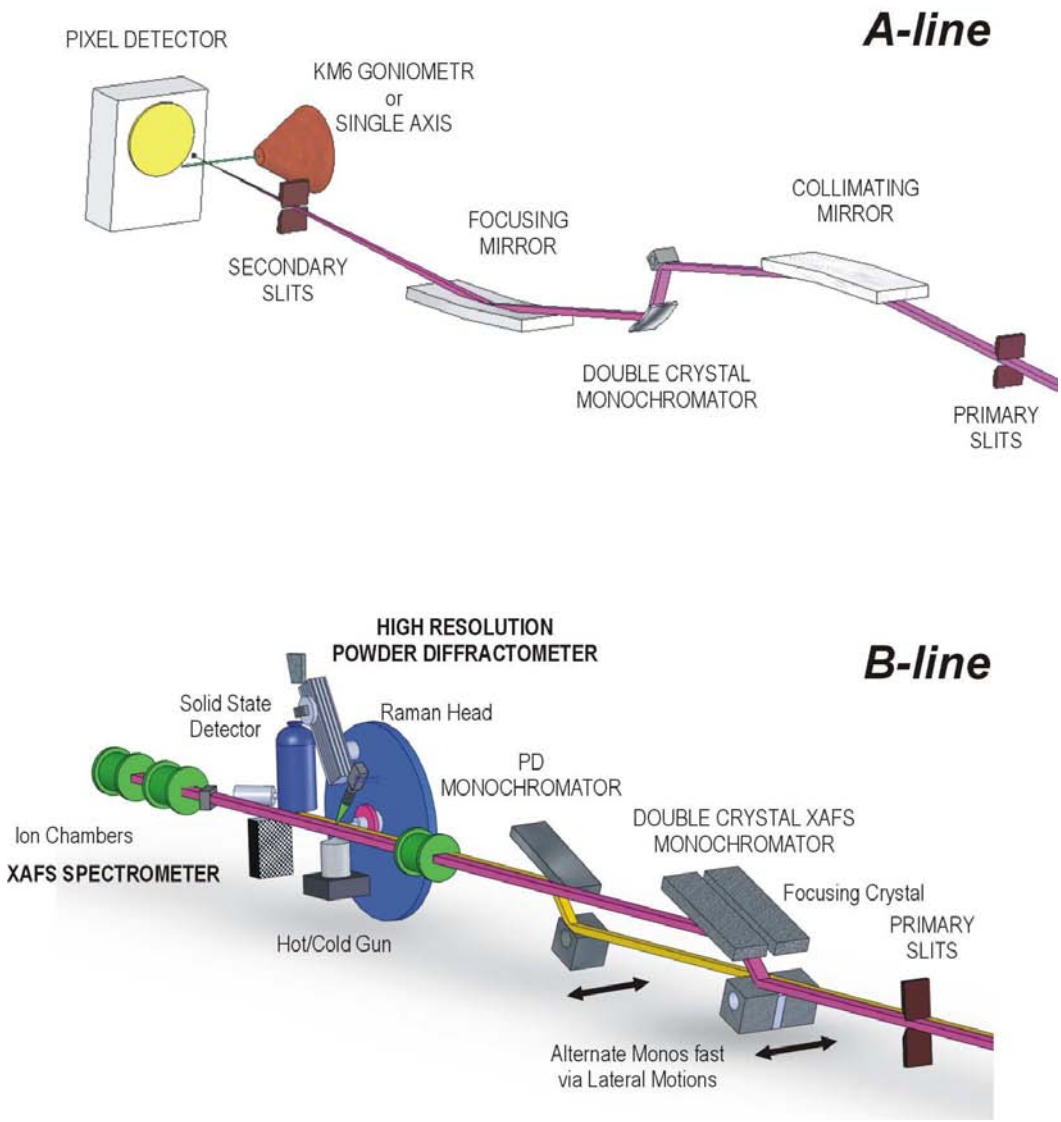

Figure III.1. *Schematic layout of the SNBL Optics*

current of 200mA) has allows us to operate the beamline without a feedback mechanism up until the present time. However, we have now invested in a commercial beam position monitor and feedback system (Huber Diffraktionstechnik GmbH) which will give us fine control of the focused beam position in the experimental hutch. This device will help us to maintain beam stability even if the electron beam current is increased in the coming years (300mA has already been tested), and will improve the performance of the secondary focused optics which is planned for installation in 2014.

Most experiments are carried out in the spectral range from about 10 keV – 20 keV, although higher energies can be accessed if the mirrors are removed. In line with the recommendations of the last beamline review, and following the requests of our user groups, we aim to extend the spectral range of the beamline while maintaining the focusing option. This goal can be achieved by reducing the grazing angle of incidence of the synchrotron beam onto the mirrors from the present value of 3mrad down to 2.5mrad or possibly lower. Although this will involve some loss of total flux in the focused beam (because of the reduced fraction of the synchrotron beam intercepted by the mirrors and the K- absorption edge of the reflective Rh layer at 23.2keV), these losses will be offset by the gain in spectral range delivered to the users. It is our goal to extend the spectrum of the focused beam up to at least 25 keV, and if possible to 30 keV. Recent tests have confirmed that 25 keV can be reached without major problems, although the flux still remains to be optimized in the higher energy range.

BM1B is dedicated to High Resolution Powder Diffraction (HRPD) and EXAFS experiments. A considerable effort has been devoted to the goal of combining these two techniques into quasi-simultaneous measurements. In order to achieve this aim, we have built and integrated two independent, water-cooled monochromators into the optics enclosure (Fig.III.3). This allows us to automatically swap between the respective monochromators and hence from HRPD to EXAFS (and vice versa) within a few seconds.

The first monochromator is an unfocused double-crystal monochromator dedicated to EXAFS measurements. It consists of two crystal pairs, a flat Si (111) and a cylindrically bent Si (111) orientated crystal, mounted on a slide transverse to the incoming beam. By means of this slide, one can quickly choose between the flat Si(111) and the focusing crystal pair, or alternatively select a position that lets the white beam pass through between the two crystals. It is in this configuration that the white beam can reach the following monochromator, which is a Si(111) channel-cut dedicated to High Resolution Powder Diffraction. This channel-cut crystal is again mounted on a transverse slide such that it can be easily moved out of the beam in case that the beam from the first monochromator for EXAFS experiments is required. A swap between the two monochromators can be performed within a few seconds only.

Figure III.2. *General view of the Optics Hutch*

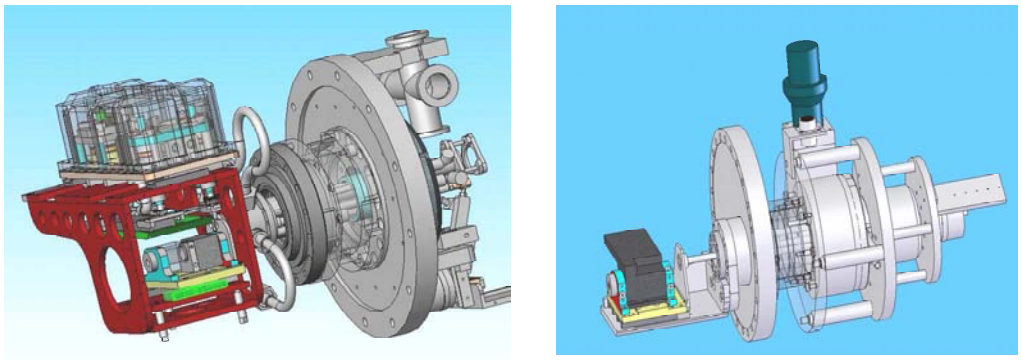

Figure III.3 *Schematic drawings of the two monochromators on the BM1B branch line*

.

III.2 Beamline BM1A

General introduction

Due to the substantial investment in infrastructure and ancillary equipment which has taken place over the last few years, we are now able to guarantee our user community access to an optimal combination of tools needed for a modern synchrotron beamline. In particular, the replacement of our aging Onyx CCD detector with the latest generation Titan detector from Agilent Technologies in March 2011 represented a major effort to keep the X-ray instrumentation at SNBL completely up-to-date. The announcement in 2011 that funding was available for the upgrade of BM01A with a Pilatus2M pixel detector from Dectris Ltd represents the largest single grant for SNBL in recent years (in excess of €1M). The fact that it has been jointly funded by the Norwegian Research Council and the Swiss National Science Foundation confirms the common interests of both countries in ensuring that SNBL continues to receive generous financial support. The new detector was delivered in May 2012, and was operational already one month later.

It remains our primary goal to provide our users with a versatile and flexible X-ray platform for a wide variety of experiments. The fact that in recent years we have been able to maintain the high productivity of the beamline year in terms of publications (averaging well over 100 papers per year in refereed journals for SNBL, of which about 60 per year come from work carried out on BM01A) confirms that we have been successful in achieving this goal. We have seen a marked increase both in the number and complexity of experiments carried out on both beamlines, with more and more frequent use of combined techniques (powder and single crystal diffraction, EXAFS, Raman and optical spectroscopy) to address modern challenges in structural chemistry and biology, as well as materials science and applied research in the fields of energy storage and catalysis. It is becoming clear that the general field of *in-situ* experiments has become a primary focus of attention at SNBL. Both beamlines have access to an on-line Raman spectrometer. In addition, considerable funds have been invested in the provision of dedicated gas supply and gas mixing systems for in-situ experiments (e.g. catalysis).

Figure III.4 *The new Titan CCD from Agilent Inc.*

Despite the closure of the entire facility for several months early in 2012 (as part of the upgrade of the ESRF), there has been little or no impact on the output from the beamline in terms of publications. It was possible, however, to take advantage of the enforced shut-down in 2012 in order to make some major improvements to the equipment on the experimental station. The main efforts and resources on BM01A have been concerned with upgrading the X-ray area detectors used on the beamline, and we will describe the impact of these developments in the following sections in more detail.

III.2.1 Current status and scientific developments

The delivery and installation of the Titan detector from Agilent Technologies in March 2011 has led to an increase in both the quantity and quality of data delivered by the KM6 diffractometer on BM01A. The availability of excellent quality diffraction data has led in turn to a resurgence of interest in chemical crystallography, and several papers had appeared in high profile chemical journals such as as ***Angew. Chemie*** or ***JACS***. An example of such work is the report by the group of Prof. A. Hauser in the University of Geneva on *Near-Infrared to Visible Light Up-conversion in a Molecular Trinuclear d–f–d Complex,* which was highlighted by the editors of ***Angew. Chemie*** as a Very Important Paper (L. Aboshyan-Sorgho, et al., 2011 [2011-1]*).* A European patent for this process of up-conversion has now been filed in 2011 by the University of Geneva. This provides an interesting illustration of the connection which can exist between fundamental work in structural chemistry and the potential relevance of such work for industry.

Another example of the impact of high quality diffraction data produced by the CCD detector is the work reported in ***Phys.Rev.Lett*** concerning the *High-Pressure γ-B_{28} Phase of Boron* (S.Mondal et al., 2011 [2011-59]). These results form part of collaboration between the University of Bayreuth and Linköping University, together with the staff of SNBL. The structure of this form of boron has been the subject of some dispute over recent years, but the latest data delivered by BM01A has now finally clarified the topology of the bonding in this polymorph. In a follow-up paper in ***Phys.Rev B*** (S. Mondal et al., 2013 [2013-28]), the same authors investigated orbital order in α-B_{12} and γ-B_{28} polymorphs of elemental boron using data from SNBL and Hamburg.

The study of the relationship between the structure and physical properties of materials continues to be one of the central themes of the work at SNBL. The investigation of potential materials suitable for hydrogen storage has been once again a major activity on both beamlines of SNBL, and the results have appeared in many publications from BM01A in the last few years. Given the strong interest in both Norway and Switzerland in this subject, it will be important to ensure that the SNBL user community continues to have access to the necessary equipment and infrastructure (such as *in-situ* gas reactors and high pressure fittings) which are vital for working in this field. A program of extended visits by scientific staff from Norway to SNBL is planned for the coming years, and this extra effort could

be very fruitfully directed towards the development of this type of *in-situ* equipment.

Another area of research at SNBL which has benefited from some extended visits of scientists (in this case two master students) from Norway has been the field of thin films. Although some papers had from time to time appeared already on this subject using data from SNBL, the use of the beamline for thin film measurements remained relatively unexplored on BM01A. Preliminary results using the new CCD detector have been most promising, and it is now clear that the use of the Pilatus2M pixel detector produces even better data (because of the low noise and zero point-spread function in pixel detectors). This is a field in which the combination of X-ray diffraction and diffuse scattering can provide the key to a successful interpretation of the structural properties of the thin films. A technical publication concerning the procedures for data collection and analysis of thin film diffraction images has appeared in ***J Synchrotron Radiation*** *On the application of a single-crystal kappa-diffractometer and a CCD area detector for studies of thin films* (H. H. Sønsteby, 2013 [2013-48]), and other papers are in preparation using recent data from the Pilatus2M set-up.

The SNBL project has benefited from a very generous equipment gift from Prof. Walter Steurer, Head of the Laboratory of Crystallography of the ETH Zurich. We are pleased to acknowledge that Prof. Steurer has given SNBL a wide range of high pressure equipment, including several Diamond Anvil Cells, replacement diamonds and a considerable amount of ancillary equipment. The availability of such an excellent selection of high pressure equipment at SNBL has transformed both the quality and quantity of experiments which can be carried out in this regime of extreme conditions, and there has been a corresponding jump in the number of publications from SNBL in the field of high pressure research.

The opportunities for collecting high quality diffraction data from single crystals in the temperature regime down to a few degrees Kelvin are very limited indeed,

Figure III.6 *Low temperature – Helium cryostat – Single crystal diffraction*

even at synchrotron radiation facilities. We have purchased and commissioned a miniature cryostat which was originally designed for low temperature optical microscopy. With a change of window material and minor mechanical modifications to the housing, we can now operate this cryostat down to a base temperature of 5 Kelvin either on the Pilatus2M setup or the KM6 multi-axis diffractometer. The first paper which appeared using this cryostat concerned the investigation of a new multiferroic material by a group from the Paul-Scherrer-Institut (*Spin Amplitude Modulation Driven Magnetoelectric Coupling in the New Multiferroic* $FeTe_2O_5Br$, **Phys. Rev. Lett**. 103, 147202, 2009 [2009-94]).

The combination of experimental techniques for *in-situ* experiments continues to be a popular theme at SNBL. The use of a Raman spectrometer in conjunction with X-ray diffraction measurements has, in the meantime, become a standard technique on both beamlines. Recently, we developed this idea somewhat further, and a group from the University of Oslo (Prof. Kristoffer Andersson) managed to carry out both Raman and optical spectroscopy on samples at 100K, during a diffraction experiment. The set-up around the sample became somewhat crowded, but in the end we achieved a configuration which is probably unique in synchrotron experiments. Several publications have since appeared exploiting this configuration, including *Tracking Flavin Conformations in Protein Crystal Structures with Raman Spectroscopy and QM/MM Calculations* **Angew. Chemie Int. Ed**., 49, 13, 2324, 2010 [2010-70], and *How different oxidation states of crystalline myoglobin are influenced by X-rays***, Biochimica et Biophysica Acta - Proteins and Proteomics**, 1814, 2011, 785 [2011-33].

Figure III.7 *Combined XRD+Raman+UV spectroscopy set-up*

III.2.2 Pilatus2M upgrade

With the aid of generous funding from Switzerland and Norway, it was possible to place an order in 2011 for the latest generation of large area pixel detectors produced by Dectris Ltd (Baden). In addition to the Pilatus2M detector itself, the funds were sufficient to cover the costs of a versatile diffractometer platform and kappa goniometry suitable for a wide range of different experiments in diffraction and X-ray scattering. The complete instrumentation was delivered and installed during the shut-down of the ESRF in the spring of 2012. The first experiments with the new setup could be conducted in June 2012, and the Pilatus2M has been in continuous use since its installation on BM01A. A comparison of the performance parameters compared with the image plate detector previously in use on BM01A underlines the dramatic improvements which the Pilatus2M has brought to SNBL. Instead of about 1 minute read-out time for the image plate, the new detector can be read-out in 2 ms. This reduction in cycle time allows a data collection to be made in shutter-less mode, which in turn speeds up the entire data collection procedure. A typical measurement time for a good quality single crystal data set has been reduced from 2 – 3 hours down to about 10 minutes. This changes not only the quantity of measurements which can be carried out (and hence improves the through-put of the beamline), but changes also qualitatively the overall performance of the instrument. Fast experiments can mean also more reliable measurements, since they place less demands on the long-term stability of the beam itself and of the sample environment. It is also easy to repeat measurements in order to check the reproducibility of an experimental result. In addition, of course, fast experiments imply that we can more easily follow dynamic processes such as phase transitions, chemical reactions etc.

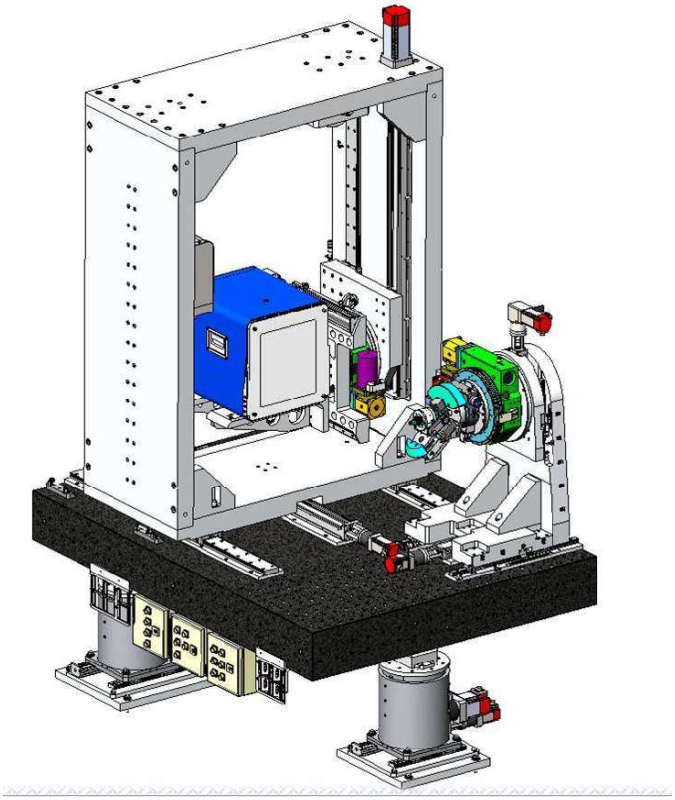

Figure III.8 *Design study for Pilatus2M setup*

Figure III.9 *The Pilatus2M diffractometer*

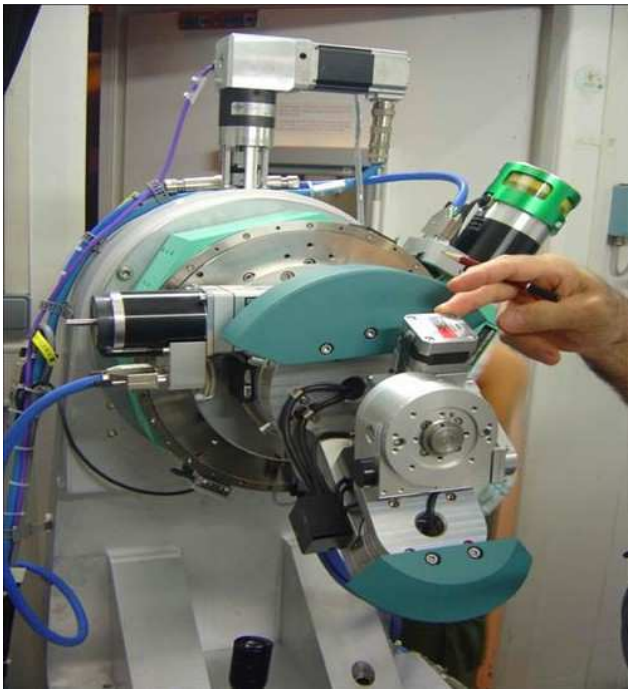

Figure III.10 *Kappa attachment for Pilatus2M diffractometer*

The Pilatus2M setup on BM01A has now been in operation for many months, and a very large number of data sets have been delivered to the users. The huge quantity of data which this implies brings its own challenges in terms of handling, processing and storing the images. Exactly this question of optimal data treatment and presentation is becoming more and more important, and several collaborations have begun with specific user groups interested in addressing this problem. In particular, groups from Stavanger and Trondheim wish to send scientists to SNBL for extended periods both to learn the how best to profit from the new instrumentation, and to optimize the data treatment.

In addition to the data analysis, it is import to learn how best to design an optimal strategy for collecting the data. Fast data collection does not automatically imply that the data will be good, and we have established a close collaboration with Dectris Ltd in order to look carefully at data quality. This collaboration includes carrying out joint experiments at SNBL to investigate the factors which can have a negative impact on data quality, such as counter dead-time and saturation effects. The Pilatus2M detector on BM01A is probably the only instrument of this type already operational on a general-purpose beamline for X-ray diffraction and scattering experiments. This presents both challenges and opportunities both for our users and for the staff of SNBL. Scientists from Dectris visited BM01A in the spring of 2013, and collected test data in order to investigate the effects of high count-rates and narrow crystal rocking curves often encountered at synchrotron beamlines. The results of these tests have already been presented at the International Workshop on Radiation Imaging Detectors 2013. Following up on these tests, Dectris will be provided SNBL with specialist software for the correction of high count-rate data, taking into account both the configuration of the beamline and detector, and, very importantly, the fill mode of the storage ring.

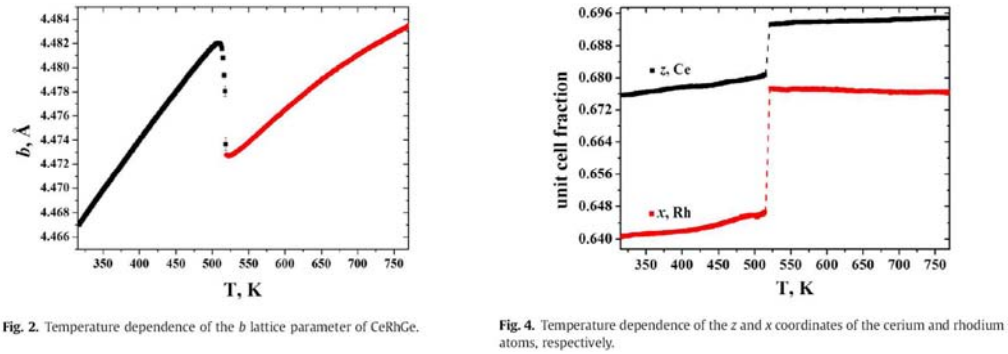

Fig. 2. Temperature dependence of the *b* lattice parameter of CeRhGe.

Fig. 4. Temperature dependence of the *z* and *x* coordinates of the cerium and rhodium atoms, respectively.

Figure III.11 *Temperature-dependent study of the crystal structure of CeRhGe*

As an example of the advantages of the fast data collection using the Pilatus2M, a recent temperature-dependent study of crystal structure of CeRhGe has recently appeared in **Solid State Sciences** *Change of the cerium valence with temperature – Structure and chemical bonding of HT-CeRhGe* (V. Svitlyk et al., 2013 [2013-51]). Over a temperature range from 350K – 700K, the high speed data acquisition mode allowed about 300 individual powder patterns to be collected. Each pattern could be analyzed to reveal not only the variation in the cell dimensions as a function of temperature, but also the individual atomic positions and displacement parameters (see figure).

III.2.3 KM6CCD diffractometer

Using internal funding through the SNX budget, a Titan CCD could be purchased from Agilent and installed on the KM6 diffractometer in 2011. After a short commissioning period, the KM6 operated for about 12 months without problems, and produced a large amount of useful data during this period. Examples of the excellent data quality obtained from the new CCD detector can be found in the section on scientific highlights. In the summer of 2012, the industrial computer running the KM6 control software failed, and a repair of the obsolete hardware

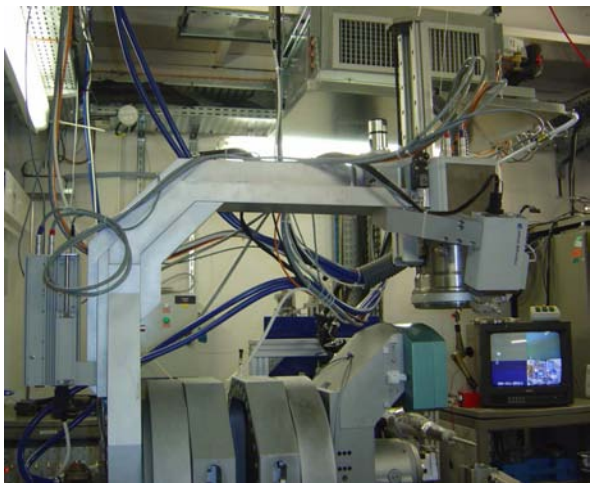

Figure III.12 *KM6 diffractometer with new CCD detector*

was no longer possible. It was therefore time to follow the earlier recommendations of our SNX Council to replace the motor controls, and work on this project is now in progress. New software has been provided by Agilent Inc to facilitate the interface between the crystallographic control package and the SPEC motor controls. The replacement of cables and other hardware connecting the motors to the new ICEPAP controls (provided by the ESRF) is under way. The new configuration should be essentially transparent to the users, since the crystallographic software will provide an identical user interface. It is planned that user experiments with the KM6 CCD to begin in the Spring of 2014.

III.3 Beamline BM1B

Improvements since last review committee meeting in 2009

SNB has undergone some profound changes in the beamline layout as well as in the acquisition strategies over the recent years. The installation of the two interchangeable monochromators has proven to be extremely beneficial to the performance of the beamline. An estimated 70-80% of our experiments are now *in-situ* measurements exploiting the versatility of the 2-monochromator approach, i.e. the speed, stability and reproducibility of the calibration when moving from EXAFS to Powder Diffraction (PD) and back again.

III.3.1 New Station Layout

Since the last review committee the B-station has gone through a complete changeover: The old experimental table at the end of the beamline hutch, as well as the previous mount for experimental equipment has been fully removed.
A new experimental layout has been designed and put in place. It comprises a solid long polished marble block for vibrational stability mounted on a set of three jacks for primary alignment. The marble has been machined with attachment holes for the fixation of a series of optical rails (X95 profiles) to allow for a fast and precise mounting and alignment of all relevant beamline components, in particular: Ion-chambers for EXAFS measurements, the 13-element flourescence detector for low concentration EXAFS, mounts for the Raman heads and adjustable supports for our cooling and heating units (Cryostreamer+He-flow cryostat, heat gun etc.), modular flight tubes to avoid air absorption, etc.
The acquisition and mounting of a solid new X-Y-Z stage allows now a much faster sample orientation as before, still improving the solidity of the mount and the precision of the alignment.
The overall design is such that this new experimental bench can be taken out as a whole (via the roof and the ESRF overhead crane) such that it can easily be removed from BM01B and installed elsewhere. This is particularly important in

(a) **(b)**

Figure III.13 *(a) New station layout, with marble block, rails and alignment stages (b) Old layout as in 2009*

the light of our recent efforts to move BM01B to another bending magnet port (see following section III.3.5 about the "Future").

The experimental table at the end of the beam line has been removed and a central supporting marble block was installed around the diffractometer location.

However, the major bottleneck for characterizing quickly evolving systems were still the high acquisition times needed for a full XAFS and/or HRPD pattern (typically ≥ 15min for both techniques). Recent progress has removed these drawbacks almost entirely.

III.3.2 Installation of a fast scanning option for our EXAFS monochromator

One of the main advantages of the SNB monochromator is the fact that we can access a wide range of energies spanning from <5-80keV without any changes to the beamline set-up. This has paid off in the last years where we repeatedly performed high energy EXAFS on rare earth doped scintillator materials (K-edges of almost all Lanthanoids) or K-edge EXAFS measurements on important catalyst elements like Cerium or Rhenium. We regularly have proposals specifically asking for the possibility to perform high energy EXAFS on our beamline.

However, especially at low energies where large angular displacements are needed to perform a complete EXAFS scan, measurement times were still far too long for many chemical reactions. In order to remedy to this situation we have modified our monochromator drive system and added a second (high torque) stepper motor in a direct coupling to the monochromator drive spindle.

To illustrate the fast scanning option of SNB EXAFS mono: A clutch (in light yellow) allows uncoupling the 1:100 harmonic drive gear box (gray cone with black stepper motor mounted on its back) from the monochromator spindle (brown).
The monochromator can now be run in two modes: When uncoupled the monochromator spindle can be driven directly via a strong stepper motor (schematically shown as violet body). When the clutch and thus the reducer

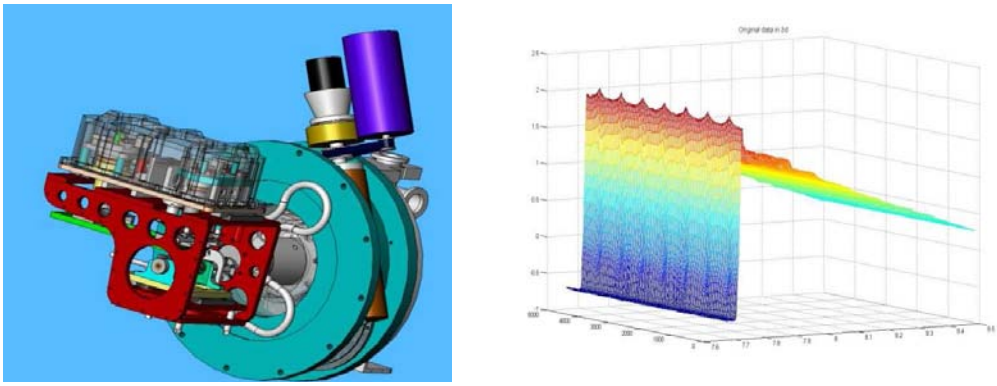

(a) **(b)**

Figure III.14 *(a) Modified EXAFS mono with fast drive*
(b) Modulation EXAFS (MES) using the fast scan option

gearbox (+motor in black) is engaged the high torque motor gets unpowered and simply spins without any resistance together with the monochromator shaft.
This rather simple change allows now for rapid, full EXAFS scans down to 10s or even less even at low energies close to 5keV. We use the stepper motor cards developed by the ESRF (ICEPAP) for this purpose since they allow us to run our system in a fast responding closed loop mode such that even at these speeds the motion is fully controlled by our high resolution angular encoder and no perceivable distortions in our EXAFS patterns are observed. Furthermore we have bought new amplifiers reducing the noise level and permitting a user friendly amplification gain change directly via the control software.

III.3.3 Acquisition of a 2D-CMOS Area Detector

With measurement times down to the second scale for the EXAFS measurements we were still hitting a strong time limitation for the powder diffraction measurements. To overcome this situation we have bought a 12 Megapixel medical detector in 2012 (normally used for mammography) and implemented on our beamline.

This new detector does not only reduce the measurement times for powder diffraction measurements down to the second scale but the high conversion efficiency of the 150um thick scintillator conversion layer (CsI) at high energies (> 40keV) opens up the door to high energy diffraction and likely even Total Scattering (PDF) measurements in the future.

It is noteworthy that this new system can work in parallel with the “old” powder diffractometer, since the conception of our new experimental bench allows mounting the 2D detector below the beam plane thus permitting parallel operation of the high speed/statistics 2D detector and the high resolution powder diffractometer. We expect this combination to be a very powerful set-up for high speed, high quality measurements, but also alleviating the problem of calibration of our new area detector since the high resolution diffractometer gives us the best reference possible showing how the intensity distribution measured by the 2D detector must (!) look like.

The following pictures show a comparison between the “old” high resolution set-up and the “new” area detector.

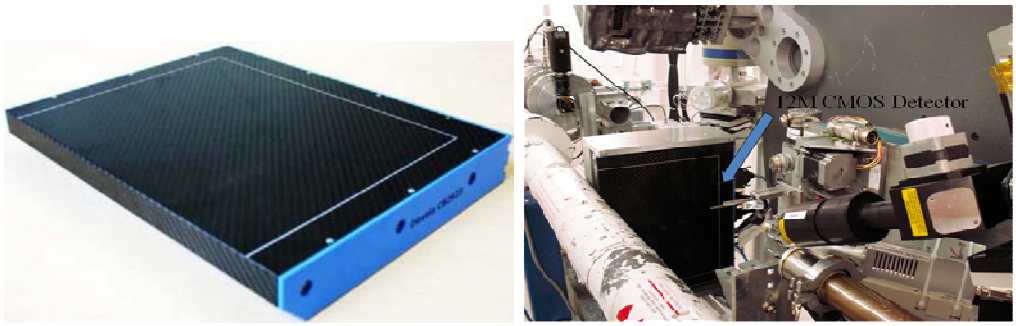

Figure III.15 *(a) Dexela CMos pixel detector, 29cm×23cm sensitive area*
(b) 2D area detector as integrated into beamline

As the LaB_6 pattern (see below) indicates, the resolution of the HRPD instrument is still 3x higher (depending on capillary size and detector distance) but the measurement times have come down to the second range.
The diffraction measurements on the ZrO + 8%Sc_2O_3 nano-powder (right image) highlights that even weak features (see magnification under red circle) which are barely visible in the HRPD pattern come out well resolved when measured with the 2D detector.

III.3.4 Focusing

Since SNB is specialized in the analysis of industrially relevant catalysis and synthesis processes. It is in the nature of these systems that they often show poorly or nano-crystalline materials and phases. Adding Total Scattering techniques to our possibilities would greatly enhance our capacities in the characterization of these "real world samples".

Since total scattering experiments need good statistics at high Q's it is in this context important to provide a high X-ray flux density at high energies. The ESRF being a high energy machine has the advantage of delivering still plenty of flux at photon energies >30keV but space constraints due to the vicinity of the two branches of SNBL (SNA and SNB) stymied any attempts of installing a sagitally focusing monochromator on the B-branch.
We therefore opted for a "new way" of focusing, using a Si(111) wafer anodically bond onto a Pyrex support with a concave cylindrical depression ground into it prior to bonding.

The dimensions of the Pyrex support are such that it fits exactly into one of the two slots of the crystal cage (of the secondary crystals) of our EXAFS two crystal monochromator.
This can be seen on the image below. The beam gets reflected by a first flat and water-cooled crystal (shown in translucent green at the right bottom). The focusing crystal sits in the crystal cage above (again in green, focusing crystal not shown) from where it bounces off for a second time before it leaves the monochromator in the horizontal plane.

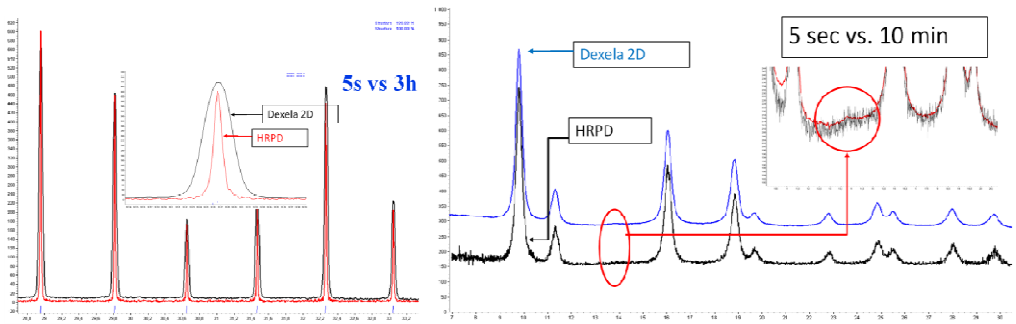

Figure III.16 *(a) LaB_6 pattern for comparison (unfocused)*
(b) ZrO+8%Sc_2O_3 nanopowder

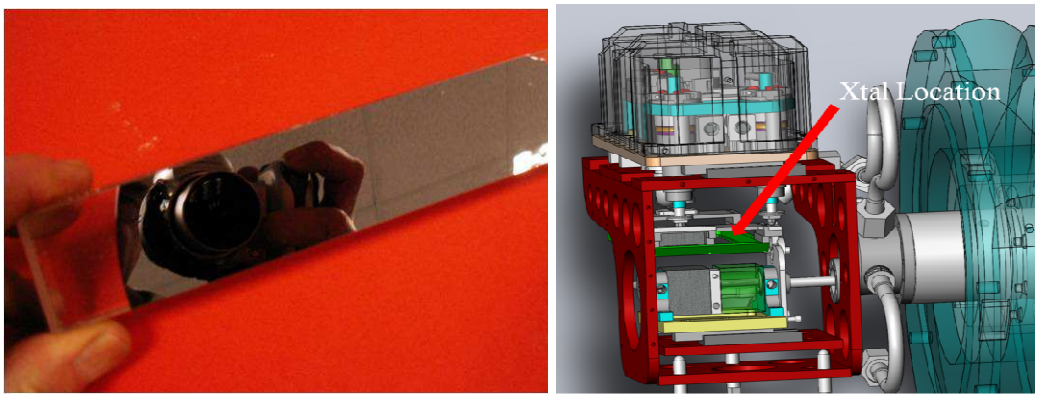

Figure III.17 *(a) Anodically bond Si(111) wafer on concave Pyrex support*
(b) Insertion of focusing crystal in existing monochromator

The radius of curvature is optimized such that we get a minimal vertical focal line width at the detector position at a photon energy of about 41keV. A horizontal slide system integrated into the crystal cage (cage in red) allows selecting either the flat or the focusing crystal pair for operation.

The absorption edge of Cs lies close to 36 keV. Above this energy absorption of x-rays in the scintillator layer of the 2D detector is high. At these energies our bending magnet source still delivers a sizable flux. Since we would like to prepare for PDF measurements where high **Q** and thus high energies are needed, 41keV was chosen as a compromise to ensure high detector efficiency one hand and high **Q** on the other.
The following picture shows the performance of this device. The flux density was increased more than 10 fold without any detrimental effects to the peak shape or peak resolution.

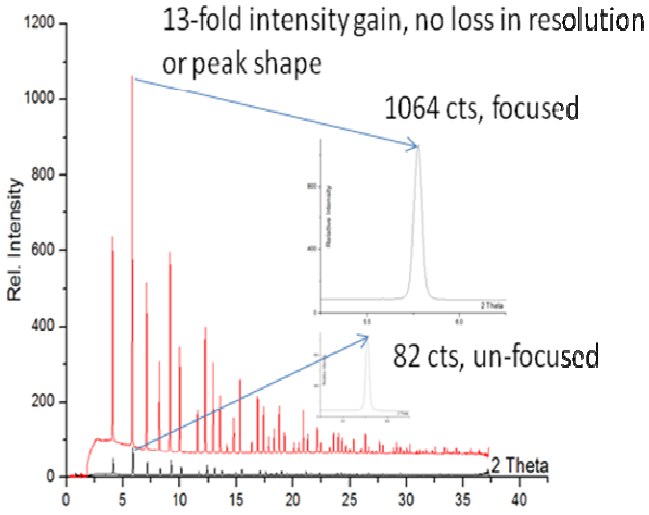

Figure III.18 *LaB_6 powder diffraction measurement using our Dexela 2D detector, comparing focusing (red) and non-focusing geometry (black spectra at bottom). Measurement times are 0.5s @ 41keV for both (focused and unfocused) measurements*

III.3.5 Future

Future developments of BM01B are more and more hampered by the vicinity of the A-branch of the Swiss-Norwegian beamlines. We would like to implement pre-monochromator mirrors for efficient harmonic rejection and heat-load reduction, post-mono deviating mirrors for crossing the beams emerging from our two monochromators on the sample spot for truly simultaneous PD/ EXAFS measurements plus the possibly to install a third – high throughput – monochromator for PDF measurements. We have therefore handed in a bid for the takeover of an unused ESRF bending magnet port. The ESRF has received our proposal with great interest, but the final decision is still not known at this moment.
Independent of the outcome of this decision we will prepare for moving to an independent beamline for SNB – be it sooner or later. In a first step we would simply move our existing equipment from BM01B to the new location before we can take full advantage of the new situation by adding new items to the beamline layout (see III..

III.4. Auxiliary equipment available for both beamlines

A. Cryostats

As far as possible we try to adapt our equipment to the need of combining different techniques. As a practical consequence we design our sample environment to be as open and accessible as possible. One example is our He-flow cryostat. By designing the cryostat around our needs, we are in a situation where we can apply all our techniques (Diffraction+EXAFS+Fluorescence+Raman) down to temperatures of 4.5K. An additional, miniature He-flow cryostat has recently been purchased for the KM6 diffractometer, and this cryostat is now in routine operation on BM01A

B. Gas mixing and gas flow control

The last year we have also developed together with our user community a gas mixing, flow and measuring system. This system is also fully integrated in the beamline and can distribute gasses to both of our experimental stations. It is a very flexible system capable of adapting to the needs of our wide user community. All gas bottles are stored outside the Experimental Hutches, and a total of 6 different gasses can be supplied via stainless steel pipework to both beamlines. The gas mixing and control system can be completely remote controlled (Figs.III.19-21). A mass spectrometer is permanently installed to characterize the gases released after the in-situ reaction. A variety of micro-reaction cells are available for gas pressures up to 100 bar. The majority of the funding for this equipment came from the Catalysis Initiative sponsored by the Norwegian Research Council.

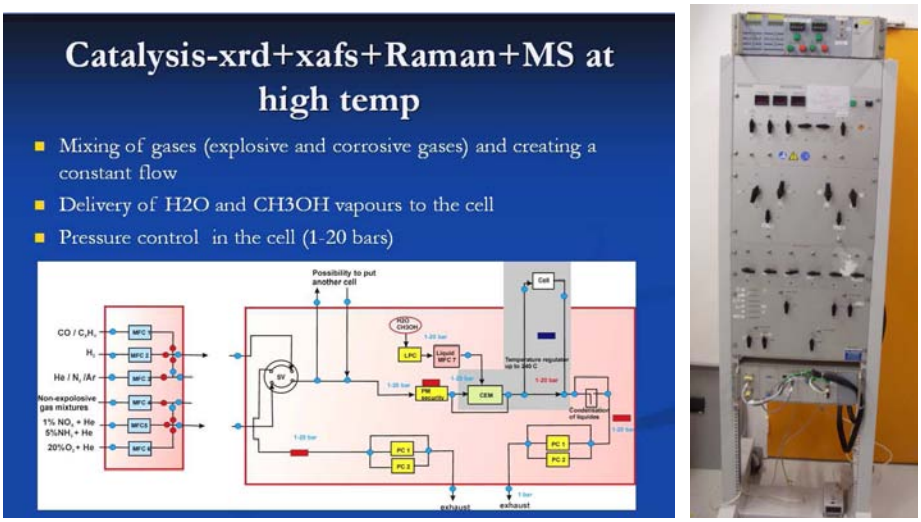

Figure III.19. *Gas mixing and flow control system.*

Figure III.20. *The array of gas bottles outside the experiment hutches*

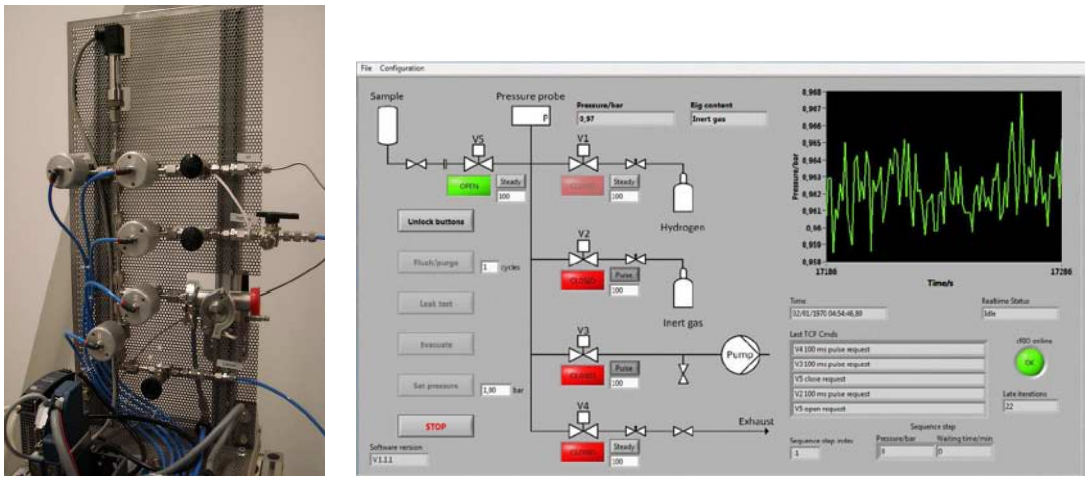

Figure III.21 *The gas mixing system designed for high gas pressures*

III.3.5 Acquisition Software

The increasing complexity of experiments and the flexibility needed to cater for quicker and combined experiments lead us to adopt SPEC as data acquisition software on BM1B in 2004. It also brought the advantage to have direct support from the ESRF software group in order to integrate new instruments and devices. This choice has turned out to be extremely fruitful be it in terms of recently added functionalities (speed, data logging, scanning modes) or in the light of speeding up and synchronizing different measurements or external parameters.

As part of the general refurbishment of the beamline, BM1A has now also adopted SPEC for beamline instrument control. In addition, SPEC is the basis for the control of PILATUS@SNBL. However, a dedicated python-based graphical user interface (Pylatus) has been implemented. Control of various ancillary equipment can be carried out via the Pylatus GUI, which greatly increases the capabilities of the new setup. We have furthermore purchased a new software interface from Agilent Inc. for the KM6 diffractometer. This interface will in turn communicate with the ESRF standard ICEPAP motor controls via a SPEC session. In this fashion, and with a minimum of disruption to our user community, we will be running the entire beamline and experimental instrumentation in a standard ESRF configuration but with our own graphical interfaces.

IV. SNBL OPERATION: on the beamlines and beyond

IV.1 BL staff

A beamline operation depends to a large extent on the staff – its flexibility, motivation, expertise and scientific interests. The following list introduces the SNBL team members and indicates their functions.

Dr. Vladimir DMITRIEV - *Project Director* - Has overall responsibility for and authority over SNBL's daily operation, as executive director of the SNX Foundation, member of its Council and chairman of ASNG (at SNBL since 1999, from January 2005 as a Director). Assists users in the performance of their experiments. Scientific interests include experimental (x-ray diffraction and Raman spectroscopy) and theoretical (symmetry analysis and phenomenological theory) study of phase transitions in condense matter; high-pressure/high-temperature study of metals, minerals and inorganic compounds.

Dr. Philip PATTISON - *Senior Beamline Scientist (A-Station), Deputy Director of SNBL* - Responsible for all scientific and technical aspects of the operation, planning, scheduling and development of beamline BM01A (1991). Assists users in the performance of their experiments. Scientific interests: Applications of synchrotron radiation to crystal chemistry and solid state physics; Design and development of X-ray optics for synchrotron beamlines.

Dr. Dmitry CHERNYSHOV – *Beamline Scientist at BM1A* - Assists users in the performance of their experiments, participates in the development of beamline BM01A (2005). Scientific interests cover field of phase transitions in molecular crystals induced by temperature, pressure, light irradiation, and physics of neutron and synchrotron scattering on periodic structures in general.

Dr. Vadim DYADKIN – *Post Doc at BM1A* - Assists users in the performance of their experiments, participates in the development of beamline BM01A (2012). Scientific interests are in the field of materials for diffraction studies (powder and single-crystal) and of their structure and phase transitions.

Mr. Herman EMERICH - *Senior Beamline Scientist (B-Station*) - Responsible for all scientific and technical aspects of the operation, planning, scheduling and development of beamline BM01B (1993). Assists users in the performance of their experiments. He has strong interest in development and instrumentation and applying these advancements in collaboration with independent research groups.

Dr. Wouter Van BEEK - *Beamline Scientist at BM1B* - Assists users in the performance of their experiments, participates in the development of beamline BM01B (1997). Has a strong track record in instrumental developments, e.g. multiple technique approaches under a wide variety of external stimuli. His research interests are focused on the study of phase transitions, synthesis and

catalytic processes with the aim to use the newly created opportunities to its full scientific potential.

Dr. Paula ABDALA – *Post Doc at BM1B* - Assists users in the performance of their experiments, participates in the development of beamline BM01B (2011). Scientific interests: mechanisms of reactivity of heterogeneous catalysts and electro-catalysts. Studies of nanostructured materials with industrial applications such as solid oxide fuel cells and gas sensors using XAS, XRD, and Raman spectroscopy, under *in situ* or operand conditions.

Dr. Olga BANDILET – *Computer Engineer* (0.25).

Mrs. Chantal HEURTEBISE - *Administrative manager* - Handles general office work; administrates all accounting operations; secretary of the SNX Council (1999).

Senior Technician – Geir WIKER

Former members (2000-2012)

Dr. Hans-Peter WEBER – Project Director (1990-2004)
Dr. Jon Are BEUKES – PostDoc (2000-2004)
Dr. Silvia CAPELLI – PostDoc (2000-2003)
Dr. Denis TESTEMALE – PostDoc (2003-2005)
Dr. Olga SAFONOVA – PosDoc (2006-2011)
Dr. Yaroslav FILINCHUK – PostDoc (2006 – 2011)
Dr. Volodimir SVITLYK – PostDoc (2011-2012)
Mr. Olexii KUZNETSOV – PhD Student (2001-2004)
Mr. Denis MACHON – PhD Student (2001-2004).
Mr. Marc PISSARD – Senior Technician (2000-2008)

IV.2 SNBL In-house research activity

Several programs in scientific research and instrumentation development are currently being carried out at SNBL by its staff. In the technical description of the beamline, some aspects of the innovative solutions in instrumentation and beam line design were presented. Two EU collaborative projects, with the participation of several groups from European universities, aim to design, construct and commission new high-pressure/high-temperature diamond anvil cells for studying the transport properties of material under extreme conditions, and for single-crystal X-ray diffraction at high pressure and temperature. We are also involved in the EU project DYNAMOL (see below) in which we can contribute towards the development of data collection strategies and improved software aimed at solving the crystal structures of complex, supra-molecular assemblies at atomic resolution.

We will collect data for change density analysis on several organic compounds, in collaboration with groups from the University of Aarhus and the Georg-August Universität Göttingen, in order to verify the performance of both our CCD and pixel detectors. High quality data have already been collected on these compounds at Spring8 and HASYLAB, and this collaboration with experienced groups in the field of charge density analysis will give us a good opportunity to confirm the quality of our data from both detector systems. Where data of the highest quality and up to the highest possible scattering angle are required (e.g. for the investigation of anisotropic displacement parameters, or for charge density studies) then the KM6CCD will be the detector of choice. For most other experiments, we expect that the Pilatus2M will be the optimal detector.

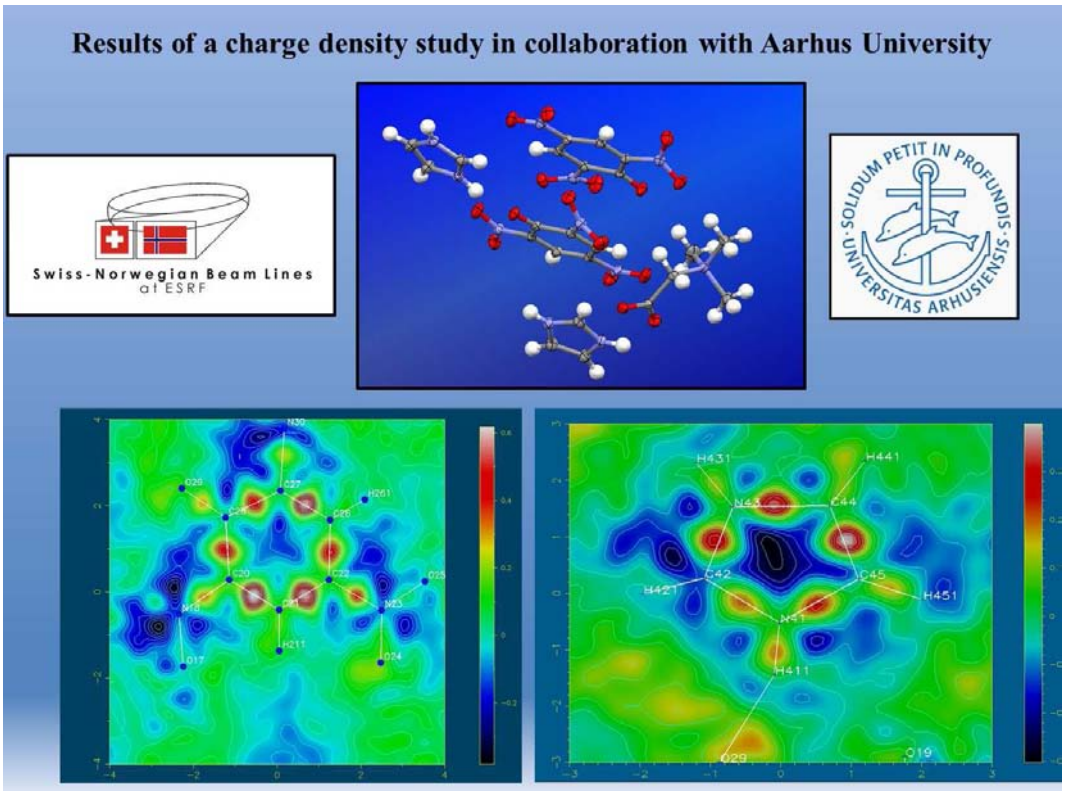

Several of our user groups are very interested in probing the borderline region between small molecule crystallography and macromolecular structures. Groups are active in this field at, for example, the Laboratory of Supramolecular Chemistry at the EPFL (Prof Kai Severin) and the University of Oslo, Department of Chemistry (Prof Karl Petter Lillerud) where metal organic complexes and new micro-porous structures are being investigated. New tools and data collection strategies are needed for these applications, because the goal is to be able to obtain information at atomic resolution on large, complex, and often disordered structures. The SNBL staff are therefore collaborating on an EU academic-industrial partnership called DYNAMOL (Dynamic Molecular Nanostructures) in which the EPFL and Global Phasing Ltd, Cambridge are participating. The samples will be provided by the group of Prof Severin, the data collection will be done at BM01A and the analysis carried out by Dr Holstein at Global Phasing Ltd. At the end of the project, the software will be installed and tested at SNBL,

and will be available to all user groups. As an example of structure complexity, we show the results of an investigation into giant manganese wheel-like structure recently measured and solved at BM01A. The crystals for this study were provided by colleagues at the University of Porto, Portugal.

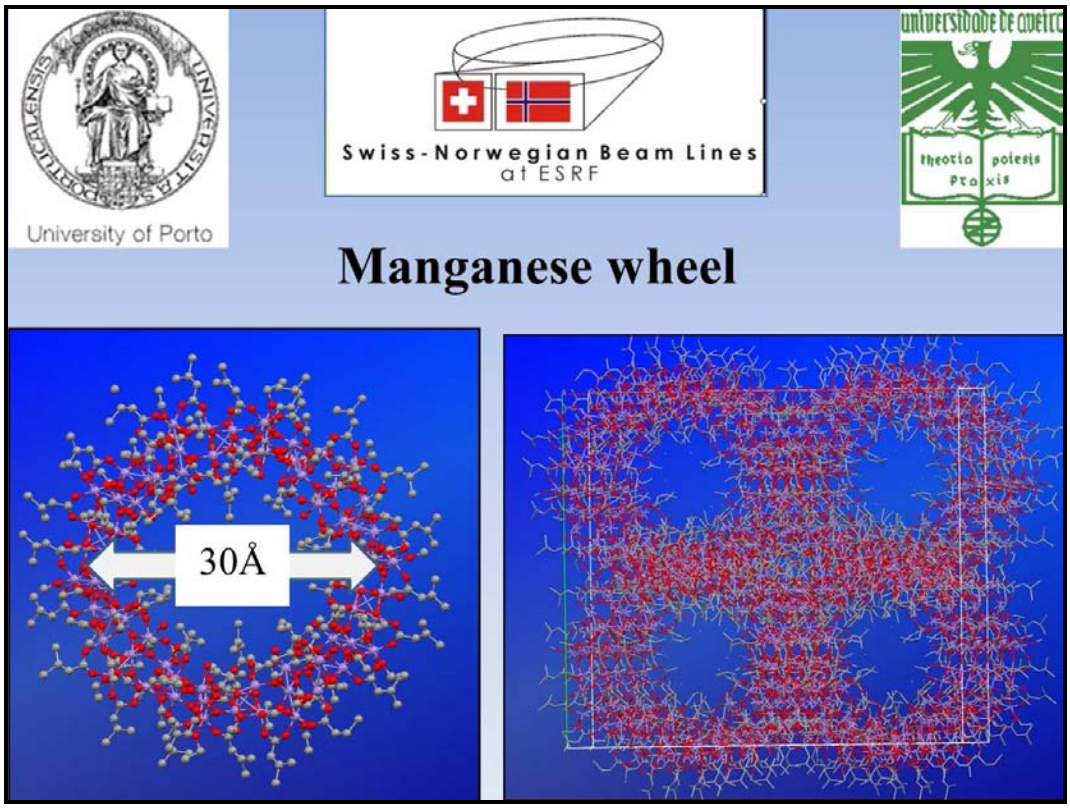

In addition to the sheer size of the crystal structures, complexity can also occur due to a myriad of possible interactions between the electrons and atoms within a crystal. These interactions can reveal themselves by the presence, for example, of satellite reflections close to the Bragg nodes in the reciprocal lattice. They can also generate clouds of diffuse scattering, whose shape depends on specific features of the Fermi surface and the Brillouin zone boundaries. Several projects on this theme have earlier generated a number of publications from data collected at SNBL using our MarResearch image plate setup. The new diffractometer equipped with the Pilatus2M detector is ideal for this kind of application. It is particularly important to be able to present the observations in three dimensions, allowing proper inspection of the diffuse scattering features. We are therefore working (in collaboration with colleagues at the ESRF and the University of Trondheim) on procedures to reconstruct the full 3D reciprocal space representation of the 2D images collected with an area detector. Several recent publications have already exploited the technical developments made at SNBL concerning reciprocal space reconstructions, and work on further improvements is in progress.

Recent publicationjs from BM01A using reciprocal space reconstruction:

Tagantsev, A. K. , Vaideeswaran, K., Vakhrushev, S. B., Filimonov, A. V., Burkovsky, R. G., Shaganov, A. et al. *The origin of antiferroelectricity in $PbZrO_3$* Nature Communications, **4**, in press, 2013

Bosak, A., Chernyshov, D., Vakhrushev, S. *Glass-like structure of a lead-based relaxor ferroelectric* J. Appl. Cryst., **45**, 6, 2012

Burkovsky, R. G., Bronwald, Yu. A., Filimonov, A. V., Rudskoy, A. I., Chernyshov, D., Bosak, A. et al. *Structural Heterogeneity and Diffuse Scattering in Morphotropic Lead Zirconate-Titanate Single Crystals* Phys. Rev. Lett., **109**, 097603-097607, 2012

Bosak, A., Chernyshov, D., Vakhrushev, S., Krisch, M. *Diffuse scattering in relaxor ferroelectrics: true three-dimensional mapping, experimental artefacts and modelling* Acta Cryst., A**68**, 1, 117-123, 2012

Bosak, A., Hoesch, M., Krisch, M., Chernyshov, D., Pattison, P., Schulze-Briese, C. et al. *3D Imaging of the Fermi Surface by Thermal Diffuse Scattering* Phys. Rev. Lett., **103**, 076403-076407, 2009

IV.3 SNBL Upgrade and Scientific Perspectives

IV.3.1 Technical developments on BM01A

The KM6 multi-axis diffractometer, equipped with the latest generation CCD detector, provides a versatile platform for a wide variety of diffraction experiments. Although smaller in x-ray sensitive area and slower in readout than the latest pixel detectors, the CCD technology (i.e. an integrating detector) is well suited for collecting very accurate data on a synchrotron beamline. On the other hand, large area 2D detectors such as the Pilatus2M can cover a vast range of applications in powder and single crystal diffraction, as well as diffuse scattering and total scattering (i.e. measurement of pair-distribution function). Therefore SNBL is already well-equipped for carrying out a wide variety of different x-ray scattering experiments. Our goal over the coming months and is to find the optimum combination of data collection strategies and data analysis procedures in order to extract the very best quality information from the available instrumentation. To this end, we have identified four areas in which we will be investing our resources.

1. *Improve the overall quality of our diffraction data*

A bending magnet beamline at the ESRF provides a stable, reliable and highly intense source of x-rays. Since we have two independent detector platforms at BM01A, we have the ideal opportunity to compare and calibrate the performance of our different detectors and associated goniometry. In collaboration with Dectris Ltd, we will also be testing and developing hardware and software for optimized data collection using the Pilatus2M pixel detector. It is well-known that photon-counting pixel detectors can suffer from a loss of counts at high count-rates. Without appropriate corrections, this problem can severely limit the dynamic range which can be covered with this type of detector. SNBL is now the test facility for new versions of data analysis software from Dectris Ltd, which will allow us to make an optimal count-rate correction for the Pilatus2M.

2. *Data collection strategies and instrument control*

For many experiments, it is essential to be able to collect diffraction data at the lowest possible temperatures. This may involve the onset of magnetic order, a low temperature phase transition, or simply the need to suppress as much as possible the effects of thermal motion. We have already carried out many measurements at helium temperatures using either our own cryostat, or else the Helijet cryo-cooler on loan from the ESRF Sample Environment Laboratory. The combination of very low temperatures provided by these devices, plus the rapid data collection possible with the Pilatus detector, suddenly opens up some very interesting opportunities for cryogenic experiments at BM01A. We will therefore, in collaboration with the ESRF, submit a joint proposal to invest significant resources in low temperature equipment optimized for our Pilatus2M setup. Our goal is to bring together the appropriate equipment and technical expertise at SNBL to allow us to perform experiments at helium temperatures in a routine and

reliable fashion. In particular, we have identified groups carrying out neutron diffraction measurements at the Paul-Scherrer-Institut, Switzerland (and potentially also at the Institute for Energy Technology at Kjeller, Norway) who would welcome the opportunity to have regular access to synchrotron measurements at helium temperatures. Reports concerning several experiments in collaboration with the PSI laboratory for Neutron Scattering can already be found in the publications list.

The controls for the Pilatus2M detector and associated instrumentation on BM01A have been developed in-house by the SNBL team (particularly thanks to the efforts of Dr Vadim Dyadkin). The software package running PILATUS@SNBL not only controls the functionality of the detector itself, but is a versatile tool able to control a large number of different types of ancillary equipment such as heaters, coolers and cryostats. Positional scans can also be performed during the data collection, in order to investigate inhomogeneous samples. In addition, we have an SNBL software "tool-box" which allows us to pipeline the Pilatus2M images into a variety of other analysis packages such as CrysalisPro (Agilent) for single crystal analysis and Fit2D (ESRF) for powder data. Other options within the tool-box prepare the powder data for batch processing using the FullProf package, for example. These developments are vital if the user wishes to exploit fully the massive amount of data which can be generated by this type of pixel detector. It is not at all unusual to have 200-300 powder patterns to analyze following a simple temperature ramp, and hence care must be taken to ensure that the users are able not only to collect the data, but also to analyze it properly.

3. *Secondary focusing for measurements on small crystals (<< 50 μm)*

We have already successfully demonstrated the use of a doubly-curved, graded multi-layer mirror from XENOXS (Grenoble) for secondary focussing. With the aid of this mirror, positioned close to the sample, the focal spot could be reduced in size from 300μm to about 30μm diameter with an increase in flux density of a factor of 30x. Up until now, it has been difficult to implement this device in practice due to space restrictions around the KM6 diffractometer, and the poor mechanical precision of the MarResearch Image Plate setup. We now have a very flexible working environment around the sample position with the Pilatus2M platform, and excellent mechanical precision. Therefore the time has come to develop a standard configuration which will allow us to install and remove the XENOXS mirror on a routine basis. The dramatic gain in flux density will make it feasible to collect good data even on weakly diffracting, small crystals. While this configuration will not compete with beamlines optimized for micro-focussing, it will extend dramatically the range of samples which can be successfully measured

at SNBL. In addition, it will be an ideal arrangement for studying crystals in high pressure diamond anvil cells, where the sample volume is necessarily very limited.

4. *Improved beam control and flux monitoring*

As the mechanical precision of our goniometry improves, there are consequently more stringent demands placed on the beam quality and stability. For this reason, we have invested in commercial beam position monitors and feed-back controls for BM01A. We have purchased from Huber Diffraktionstechnik GmbH a high precision beam position monitor, slit screens, filter wheel, ultra-fast shutter, beam stop and an in-line microscope. This equipment has been kindly provided at favourable terms in order to evaluate the performance of these components on a synchrotron beamline. Although the overall stability of the synchrotron beam on a bending magnet source is very good (ie until now, no feed-back system has been required), we now wish to work in a regime where beam position control of a few microns or better is necessary. We therefore welcome the opportunity to work together with Huber GmbH on perfecting the performance of this equipment. With the aid of this beam monitor and feedback control, we should also be in a good position to handle the increased flux associated with an eventual increase in the beam current in the storage ring.

Summary

The combination of initiatives outlined above should allow us to improve further the overall quality of the diffraction data collected at BM01A. We will extend the temperature range and reduce the sample size required for routine experiments performed at SNBL. Experiments on complex materials with large unit cells should become feasible. Strategies will be developed which will allow us to convert optimally the 2D data collected with an area detector into the full 3D reciprocal space information. These procedures will be vital if we are to be able to visualize the structure of the diffuse scattering and interpret its dependence on complex interactions between electronic and crystal structure. The performance of the instrumentation in the experimental station will be optimized, and the stability and reliability of the focused beam will be guaranteed. Finally, we will provide the data analysis pipelines which are essential for handling and interpreting the massive amounts of data generated by pixel detectors.

IV.3.2 Technical developments on BM01B

All the room needed to run SNB on BM01 is almost full. We are reaching the limits of what we can do with the available space both in the optics and the experimental hutch. Any further upgrade is difficult to implement, time consuming, unnecessary expensive compared to a similar upgrade on a standard beamline. Further progress is not impossible on BM1B but it will always remain inefficient.

The following in-house project aims at alleviating the well-known space constraints of BM1B by moving it to a different bending magnet port (BM18).

The major advantages can be summarized as follows:

A) Improved operational efficiency of SNBL
B) Facilitating future developments to extend the range and variety of high quality techniques available to our users
C) No additional funding resources required in the short and long termat the expense of only a minor loss of beamtime

In its current form with two beamlines on one bending magnet port the SNBL management already presented a roadmap for future investments. This roadmap is in line with the recommendations of the SNX Committee of the Future presented in November 2008 and the SNX EXAFS commission presented in December 2009. It includes major changes to the B-line optics both for EXAFS and HRPD. These planned developments would allow SNBL not only to increase the scientific capability of the beamline in the short term but also opens new perspectives for its development in the long term.

A design study preparing this upgrade revealed however, a whole set of technical difficulties. The basic problem is the vicinity of the two beamlines, A and B, and as a direct consequence an unfavorable geometry and extremely limited room available for (new) B-station related optical elements and instruments be it in the common optics enclosure or in the experimental hutch. It became evident that above problems cannot be satisfactorily solved in the model of coexistence of the two stations at the same bending magnet port. Major progress on the B-station capabilities is difficult to implement, time consuming, and therefore expensive.

The SNX has put out a bid on an obsolete infrastructure (BM16) in 2012. The SNX proposal was well received by ESRF management and council. Two parties were bidding at the same time on this BM16 port and it was impossible for the ESRF to make a decision based on scientific and technical criteria. See recommendation from ESRF SAC chairman: “In view of the difficulty to take a decision based solely on the scientific and technical merits of the two projects, and considering the effect of the two projects on the quantity of public beam time and external investment on the ESRF operations the SAC would like to make the recommendation for the Council that the FAME proposal should be granted the BM16. However, the SAC urges the ESRF management to find an alternative solution for the SNBL proposal in another location on the ESRF experimental hall.”

A twofold decision was finally taken at the ESRF council meeting in June 2012:

- The acceptance of the French proposal as a new CRG beamline to be constructed on the existing BM16 premises; and that
- Management will continue technical, financial and logistical discussions with the representatives of the SNBL proposal, with the objective of finding, as soon as possible, a suitable solution for the timely assignment to this proposal of an available bending magnet port on the ESRF experimental floor.

The SNBL representatives were in response to the council decision contacted in June 2013 by the ESRF managements with an alternative solution: BM18.
The ESRF offer can be roughly broken down in three:

- An empty bending magnet port.
- A complete infrastructure design suitable and ready to receive BM01B.
- The planning and supervision of the infrastructure construction during the winter of 2014.

IV.4 SNBL Workshop: Diffuse Scattering from Crystalline Materials (June, 2009)

As part of our policy of seeking ways to facilitate the exchange of information between the SNBL team and the synchrotron user community, the SNBL management has organized a series of workshops at the ESRF based on themes of current and future interest both to the SN community and a wider scientific audience. The first of these meetings on the topic of nanoscale materials was held in 2006, followed by a workshop on the subject of high gas pressures for *in-situ* experiments in 2007. Both of these meetings were attended by 30-40 participants, including participants from various synchrotron beamlines as well as external users. The next meeting, which took place in June 2008, continued the theme of *in-situ* experiments, but specifically includes the use of our new Raman spectrometer in combination with x-ray absorption and diffraction measurements. 80 participants, came from 14 countries.

The first joint SNBL-ESRF workshop took place June 25-26 2009 at the ESRF, Grenoble. The goal of this 2-day workshop was to bring together people interested in diffuse scattering, in order to share their experience in experiment and theory and to present and discuss new problems in physics and chemistry in which disorder phenomena are important.

More than fifty participants from 10 countries (France, Switzerland, Norway, Germany, Austria, Russia, Spain, Australia, UK, USA) created a very stimulating, constrictive and friendly environment for exchanging theoretical ideas and experimental know-how. The list of participants shows the presence of world-leading experts in the field of diffuse scattering such as Hans-Beat Bürgi (Switzerland), Richard Welberry (Australia), Tai-Chang Chiang (USA), Reinhard Neder (Germany), Harold Reichert (Germany/ESRF), Sergey Vakhrushev (Russia), together with young scientists and Ph.D. students. The study of disordered phenomena has a long tradition in Switzerland and Norway; there were 10 Swiss and 3 Norwegian participants. There were also visitors from ESRF and

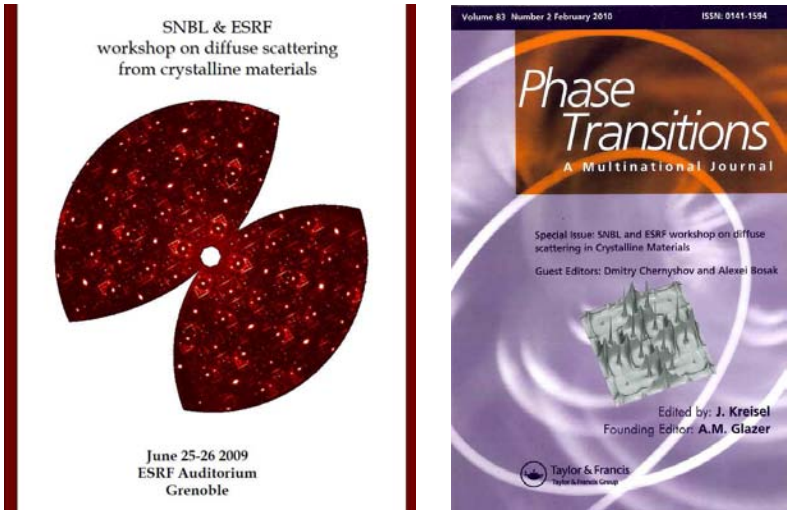

Figure IV.1 *Programme booklet and Proceedings of the Workshop*

ILL interested in diffuse scattering.

There were many interesting lectures presenting new approaches in data analysis, illustrating the use of combination of diffuse and inelastic scattering techniques, showing new challenging problems to be solved in future, and offering new experimental methods. To have a record of the main results, a selected collection of presentation was published in a special issue of "Phase Transitions" international journal (PT, 2010, **83**, no.2).

The workshop also gave an opportunity for our users to see what can already be done at ESRF and SNBL today and, with their help, what might be possible in the future. For a synchrotron facility offering beamtime for user community, such as SNBL or ESRF beamlines, the workshop helped to define the direction in which we have to develop in order to fulfil the requirements of our user community. In particular, it becomes clear that the best data quality of diffuse scattering experiments can be achieved with a PILATUS detector; and a corresponding proposal for detector and goniostat has been therefore submitted at that time. We are offering now 3D inspection of reciprocal space that can be done shortly after data collections with help of software developed together with colleagues from ID28 ESRF beam line. Fast and reliable measurements of diffuse scattering data assume that there will be a large amount of information to be analysed and require fast computers operating with large amounts of graphical information. Analytical tools facilitating data analysis have been in particular developed at ETHZ and tested with data collected at SNBL.

The workshop also gave an example of constructive collaboration between SNBL and ESRF in terms of organization and finance issues. Scientific collaboration with ID28 has been successfully continued and we have 16 common publications in 2009-2013. This fruitful combination of mapping of diffuse scattering with inelastic scattering could be further explored by Swiss and Norwegian users as well as our know-how and experimental protocols on data collection and analysis.

IV.5 SNBL Collaborations

Active cooperation of efforts, in different fields, with user’s institutes and similar facilities is an important aspect of the SNBL management policy. The collaborations had a significant impact affecting the beam line configuration, priorities in its technical development and financial issues. It helps us in ensuring the SNBL’s current solid equipment and financial base, and gives confidence in its successful future.

Cooperation with Swiss and Norwegian institutes has the highest priority in the “external” affairs of SNBL. An active role of the SNBL in seeking and establishing close relations with bi-national research groups, institutes and centres is a key part of the strategy of the management team.

A. Interaction with national institutions

An example of such interaction is the involvement of SNBL in the long-term Norwegian Natural Gas Processes and Products program (*inGAP*). Partners in the project are both academic, such as the University of Oslo, NTNU Trondheim, SINTEF, as well as industrial: Statoil ASA, Hydro Polymers AS, Norsk ASA, and Borealis. The Research Council of Norway launched, on March 2007, the *inGAP* center. The aim of the project "In-situ@SNBL" was to build up a state-of-the-art facility for synchrotron X-ray based in-situ studies of catalysts. As in situ studies will play a key role in many of the projects in *inGAP*, the construction of this facility was prioritised in the early stages of the *inGAP* collaboration. The construction of the facility at SNBL is now completed and operational. It ensures a long-term perspective for the SNBL operation in the field of catalysis.

Another initiative, coordinated by the SNX Council representatives, was the purchasing and installation on the beam line of a new diffractometer equipped with Pilatus2M pixel detector. A joint request submitted by the group of Swiss and Norwegian universities and technological institutes received full support from the Swiss National Science Foundation and the Research Council of Norway with funding in excess of €1M. The research councils of the two countries contributed, in equal parts, to the Raman project at SNBL with a total sum of €960'000.

SNBL admits on the short-, middle- or long-term basis (from few weeks to one year) PhD students, PostDocs, and researchers granted by the Research Council of Norway. Visiting scientists from University of Oslo, Technical University of Trondheim and Institute of Energy Technology (IFE, Kjeller) already worked at SNBL. We expect new collaborators and trainees from UiO, IFE, and NTNU in 2014.

B. Links to SLS/PSI

Collaboration with Swiss Light Source (SLS/PSI) is developing in a very constructive and stable manner. The SNBL staff members share their expertise in X-ray optics and combined measurement techniques (Raman+XRD+EXAFS) with colleagues from SLS. SNBL director, Dr. V.Dmitriev, is a member of the Proposal Review Committee at SLS for several years.

It is well recognised by the Swiss users community that SNBL is complimentary to SLS facility since it can cover the hard X-ray range of the synchrotron spectrum. In order to give a full picture of accessible facilities to our users, SNBL regularly presents reports on its status at SLS User Meetings in Villigen – a practice requested by the SLS management since 2005.

C. SNBL and MAXLAB

Until recently, there were no direct links between these two facilities which are oriented in part towards the Norwegian synchrotron community. The

reason lies mainly in the significantly different energy ranges in which SNBL and MAXLAB operate. While the former uses a bending magnet source of the ESRF optimised for hard X-rays, the latter is an excellent facility for studies with low energy synchrotron radiation. The corresponding user groups usually belong to different research fields, and their interests rarely overlap. The new MAX-IV project envisages the extension of the energy range available to the MAXLAB users towards higher energies. Therefore a Memorandum of Understanding has been established between MAXLAB and SNBL. The contacts with MAXLAB have already been useful in terms of comparing the performance of instrumentation at the two sites, and have included visits by beamline staff to SNBL and MAXLAB. We have also been able to provide some input for the design studies related to the planned beamlines for MAX-IV, and we have participated in the scientific and technical evaluation of these projects as members of the MAX-IV beamline review panels.

D. On-site collaborations

SNBL has a privilege being installed at the ESRF, in an exceptional environment of modern synchrotron beam lines operated by experienced instrument scientists. Regular contacts with ESRF and other CRGs staff members are realised in several forms.

SNBL has a well-established collaboration with the Dutch-Belgium CRG (DUBBLE). This collaboration has been formalized since November 2005 with a Memorandum of Understanding (MoU) which regulates the cooperation between the two facilities. The agreement provides beamtime access to both facilities for user groups from Norway, Switzerland, Belgium and the Netherlands. In addition, the MoU foresees the exchange of equipment and personnel between the two CRGs, and provides access to in-house research time on both beamlines. In practice, it means an enlargement of the instrumentation toolbox for the Swiss and Norwegian synchrotron user communities. The agreement provides a route for access to the SAXS technique as well as an XAFS set-up which is optimised in a different energy range than at SNBL. This agreement allows SNBL to economise resources and concentrate these resources more effectively on a limited number of topics.

Numerous other collaborations exist, such as a very fruitful scientific collaboration with a ESRF beam line ID-28 (BL responsible Dr. M.Krisch, BL scientist Dr. A.Bosak) specialised in inelastic X-ray scattering. The combination of X-ray diffraction under extreme conditions, or diffuse scattering method presented at SNBL, with the state-of-the-art inelastic scattering technique developed at ID-28, proved to be very efficient and informative.

V. SCIENTIFIC HIGHLIGHTS

V.1 Users contributions

V.1.1 User contributions highlighted by the ESRF

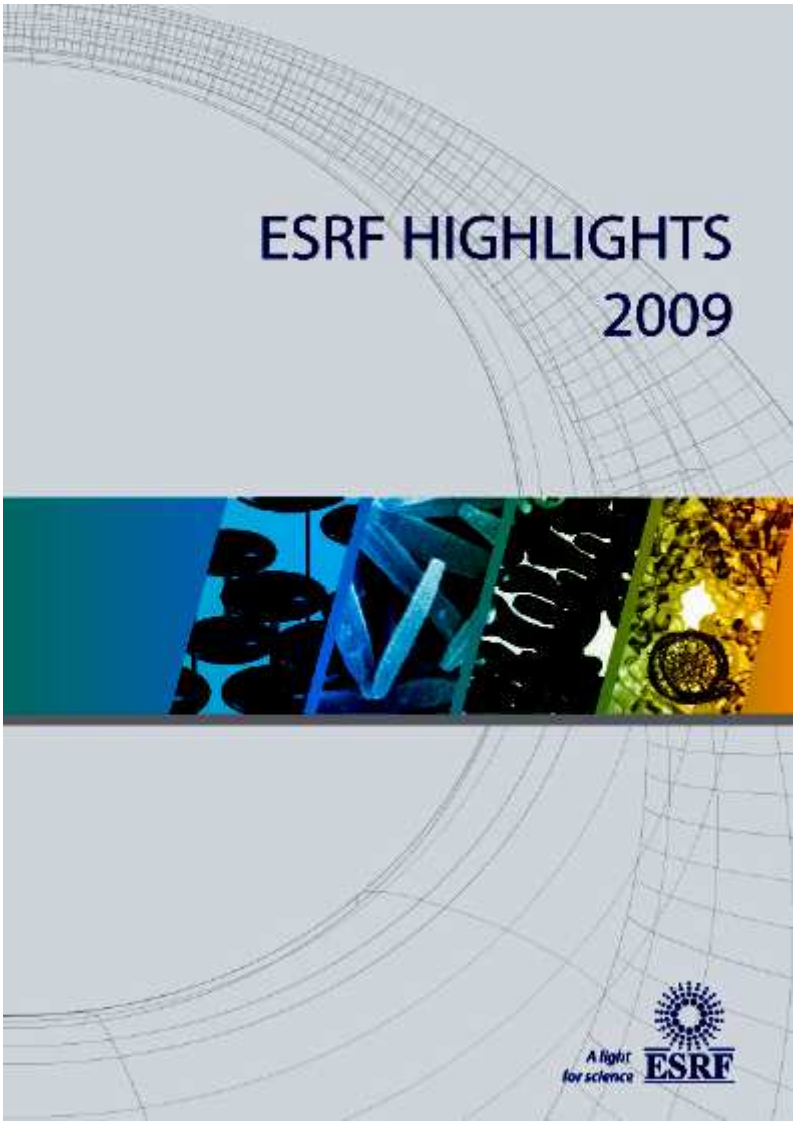

Structure and properties of single crystals of high-pressure boron

Boron is an unusual element. Its three valence electrons are too localised to make it metallic but insufficient in number to form a simple covalent structure. As a compromise, boron atoms form quasimolecular B_{12} icosahedra that become building blocks of boron and boron-rich crystalline phases. Only α-rhombohedral and β-rhombohedral boron, obtained at ambient pressure, are established as pure boron crystalline forms. The high-pressure behaviour of boron is of considerable interest in physics and materials science. Our investigations of superconducting polycrystalline boron-doped diamonds [1] revealed boron segregation in an intergranular space that may influence the mechanism of superconductivity.

Many of the fundamental questions regarding the solid-state chemistry of boron are still unanswered. Synthesis of single-phase products in macroscopic quantities and in the form of single crystals remains one of the great challenges of boron chemistry [2]. Using a large volume press, at 20 GPa and 1700 K, we have grown single crystals of a high-pressure high-temperature orthorhombic B_{28} boron phase for the first time. The crystals appeared to have a dark-red colour and an elongated prismatic shape (Figure 59). We confirmed the purity of the crystals by chemical analysis, collected single-crystal X-ray diffraction data (BM01), then solved and refined the crystal structure. There is remarkable

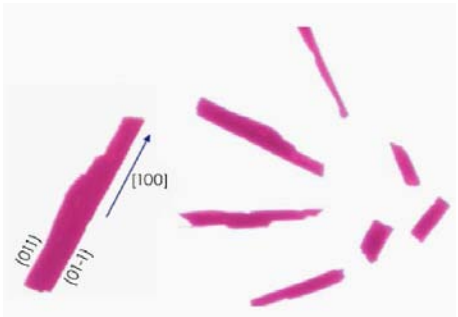

Fig. 59: Single crystals of the orthorhombic high-pressure boron phase.

Principal publication and authors
E.Yu. Zarechnaya (a), L. Dubrovinsky (a), N. Dubrovinskaia (b,c), Y. Filinchuk (d), D. Chernyshov (d), V. Dmitriev (d), N. Miyajima (a), A. El Goresy (a), H.F. Braun (e), S. Van Smaalen (c), I. Kantor (f), A. Kantor (f), V. Prakapenka (f), M. Hanfland (d), A.S. Mikhaylushkin (g), I.A. Abrikosov (g) and S.I. Simak (g), *Phys. Rev. Lett.* **102**, 185501 (2009).
(a) Bayerisches Geoinstitut, University of Bayreuth (Germany)
(b) Institut für Geowissenschaften, University of Heidelberg (Germany)
(c) Lehrstuhl für Kristallographie, Physikalisches Institut, University of Bayreuth (Germany)
(d) ESRF
(e) Experimentalphysik V, Physikalisches Institut, University of Bayreuth (Germany)
(f) GeoSoilEnviroCARS, University of Chicago (USA)
(g) Department of Physics, Chemistry and Biology, Linköping University (Sweden)

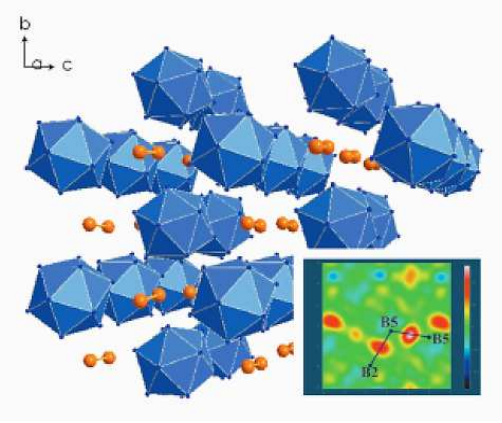

Fig. 60: The structure of the HPHT boron phase shown in the *bc* projection. The insert shows difference electron density plots around the atoms B5 (dumbbell, upper right) and B2 and B5 (dumbbell-icosahedron contact) extracted from single-crystal X-ray diffraction data. The maximum electron density is centred on the middle of the bond, suggesting covalent bonding between the B_2 dumbbell and the B_{12} icosahedron.

agreement between structural parameters obtained from single crystal and powder X-ray diffraction data [3] and those from our *ab initio* calculations. The *bc* projection (**Figure 60**) shows that the structure is built of B_{12} icosahedra and B_2 dumbbells linked together, thus forming a three-dimensional network. The distances B-B within a B_{12} icosahedron (1.766(3)-1.880(3) Å) are slightly longer than those within a dumbbell (1.721(4) Å). Chemical bonds within B_2 dumbbells and B_{12} icosahedra, as well as between icosahedra and dumbbells, are strongly covalent, as evident from the presence of residual electron density in the difference Fourier maps.

The high density and strong covalent bonding in this B_{28} phase suggest that it could be less compressible than the other known boron phases. This was confirmed in the compression experiment (**ID09**) up to ~30 GPa in a diamond anvil cell with Ne as a pressure transmitting medium and a powder of B_{28} that gave values for the bulk modulus of $K_{300} = 227(2)$ GPa and its pressure derivative $K' = 2.2(2)$. Pure orthorhombic B_{28} is a poor electrical conductor with a resistivity of the order of 10^6 Ω cm at ambient conditions. With increasing temperature, the resistivity decreases indicating semiconducting behaviour. The activation energy (1.9(2) eV) is in reasonable agreement with the value of the band-gap energy (2.1 eV) determined from optical spectroscopy measurements.

Boron is known as a hard material (with the Vickers hardness reported as high as 25-30 GPa for β-boron). We found that samples of B_{28} with submicrometre grain sizes have a hardness of 58(5) GPa. This value is in the range of polycrystalline cBN which makes B_{28} the second (after diamond) elemental superhard material.

In summary, our study demonstrates that the orthorhombic high-pressure high-temperature boron phase, synthesised above 9 GPa, has a structure consisting of covalently bonded B_{12} icosahedra and B_2 dumbbells, and combines unusual properties – it is a wide band gap semiconductor that is superhard, optically transparent, and thermally stable (above 1000 K in air). We have demonstrated the possibility to grow single crystals of this phase, which opens prospects for applications of this material in areas of electronics and optics.

References

[1] N. Dubrovinskaia, R. Wirth, J. Wosnitza, T. Papageorgiou, H.F. Braun, N. Miyajima and L. Dubrovinsky, *Proc. Natl. Acad. Sci. USA* **105**, 11619 (2008).

[2] B. Albert and H. Hillebrecht, *Angew. Chem. Int. Ed.* **48**, 2 (2009).

[3] E. Yu. Zarechnaya, L. Dubrovinsky, N. Dubrovinskaia, N. Miyajima, Y. Filinchuk, D. Chernyshov and V. Dmitriev, *Sci. Tech. Adv. Mater.* **9**, 044209 (2008).

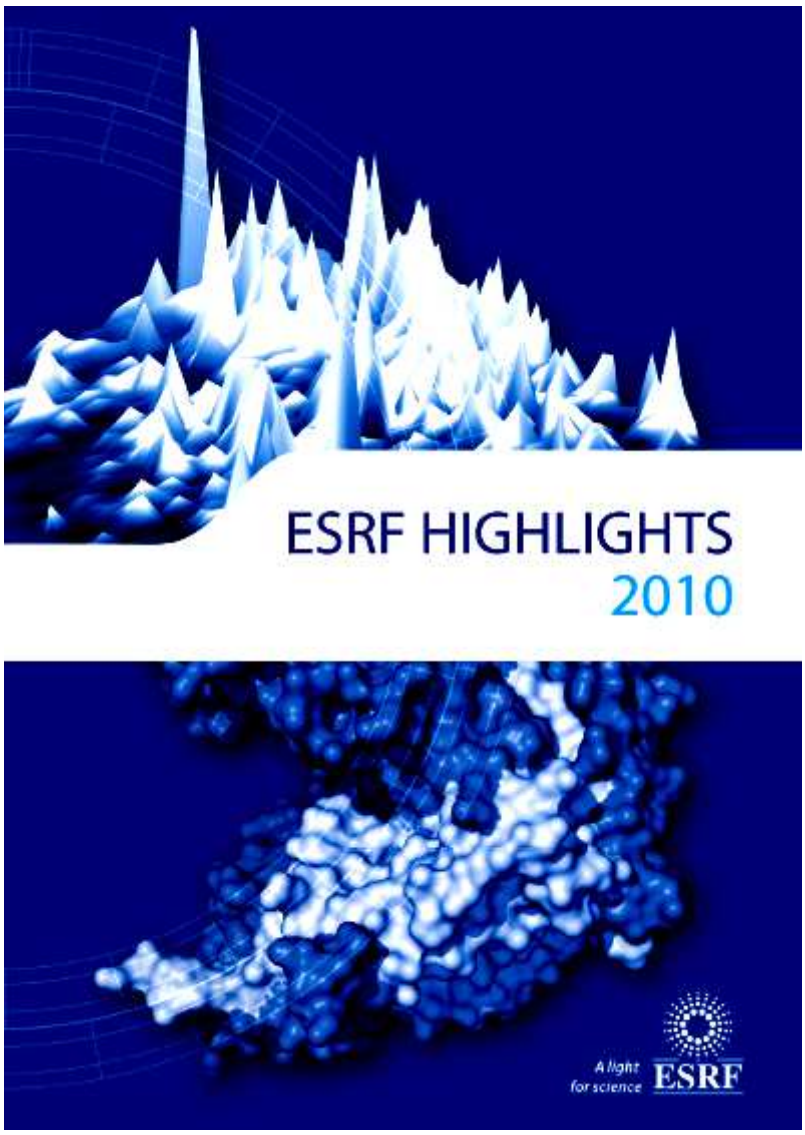
ESRF HIGHLIGHTS
2010
A light for science
ESRF

Principal publication and authors
Å.K. Røhr, H.-P. Hersleth and K.K. Andersson, *Angew. Chem. Int. Ed.* 49, 2324-2327 (2010).
Department of Molecular Biosciences, University of Oslo (Norway)

Consequences of using X-rays when studying redox cofactors

Flavin cofactors are involved in numerous biological processes including light sensing, oxygen activation, electron transfer, and DNA-repair. During these processes the flavin cofactor undergoes subtle conformational changes depending on its state. It is of great importance to understand the connection between flavin conformations and the nature of the chemistry performed.

In the literature, questions regarding flavin structure and function have been addressed many times using spectroscopic methods, theoretical calculations, and X-ray crystallography. The protein data bank (PDB) contains more than 1400 crystal structures containing either a flavin mononucleotide (FMN) or flavin adenine dinucleotide (FAD) cofactor. The redox and protonation states of these cofactors are usually assumed to reflect the situation in the protein crystal prior to X-ray data collection. This is a problematic assumption since redox cofactors are susceptible to react with photoelectrons generated in the crystal by X-rays during data collection. The large distribution of the so-called flavin butterfly bending angle, which is an indicator of flavin red-ox and protonation state, in the PDB-deposited flavoproteins indicate a large diversity of flavin states among these structures [1].

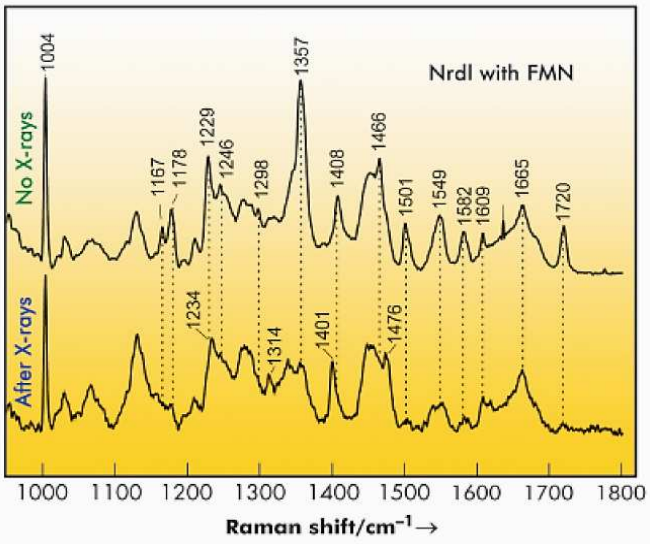

Fig. 116: Single-crystal *in situ* Raman spectra recorded for the flavoprotein NrdI before and after X-ray data collection.

We have solved crystal structures of the flavodoxin-like protein NrdI to 1.12 and 1.15 Å resolution at beamline **BM01** using crystals containing the yellow, oxidised FMN ($NrdI_{ox}$) and the blue, neutral semiquinone FMNH• cofactor ($NrdI_{sq}$), respectively. Before and after X-ray data collection, Raman spectra were collected *in situ* from both crystals. For both crystals, Raman bands confirmed the initial redox states. However, as shown in Figure 116, dramatic changes in the Raman spectra recorded before and after X-ray data

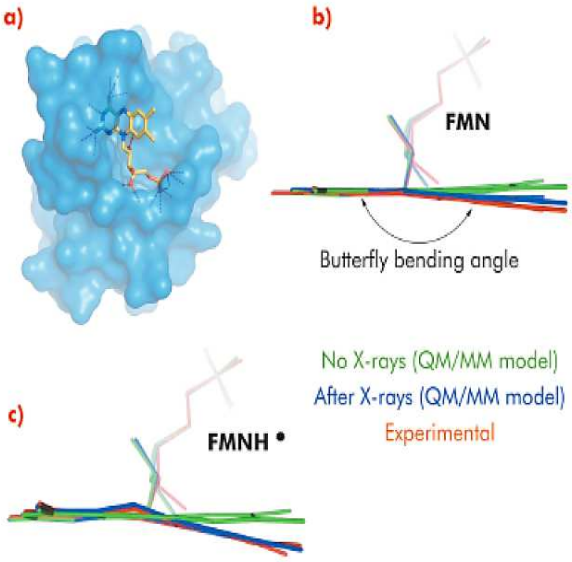

Fig. 117: a) Stick representation of the flavin cofactor bound in a surface pocket of NrdI, b) QM/MM models of flavins in NrdI containing the oxidised FMN cofactor (green), the one-electron reduced ($FMN^{\bullet -}$) cofactor (blue), and the flavin conformation in the crystal structure of $NrdI_{ox}$ (red), c) QM/MM models of flavins in NrdI containing the neutral semiquinone ($FMNH^{\bullet}$) cofactor (green), the one-electron reduced ($FMNH^{-}$) cofactor (blue), and the flavin conformation in the crystal structure of $NrdI_{sq}$ (red). In both b) and c) the QM/MM models confirm a one electron reduction of the flavin during X-ray data collection.

collection were observed. When starting with $NrdI_{ox}$ all flavin Raman bands either shift in energy or disappear after X-ray data collection, indicating a change in the flavin state. For $NrdI_{sq}$ all Raman bands decrease in intensity upon X-ray exposure, indicating a one-electron reduction to the fully reduced anionic form $FMNH^{-}$. These observations coincide with the crystal structures in which the flavin in both models have a butterfly bend deviating from the planarity predicted for FMN and $FMNH^{\bullet}$ (Figure 117).

To shed light on our experimental observations, which indicate that the state of the flavin cofactor is influenced by exposure to X-rays, QM/MM models of possible flavin redox and protonation states were built and their geometry optimised. Of the different models containing FMN, $FMN^{\bullet -}$, $FMNH^{\bullet}$, $FMNH^{-}$, or $FMNH_2$, the one-electron reduced forms of the initial states in the crystals, $FMN^{\bullet -}$ and $FMNH^{-}$, corresponded to the experimentally determined ($NrdI_{ox}$) and ($NrdI_{sq}$) crystal structures respectively.

The combination of single-crystal *in situ* Raman crystallography with QM/MM calculations demonstrate the importance of monitoring active site cofactors during X-ray data collection in order to track and characterise eventual radiation damage, which, if unaccounted for, can result in erroneous interpretation of crystal structures [2-5].

References
[1] T. Senda, M. Senda, S. Kimura and T. Ishida, *Antioxid. Redox Signaling* 11, 1741-1766 (2009).
[2] H.-P. Hersleth, T. Uchida, Å.K. Røhr, T. Teschner, V. Shünemann, C.H. Görbitz, T. Kitagawa, A.X. Trautwein and K.K. Andersson, *J. Biol. Chem.* 278, 23372 – 23386 (2007).
[3] H.-P. Hersleth, Y.-W. Hsiao, U. Ryde, C.H. Görbitz and K.K. Andersson, *Biochem. J.* 412, 257–264 (2008).
[4] H.-P. Hersleth, Y.-W. Hsiao, U. Ryde, C.H. Görbitz and K.K. Andersson, *Chem. Biodiversity* 5, 2067-2089 (2008).
[5] H.-P. Hersleth and K.K. Andersson, *Biochem. Biophys. Acta* (2010) (in press doi:10.1016/j.bbapap.2010.07.019).

Flexible porous coordination polymers for selective adsorption

Among crystalline porous solids, metal organic frameworks (MOFs) deserve special interest. These hybrid solids, built up from inorganic subunits connected through polytopic ligands (such as poly-carboxylate and poly-pyrazolate) have the faculty to change their pore size reversibly upon external (temperature, pressure, light) or internal (entrapped guests) stimuli while remaining crystalline. This dynamic porosity leads to unusual sorption properties, which are attractive for applications in the area of fluid storage, capture or separation. One of the most archetypical examples of such a solid is MIL-53(M) (MIL stands for Materials Institute Lavoisier), a metal (M = Al, Cr, Fe) terephthalate built up from inorganic chains and linear ligands presenting one dimensional diamond-shaped micropores. In the last few years, a multi-technique approach has been developed to study the adsorption of important gases (H_2, CH_4, CO_2, alkanes, etc.) in these solids [1]. It could be of interest in industrial applications to obtain alcohol of very high purity. Therefore, the sorption of polar vapours (water, methanol and ethanol) in MIL-53(Cr) has been explored. Upon adsorption, the solid evolves from a large-pore form to a narrow-pore form (Figure 52), for which the pore volume depends on the nature of the guest. At higher alcohol pressure, the structure evolves once again to a large-pore form, whereas the narrow pore form is retained in the presence of water. The specific host-guest interactions associated with these adsorption processes were probed by microcalorimetry, X-ray structure investigation, IR and Raman spectroscopy, thermal analysis and molecular modelling. The *in situ* powder X-ray diffraction experiments were carried out at beamline **BM01A**. These studies revealed that the strength of the interaction depends on the nature of the adsorbed species (water < alcohols), and finally concludes that this solid is potentially interesting for the selective adsorption of alcohol from

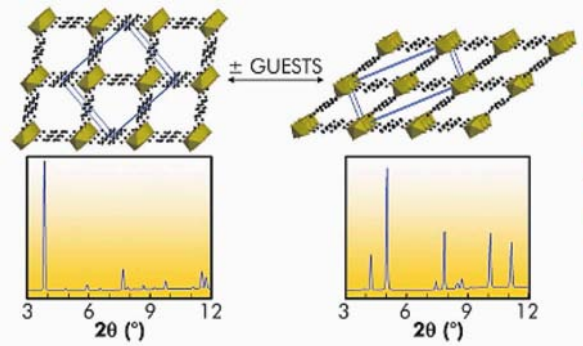

Fig. 52: The "breathing" behaviour of MIL-53 upon adsorption/desorption of guests, and the corresponding powder X-ray diffraction patterns which allow a direct evaluation of the pore size. Left: large-pore form; right: narrow-pore form.

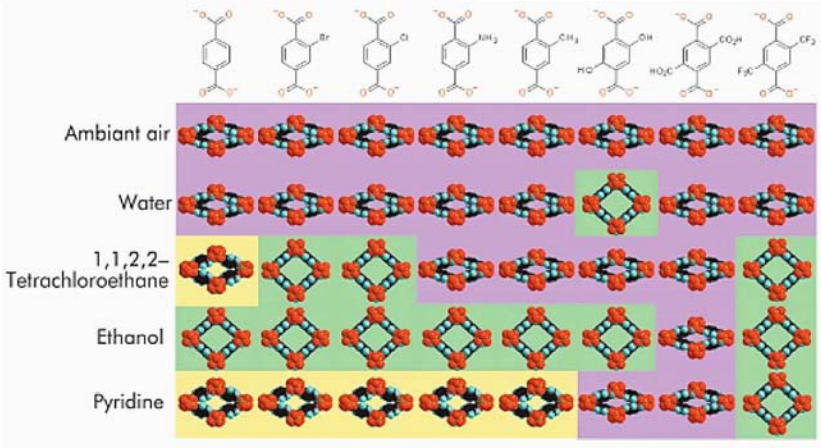

Fig. 53: Effect of the nature of the grafted organic group on the pore opening of functionalised MIL-53(Fe)s upon adsorption of various liquids. Pink: narrow-pore form; green: large-pore form; yellow: intermediate-pore form.

Principal publications and authors
S. Bourrelly (a), B. Moulin (b), A. Rivera (c), G. Maurin (c), S. Devautour-Vinot (c), C. Serre (d), T. Devic (d), P. Horcajada (d), A. Vimont (b), G. Clet (b), M. Daturi (b), J.-C. Lavalley (b), S. Loera-Serna (a), R. Denoyel (a), P.L. Llewellyn (a) and G. Férey (d), *J. Am. Chem. Soc.* 132, 9488-9498 (2010); T. Devic (d), P. Horcajada (d), C. Serre (d), F. Salles (c), G. Maurin (c), B. Moulin (b), D. Heurtaux (d), G. Clet (b), A. Vimont (b), J.-M. Grenèche (e), B. LeOuay (d), F. Moreau (d), E. Magnier (d), Y. Filinchuk (f), J. Marrot (d), J.-C. Lavalley (b), M. Daturi (b) and G. Férey (d), *J. Am. Chem. Soc.* 132, 1127-1136 (2010).
(a) Laboratoire Chimie Provence, CNRS, Université Aix-Marseille (France)
(b) Laboratoire Catalyse et Spectrochimie, CNRS, ENSICAEN, Université de Caen (France)
(c) Institut Gerhardt, CNRS, ENSCM, Université de Montpellier (France)
(d) Institut Lavoisier de Versailles, CNRS, Université de Versailles St-Quentin en Yvelines (France)
(e) Laboratoire de Physique de l'Etat Condensée, CNRS, Université du Maine (France)
(f) Swiss Norwegian Beamline,

Reference
[1] C. Serre, S. Bourrelly, A. Vimont, N.A. Ramsahye, G. Maurin, P.L. Llewellyn, M. Daturi, Y. Filinchuk, O. Leynaud, P. Barnes and G. Férey, *Adv. Mater.* 19, 2246-2251 (2007).

water/ethanol mixtures. Alternatively, the introduction of functional groups on the organic linker is an easy way to modify the pore surfaces, and thus to tune the sorption properties, affecting both the strength of the host-guest interactions and the pore opening. With this aim, various functionalised MIL-53(Fe) solids were prepared. While the hydrated form (under ambient air) of all these solids is associated with a narrow-pore form (see Figure 53), they present contrasting behaviours when immersed in liquids. Powder X-ray diffraction indeed reveals that the pore opening (and thus the number of adsorbed molecules), strongly depends on the nature of both the liquid and the grafted group (Figure 53). Besides the appearance of a large-pore form requires that the host-guest interactions (hydrogen bonding) overcome the intraframework interactions. Providing that this requirement is fulfilled, the adequacy of the chemical nature of both components (liquids-grafted groups) could lead to selective adsorption.

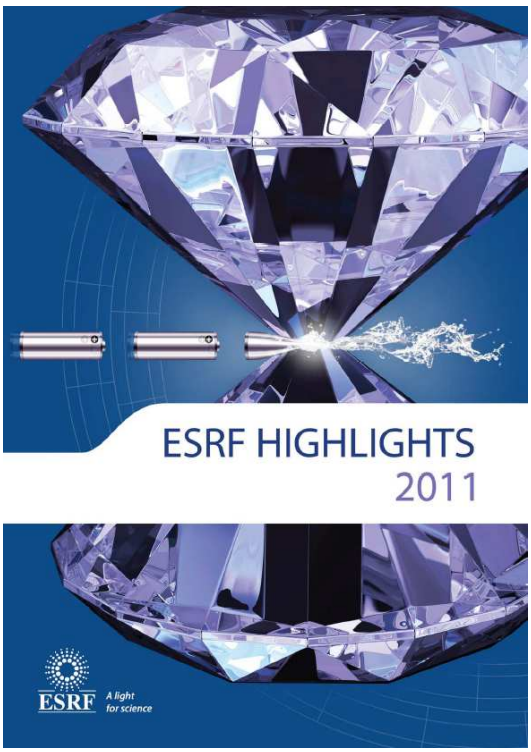
ESRF HIGHLIGHTS
2011
ESRF
A light for science

Molecular near-infrared to visible light upconversion

Principal publication and authors
L. Aboshyan-Sorgho (a), C. Besnard (b), P. Pattison (c,d), K.R. Kittilstved (e), A. Aebischer (f), J-C. G. Bünzli (f), A. Hauser (e) and C. Piguet (a), *Angew. Chem. Int. Ed.* **50,** 4108–4112 (2011).
(a) Department of Inorganic, Analytical and Applied Chemistry. University of Geneva (Switzerland)
(b) Laboratory of Crystallography, University of Geneva (Switzerland)
(c) Laboratory of Crystallography Ecole Polytechnique Fédérale de Lausanne (Switzerland)
(d) Swiss Norwegian Beamline (SNBL), ESRF
(e) Department of Physical Chemistry University of Geneva (Switzerland)
(f) Laboratory of Lanthanide Supramolecular Chemistry Ecole Polytechnique Fédérale de Lausanne (Switzerland)

Near-Infrared to visible photon up-conversion is a process in which photoexcitation at a certain wavelength in the near infrared is followed by luminescence at a shorter wavelength in the visible. In this process, low energy photons are "converted" to higher energy photons. This phenomenon could be of potential use in liquid solar cell applications in order take advantage of the infrared part of the solar spectrum or in biological imaging to design visible emitting bio-luminescent probes which are excited with infrared radiation. Using a longer excitation wavelength than in the visible range, infrared presents several advantages such as less phototoxicity and a deeper penetration depth into living tissues. Moreover, compared to classical fluorescence spectroscopy, up-conversion microscopy does not suffer from noise due to the auto-luminescence of the sample [1].

The minimum prerequisite for the generation of upconversion luminescence by a material is the existence of two metastable excited states, the first serving as an excitation reservoir, and the second as the emitting state. Different possible processes of up-conversion have been described [2], the two most common being excited-state absorption (ESA) and energy transfer upconvertion (ETU). ESA is a single ion mechanism which involves two sequential absorption processes. In the ETU process, at least two closely spaced ions are required. A sensitiser, which is excited to an intermediate excited state, transfers its energy to a neighbouring chromophore called acceptor, also in an intermediate excited state, promoting it to the upper emitting level (**Figure 95**). The existence of several excited states located between the ground state and the target excited state in lanthanide complexes makes them good candidates for such an upconversion mechanism, although it has long been thought that the vibrational oscillation of the organic ligands would quench this process for trivalent lanthanide ions [3]. However, with the development of the supramolecular chemistry of lanthanide complexes, using specially designed ligands, assemblies can be made where the geometry of the metal centre is controlled. This control enables chemists to synthesise assemblies with specific structural properties in order to tune the physical properties.

With a two-photon excitation model in mind, we therefore designed a molecular complex which can maximise the probability of the ETU process. It consists of the connection of two chromium(III) sensitisers around a central erbium(III) acceptor in a linear self-assembled cation (see **Figure 95**). This system presents several characteristics that can favour the ETU upconversion mechanism such as the high local concentrations of sensitisers, the choice of metals that gives a high efficiency for the Cr-Er energy transfer, and the wrapping of the helical ligand strands around the metal ion that protects them from the solvent.

The structure of such highly paramagnetic slow-relaxing complexes is difficult to assess without the use of X-ray diffraction. NMR and EPR techniques are difficult to

Fig. 95: The molecular triple-metallic complexes with the three metal atoms aligned and wrapped by three helical ligands. The simplified energy diagram shows the energy transfer between the two chromium atoms (sensitiser) and the erbium atom (acceptor) for the proposed ETU mechanism.

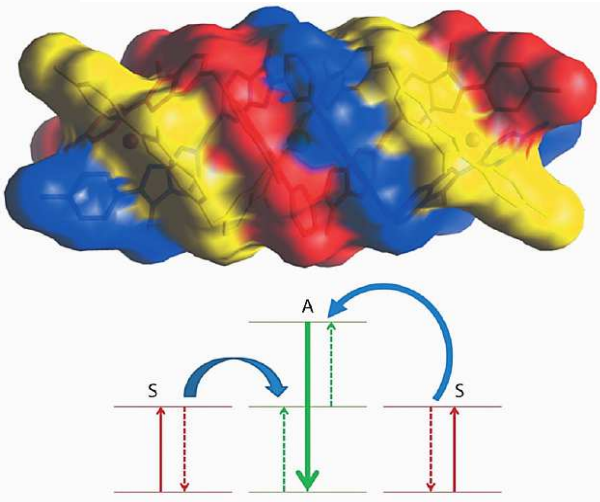

References
[1] D.H. Kim and J.U. Kang in *Microscopy: Science, Technology, Applications and Education* **1**, 571-582 (2010).
[2] F. Auzel, *Chem. Rev.* **104**, 139–173 (2004).
[3] C. Reinhard *and* H.U. Güdel, *Inorg. Chem.* **41**, 1048–1055 (2002).

use in these systems: NMR suffers from large line widths due to chromium(III) and EPR suffers from complications due to zero-field splitting, TIP effects and large line widths due to erbium(III). But as this compound crystallises with two complexes in the asymmetric unit, the unit-cell is large (volume 47200 Å^3). Moreover, disordered solvent molecules occupy channels inside the crystal, and the diffraction data from conventional sources in our laboratory were of poor quality. The higher quality of the data obtained from **BM01A**, the Swiss-Norwegian beamline, allowed us to unambiguously solve the structure and proved the organisation of the molecule.

The carefully chosen molecular design permitted green emission to be observed upon NIR irradiation of the sample, characteristic of the Er($^4S_{3/2}\rightarrow{}^4I_{15/2}$) transition. This first example of upconversion in an isolated molecular complex opens a new playground for synthetic chemists. New molecular designs connecting three Cr ions to the Er ion could for instance lead to unprecedented molecular three-photon upconversion luminescence.

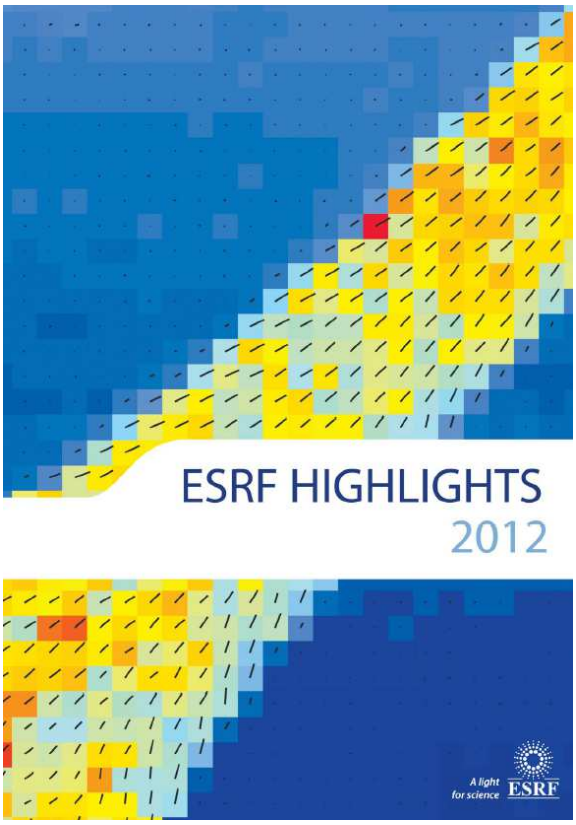

Microscopic and mesoscopic structure of functional perovskite ferroelectrics

Piezoelectric materials change their physical dimensions under application of an electric voltage and generate voltage under mechanical stress. Today they are widely used as sensors and actuators in various industries. In general, the most efficient piezoelectrics are mixed perovskites with composition close to the so-called morphotropic phase boundary (MPB). Near the MPB the ferroelectric phases of different symmetry have nearly the same energy and are separated by a rather small potential barrier. As a result, the different states can be easily switched by a small electrical or mechanical signal providing high electromechanical coupling. The exact structure and switching mechanisms are, however, challengingly complex and not yet understood. We combine diffuse and inelastic X-ray scattering experiments to reveal the character of structural heterogeneity in the most extensively used MPB piezoelectric – PZT.

Lead zirconate-titanate $PbZr_{1-x}Ti_xO_3$ (PZT) holds about 80% of the piezoelectric market. It is also a model system for studying the MPB phenomenon, which is observed for compositions when x is

Principal publications and authors
R.G. Burkovsky (a,b), Y.A. Bronwald (a), A.V. Filimonov (a), A.I. Rudskoy (a), D. Chernyshov (c), A. Bosak (b), J. Hlinka (d), X. Long (e), Z.-G. Ye (e) and S. Vakhrushev (f,a), *Phys. Rev. Lett.* **109**, 097603 (2012).
(a) St. Petersburg State Polytechnical University (Russia)
(b) ESRF
(c) SNBL at ESRF (France)
(d) Institute of Physics, Academy of Sciences of the Czech Republic, Prague (Czech Republic)
(e) Department of Chemistry and 4D LABS, Simon Frazer University, Burnaby (Canada)
(f) Ioffe Physical-Technical Institute, St. Petersburg (Russia)

around 0.48. Many diffraction studies have been devoted to understanding the structure of PZT near the MPB, but despite these efforts, the results and their interpretation remain controversial [1]. This is mainly due to the fact that diffraction studies reveal in almost all cases a structure, which is more complex than the single phase long-range ferroelectric order. The real microscopic structure can be studied effectively by analysing the scattering outside Bragg peaks by diffuse and inelastic scattering methods. We used these methods at beamlines **BM01A** and **ID28**, respectively. PZT single crystals of sufficient size and quality were grown at the Simon Frazer University (Canada).

Our diffraction measurements reveal the appearance of strong anisotropic diffuse scattering around Bragg spots (**Figure 47 a,c**) at temperatures just below the transition between two different ferroelectric phases (about T = 430 K). The observed scattering does not correspond to the polarisation fluctuations near the phase transition because it is absent on the high-temperature side of the ferroelectric-ferroelectric transition and also near the ferroelectric-paraelectric transition (about T = 663 K). Consequently, we have to assume another mechanism, which takes into account some structural inhomogeneity.

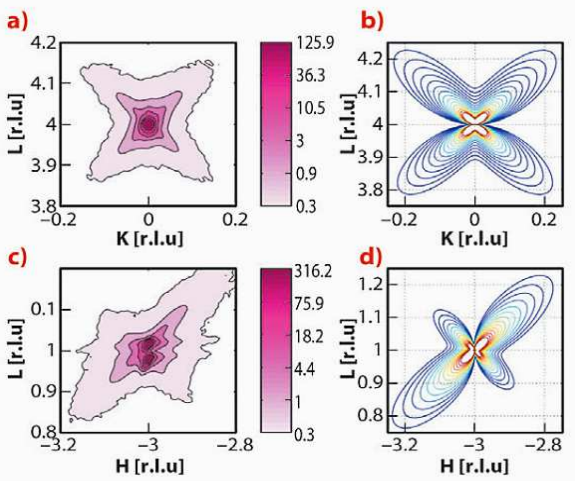

Fig. 47: Experimental diffuse scattering maps (a,c) and corresponding calculations (b,d).

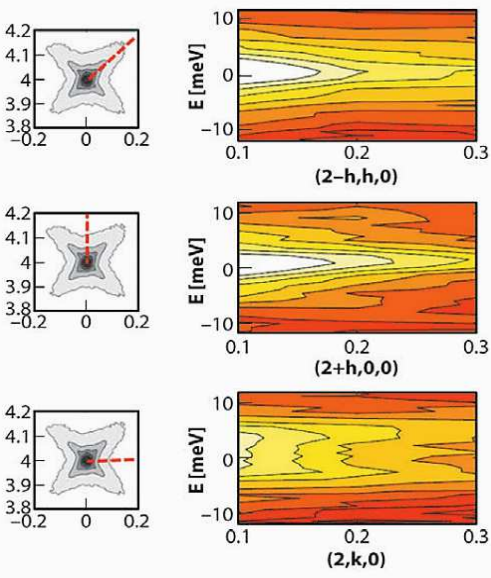

Fig. 48: Inelastic X-ray scattering maps along the three key directions of the (0 0 2) Brillouin zone.

To further understand the origin of diffuse scattering we used inelastic X-ray scattering (IXS). This technique allows static and dynamic components of diffuse scattering to be disentangled due to the meV energy analysis of the scattered photons. **Figure 48** schematically shows the IXS intensity maps along the inspected directions in reciprocal space. We observe strong quasielastic scattering (centred at zero energy-transfer) in diagonal and longitudinal directions, while in transverse directions the scattering is almost purely inelastic. Therefore, the observed diffuse scattering (**Figure 47a**) is a superposition of two contributions: one is due to phonons and the other one is due to static deviations from long-range order. The important feature of this second component is the absence of any intensity along the transverse direction. To reproduce this feature with models by considering the diffuse scattering as a Fourier image of real-space objects or 3D correlators was not possible. In contrast, it is consistent with Huang scattering – scattering due to inhomogeneous deformations of the lattice. More specifically, we note a very good agreement (**Figure 47 b,d**) with experimental data when the deformations are modelled as being due to tetragonal-symmetry point defects in a matrix that is nearly cubic. From the anisotropy of the diffuse scattering, it can be deduced that these defects produce very small volume strain due to the specific ratio between tensile strain along the main tetragonal direction and compressive strain along the two other directions. The emerging physical picture behind this model assumes that small clusters of the tetragonal phase remain in the matrix of the new average structure below the ferroelectric-ferroelectric phase transition temperature. In this model

we associate the diffuse scattering with the scattering by the matrix surrounding the clusters (not with the scattering by the clusters themselves, which are too small for direct observation) because the matrix is deformed on a larger, mesoscopic scale.

Last, but not least, the observed morphotropic PZT diffuse scattering appears at first sight to be very similar in shape to that of relaxor ferroelectrics **[2]** – a different and special class of disordered perovskites. However there are clear topological differences with respect to the relaxor case – in (0 0 L) Brillouin zones of PZT the transverse diffuse scattering component is suppressed, while for diffuse scattering in relaxors, the minimum of intensity appears along the longitudinal direction. This forms a solid basis for the assumption that the origin of diffuse scattering in these two classes of materials is also different. We believe that the present work on PZT will further stimulate the development of a common understanding of disorder phenomena in functional perovskite ferroelectrics.

References
[1] J. Kreisel, B. Noheda and B. Dkhil, *Phase Transitions* **82**, 633 (2009).
[2] A. Bosak, D. Chernyshov, S. Vakhrushev and M. Krisch, *Acta Crystallographica* **A68**, 117 (2012).

Design of zeolite by inverse sigma transformation: Cut and paste zeolites

Principal publication and authors
E. Verheyen (a), L. Joos (b), K. Van Havenbergh (c), E. Breynaert (a), N. Kasian (a,d), E. Gobechiya (a), K. Houthoofd (a), C. Martineau (e), M. Hinterstein (f), F. Taulelle (e), V. Van Speybroeck (b), M. Waroquier (b), S. Bals (c), G. Van Tendeloo (c), C.E.A. Kirschhock (a) and J.A. Martens (a), *Nat. Mater.* **11**, 1059–1064 (2012).
(a) Center for Surface Chemistry and Catalysis, KU Leuven (Belgium)
(b) Center for Molecular Modeling, Ghent University (Belgium)
(c) Electron Microscopy for Materials Science, University of Antwerp (Belgium)
(d) L.V. Pisarzhevsky Institute of Physical Chemistry, National Academy of Sciences of Ukraine, Kyiv (Ukraine)
(e) Tectospin, Institut Lavoisier, UMR 8180 Université de Versailles (France)
(f) Institut für Werkstoffwissenschaft, Technische Universität Dresden (Germany)

Zeolites are crystalline microporous aluminosilicates which consist of corner-sharing TO_4 tetrahedra. They are workhorses in industry for adsorption, separation and catalysis. Heteroelements are often inserted to enhance desired properties such as catalytic activity and selectivity. The introduction of germanium however results in stability problems.

Germanosilicate IM-12 zeolite (UTL topology) consists of dense silicate layers connected by double-four rings (D4Rs), the preferential location of germanium (**Figure 138**). The systematic instability of the UTL zeolite can be used to harvest building units that can be rearranged to transform UTL zeolite into a new and stable zeolite. Acid leaching removes the germanium from the UTL framework while preserving the dense silicate layers and reconnects these layers to form new zeolite topologies –COK-14 or COK-14. –COK-14 is a new all-silica interrupted framework topology with a two-dimensional channel system and interconnecting 8-, 10- and 12-membered rings (**Figure 138**). Upon drying in the absence of water, silanol condensation takes place and COK-14 is formed (**Figure 138**). The transformation from UTL zeolite to COK-14 involves the systematic removal of one layer of T-atoms and as such is the first experimentally observed inverse sigma transformation.

To verify if a true inverse sigma transformation occurred, an intermediate state was captured named Ge-COK-14. This sample was synthesised by reducing transformation time. ^{29}Si-NMR and ^{1}H-NMR indicated this sample contained Q^3 silicon environments, associated with silanol groups, while still having Si-O-Ge bonds. Approximately 50 wt% of the original germanium content was still present in Ge-COK-14. High-resolution powder X-ray diffraction data and X-ray absorption spectra for Ge-COK-were collected at room temperature at beamline BM01B (the Swiss Norwegian Beamline SNBL) in collaboration with beamline BM26 (DUBBLE) (**Figure 139**). Indexing of the powder pattern of Ge-COK-14 resulted in a unit cell of a = 24.43 Å, b = 13.90 Å, c = 12.28 Å and a monoclinic angle of 108.97° compared to a = 24.64 Å, b = 13.92 Å, c = 12.26 Å and β = 109.20° for –COK-14 and a = 29.00 Å, b = 13.98 Å, c = 12.45 Å and β = 104.91° for the parent UTL zeolite. This indicated that Ge-COK-14 already had the interlayer spacing of –COK-14 but still contained germanium. Ge K-edge EXAFS spectra revealed the local environment

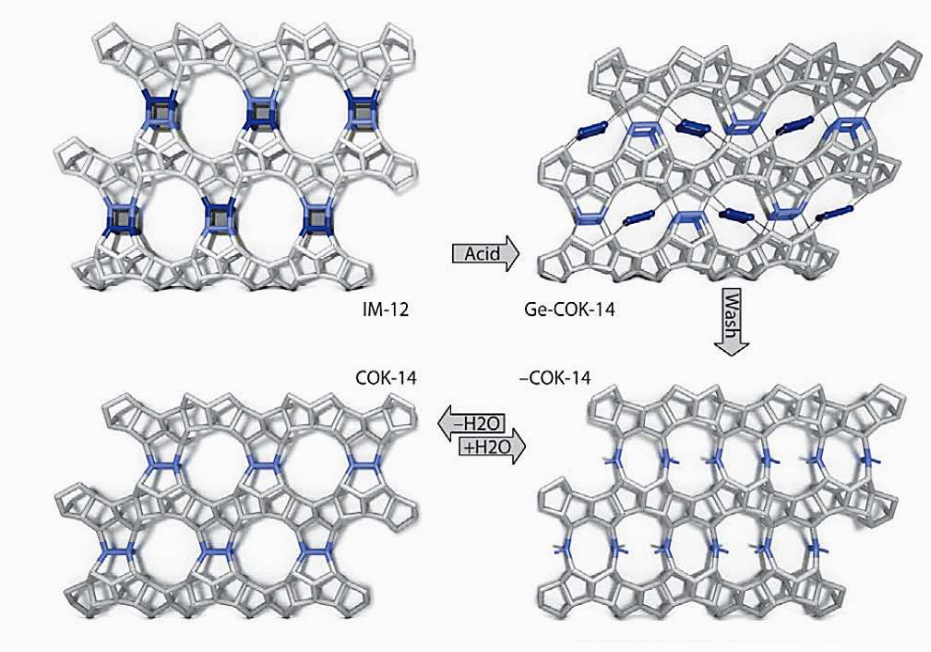

Fig. 138: Acid leaching of IM-12 zeolite can dislodge the germanate four-ring (dark blue) and shift it into the channels of the contracted framework of Ge-COK-14. Further acid leaching fully eliminates the germanate four-ring resulting in the interrupted (-COK-14) or fully condensed framework (COK-14) depending on the conditions.

and coordination of Ge in Ge-COK-14 (**Figure 139**). Each Ge atom had two Ge neighbours at 3.2 Å. A combination of HRXRD and Ge-K-edge EXAFS measurements allowed the structure of Ge-COK-14 to be unravelled (**Figure 138**, **Figure 139**). In this sample, germanium was present as a germanate four-ring in the position that would later become the 12-membered ring of COK-14. Ge-K-edge EXAFS measurements of the parent UTL zeolite revealed this germanate four-ring was already present (**Figure 138**).

Acid leaching removes the germanate four-ring from the UTL zeolite and shifts it into the channels of Ge-COK-14. Prolonging the transformation and washing leads to full elimination of germanium and results in the new zeolite frameworks –COK-14 and COK-14 (**Figure 138**). The COK-14 zeolite family is a valuable addition to the all-silica large-pore zeolite types. More new zeolites with attractive pore architectures may be obtained by this inverse sigma transformation approach.

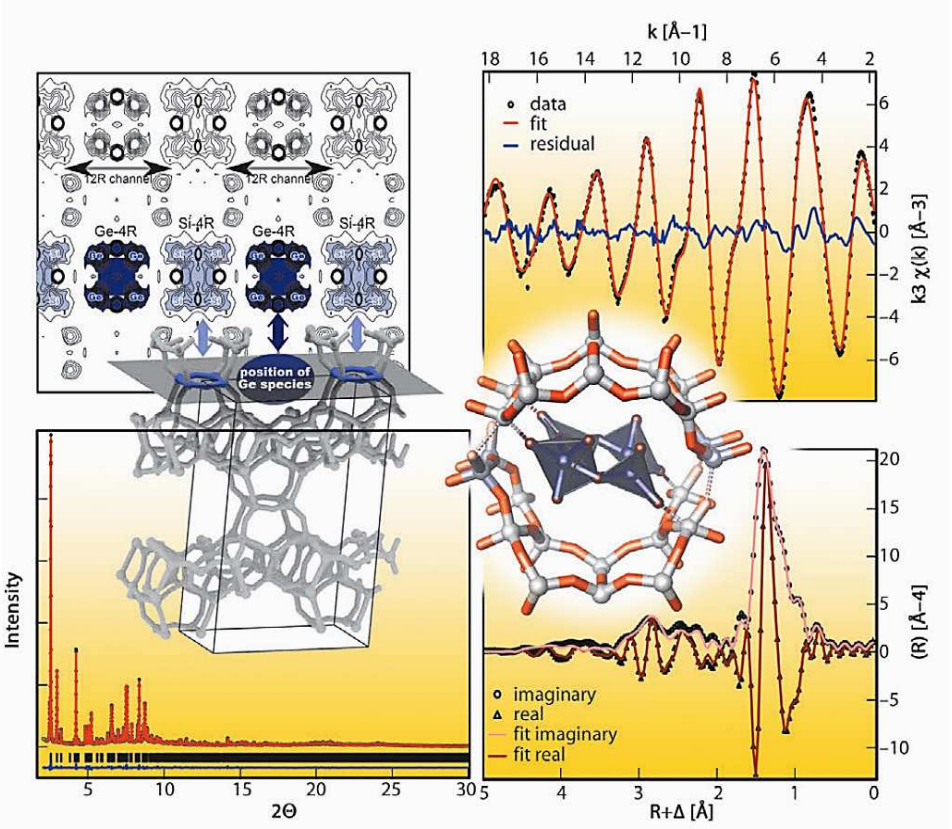

Fig. 139: Rietveld refinement (bottom left), observed electron density (upper left) and fitted EXAFS data (right) of Ge-COK-14. EXAFS analysis was based on the inserted fragment from Rietveld refinement. Inset on the left indicates the shown plane of observed electron density.

V.1.2 Recent User contributions

Ionothermal Synthesis and Structure Analysis of an Open-Framework Zirconium Phosphate with a High CO_2/CH_4 Adsorption Ratio

Lei Liu[(a)], Jiangfeng Yang[(a)], Jinping Li[(a)], Jinxiang Dong[(a)], Dubravka Sisak[(b)], Marisa Luzzatto[(b)], and Lynne McCusker[(b)]

(a) Research Institute of Special Chemicals, Taiyuan University of Technology, Taiyuan, Shanxi (P.R. China)
(b) Laboratorium für Kristallographie, ETH Zürich, Zürich (Switzerland)

Zirconium phosphate materials have been investigated extensively because of their potential for application in the fields of ion-exchange, catalysis, photochemistry, and biotechnology. Most studies of these materials have focused on the two layer compounds α-$Zr(HPO_4)_2 \cdot H_2O$ and γ-$ZrPO_4$-$(H_2PO_4) \cdot 2H_2O$ and their derivatives, which are obtained by post-synthesis processing techniques (for example ionexchange, intercalation, or grafting). The main reason most other zirconium phosphate materials have been neglected can probably be attributed to their poor thermostability.They have generally been synthesized using organic amines as structure-directing agents in a hydro-/solvothermal procedure. Of these templated zirconium phosphate materials, those with framework (rather than layer) structures tend to have a higher thermostability, but they are difficult to synthesize using this conventional synthetic approach. In fact, only two open-framework structures have resulted from these efforts. Unfortunately, neither is stable to the removal of the occluded organic species by calcination, so they cannot be used as microporous materials for gas adsorption or separation, or for shape-selective catalysis.

Recently, our group reported the ionothermal synthesis of a zirconium phosphate using a deep-eutectic solvent (DES), which consisted of carboxylic acid and quaternary ammonium salts. The resulting framework structure was found to depend on the structure and steric effect of the quaternary ammonium cation. Herein, we combined ethylammonium chloride and oxalic acid to form a DES with a melting point below 100ºC, and then used it to synthesize a novel open-framework zirconium phosphate, $C_2H_7NH)_8(H_2O)_8][Zr_{32}P_{48}O_{176}F_8(OH)_{16}]$ (denoted hereafter as ZrPOF-EA). The crystal structure of ZrPOF-EA (Fig.1) was solved from high resolution powder diffraction data collected on the Swiss–Norwegian Beamline, BM01B, in the orthorhombic system (a=6.165Å, b=19.955Å, c=37.062Å) and reflection intensities were extracted assuming the space group P*mc*2_1. These data were used as input to the powder charge-flipping (pCF) algorithm in the program Superflip for structure solution. The best electron density map from the first pCF run was used as a seed to generate the starting phase sets for the second run, and the best of the resulting maps was interpreted to yield the positions of all 16 zirconium, 23 of the 24 phosphorus, and 55 of the 77 oxygen atoms. A series of difference electron density maps led to the location of the missing phosphorus atom, the terminal oxygen atoms, and the non-framework species. Atoms bridging between two zirconium atoms were assigned as fluorine. During the course of the refinement, it became apparent that most of the framework atoms followed the symmetry of the higher space group P*bam*, so refinement was completed in that space group even though it meant that

the terminal P-OH groups and the organic cations were disordered. This refinement, with 8 zirconium, 12 phosphorus, 40 oxygen, 2 fluorine, 2 water, and 3 ethyl ammonium ions in the asymmetric unit, converged with the R values R_F=0.038, and R_{wp}=0.170 (R_{exp}=0.171).

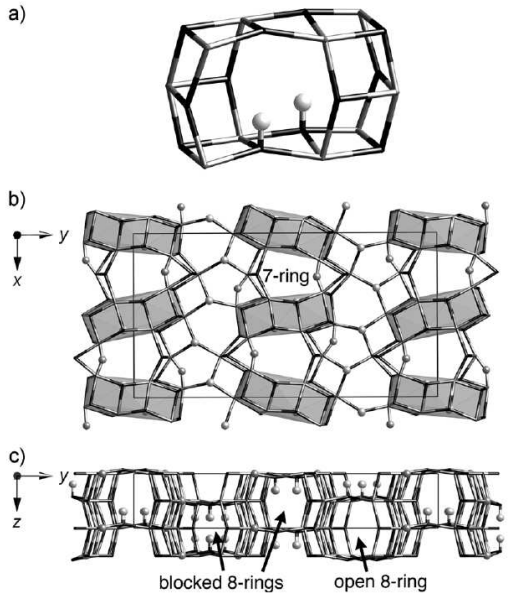

Figure 1. ZrPOF-EA framework structure showing a) the characteristic [$4^{14}8^2$] unit, b) the projection along the *c* axis with the [$4^{14}8^2$] units highlighted, and c) the projection along the *a* axis. Bridging O atoms have been omitted for clarity. Terminal O atoms and bridging F atoms are shown as balls, Zr gray, and P black.

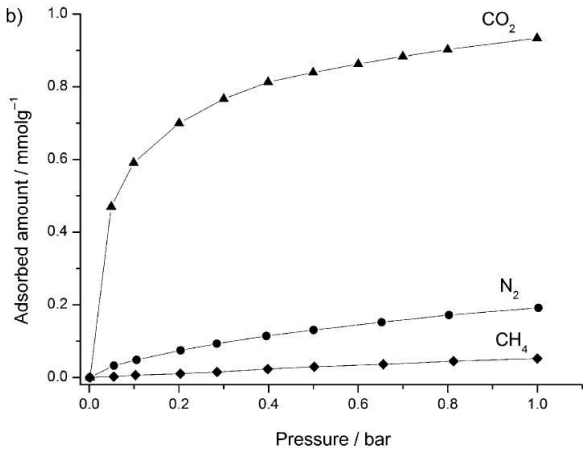

Figure 2. Adsorption isotherms of CO_2, N_2, and CH_4 for ZrPOF-EA at 25ºC, in the low-pressure range (0–1 bar).

In ZrPOF-EA, the oval 7- and 8-ring windows have dimensions of about 4.0 x 3.0 Å and 3.9 x 3.2 Å, respectively. To establish its adsorption properties, CO_2, N_2, and CH_4 adsorption experiments were carried out on an intelligent gravimetric analyzer (IGA-001, Hiden Isochema) at 25ºC. Before each adsorption experiment, the activated ZrPOF-EA was outgassed at 300ºC under vacuum for 10 h. From the adsorption isotherms shown in Fig.2, it is evident that the adsorption capacity for CO_2 is markedly higher than that for CH_4, with a CO_2/CH_4 adsorption ratio ranging from 67.2 at 0.2 bar to 17.3 at 1 bar. The selective adsorption of CO2 may be a result of the complicated pore structure and the polar hydroxy groups directed into the pore channels. The small 7- and 8-ring pore openings allow CO_2 molecules (3.3 Å kinetic diameter) to enter the channels, but block the larger CH_4 molecules (3.8 Å kinetic diameter). Furthermore, the low N_2 adsorption capacity indicates that even the intermediate-sized N_2 (3.6 Å kinetic diameter) has difficulty in entering the pores, leading to a CO_2/N_2 adsorption ratio ranging from 12.2 at 0.2 bar to 4.9 at 1 bar.

One of the applications of CO_2 separation technologies is in the upgrade of biogas to pure or more concentrated methane. Biogas, which is essentially a mixture of CO_2 (ca. 25–45%) and CH_4, is a very important source of renewable methane produced by the anaerobic digestion of waste materials. Although ZrPOF-EA has a relatively low adsorption capacity, its high CO_2/CH_4 adsorption ratio may find industrial application in membrane separation technology for upgrading such natural gas.

Principal publication

Lei Liu, Jiangfeng Yang, Jinping Li, Jinxiang Dong, Dubravka Sisak, Marisa Luzzatto, and LynneB. McCusker, *Angew. Chem. Int. Ed.* 2011, **50**, *8139 –8142.*

The influence of X-rays on different redox states of crystalline myoglobin.

Hans-Petter Hersleth and K. Kristoffer Andersson
Dept.of Biosciences, University of Oslo, PO Box 1066 Blindern, 0316 Oslo, Norway

X-ray induced radiation damage of protein crystals is well known to occur even at cryogenic temperatures, and redox active sites like metal and radical sites seem especially vulnerable for these radiation-induced reductions. It is essential to know correctly the oxidation state of metal-ion sites in protein crystal structures to be able to interpret the structure-function relation. To better understand how metalloproteins are influenced by X-rays during crystallographic data collection we have chosen to study different redox states generated in the reaction between myoglobin (Mb) and peroxides (coloured red in *Fig. 1*). These different states have characteristic light absorption spectra in the 450-700 nm, and can therefore be monitored by single-crystal online microspectrophotometry (*Fig. 1*). The radiation-influenced structures of these states have previously been determined at SNBL and ESRF (*Fig. 2*).

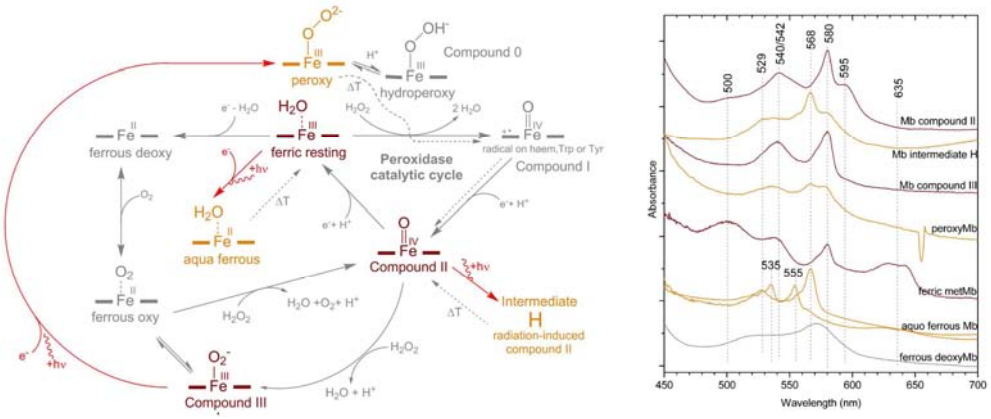

Figure 1: Reaction scheme showing the different Mb redox states with corresponding single-crystal light absorption spectra.

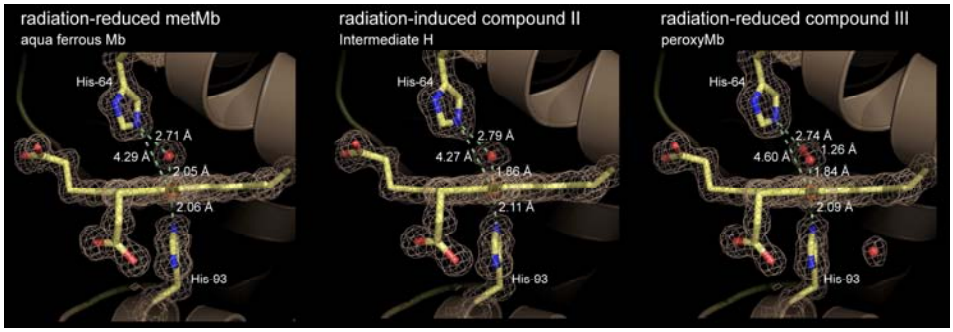

Figure 2: Structures of radiation-influenced states of Mb (PDB codes: 2V1I, 2V1E, 2VLX)

In this study, we have in detail investigated the impact that X-rays have on these different oxidation states of Mb, to understand how fast these states are influenced, and to determine how much X-rays you can use before the different states are too heavily influenced/reduced by X-rays. In order to investigate how the lifedoses vary among different oxidation states of metalloproteins we have systematically analysed the effect X-rays have on the ferric Fe^{III} metMb, compound II Fe^{IV}=O ferrylMb and Mb compound III Fe^{III}-O_2^- states with single-crystal spectroscopy.

Fast X-ray influence of the ferric metMb – determination of lifedose

The metMb state have characteristic light absorption peaks at 500, 540, 581 and 635 nm, while the radiation-reduced state have the most dominant peaks at 529 and 568 nm. *Fig 3* shows that the influence/reduction begins immediately; from the first X-ray photon that hits the crystal. The appearance of the 568 nm peak is clearly seen after an absorbed dose of only 0.0053 MGy (*Fig. 3*; middle).

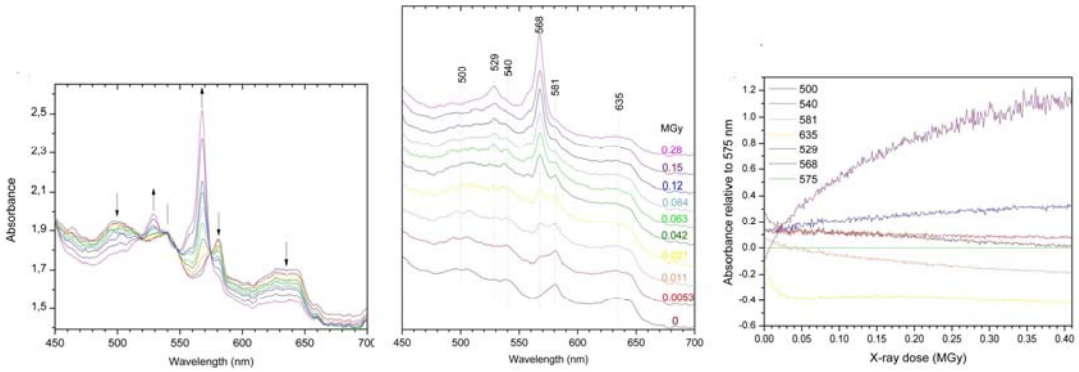

Figure 3: Single-crystal light absorption spectra of a ferric Fe^{III} metMb: (left) overlay of spectra at selected time/dose points, (middle) selected spectra at increasing time/dose points; (right) propagation of the different peaks of metMb and the radiation-induced state relative to the isosbestic point at 575 nm.

To determine a suitable lifedose, which can be used for composite data collection strategies, is not trivial. Remaining of ~90% of the initial state might be a suitable limit. However, the background is considerably increased by the solvated electrons during the first seconds of irradiation. This elevation reaches a maximum and then decays slowly. To remove the background effect, the absorbance of the different peaks have in *Fig. 3* (right) been retracted the absorbance of the isosbestic point at 575 nm. This result in a figure showing the increase and decrease of the different peaks with respect to X-ray exposure/absorbed X-ray dose (*Fig. 3*; right). The 568 and 529 nm peaks of the radiation-induced state increase, especially 568 nm, while the 500, 540, 581 and 635 of metMb decrease slowly. The lifedose has been taken to be the dose it takes for the original state to decay to 90%. To be able to calculate this value, we have taken the absorbance at 581 nm and retracted the absorbance at the closest isosbestic point at 575 nm to correct for the background. The decrease of this peak to 90% has been determined to be ~0.01 MGy (equals ~12 seconds of exposure at ID14-2 with 37.7% transmission).

The radiation-reduced ferric metMb state is believed to be an aquo or hydroxy ferrous state. An interesting observation is that an annealing of this state, seems to regenerate the original metMb state as observed with both light absorption and Raman spectroscopy. The single-crystal off-resonant Raman spectrum of ferric metMb is shown in *Fig. 4*, exhibiting the characteristic ferric haem modes (e.g. the $\square_4$ oxidation state marker at 1371 cm^{-1}). After X-ray irradiation corresponding to a dose of 1.4 MGy, the Raman signal is much weaker than for the resting state (*Fig. 4*). For this radiation-induced ferric metMb state most of the haem modes have diminished, moved and/or become more undefined. After a short annealing, several of the haem modes of the ferric metMb state reappear.

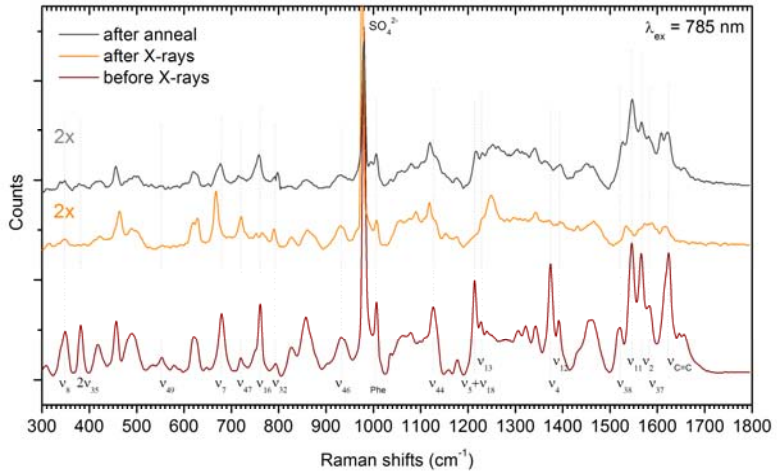

Figure 4: Single-crystal off-resonant Raman spectra of a ferric Fe^{III} metMb crystal: (dark red) before irradiation with X-rays, (orange) after irradiating with X-rays corresponding to an absorbed dose of ~1.4 MGy, and (grey) after annealing.

Influence on the different redox states of Mb – determination of lifedoses

The fast influence/reduction observed for metMb is also observed for the compound II Fe^{IV}=O ferrylMb and Mb compound III Fe^{III}-O_2^- (*Fig. 5*).

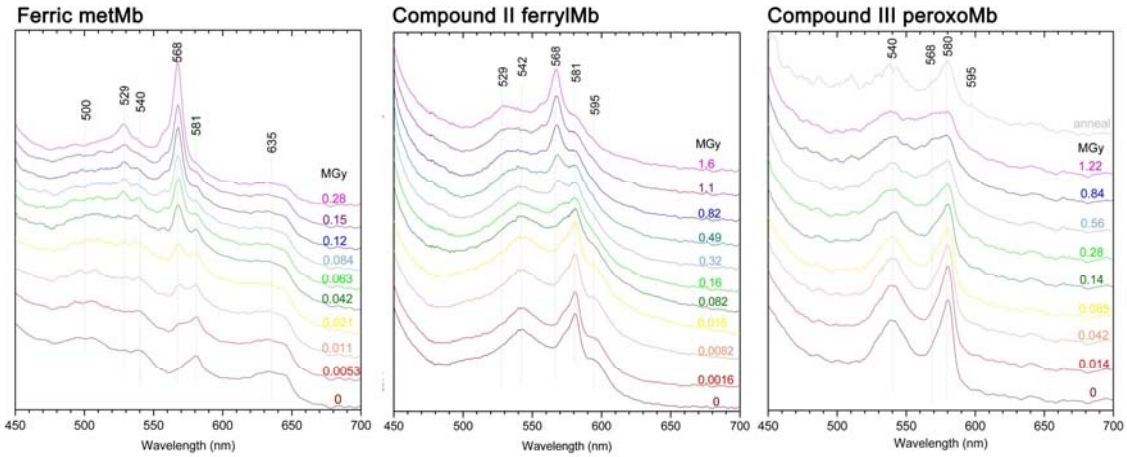

Figure 5: Selected single-crystal light absorption spectra of different redox states of Mb with increasing time/dose points: (left) ferric Fe^{III} metMb; (middle) compound II Fe^{IV}=O ferrylMb; (right) Mb compound III Fe^{III}-O_2^-.

The characteristic ferrylMb peaks at 542, 581 and 595 are slowly decreasing, while the peaks for the radiation-reduced state gradually appears at 529 and 568 nm with well defined isosbestic points at 528, 556 and 572 (*Fig. 5*; middle). A calculation of the lifedose in a similar way as for metMb gives doses of ~0.02-0.03 MGy (90% of 581 nm). The lifedose estimations therefore indicate the striking fact that the Compound II ferrylMb is not as easily reduced as the lower oxidation state of ferric metMb. A time/dose

monitoring with light absorption is therefore needed for each individual oxidation state. The fact that it is the same peaks that appears for both ferricMb and ferrylMb raise the question if it is a real and similar reduction to aquo ferrous of both states, or if it is some part of the haem moiety that is reduced similarly in the two states. However, the increase of the 568 nm differs between the ferric and ferryl states. The crystal structures of the radiation-reduced states of metMb and ferrylMb show also a different Fe-O distance, 2.05 and 1.84 Å, respectively, demonstrating that these radiation-induced states cannot be identical with respect to the iron (*Fig. 2*).

For Mb compound III Fe^{III}-O_2^- the characteristic compound III peaks at 540 and 580 nm decrease with increasing dose (*Fig. 5*; right). The 568 nm peak increase very slowly for this state, compared to the ferric and ferryl states. The estimation of the lifedose for this state results in quite similar values: ~0.02 MGy (90% of 580 nm) Table1,

Table 1

Redox state	**Lifedose***
Ferric Fe^{III} metMb	~ 0.01 MGy
Compound II $Fe^{IV}O$ ferrylMb	~ 0.02 MGy
Compound III Fe^{III}-O_2^- peroxoMb	~ 0.02 MGy

***** When 90% of the original state remains: Dose at which the 581 nm peak has fallen to 90% of the initial absorbance relative to the isosbestic point

Summary

All the three Mb states (ferric Fe^{III} metMb, compound II Fe^{IV}=O ferrylMb and Mb compound III Fe^{III}-O_2^-) are influenced / reduced by the X-rays used for structure determination. How fast these changes occur vary slightly between the different crystalline states. However, all these lifedoses are on a much shorter timescale than the lifedoses used for protein crystals in general. The lifedose / Hendersson limit for a "normal" protein crystal (without a redox site) is ~20 MGy. The lifedoses we have estimated here for obtaining the structure of unreduced Mb redox states are therefore about 1000 times less than the general Hendersson limit. In general, we would argue that monitoring of a spectroscopic property as a function of time / dose should always accompany the structure determination of a metalloprotein to confirm its correct oxidation state.

Publication:

Hersleth, H.-P. & Andersson, K.K. (2011) How different oxidation states of crystalline myoglobin are influenced by X-rays. *Bichim. Biophys. Acta, Proteins Proteomics*. **1814**, 785-796.

Fischer–Tropsch synthesis: An XAS/XRPD combined in situ study from catalyst activation to deactivation

Nikolaos E. Tsakoumis[a], Alexey Voronov[a], Magnus Rønning[a], Wouter van Beek[b], Øyvind Borg[c], Erling Rytter[a,c], Anders Holmen[a,*]

[a]*Department of Chemical Engineering, Norwegian University of Science and Technology (NTNU), Trondheim, Norway.*
[b]*The Swiss-Norwegian Beam Lines (SNBL) at ESRF, BP 220, F-38043 Grenoble, France.*
[c]*Statoil R&D, Research Centre, Postuttak, NO-7005 Trondheim, Norway.*

A Re promoted Co/γ-Al_2O_3 and an un-promoted Co/γ-Al_2O_3 Fischer–Tropsch catalysts were studied *in situ* throughout the common steps of laboratory catalyst testing i.e. reduction, pressurization, the initial period before reaching pseudo-steady state, deactivation and post mortem analysis. High-resolution X-ray powder diffraction (HR-XRPD) was combined with X-ray absorption spectroscopy (XAS) in order to reveal changes occurring during the experimental procedure. A mass spectrometer (MS) connected to the reactor outlet allow monitoring of the gas phase and accordingly the catalyst performance with respect to activity. Fischer–Tropsch synthesis was performed at industrially relevant conditions (493 K, 18 bar, H_2/CO=2.1 and >50% CO conversion).

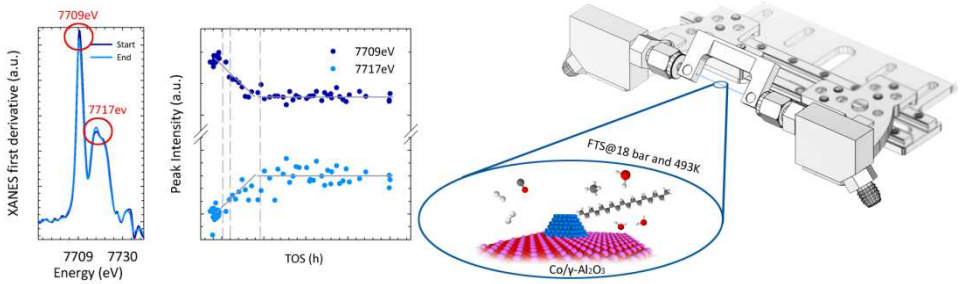

Motivation

Co-based catalysts appear more attractive for the conversion of natural gas derived synthesis gas to hydrocarbons, due to their high activity per pass, high selectivity to linear paraffin's, and low water–gas shift activity. However, because of the high price of the Co metal, catalyst stability has become a major issue to be addressed and a lot of effort has been devoted to deactivation studies from both industry and academia [1]. Ultimately, all supported FTS cobalt catalysts lose activity with time on stream. The main causes of catalyst deactivation as they are documented in the literature are poisoning, formation of inactive cobalt phases (re-oxidation, carbidization, and metal-support mixed compound formation), sintering, carbon formation, surface reconstruction, and attrition.

The investigation of the origin of catalyst deactivation in all catalytic applications is primarily a characterization-oriented subject, and commonly, the employed analytical procedures are applied *ex situ* on spent catalysts, *in situ* at moderate conditions or under vacuum on model systems [1–3]. *Ex situ* characterization of FTS cobalt catalysts requires a demanding sample handling since the results can be significantly affected by the pyrophoric nature of metallic Co existing in the spent catalyst. Furthermore, the procedure is hampered by catalyst encapsulation by long-chain hydrocarbons (FTS waxes). In addition, at reaction conditions the partial

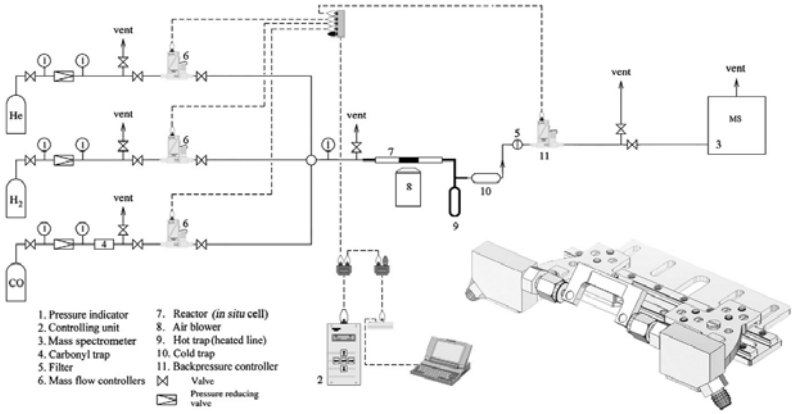

Figure 1. Sketch of the experimental setup and a 3D drawing of the *in situ* cell.

pressures of reactants and products dramatically affect catalyst behaviour. The impact of the gaseous FTS environment toward potential re-oxidation (high partial pressures of steam) or reconstruction during reaction makes the use of realistic FTS conditions vital. *In situ* and preferably *operando* studies of well-defined catalytic systems at realistic conditions have been employed by combining various complementary techniques in order to increase our understanding in the complicated Fischer–Tropsch synthesis reaction [1,2,4,5].

Catalyst activation

Data deriving from *in situ* XANES on the Co k edge (7709 eV) suggests that the reduction of calcined catalyst passes through a two-step procedure as previously reported[2]. The transition from Co_3O_4 via a CoO intermediate to metallic cobalt and a fraction of unreduced Co is illustrated by XANES (Fig. 2). A mixture of face centred cubic (*fcc)* Co and hexagonal close packed (*hcp)* Co on the reduced catalysts could be identified by XRPD. Full pattern decomposition by models of pure Co-*fcc* and Co-*hcp* crystallites was not viable indicating the intergrowth of the two phases and possible existence of staking faults or other grain boundaries[4].

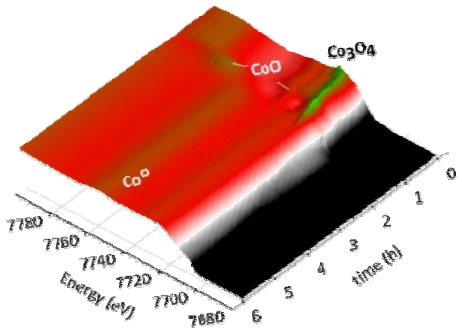

Figure 2. 3D representation of the species detected by Co-XANES during catalyst reduction at a ramp rate of 3°C/min to 400°C and dwell for 4 hours.

Quantitative results obtained by linear combination analysis of reference materials (cobalt oxides and foils) allowed evaluation of the reduction rates of Rhenium (Re) promoted Co-Re/γ-Al_2O_3 and un-promoted Co/γ-Al_2O_3 catalysts. It appears that Re addition accelerated only the second reduction step from CoO to metallic cobalt.

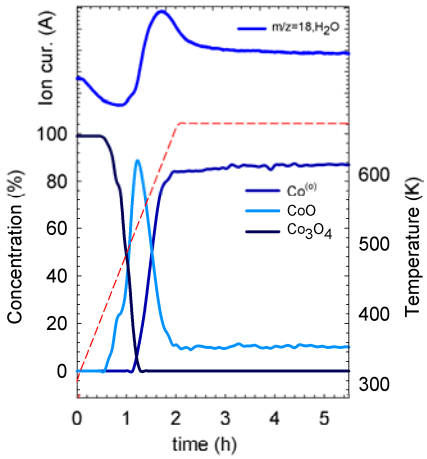

Figure 3. The formation of water as monitored by mass spectrometry together with the concentration of Co species during reduction.

Hydrocarbon synthesis

The reduced catalyst was subjected at realistic Fischer-Tropsch synthesis (FTS) environment for 40 hours. A quartz capillary reactor was used. Activity and deactivation behaviour shows good agreement with results obtained from a laboratory fixed-bed reactor (Fig. 4). Throughout the experiment a large number of X-ray scans were recorded showing very good repeatability and allowing detection of minor changes. Pressurization, induction period and steady-state/deactivation period were studied. Different observations in each of them are briefly discussed.

Already at the pressurization under synthesis gas environment it is expected that the cobalt surface reconstructs due to the invasive nature of CO. However, no change in the EXAFS signal was detected during that period. Here it should be mentioned that the surface to volume ratio of cobalt particles in the present study (0.085) may be insufficient for such information to be extracted.

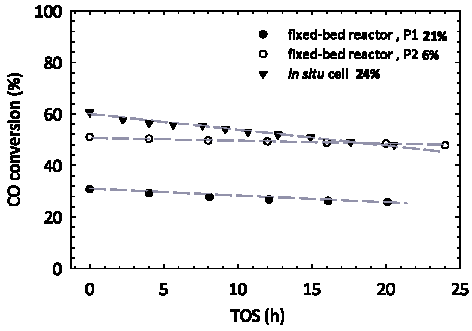

Figure 4. FTS activity profile from FBR and the in situ cell.

During the induction period XANES data suggest re-oxidation of the Re-promoted catalyst into a divalent cobalt (Co^{+2}) in the expense of metallic Co. Apparently a reduction in the feature related to metallic cobalt at edge energy is more observable than the formation of the divalent cobalt phase (Fig. 5).

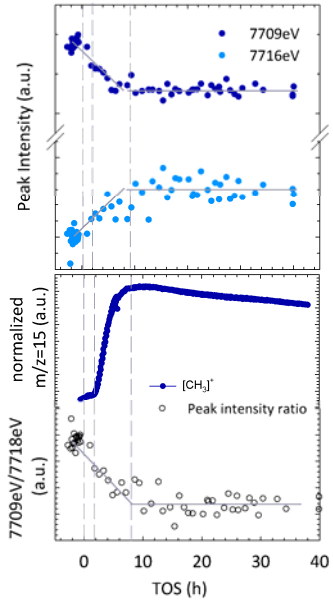

Figure 5. Evolution of features existing in the first derivative of XANES spectra and related to metallic and Co^{+2} phases (upper) MS signal of the methane formation (lower).

Simulation by linearly combined XANES spectra of the clearly demonstrated that the formed species are closer to the tetrahedral configuration found in the surface $CoAl_2O_4$–like compound or wurtzite-type CoO than the octahedrally coordinated CoO. Water may play a key role in this transformation since it is been produced throughout the induction period and is known to interact with the alumina surface by a hydrating mechanism and Co.

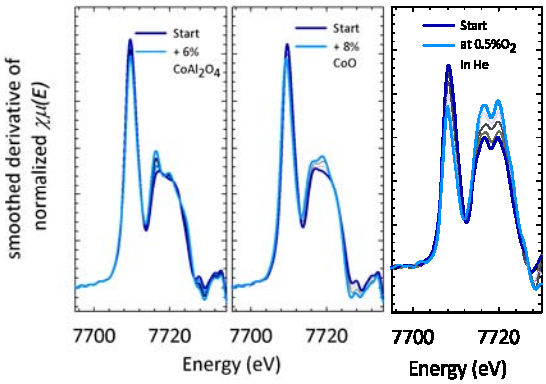

Figure 6. Simulation of the formation of $CoAl_2O_4$, CoO on reduced catalyst Co-Re/γ-Al_2O_3 catalyst together with model experiments on reduced catalyst under diluted O_2 stream.

This result implies that a mechanism of aluminate formation passes directly from the metallic cobalt to the Co-aluminate compound, without the CoO intermediate. However, the resolution of the technique in addition to the broad size distribution of the high surface area catalyst may be insufficient to detect such an intermediate. Alternatively, the formation of a wurtzite-type CoO at FTS conditions should not be excluded. On the other hand the Co/γ-Al_2O_3 catalyst exhibits further reduction during the evolution of reaction as was previously shown [2].

From the correlation of the MS signal and the XANES spectra it is evident that the formation of divalent cobalt is taking place during the induction period and not in the steady-state Fischer-Tropsch synthesis. In addition, it is encountered only in the promoted catalyst. Similar results have been obtained by temperature programmed and gravimetric techniques or ex situ XANES on spent catalysts by other researchers. Though, the interpretation was different since the ex situ studies lack a clear overview of the reaction evolution with time. Work from our group [6] on the effect of water in similar catalysts is suggesting a rapid irreversible deactivation of the small Co particles when high partial pressures of steam are introduced.

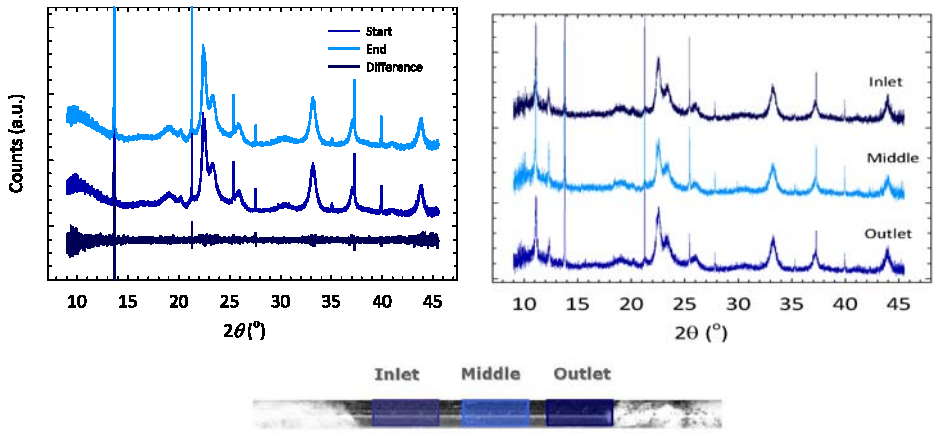

Figure 7. XRPD patterns of the catalyst after reduction and after 40h of FTS (upper). The different parts of the catalytic bed were probed (lower).

Monitoring of the catalyst during the Fischer – Tropsch synthesis at industrially relevant conditions by using a combination of X-ray characterization techniques with simultaneous activity measurements, suggests that the bulk of the cobalt remains unaffected during the run. That implies absence of bulk transformations that previously have been proposed to be reasons for the initial deactivation in FTS (i.e. re-oxidation and carbide formation). No indication of crystallite growth due to sintering was detected during the run (Fig. 7). In addition no significant gradients in the concentration of cobalt species or the size of the crystallites has been found as a function of the length of the catalytic bed (Fig. 7 and 8).

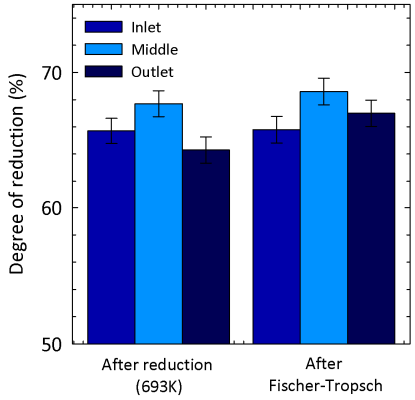

Figure 8. Degree of reduction as a function of catalyst bed position before and after FTS.

Summary

Common laboratory FTS activity test has been performed into a micro-system using a quartz capillary as reactor. Two catalysts were tested: Co-Re/γ-Al_2O_3 and a Co/γ-Al_2O_3. The setup has been optimized for performing FTS for more than a day at industrially relevant conditions (18 bar, 493 K, and CO conversion >50%). XAS and HR-XRPD were combined in order to reveal information on the catalyst phases during all the stages of the experimental procedure. The induction period appears to be of particular interest since the formation of tetrahedrally coordinated divalent cobalt is detected in the Co-Re/γ-Al_2O_3 catalyst. The phase appears to be similar to a surface $CoAl_2O_4$-like compound. On contrary the Co/γ-Al_2O_3 catalyst is subjected to further reduction during the induction and reaction periods. This further reduction is mainly taking place at the outlet of the reactor. Initial deactivation was detected by the MS but no apparent change in the X-ray signal could be observed. Results suggest that catalyst deactivation observed in the inisiat stages of FTS is surface-related phenomenon.

Publications

[1] N. E. Tsakoumis, M. Rønning, Ø. Borg, E. Rytter, A. Holmen, *Catalysis Today* **2010**, *154*, 162–182.
[2] M. Rønning, N. E. Tsakoumis, A. Voronov, R. E. Johnsen, P. Norby, W. van Beek, Ø. Borg, E. Rytter, A. Holmen, *Catalysis Today* **2010**, *155*, 289–295.
[3] N. E. Tsakoumis, Deactivation of Cobalt-based Fischer-Tropsch Synthesis Catalysts, **2011**.
[4] N. E. Tsakoumis, R. Dehghan, R. E. Johnsen, A. Voronov, W. van Beek, J. C. Walmsley, Ø. Borg, E. Rytter, D. Chen, M. Rønning, et al., *Catalysis Today* **2012**, 10.1016/j.cattod.2012.08.041.
[5] N. E. Tsakoumis, A. Voronov, M. Rønning, W. van Beek, Ø. Borg, E. Rytter, A. Holmen, *Journal of Catalysis* **2012**, *291*, 138–148.
[6]S. Lögdberg, M. Boutonnet, J. C. Walmsley, S. Järås, A. Holmen, E. A. Blekkan, *Applied Catalysis A: General* **2011**, *393*, 109–121.

Porous and Dense Magnesium Borohydride Frameworks: Synthesis, Stability, and Reversible Absorption of Guest Species

Y. Filinchuk[a,b,c], B. Richter[b], T.R. Jensen[b], V. Dmitriev[c], D. Chernyshov[c], H. Hagemann[d]

(a) Université Catholique de Louvain (Belgium); (b) Aarhus University (Denmark)
(c) SNBL at ESRF (France); (d) University of Geneva (Switzerland)

Crystalline hydrides, made of hydrogen and light elements such as boron, contain huge quantities of hydrogen but do not release it easily, due to their strong chemical bonds. Scientists have now, for the first time, succeeded in crystallising a highly porous hydride that can take up even more gas and release this additional amount when needed, like a reservoir or a gas bottle. The results are published in Angewandte Chemie, and highlighted by an inside cover page in the November 2011 issue.

The international team included researchers from the universities of Louvain-la-Neuve (Belgium), Aarhus (Denmark) and Geneva (Switzerland), along with the European Synchrotron Radiation Facility. The main author is Yaroslav Filinchuk from the Université Catholique de Louvain, University of Aarhus and ESRF.

Hydrogen is the most promising candidate fuel for future clean cars and trucks. The main reason it is not widely used today is the lack of affordable and safe mobile storage systems. Research into storage systems is focusing on two classes of materials: complex hydrides containing light elements such as boron, nitrogen or aluminium (borohydrides, amides, alanates); and porous materials, so-called metal-organic frameworks (MOFs). Unfortunately, whilst hydrides store large amounts of hydrogen, they release it only at relatively high temperatures. On the other hand, MOFs store and release molecular hydrogen easily, but only at cryogenic temperatures. The two groups of materials are made of completely different building blocks, representing two diverse fields of chemistry.

The new substance, obtained by Bo Richter from the University of Aarhus, combines the properties of both: it is highly porous like a MOF but entirely made of a hydride. This new form of magnesium borohydride (γ-$Mg(BH_4)_2$) stores 15 weight percent of hydrogen in the bulk material, representing an energy density equivalent to 50% of that of diesel fuel. In the pores, the material has the capability to store another 3 weight percents of H_2, at low temperatures, which alone represent 5 times the energy density of a modern lithium-ion battery.

As the material is crystalline, the researchers could study its gas uptake and release as well as its pressure- and temperature-induced transformations by X-ray diffraction. Most of these experiments were carried out at BM01A. The scientists discovered that about one third of the new material is empty and this space can store various guest molecules,

including hydrogen, nitrogen and even small organic molecules. It holds these gases at higher temperatures than most other porous solids. The nature of interaction between the "guest" gas molecules and the "host" nanoporous framework was also revealed by X-ray diffraction.

Information on the structure and properties of the new material allowed the researchers to infer the nature of the chemical bonds and building principles in metal borohydrides. This research opens a door, via combining the BH_4 anions with more complex ligands, to novel hybrid materials which could be highly selective gas storage and/or separation systems.

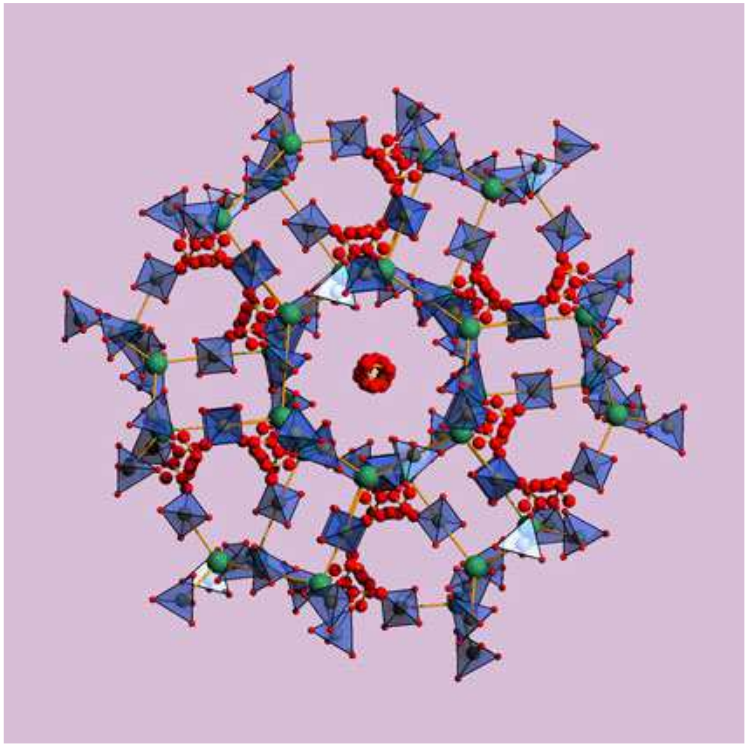

Hydrogen gas molecules (red spheres) stored within the crystalline magnesium borohydride structure (Mg green, BH_4 blue).

Publication

Y. Filinchuk, B. Richter, T.R. Jensen, V. Dmitriev, D. Chernyshov, H. Hagemann, Porous and Dense Magnesium Borohydride Frameworks: Synthesis, Stability, and Reversible Absorption of Guest Species, *Angew. Chem. Int. Ed.* **50**, 47, 11162–11166, 2011

V.2 In-house research

V.2.1 SNBL staff contributions highlighted by the ESRF

Pressure-induced insulator-to-metal transition in $TbBaCo_2O_{5.48}$

A key aspect of cobalt oxides that eclipses the conventional charge, spin and orbital degrees of freedom, is the possible variety of spin states of the cobalt ions. For this reason, cobalt layered perovskites represent a unique system that allows the study of the effect of spin-state degrees of freedom on the metal-insulator charge- and spin-ordering transitions.

There are several reasons to also expect a change in structural and transport properties of insulating oxides of 3d-metals as a function of pressure. Pressure could favour the orbitally-disordered phase thus giving an increase of conductivity. A change of spin-state for cobalt ions from HS or IS to LS is accompanied by a decrease of ionic radius, thus pressure could favour the spin conversion toward LS states. In this case one would not expect an increase of conductivity under pressure since LS states effectively block electron mobility via the "spin blockade" mechanism. One more possible pressure effect may be foreseen from symmetry analysis that links the structure and conductivity via an electron transfer integral through the Co-O-Co path. For this mechanism, one would expect a symmetry change under pressure.

The complex oxide $TbBaCo_2O_{5.5}$ contains Co^{3+} ions in octahedral or pyramidal coordination of oxygen atoms. Each Co^{3+} ion can be found in a low, intermediate, or high spin state (LS, IS, or HS) having different ionic radii. $TbBaCo_2O_{5.5}$ shows an insulator-to-metal transition on heating, and at the same temperature, T_c~335K, there is a structural change from Pmma ($2a_c \times 2a_c \times 2a_c$) to Pmmm ($a_c \times 2a_c \times 2a_c$). This transition agrees with a partial ordering of cobalt ions in different spin and orbital states. The deactivation of a "spin blockade" mechanism (associated with the LS states) has been suggested for this insulator-to-metal transition, assuming that heating would promote HS states and suppress LS states [1].

As no change in physical and structural properties has been found so far between ambient pressure and 1.2 GPa [2], the "spin blockade" has been considered the primary mechanism for the temperature induced metal-to-insulator transition in rare earth cobaltites.

By combining diffraction and transport measurements, we have recently shown that there is an insulator-to-metal transition, but at pressures higher than probed before, at ~10 GPa (Figures 6 and 7). In the same pressure range we observe changes in resistivity and in the ratio of the lattice constants of the average orthorhombic Pmmm ($a_c \times 2a_c \times 2a_c$) cell; the same behaviour holds for the spontaneous strains. The change in the ratio of the lattice constants is very similar to that observed as a function of temperature (Figure 7), thus suggesting a common mechanism for the two transitions. We can exclude the spin blockade mechanism as candidate, as it should be suppressed under pressure due to the higher ionic radius of HS ions. Temperature favours disorder

Principal publication and authors

D. Chernyshov (a), G. Rozenberg (b), E. Greenberg (b), E. Pomgakushina (c) and V. Dmitriev (a), *Phys. Rev. Lett.* **103**, 125501 (2009).

(a) Swiss-Norwegian Beam Lines at ESRF, Grenoble (France)
(b) School of Physics & Astronomy, Tel-Aviv University (Israel)
(c) Laboratory for Developments and Methods, PSI Villigen (Switzerland)

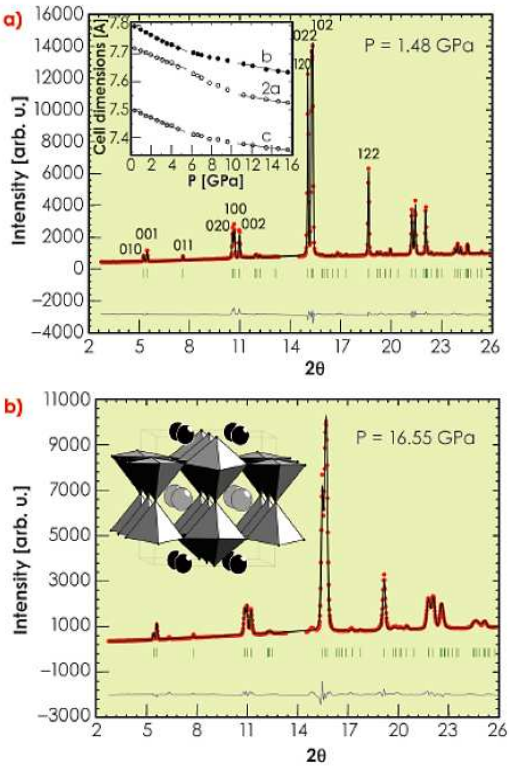

Fig. 6: Diffraction patterns for $TbBaCo_2O_{5.48}$ with experimental points, fitted profile, difference curve (bottom), and positions of Bragg reflections (vertical bars). a) P=1.48 GPa; the inset shows the unit cell dimensions as a function of pressure. b) P=16.55 GPa; the inset shows the high temperature/high pressure orthorhombic Pmmm ($a_c \times 2a_c \times 2a_c$) structure. Colour code: Tb (black), Ba (grey), cobalt ions are coordinated by oxygen forming octahedrons and pyramids.

via the entropy term, but pressure does not; ordering of spin states can therefore be excluded as well as common mechanisms. We propose instead that the change of the Co-O-Co angle affects the electron transfer integral, and consequently the conductivity. This mechanism assumes a strong link between structural deformation and transport properties while the spin-state degree of freedom only plays a secondary role.

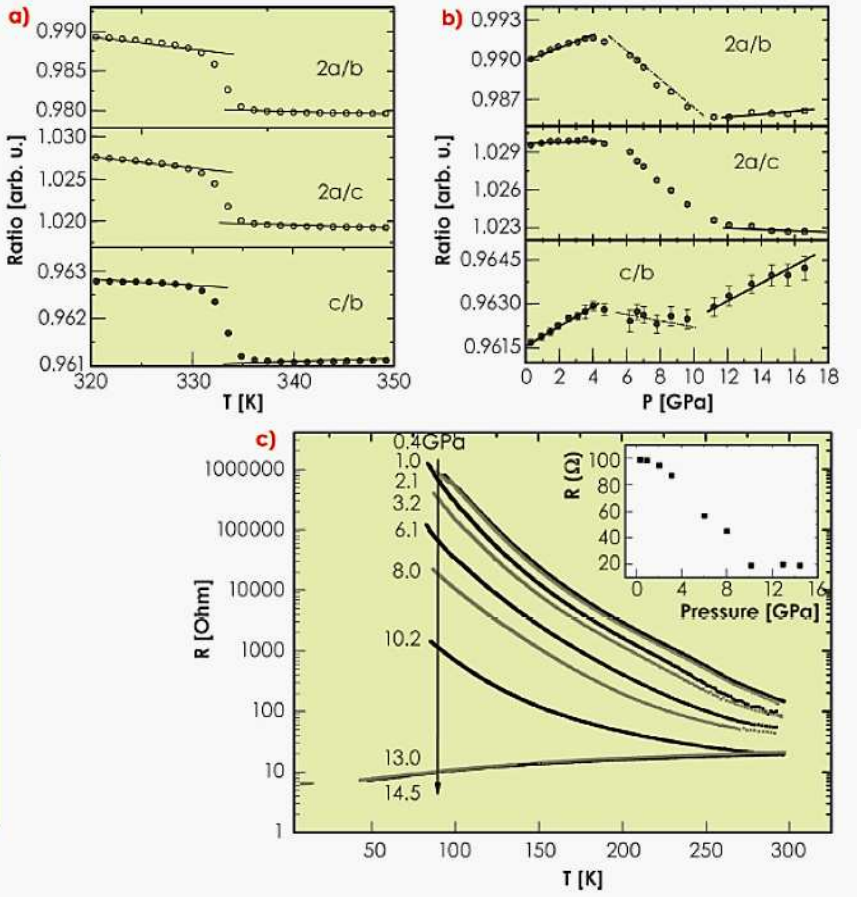

Fig. 7: Ratio of unit cell dimensions as a function of a) temperature, and b) pressure. c) Temperature dependence of the resistivity measured at different pressures. The inset shows the pressure dependence of the resistivity at 298 K.

References

[1] A. Maignan, V. Caignaert, B. Raveau, D. Khomskii and G. Sawatzky, *Phys. Rev. Lett.* **93** 026401 (2004).

[2] A. Podlesnyak, S. Streule, K. Conder, E. Pomjakushina, J. Mesot, A. Mirmelstein, P. Schützendorf, R. Lengsdorf, and M.M. Abd-Elmeguid, *Physica B-Condensed Matter* **378-80**, 537 (2006).

V.2.2 Recent SNBL staff contributions

Development and implementation of modulation enhanced techniques

Wouter van Beek
SNBL at ESRF (France)

Chemical and physical processes of both technological and fundamental importance are often very complex. Better understanding of these processes, necessary for their optimization, often come through the use of *in situ* experimental techniques. These processes intrinsically take place at the atomic level and proceed extremely fast (from pico- to nanosecond scale). On the other hand kinetic effects, fundamental for lifecycle considerations, are much slower (from millisecond, minutes, to hours). In general, *in situ* techniques now routinely probe minutes to hours time scales, while the investigation of millisecond to second time scale is on its way to becoming routine. When *in situ* techniques are applied to, for instance catalysts, an additional difficulty arises due to the dilution of the active catalytic centres that are often supported or embedded on/in an inert matrix. As a consequence, the actual active constituent only represents a minute fraction of the overall catalytic body. It is a big challenge to develop techniques that are capable of addressing both the fundamental and practical aspects of catalyst design. These techniques need to span over many orders of *time* and *length* scales with sufficient *sensitivity* in order to spot the active centres and reveal how these are influenced or not by the surrounding structure. There is a clear tendency towards combining several analytical tools in a complementary fashion [1]. The most prominent advantage of such multi-technique approaches lies in the enhanced, correlated information of dynamic chemical and physical processes when (quasi-) simultaneous, synchronized data acquisition is ensured. As a result one obtains information about the material structure that goes beyond the sum obtained by individual experimental methods. SNBL has been playing a leading role in combining diffraction with vibrational spectrocopies in the past. The palette of users has hence broadened and spectroscopy specialists started to appear on the beamline during the last 4 years. This has led to the introduction of the concept of modulation on the beamline [2, 3]. In brief when a system is perturbed by a periodic external stimulation, e.g. concentration, pH, light flux, pressure and temperature, for many materials the structural response is also periodic. Periodic perturbations are used frequently in spectroscopic investigations because they enhanced Sensitivity or Signal to Noise and introduce selectivity into experiments. This technique has been called Modulation Excitation Spectroscopy (MES). This had made the diffraction oriented beamline scientists think about the implications of modulation to diffraction. We have subsequently adapted this methodology for diffraction and named it Modulation-Enhanced Diffraction (MED). First we developed the theory to explain the kinematic diffraction response of a crystal when it is subjected to a periodically varying external perturbation [4]. We show that if a part the local electron density varies linearly with an external stimulus, the diffracted signal is not only a function of the stimulation frequency Ω, but also of its double 2Ω. These frequency components can provide selective access to partial diffraction contributions that are normally summed up in the interference pattern.

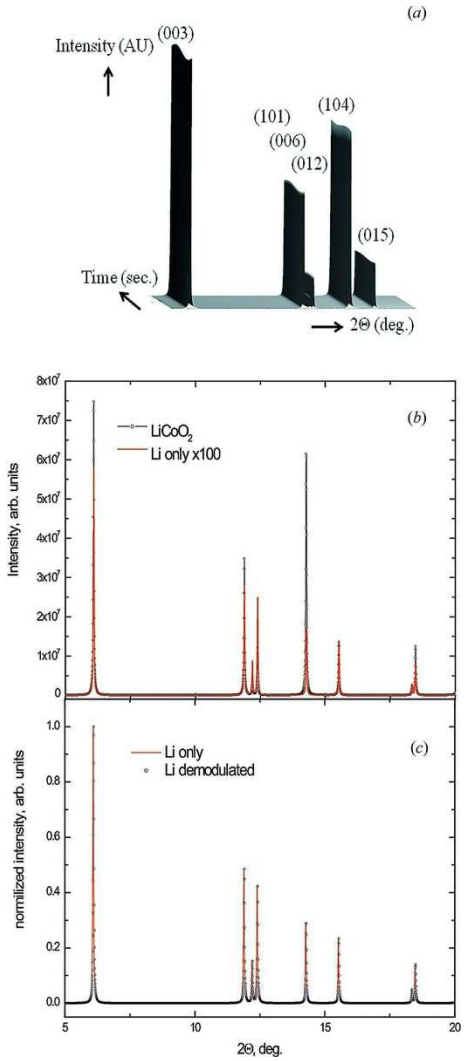

Figure 1 *Simulation of of a MED experiment where Li is going in and out periodically from $LiCoO_2$. Adapted from [4].*

As an illustration, we have carried out a simulation of a MED experiment with a sinusoidal modulation of Li occupancy, assuming linear response and zero time delay. A total of 60 powder patterns of LixCoO2, with x = 0.3–0.5, have been calculated with the help of the TOPAS software and Fig. 1(a) illustrates the time evolution of the diffraction pattern. For the sake of simplicity we have neglected the variation of the unit-cell dimensions and oxygen displacement, since they are expected to be small in this region. The comparison of the Li contribution with the total intensity from LixCoO2 is illustrated in Fig. 1(b). The extraction of the demodulated diffraction intensities at twice the stimulation frequency have been carried out with a locally developed script. The comparison of the demodulated pattern with the diffraction pattern of the Li sub-lattice alone is shown in Fig. 1(c); the patterns are the same as expected. Experiments were done where a phasing process applied to partial diffraction terms allow to recover *only* the substructure actively responding to the stimulus [5, 6] confirming the theoretical work. The proposed technique is targeted towards making efficient use of modern detectors now available at SNBL and alleviating the data analysis bottleneck by only extracting the

changing part from the data. Hundreds or even thousands of diffraction images can be collected in matter of minutes. MED proposes a new way of performing experiments and automated means of extracting information from these large quantities of data. Developments are still ongoing also in the field of EXAFS.

1. Newton, M. A., van Beek, W. *Combining synchrotron-based X-ray techniques with vibrational spectroscopies for the in situ study of heterogeneous catalysts: a view from a bridge.* Chem. Soc. Rev., **39**, 4845-4863, 2010
2. Urakawa, T. Bürgi, A. Baiker, Chemical Engineering Science **63**, 4902-4909 (2008).
3. Urakawa, A., van Beek, W., Monrabal-Capilla, M., Galn-Mascars, J.R., Palin, L., Milanesio, M. *Combined, Modulation Enhanced X-ray Powder Diffraction and Raman Spectroscopic Study of Structural Transitions in the Spin Crossover Material [Fe(Htrz)2(trz)](BF4).* J. Phys. Chem. C, **115**, 4, 1323–1329, 2011
4. Chernyshov, D., van Beek, W., Emerich, H., Milanesio, M., Urakawa, A. et al. *Kinematic diffraction on a structure with periodically varying scattering function.* Acta Cryst., **A67**, 4, 327-335, 2011
5. van Beek, W., Emerich, H., Urakawa, A., Palin, L., Milanesio, M., Caliandro, R., Viterbo, D., Chernyshov, D. *Untangling diffraction intensity: modulation enhanced diffraction on ZrO_2 powder.* J. Appl. Cryst., **45**, 4, 738-747, 2012
6. Caliandro, R., Chernyshov, D., Emerich, H., Milanesio, M., Palin, L., van Beek, W., Viterbo, D. *Patterson selectivity by modulation-enhanced diffraction.* J. Appl. Cryst., **45**, 3, 458-470, 2012

Diffuse Scattering and Disorder in Perovskite Ferroelectrics

D. Chernyshov
Swiss-Norwegian Beam Lines at ESRF, Grenoble, France

Perovskite structure is one of the simplest among the double oxides; following the paradigm "structure defines property" one would not expect perovskite family to be a Pandora’s Box for so many fascinating physical phenomena. The perovskites and structurally similar compounds show a spectacular variety of physical properties, and many of them are of great technological value. Structural disorder is one of important contributors to such diversity. Dynamic disorder associated with phonons often manifests itself in the ferroelectrics experiencing phase transformations [1], chemical disorder strongly influences magnetic ordering in perovskites with giant magneto-resistance [2], short-range correlated polar displacements is apparently the kernel of the relaxor behaviour [3] – to mention only a few key directions. Mixing different ions at the same position in the structure allows to tune physical properties and control conducting, magnetic and polar response. Such a mixing also implies a compositional or chemical disorder that makes real perovskite structure extremely complex.

The disorder in a structure rarely means a chaos but rather represents certain temporal and spatial correlations between different sites. While sharp Bragg reflections correspond to the average structure, broad diffuse scattering carries information of the correlation characteristics of a disorder. At variance with the average structural descriptors like space group and unit cell dimensions, real disordered structure is characterized by correlation and probabilistic properties.

Here we shortly review a set of publications based on SNBL BM01A data where our experiments helps to uncover disordered structure of $BaMg_{1/3}Ta_{2/3}O_3$ [4], Huang scattering in $PbZr_{1-x}Ti_xO_3$[5], thermal diffuse scattering in lead zirconate[6] and, as a most complex case, polar glass-like structure of relaxor ferroelectric $PbMg_{1/3}Nb_{2/3}O_3$ [7,8]. We also present a variety of tools and methods applied for the data analysis and presentation. At variance with Bragg scattering, there is no unique protocol for analysis of diffuse scattering data. Our examples serve as an illustration on how difficult such unification could be even for structurally similar perovskites.

According to the theory of scattering on disordered materials [9], we approximate the diffuse intensity in terms of Fourier components of concentration fluctuations, c_q:

$$I_{diff}(q) = N\left|c_q^2\right|\left(\Delta f(q) - \bar{f}qA_q\right)^2 + TDS$$

here N plays role of a scale factor, $\Delta f(q)$is a difference form factor for an atom and its substitutuent. The second term in square brackets accounts for the displacive component, the latter appears due to the structural deformation near a defect and is proportional to the atomic displacements induced by a defect and can be calculated from elastic moduli. The last term stays for thermal diffuse scattering [10] and can be calculated for a given lattice dynamics model [11].
If contributions from static displacements and TDS could be neglected, the corresponding diffuse scattering $I_{diff}(q) = N\left|c_q^2\right|\left(\Delta f(q)\right)^2$ carries information on correlation coefficients $\left|c_q^2\right|$or conditional probabilities directly linked to these coefficients [12]. This situation is realized in $BaMg_{1/3}Ta_{2/3}O_3$, where the diffuse scattering has dominating contribution from the $Mg_{1/3}Ta_{2/3}$ disorder (Fig. 1). Modeling of such a disorder can be done with Monte-Carlo method and recovered disordered structure is a subject of correlation analysis. This analysis shows that the electrostatic energy and the entropy points to this disordered phase of BMT as a metastable state, kinetically locked, which could be the equilibrium state just below the melting point [4].

When the disordered state is formed by non-interacting defects of low concentration, than the correlation between defects can be ignored and diffuse scattering has dominating contribution from elastic deformation induced by a defect, this is the case of Huang scattering:

$$I_{diff}(q) \propto \left(\bar{f}_q A_q\right)^2 . \qquad (1)$$

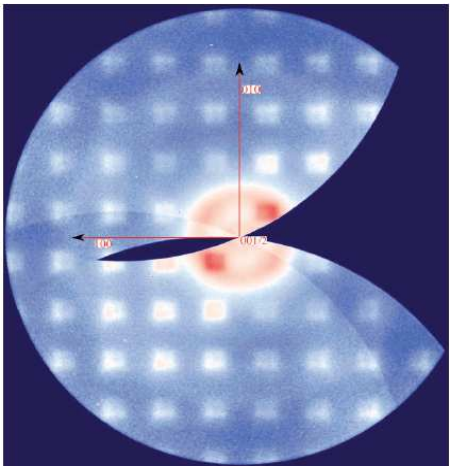

Figure 1 *The diffuse scattering observed for sections (100)-(010) section through (0, 0, ½) node for BMT. The square diffuse feature, which turn out to be cubes of diffuse scattering, has the intensity largely concentrated in the range from (h + 1/3,k + 1/3,l + 1/3) to (h + 2/3,k + 2/3,l + 2/3).*

Huang scattering is expected in the mixed perovskites for compositions close to the morphotropic boundary, in this case few phases of different symmetry may coexist in form of minor inclusions eforming the major phase. For the lead titanate-zirconate we have observed such a highly anisotropic scattering in the temperature range 293 K < T < 400 K. This scattering component disappears above 400 K at variance with otherwise very similar TDS (Fig. 2). Its main features can be reproduced by the model of inhomogeneous lattice deformations caused by inclusions of a tetragonal phase into a rhombohedral or monoclinic phase. This observation supports the idea that PZT at its morphotropic phase boundary is essentially structurally inhomogeneous.

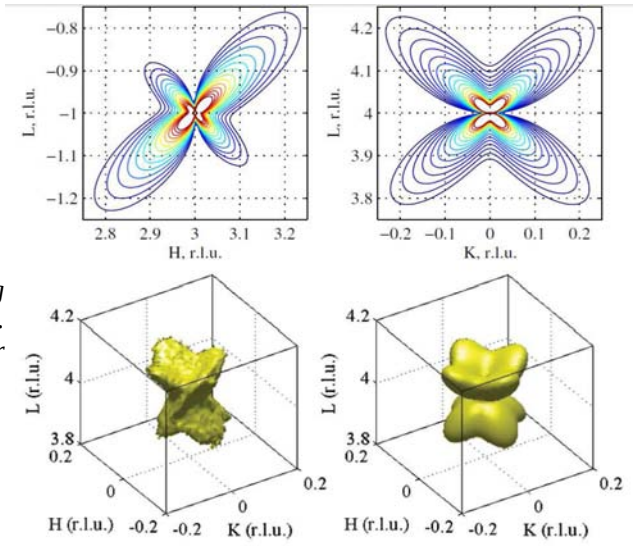

Figure 2 *Model calculation of Huang scattering maps for (0 0 4) and (-3 0 1) Bragg nodes (top). Experimental and calculated 3D diffuse clouds for (0 0 4) (bottom)*

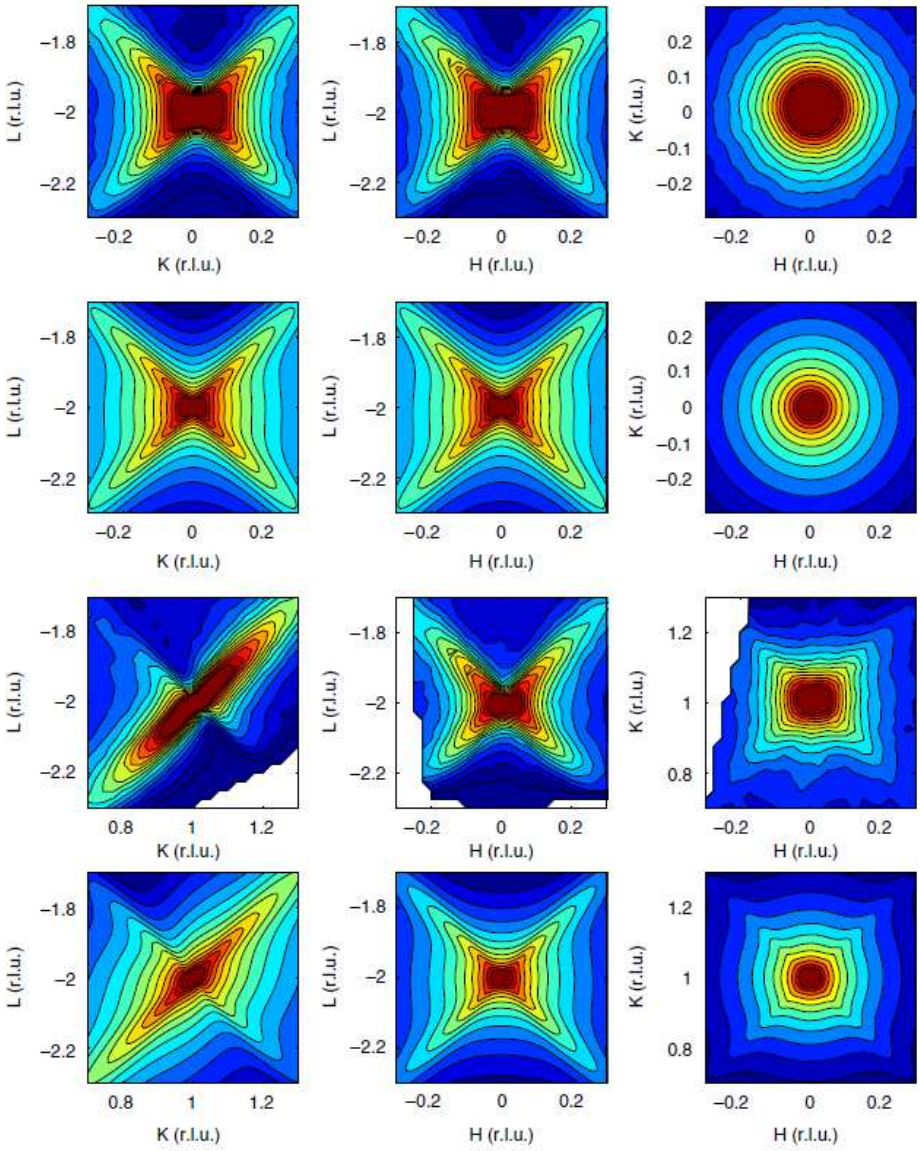

Figure 3 *Experimental and calculated diffuse scattering maps for PbZrO3, the calculation accounts for flexoelectric coupling.*

For many displasive phase transitions a phonon softening has been observed. Any soft mode would contribute strongly in the thermal diffuse scattering since the scattered intensity is inversely proportional to the square of the phonon frequency. Therefore TDS may carry very important information on the behavior of the phonon system close to phase transition. We have examined lattice dynamics of the antiferroelectric lead zirconate using inelastic and diffuse X-ray scattering techniques and the Brillouin light scattering. The analysis of the results reveals that the antiferroelectric state is a 'missed' incommensurate phase, and that the paraelectric to antiferroelectric phase transition is driven by the softening of a single lattice mode via flexoelectric coupling [6], the diffuse data supporting this conclusion are shown at Fig. 3. These findings resolve the mystery of

the origin of antiferroelectricity in lead zirconate and suggest an approach to the treatment of complex phase transitions in ferroics.

The parameterization of diffuse scattering given by eq. (1) seems to cover effectively a broad range of disordered phenomena in perovskites such as short-range chemical order, nano-regions of inclusions or phonons. There are however examples of very slow hindered dynamical systems where a direct application of the eq. (1) fails. Diffusion, ionic conductivity, glass-like behaviour may serve as examples. This is also the case for so-called relaxor ferroelectrics. Relaxor ferroelectrics have been known for more than 50 years and have been arousing significant interest because of their numerous unusual properties, such as the appearance of a broad peak in the real part of the dielectric susceptibility as a function of temperature. No structural change has been found to accompany this peak and this unusual polar response in the cubic perovskite has been linked with formation of polar nano-regions or nano-domains. Diffuse scattering data were actively used to support this idea.

We have undertaken a synchrotron x-ray diffuse scattering study of lead magnesium niobate-titanate $PbMg_{1/3}Mb_{2/3}O_3$-$PbTiO_3$ (PMN-PT) [7]. We have shown that the widely

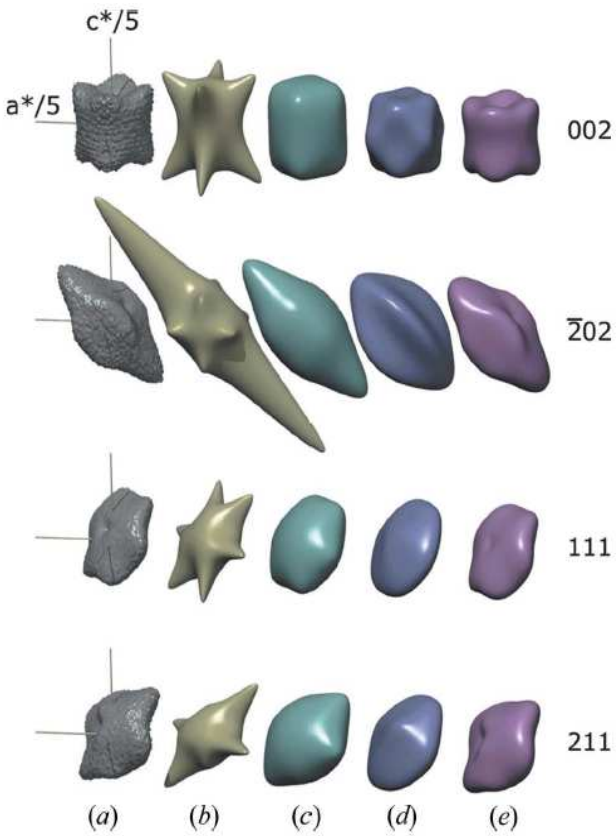

Figure 4 *Diffuse scattering near different Bragg reflections in PMN-PT. Column (a) represents the experimental observations, columns (b), (c), (d) show what is expected for different models of polar nano-regions, column (e) stays for the parametrization proposed.*

used concept of polar nanoregions as individual static entities is incompatible with the experimental diffuse scattering results. Based on the synchrotron diffuse scattering 3D dataset taken for the prototypical ferroelectric relaxor lead magnesium niobate-titanate (PMN-PT), we present a new parameterization of diffuse scattering in relaxors and propose a simple phenomenological picture to explain the unusual properties of the relaxor behavior (Fig. 4). Our model assumes a specific slowly changing displacement pattern, which is indirectly controlled by the low-energy acoustic phonons of the system. We have applied the parameterization to generate the disordered atomic configurations [8]. The analysis of the resulting displacement patterns retrieved for lead ions shows that a static snapshot of the relaxor structure corresponds to the specific dipole glassy state that is characterized by local polarization and its projection onto the selected direction. The recovered structural model agrees with the observed behavior of dielectric susceptibility as well as the existence of a wide-range hierarchy in the relaxation times in these materials.

Taken together, experiments on diffuse scattering from ferroelectric perovskites have uncovered a rich variety of disordering phenomena. Each individual case needs a special modeling that should not only satisfy local chemistry but also correspond to the physical properties. Thus various versions of Monte-Carlo and reverse Monte-Carlo approach work well for static compositional disorder but could give a meaningless result being applied for thermal diffuse scattering. A complimentary experiment on inelastic scattering helps to uncover static or dynamic nature of observed diffuse scattering, on the other hand diffuse scattering maps serve as a road map for time inelastic scattering; the other important option is temperature of pressure evolution of diffuse signal. Thanks to fast low-noise PILATUS detectors diffuse scattering measurements become routine, and, together with colleagues from ID28, we are working of the tools to manipulate, represent and analyze diffuse scattering.

[1] M. D. Fontana, G. Dolling, G. E. Kugel, and C. Carabatos, *Phys. Rev. B* **20**, 3850 (1979).
[2] S. Biswas, S. Chatterjee, P. Chatterjee, A.K. Nigam, S.K. De, *J. Mater. Res*. **20**, 813 (2005).
[3] S.B. Vakhrushev, A.A. Naberezhnov, N.M. Okuneva, and B.N. Savenko, *Phys. Solid State* **37**, 1993 (1995).
[4] A. Cervellino , S. N. Gvasaliya , B. Roessli , G. M. Rotaru , R. A. Cowley , S. G. Lushnikov, T. A. Shaplygina , A. Bossak , D. Chernyshov, *Phys. Rev. B* **86**, 104107 (2012)
[5] R. G. Burkovsky, Yu. A. Bronwald, A. V. Filimonov, A. I. Rudskoy, D. Chernyshov, A. Bosak, J. Hlinka, X. Long, Z. -G. Ye, S. B. Vakhrushev, *Phys. Rev. Let*., **109**, 097603 (2012)
[6] A.K. Tagantsev, K. Vaideeswaran, S.B. Vakhrushev, A.V. Filimonov, R.G. Burkovsky, A. Shaganov, D. Andronikova, A.I. Rudskoy, A.Q.R. Baron, H. Uchiyama, D. Chernyshov, A. Bosak, Z. Ujma, K. Roleder, A. Majchrowski, J.-H. Ko, N. Setter, *Nature Communications*, **4**, 2229 (2013)
[7] A. Bosak, D. Chernyshov, S. Vakhrushev, M. Krisch, *Acta Cryst*. **A68**, 117 (2011)

[8] A. Bosak, D. Chernyshov, S. Vakhrushev, *J. Appl. Cryst*., **45**, 1
[9] M.A. Krivoglaz, Diffraction of X-Rays and Thermal Neutrons in Imperfect Crystals, Springer, Berlin, 1992
[10] A. Bosak, D. Chernyshov *Acta Cryst*. **A68**, 117 (2011)
[11] Xu, R. & Chiang, C. *Z. Kristallogr*. **220**, 1009, (2005).
[12] D. Chernyshov, A. Bosak, *Phase Transitions*. **83** 115 (2010)

Polyhedral CeO_2 nanoparticles: Correlation between geometrical and electronic structure

C. Paun, O.V. Safonova, J. Szlachetko, P.M. Abdala*, M. Nachtegaal, J. Sa, E. Kleymenov, A. Cervellino, Frank Krumeich, J.A. van Bokhoven

**SNBL at ESRF, 38043 Grenoble, France*

Ceria, (CeO_2) is a well-known functional compound from the rare earth family. Ceria-based materials are technologically relevant materials with applications in a wide range of fields such as catalysis, solide oxide fuel cells, optics, gas sensors, and biology[1]. The reactivity of ceria is related to the low redox potential of the Ce^{3+}/Ce^{4+} pair and to the high oxygen storage capacity (OSC) that allow to store oxygen under oxidizing conditions (Ce^{4+}) and to release it under reducing ones. Recently, many researches have been focused on the understanding of the correlations between the morphology of CeO_2 nanoparticles (NPs) and their surface chemistry. The ultimate goal is the development of advanced materials having high OSC, improved catalytic activity, selectivity and stability. One of the main questions that still remain unanswered is how the concentration of defects in CeO_2 structure changes as a function of particle size and morphology and how this affects the OSC. The aim of this work is to determine systematically how the size of well-defined polyhedral ceria NPs prepared by a number of wet-chemical methods affects their electronic properties and the unit cell parameter under ambient conditions.

Well-crystallized ceria NPs of different size (2-10 nm), having polyhedral shapes and narrow size distribution were prepared by slightly modified microemulsion (M), precipitation (P) , solvothermal (S), and hydrothermal (H) methods (Table 1). HRTEM, XRD and EXAFS were used to characterize the morphology and the crystallographic structure of the NPs, while XANES at the Ce K- and L_3-edges was applied to probe the electronic properties, in particular, the concentration of Ce^{3+}. CeO_2 NIST was measured as reference.

Table 1. Samples used in the study: preparation methods, annealing conditions, particle size (d), unit cell parameter (a) and concentration of Ce^{3+}.

Samples	Preparation method	Precursor	Annealing conditions
M_110	Microemulsion	$Ce(NO_3)_3 \cdot 6H_2O$	110°C, 24h
M_200			200 °C, 6h
M_300			300 °C, 6h
M_400			400 °C, 6h
M_500			500 °C, 6h
P1_60	Precipitation_1	$Ce(NO_3)_3 \cdot 6H_2O$	60 °C, 24h
P2_50	Precipitation_2	$(NH_4)_2Ce(NO_3)_6$	50 °C, 24h
P2_400			400 °C, 6h
H_60	Hydrothermal	$Ce(NO_3)_3 \cdot 6H_2O$	60 °C, 24h
S_500	Solvothermal	$Ce(NO_3)_3 \cdot 6H_2O$	500 °C, 6h

The HRTEM (Figure 1) images reveal that the NPs are well-crystallized and have polyhedral shapes regardless of the preparation method. Figure 2 shows that the cell parameters of CeO_2 increased as the NPs size decreased independently on the preparation method, while the cell parameter shows significant discrepancy with the synthesis method. These results showed good agreement with the theoretical curve (dash line) proposed by Perebeinos *et al.*[2] who explained the lattice expansion in ceria by effective negative Madelung pressure taking place in ionic crystals.

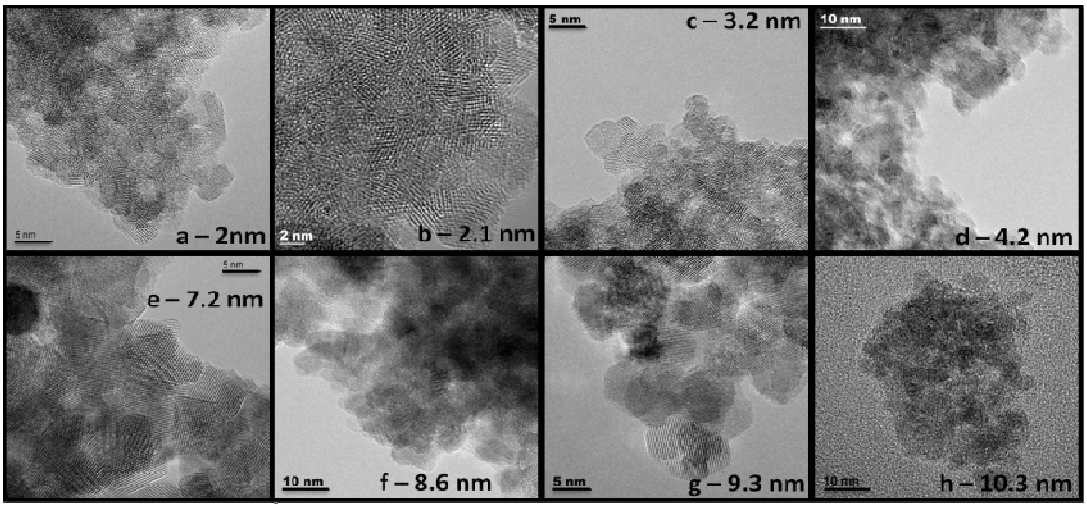

Figure 1. *HRTEM images of polyhedron NPs with synthesized by different procedures: a) M_110; b) P2_50; c) M_200; d) M_300; e) M_500; f) P2_400; g) H1_60; h) S_500.*

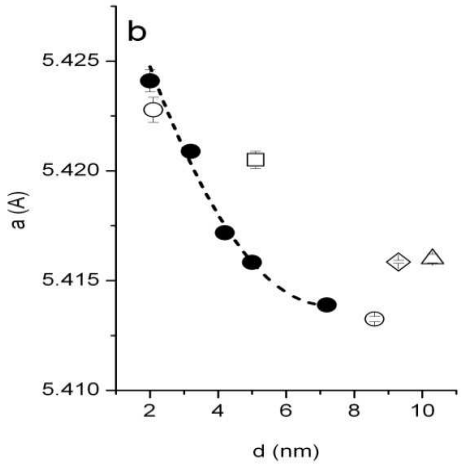

Figure 2. *Estimated CeO_2 unit cell parameters as a function of particles diameters synthesized by different methods: ● microemulsion; □ precipitation; ○; ◊ hydrothermal; Δ Solvothermal.*

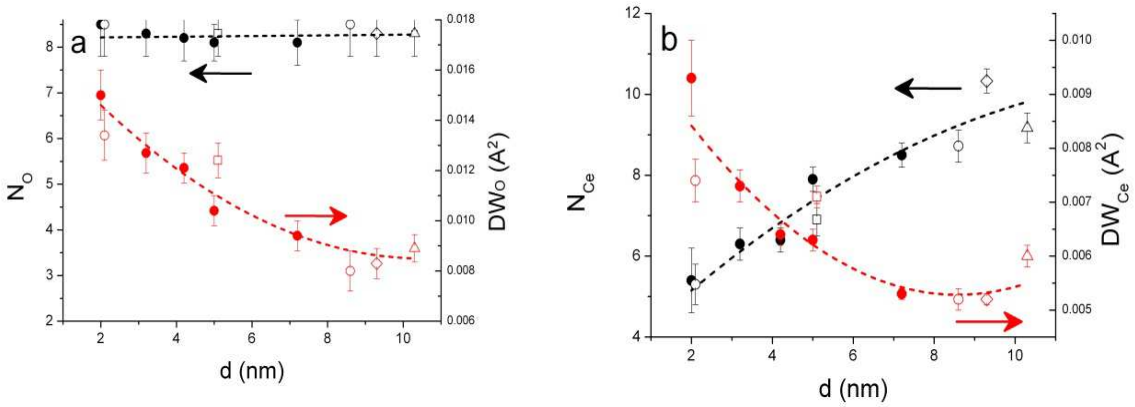

Figure 3. *The coordination numbers (N, in black) and the Debye-Waller factors (DW, in red) of oxygen in the first coordination shell (a) and cerium in the second coordination shell (b) estimated from EXAFS for ceria NPs as a function of the particle size.*

Figure 3 shows the EXAFS results (Ce K-edge) of all samples. The coordination number of cerium-oxygen in all the samples was close to the value of 8 while the corresponding values of Debye-Waller factors (DW) decreased when the NPs size increased. In the second coordination sphere, the DW_{Ce} decreases as the size of the NPs grows. The Debye-Waller factors typically increase for small crystallites due to the increased structural disorder on the NPs surface. The correlation between the Debye-Waller factors and the sizes of CeO_2 NPs shows that the structural disorder increases as the size of the NPs decreases.

From linear combination analysis on Ce K-edge XANES data, all samples show a concentration of Ce^{3+} smaller than 5%. No correlation was observed between the Ce^{3+} concentration and NPs size. However, the concentration of Ce^{3+} was related to the preparation method. Samples that were prepared using a Ce^{3+} precursor showed traces of Ce^{3+} in the NPs. The NPs prepared using a Ce^{4+} precursor showed no Ce^{3+}.

Figure 5 compares the Ce L_3-edge HERFD XANES for the ceria NPs of different size to the spectrum of CeO_2 NIST and $Ce_2(CO_3)_3$•xH2O. The spectra of the nanoceria had similar shape as that of CeO_2 NIST and also is in agreement with Kvashnina *et al.*[3]. The intensity and position of the two doublet features above the edge jump at 5730−5735 (B and C) and 5740−5745 eV (A1 and A2), are size-dependent. These features are broader and showed systematic energy shifts for small NPs. However, no significant edge shift, characteristic of Ce^{3+}, was observed in any of the spectra.

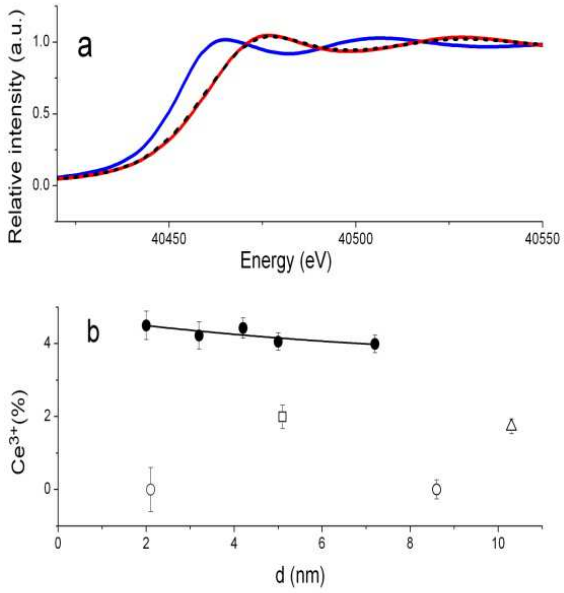

Figure 4. *(a) Ce K-edge XANES spectra of CeO2 NIST (red curve), $Ce_2(CO_3)_3 \cdot xH_2O$ (blue curve) and M_300 sample (black dash curve); (b) Variation of the Ce^{3+} concentration estimated from XANES Ce K edge spectra as a function of particle size: ● – M_110, 200, 300, 400 and 500 (2, 3.2, 4.2, 5 and 7.2 nm); □ – P1_60 (5.1 nm); ○ – P2_50, 400 (2.1 and 8.6 nm); Δ – S_500 (10.3 nm).*

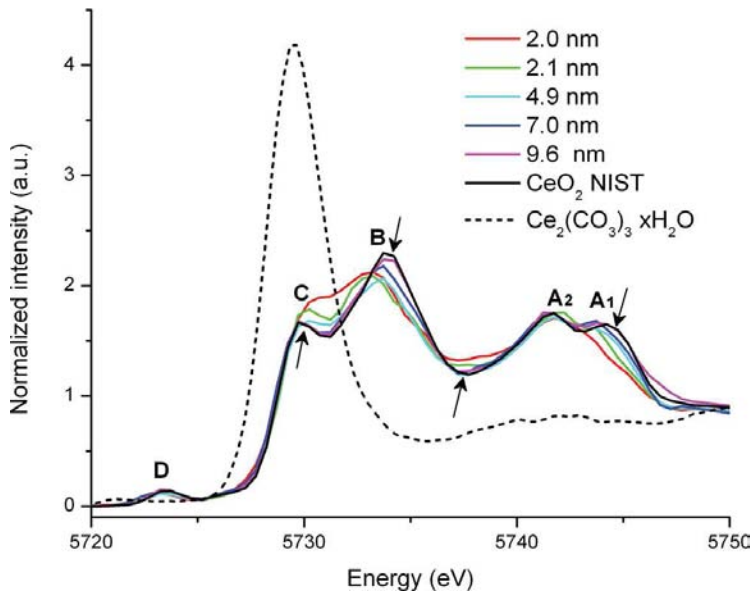

Figure 5. *The normalized Ce L3 HERFD XANES spectra of CeO_2 with different particles sizes: 2 nm (M_110), 2.1 nm (P2_50), 5.1 nm (P1_60) , 7.2 nm (M_500), 10.3 nm (S_500), 380 nm (CeO2 NIST) and $Ce_2(CO_3)_3 \cdot xH_2O$ standard.*

The results of the theoretical simulations of HERFD Ce L_3 XANES of octahedral ceria NPs qualitatively reproduced the size-dependent changes in the first doublet feature as the NP size decreased. The changes in the shape of features B and C toward smaller size can be explained by an enhanced contribution of cerium atoms situated on the NP surface and having a different local environment compared to the bulk atoms. The observed size-dependent changes in the geometric and the electronic structure of CeO_2 can explain the enhanced oxygen mobility, reducibility, and OSC of nanoceria reported in the literature. During longer exposure of nanoceria to the X-ray beam, the L_3-edge position was progressively and significantly shifting toward lower energy, indicating the photoreduction of Ce^{4+} into Ce^{3+}. For smaller NPs, the shift was more pronounced, while for bulk ceria it was not observed. Thus, the reduction likely occurred on the NP surface and shows a dependence on particle size.

Using a combination of structure-sensitive techniques applied under identical experimental conditions we established that a correlation between the NPs size, the cell parameter, and the structural disorder exist. The unit cell parameter increases when the NPs size decrease (up to 0.2% for 2 nm NPs). Also, the smaller the particles are, the larger the structural disorder. The Ce^{3+} concentration was in all samples below 5% and showed no correlation with the size and it depend on the preparation method. The amount of Ce^{3+}, which formed because of the damage by irradiation with X-rays, scales with surface area, thus producing significantly higher fractions of Ce^{3+} in smaller particles.

References

[1] Trovarelli, A.; Catalysis by ceria and related materials;
[2] Hutchings, Perebeinosa, V.; Chanb, S.-W.; Zhang, F. Solid State Commun. 2002, 123, 295−297.
[3] G.J., Ed., Catalytic Science Series; Imperial College Press: London, 2002. Kvashnina, K. O.; Butorin, S. M.; Glatzel, P. J. Anal. Atmos. Spectrom. 2011, 26, 1265−1272.

Publication

C. Paun, O.V. Safonova, J. Szlachetko, P.M. Abdala, M. Nachtegaal, J. Sa, E. Kleymenov, A. Cervellino, Frank Krumeich, J.A. van Bokhoven, “Polyhedral CeO2 Nanoparticles: Size-Dependent Geometrical and Electronic Structure”, *Journal of Physical Chemistry* **C116** (2012), 7312-7317.

Absolute structure and properties of inorganic helimagnets

V.A. Dyadkin
Swiss-Norwegian Beamlines at ESRF, Grenoble, France

Chirality is an enigmatic characteristic of biological materials where the sense of chirality (handedness) may change a property drastically. At variance, for inorganic materials both structural forms of opposite chirality have the same physical properties and are equally probable. However, as it follows from general symmetric arguments, the structural chirality may still make an effect on, at least, some physical properties that are also of chiral symmetry.

We have shown that for the case of cubic helimagnets (MnSi, MnFeSi, FeCoSi, MnGe, FeGe, MnFeGe, FeCoGe, Cu_2OSeO_3) with $P2_13$ symmetry the chiral crystal structure governs the chirality of the magnetic structure [1-4]. A lack of inversion symmetry in the above listed magnetic materials makes possible antisymmetric Dzyaloshinsky-Moriya interaction and results in a variety of magnetic phenomena. Chiral helicoidal order [5-6], skyrmion lattices [7-8], a quantum blue fog [9], soliton lattices [10], topological Hall effect [11], peculiar phase transitions [12] exemplify some of the topics attracting attention of wide range of physicists.

Here we review a series of recent papers where the data from SNBL were used to identify structural chirality while magnetic chirality was probed with help of the small angle diffraction of polarized neutrons. The structural chirality is set by an absolute crystal structure refined with via refining so-called Flack parameters [13-14]. The analysis is based on the difference between Friedel mates (I(h k l) – I(h k l)) due to resonant contribution in the x-ray scattering amplitudes. The difference caries information on the ratio between two opposite handed structural domains. The Flack parameter equals to zero corresponds to a single domain of the chiral structure (enantiopure) and atomic coordinates calculated during such a refinement give an absolute (i.e. with the fixed handedness) structural configuration. The measurement of the magnetic chirality is based on the difference between two small angle diffraction intensities collected at the same point of q-space for two opposite polarizations of the incident neutron beam [15]. Due to the large helical period (50 – 2000 Å) the first diffraction peak is expected at the q-range that is easily accessible with the small angle neutron scattering machine.

In spite of simplicity of the crystal structure the refinement of the Flack parameters for all mentioned above compounds was quite recently done by us for the first time. Almost all the tested crystals are enantiopure and they present a single structural domain of a fixed chirality, defined left or right according to a spiral Si atoms propagating along <111> axis, Fig. 1.

Having characterized the chirality of first available crystals, we have studied how the chirality of a seed affects the chirality of crystals grown by the Czochralski technique [3]. We have shown that the structural chirality can be control during the growth by the proper choice of the seed. In total, more than 50 crystals have been tested. We have to note that till now all the data suitable for the Flack refinement have been collected at SNBL BM01A diffractometers (Fig. 2).

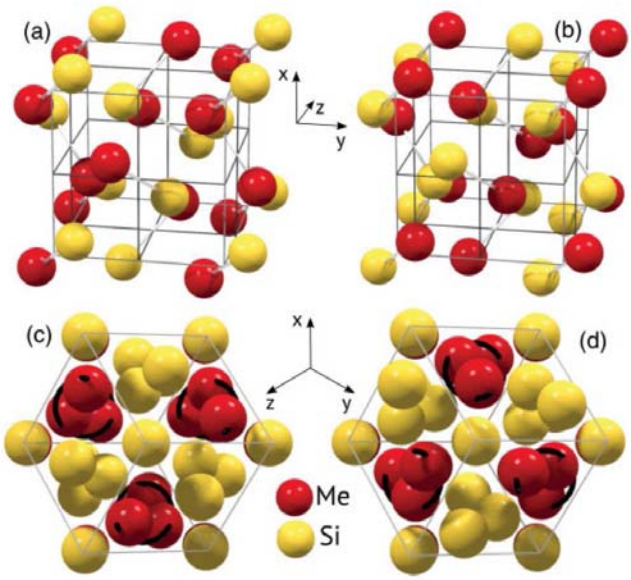

Figure 1. *View of a B20 cubic crystal (space group $P2_13$) along the <001> (a), (b) and <111> (c), (d) axes for two chiral configurations: (a), (c) right-handed with u_{Si}= 0.164 and u_{Me} = 0.862 and (b), (d) left-handed with u_{Si} = 0.846 and u_{Me} = 0.138. The black spirals help to identify the sense of the skewing.*

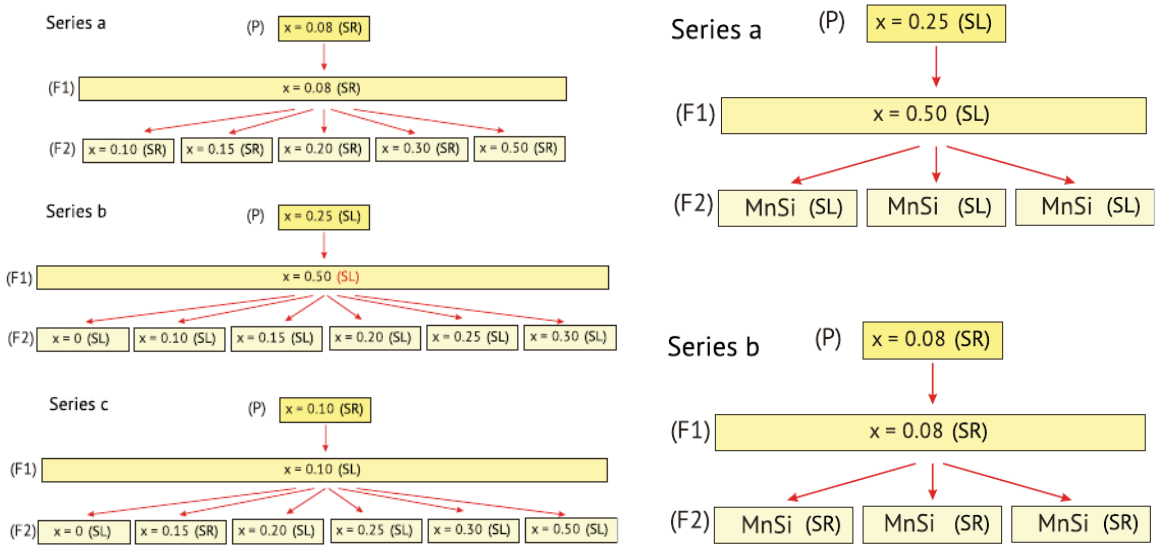

Figure 2. *$Fe_{1-x}Co_xSi$ samples (left) grown from the right-handed (P) seed (series a), from the left-handed (P) seed (series b), and from another right-handed (P) seed (series c). The structural handedness determined in the experiment is denoted as (SR) for right-handed crystals and as (SL) for left handed crystals. Series of the MnSi samples (right) grown from the left-handed (P) seed (series a) and from the right-handed (P) seed(series b).*

The magnetic chirality uncovered with polarized neutrons is found to be correlated with the structural one. With no exceptions enantiopure in the magnetic sense single crystals were enantiopure also structurally. The helicoidal magnetic structure is stabilized by the Dzyaloshinski-Moriya interaction. The coupling between structural and magnetic chiralities can be rationalized within phenomenological Landau theory as bi-linear; it implies that one cannot change, say, structural chirality without changing its magnetic counterpart [16]. However, the microscopic mechanism of this coupling and phenomenological DMI is still unknown. Recently, we have shown that the sign of the Dzyaloshinski constant D can be set by the proper choice of a 3d metal in silicides and germanides [4]. Together with the growth control of structural chirality this observation allows to control the magnetic chirality in these materials. Such a control becomes especially interesting for an exotic magnetic structure like skyrmions whose chirality obeys the same rules the chirality of the ground state helicoids [17].

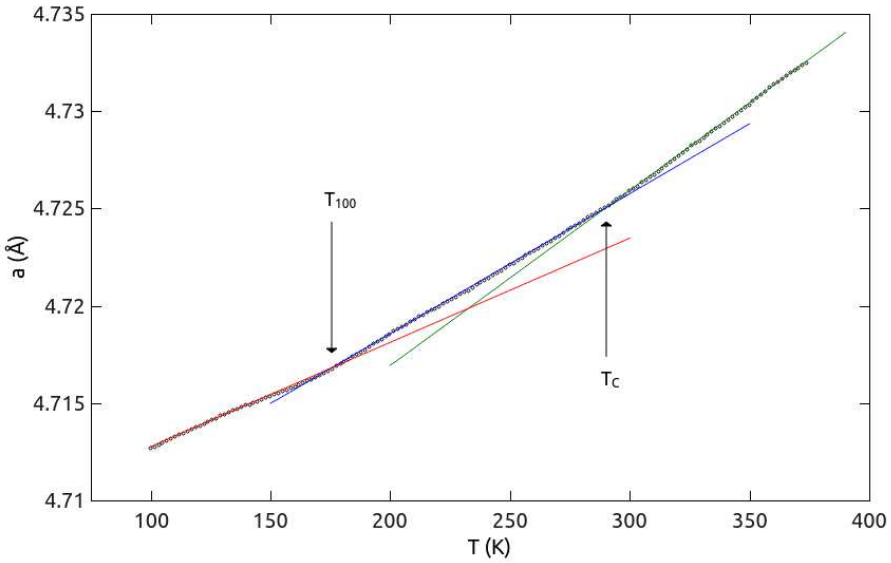

Figure 3. *The temperature dependence of the lattice constant of FeGe. T_c is the Curie temperature, T_{100} is the temperature of the phase transition from <111> to <100>.*

Recently, characterizing new FeGe crystal as a function of temperature with the novel Pilatus2M detector, we have observed another coupling between crystal structure and magnetism manifested in the thermal expansion (Fig. 3). The unit cell volume of FeGe seems to be sensitive to the formation of the helicoidal structure with <111> propagation vector at T_c = 280 K and a switch to the new propagation vector <100> at T_{100} = 175 K. Although the changes are small they are detectable with the equipment available at SNBL.

In collaboration with colleagues at EPFL and PNPI we now apply the same experimental approach to the new compounds that show similar chiral magnetic properties. As an example crystal structure of chiral helimagnet Cu_2OSeO_3 refined from SNBL data (R_1 = 0.03, R_w = 0.0685) is shown in Fig 4.

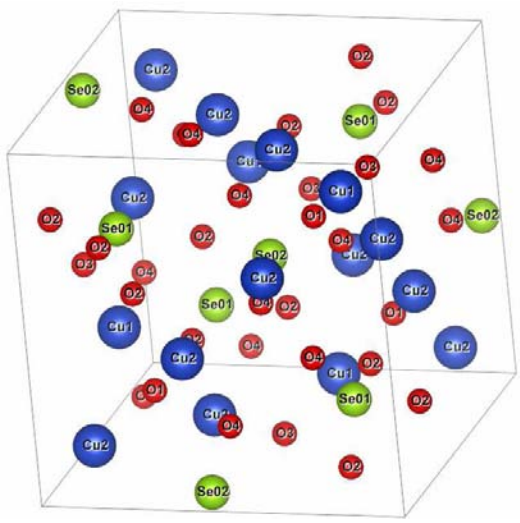

Figure 4. *The refined structure of the chiral helicoidal magnet Cu_2OSeO_3 with the $P2_13$ space group.*

Contributors:

D. Chernyshov, V. Dmitriev (SNBL at ESRF, Grenoble, France), S. Grigoriev (PNPI, St. Petersburg, Russia), K. Prsa (EPFL, Lausanne, Switzerland), A. Tsvyaschenko (IHPP, Troitsk, Russia).

[1] S. V. Grigoriev, D. Chernyshov, V. A. Dyadkin, V. Dmitriev, S. V. Maleyev, E. V. Moskvin, D. Menzel, J. Schoenes, and H. Eckerlebe, *Phys. Rev, Lett*., **102** (2009), 037204.
[2] S. V. Grigoriev, D. Chernyshov, V. A. Dyadkin, V. Dmitriev, E. V. Moskvin, D. Lamago, T. Wolf, D. Menzel, J. Schoenes, S. V. Maleyev, and H. Eckerlebe, *Phys. Rev. B*, **81** (2010), 012408.
[3] V. A. Dyadkin, S. V. Grigoriev, D. Menzel, D. Chernyshov, V. Dmitriev, J. Schoenes, S. V. Maleyev, E. V. Moskvin, and H. Eckerlebe, *Phys. Rev. B*, **84** (2011), 014435.
[4] S. V. Grigoriev, N. M. Potapova, S.-A. Siegfried, V. A. Dyadkin, E. V. Moskvin, V. Dmitriev, D. Menzel, C. D. Dewhurst, D. Chernyshov, R. A. Sadykov, L. N. Fomicheva, and A. V. Tsvyashchenko, *Phys. Rev. Lett*., **110** (2013), 207201.
[5] P. Båk and M. H. Jensen,, *Journal of Physics C: Solid State Physics*, **13** (1980), L881.
[6] S. V. Maleyev, *Physical Review B*, **73** (2006), 174402.
[7] Mühlbauer, S., Binz, B., Jonietz, F., Pfleiderer, C., Rosch, A., Neubauer, A., Georgii, R., Böni, P., *Science* **323**(2009), 915.
[8] X. Z. Yu, Y. Onose, N. Kanazawa, J. H. Park, J. H. Han, Y. Matsui, N. Nagaosa, and Y. Tokura, *Nature*, **465** (2010), 901.
[9] S. Tewari, D. Belitz, and T. R. Kirkpatrick, *Phys. Rev. Lett*., **96** (2006), 047207.
[10] Y. Togawa, T. Koyama, K. Takayanagi, S. Mori, Y. Kousaka, J. Akimitsu, S. Nishihara, K. Inoue, A. S. Ovchinnikov, and J. Kishine, *Phys. Rev. Lett*., **108** (2012), 107202.

[11] R. Ritz, M. Halder, C. Franz, A. Bauer, M. Wagner, R. Bamler, A. Rosch, and C. Pfleiderer, *Phys. Rev. B*, **87** (2013), 134424.
[12] Stishov, Sergei M., Petrova, Alla E., Shikov, Anatoly A.,Lograsso, Thomas A., Isaev, Eyvaz I., Johansson, Börje, Daemen, Luke L., *Phys. Rev. Lett.* **105**(2003) 236403.
[13] H. D. Flack, *Acta Crystallographica* **A39** (1983), 876.
[14] H. D. Flack and G. Bernardinelli, *Acta Crystallographica* **A55** (1999), 908-915.
[15] S. V. Maleyev, *Physical Review Letters*, **75** (1995), 4682.
[16] V. Dmitriev, D. Chernyshov, S. Grigoriev, and V. Dyadkin, *J. Phys.: Condens. Matter*, **24** (2012), 366005.
[17] D. Morikawa, K. Shibata, N. Kanazawa, X. Z. Yu, and Y. Tokura, *Phys. Rev. B*, **88** (2013), 024408.

VI. SNBL – FACTS and FIGURES

VI.1 Beam time allocation and user groups

The two Swiss-Norwegian Beam Lines, BM1A and BM1B, provide around 800 shifts per annum to its users. This allows the user groups to carry out on average about 80 projects every year. The Agreement between ESRF and SNX attributes 1/3 of this time to the international use, while 2/3 of the beam time should be allocated to Swiss and Norwegian users. It is worth noting that both collaborating countries are contributing members of ESRF, and researchers from Switzerland and Norway have a legal right to submit their proposals to ESRF, requesting nevertheless beam time at BM1A and BM1B lines.

Although the demand for beam time on the SNBL fluctuates from year to year, the beam lines remain very attractive for users. Figures VI.1 and VI.2 show the statistics for requested and allocated shifts over 2009-2013 years. In international part the mean overbooking ratio for these years reach 3.3. It drops down to 2.2 for Swiss and Norwegian users indicating a bit easier their access to the facility.

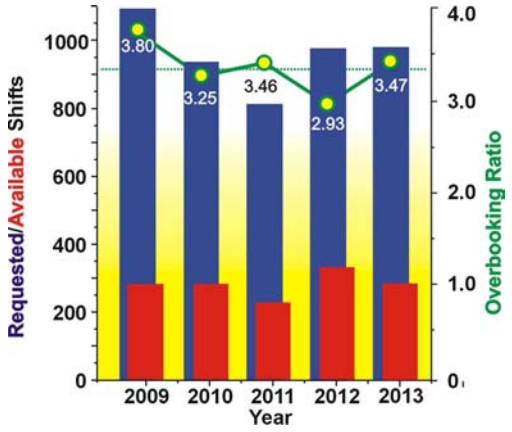

Fig. VI.1 *Requested and allocated at SNBL beam time for ESRF users*

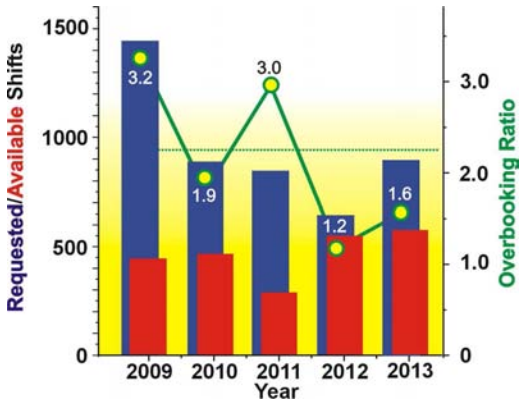

Fig. VI.2 *Requested and allocated at SNBL beam time for Swiss and Norwegian users*

The distribution of the allocated shifts by countries (Fig. VI.3) demonstrates the fact that research groups from three countries (Italy, France, and Germany) constitute an important part of international users at SNBL. Swiss and Norwegian users are well presented in this part. In the bi-national statistics (Fig. VI.4), Norwegian users are more active in using SN-attributed beam time.

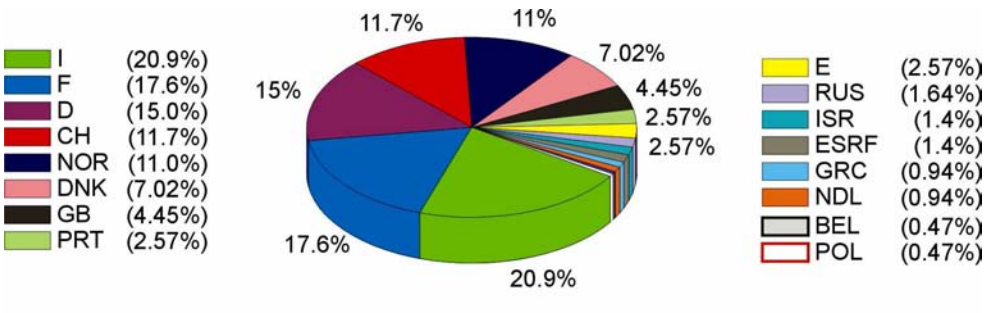

Fig. VI.3 *Distribution of the ESRF attributed beam time at SNBL by countries*

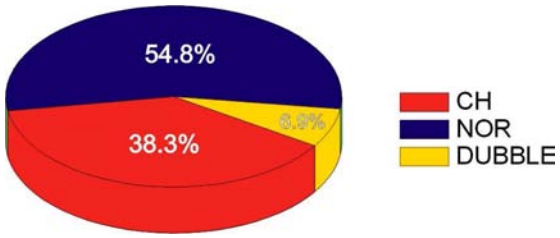

Fig. VI.4 *The use of SN beam time by Swiss and Norwegian groups*

The research groups from the two partner countries, belong to leading Swiss and Norwegian universities and research institutes. They both show considerable interest and a serious contribution to the SNBL activity. Figures VI.5 and VI.6 list Swiss and Norwegian institutes present at SNBL and show their respective use of beam time.

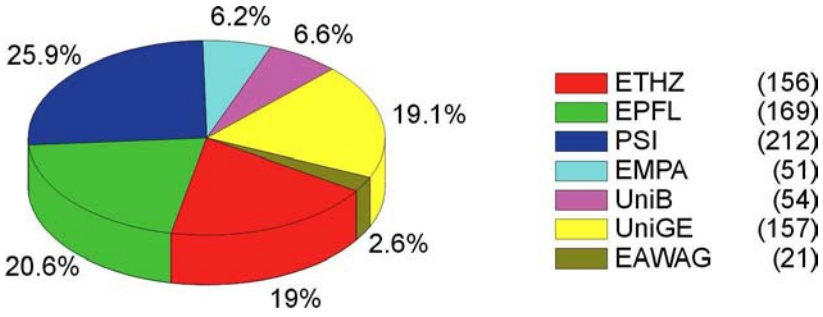

Fig. VI.5 *Distribution of the beam time by Swiss institutes in 2009-2013 (abbr. see in Appendix C)*

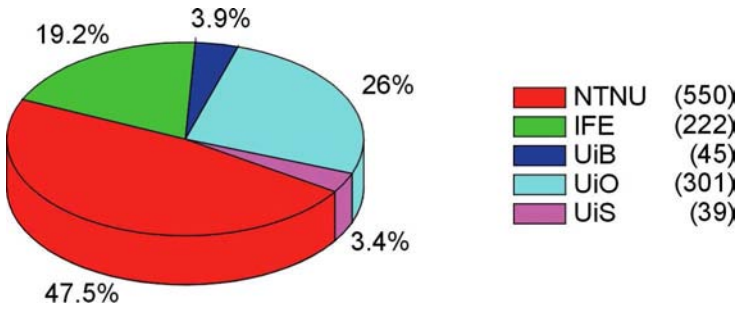

Fig. VI.6 Distribution of the beam time by Norwegian institutes in 2009-2013 *(abbr. see in Appendix C)*

The variety of Review Committees selecting projects for SNBL (Figs. VI.7) reflects the concept formed after discussions by the beamline management with the SN user community; it had strong links to their research strategy, and aimed to providing the most appropriate assistance to their projects, both those already running and others still in planning. The SN beam lines are seen as multifunctional, dedicated to complex *in situ* experiments requiring combinations of diffraction and spectroscopic techniques. The approach seems to be well received also beyond the SN users community.

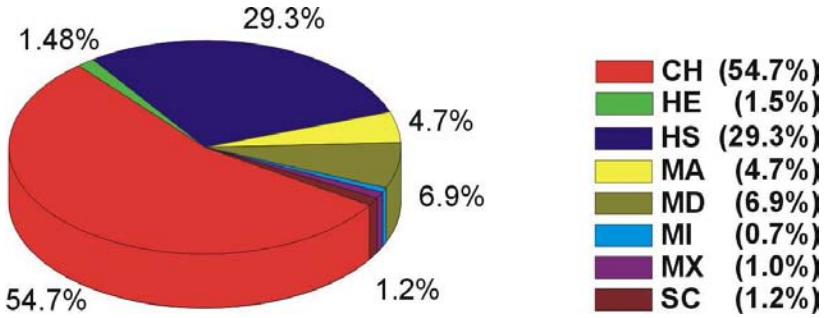

Fig. VI.7 *Distribution of beam time allocated to international users at SNBL by Review Committees in 2009-2013 years*

VI.2 Publication Output

The SNBL users exploited the high efficiency of the beamlines with an increase in the publication rate. So far more than 1100 papers from SNBL were published in peer-reviewed journals. The number of papers which appeared in the period 2009-2012 using data collected on SNBL reached an unprecedented level of 131 in publications 2009, and it shows a stable trend to keep the high level in 2010-13 (see Appendix A). Taking into account the typical number ~80 of projects carried out at the beamlines one finds the efficiency of the SNBL users in using beam time quite impressive. Figure VI.9 compares the number of papers published by the users, both international and SN, to the precise numbers of projects for years 2009-2012.

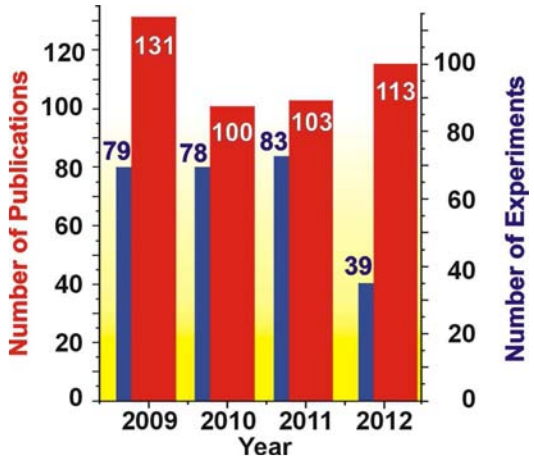

Fig. VI.9 *Publication rate of SNBL compared to the number of projects carried out every year*

It is worth noting steady increasing of the quality of SNBL users' publications. Figure VI.10 shows evolution of the average Impact Factor of journals where the corresponding papers appeared.

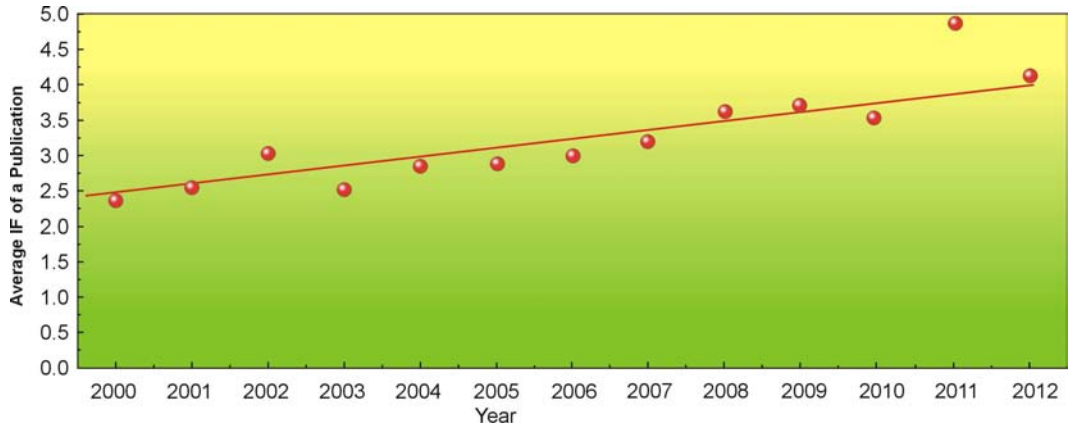

Fig. VI.10 *Average Impact Factor of SNBL publications*

Last but not least, SNBL serves as an important facility for PhD students from Swiss and Norwegian universities. In 2009-2012 thirteen theses were carried out and defended using data obtained at SNBL (see the list in Appendix B).

VII. CONCLUSIONS

- We have just concluded a major detector refurbishment of SNBL. This represents a substantial investment in the project by our funding agencies, and puts us in an excellent position to exploit the facility for many years to come.

- An active and efficient user community has been formed around SNBL. It has strong research programs in several fields, including energy storage materials, the chemistry of catalysis and the characterization of new materials using a combination of in-situ techniques.

- The presence of several groups of researchers from various institutes in Switzerland and Norway carrying out long-term programs at SNBL ensures that our facility will continue to benefit from the input from our user community and that the beamtime will be in high demand.

- The solid financial basis ensured by the national governmental agencies, as well as the important additional contributions made by the user's institutes, allow SNBL not only to maintain the existing level of the activity on the beam lines but also continue to upgrade and develop our instrumentation.

- The staff of SNBL show their motivation, expertise, and efficiency both in providing a high-level service to users, and in developing their own research and instrumentation programs.

VIII. ACKNOWLEDGEMENTS

On behalf of the SNBL team we would like to gratefully acknowledge all of the people who have supported us in our work and who have contributed significantly to the success of our common project named SNBL:

- Former and current SNX Council members, including: D.Nicholson (NTNU), G.Chapuis (EPFL), H.Fjellvag (UiO), B.Hauback (IFE), M.Ronning (NTNU), K.Knudsen (IFE), H.Larsen (UiS), J.van Bokhoven (ETHZ), P.Macchi (UniB), and C.Quitmann (PSI/MAXLab).

- Former and current SNX observers: M.Steinacher (SER), A.M.Hundere and C.A.Mathiesen (NSR).

- SNX Council advisers S.Margadona (UiO) and R.Cerny (UniGE).

- ESRF contacts for CRGs: A.Kaprolat and his team.

- ESRF technical support (E.Dettona) and computer support (R.Homs).

The proactive role of our users in forming the strategy for the development of SNBL has been invaluable. Moreover their contributions both financially and intellectually have played a crucial role in the ongoing development of the project.

APPENDIX A

List of Publications

2009

2009-1. **Afanasiev, P., Bouchu, D., Kudrik, E., Millet, J.-M., Sorokin, A.** *Stable N-bridged diiron (IV) phthalocyanine cation radical complexes: synthesis and properties* Dalton Trans., 9828 - 9836, 2009

2009-2. **Arnbjerg, L. M., Ravnsbæk, D. B., Filinchuk, Y., Vang, R. T., Cerenius, Y., Besenbacher, F., Jørgensen, J. - E., Jakobsen, Jensen, T. R.** *Structure and Dynamics for $LiBH_4$-LiCl Solid Solutions* Chem. Mater., **21**, 24, 5772–5782, 2009

2009-3. **Baldansuren, A., Dilger, H., Eichel, R.-A., Van Bokhoven, J.A., Roduner, E.** *Interaction and Reaction of Ethylene and Oxygen on Six-Atom Silver Clusters Supported on LTA Zeolite* J. Phys. Chem. C, **113,** 45, 19623–19632, 2009

2009-4. **Bezverkhyy, I., Safonova, O. V., Afanasiev, P., Bellat, J.-P.** *Reaction between Thiophene and Ni Nanoparticles Supported on SiO_2 or ZnO: In Situ Synchrotron X-ray Diffraction Study* J. Phys. Chem. C, **113**, 39, 17064–17069, 2009

2009-5. **Boldyreva, E.** *Combined X-ray diffraction and Raman spectroscopy studies of phase transitions in crystalline amino acids at low temperatures and high pressures: selected examples* Phase Transitions A, **82**, 4, 303 – 321, 2009

2009-6. **Borg, Ø., Hammer, N., Eri, S., Lindvag, O., Myrstad, R., Blekkan, E., Ronning, M., Rytter, E., Holmen, A.** *Fischer–Tropsch synthesis over un-promoted and Re-promoted γ-Al_2O_3 supported cobalt catalysts with different pore sizes* Catalysis Today, **142**, 1-2, 70-77, 2009

2009-7. **Bosak, A., Hoesch, M., Krisch, M., Chernyshov, D., Pattison, P., Schulze-Briese, C. et al.** *3D Imaging of the Fermi Surface by Thermal Diffuse Scattering* Phys. Rev. Lett., **103**, 076403-076407, 2009

2009-8. **Bras, W., Clark, S.M., Greaves, G.N., Kunz, M., Van Beek, W., Radmilovic, V.** *Nanocrystal Growth in Cordierite Glass Ceramics Studied with X-ray Scattering* Cryst. Growth Des., **9**, 3, 1297–1305, 2009

2009-9. **Buchter, F, Lodziana, Z., Remhof, A., Friedrichs, O., Borgschulte, A., Mauron, Ph., Zuttel, A.** *Structure of the Orthorhombic γ-Phase and Phase Transitions of $Ca(BD_4)_2$* J. Phys. Chem. C, **113,** 39, 17223–17230, 2009

2009-10. **Calamiotou, M., Gantis, A., Lampakis, D., Siranidi, E., Liarokapis, E., Margiolaki, I., Conder, K.** *Pressure-induced phase separation in the Y123 superconductor* EPL, **85**, 26004-26010, 2009

2009-11. **Calamiotou, M., Gantis, A., Siranidi, E., Lampakis, D., Karpinski, J., Liarokapis, E.** *Pressure-induced lattice instabilities and superconductivity in $YBa_2Cu_4O_8$ and optimally doped $YBa_2Cu_3O_{7-\delta}$* Phys. Rev. B **80**, 214517-214524, 2009

2009-12. **Chambrier, M.-H., Le Bail, A., Kodjikian, S., Suard, E., Goutenoire, F.** *Structure Determination of $La_{18}W_{10}O_{57}$* Inorg. Chem., **48**, 14, 6566–6572, 2009

2009-13. **Chen, W., Williams, A.J., Ortega-San-Martina, L., Li, M., Sinclair, D.C., Zhou, W., Attfield, J.A.** *Robust Antiferromagnetism and Structural Disorder in $Bi_xCa_{1-x}FeO_3$ Perovskites* Chem. Mater., **21**, 10, 2085–2093, 2009

2009-14. **Cerný, R., Filinchuk, Y., Brühne, B.** *Local atomic order in the vicinity of Cu_2 dumbbells in $TbCu_7$-type $YCu_{6.576}$ studied by Bragg and total scattering techniques* Intermetallics, **17**, 10, 818-825, 2009

2009-15. **Cerný, R., Penin, N., Hagemann, H., Filinchuk** *The First Crystallographic and Spectroscopic Characterization of a 3d-Metal Borohydride: $Mn(BH_4)_2$* J. Phys. Chem. C, **113,** 20, 9003–9007, 2009

2009-16. **Chernyshov, D., Rozenberg, G., Greenberg, E., Pomyakushina, E., Dmitriev. V.** *Pressure-induced insulator-to-metal transition in $TbBaCO_2O_{5.48}$* Phys.Rev.Lett., **103**, 125501-12505, 2009

2009-17. **Chernyshov, D., Vangdal, B., Törnroos, K.W., Bürgi, H.-B.** *Chemical disorder and spin crossover in a mixed ethanol–2-propanol solvate of Fe^{II} tris(2-picolylamine) dichloride* New J. Chem., **33**, 1277 - 1282, 2009

2009-18. **Croce, G., Carniato, F., Milanesio, M., Boccaleri, E., Paul, G., Van Beek, W., Marchese, L.** *Understanding the physico-chemical properties of polyhedral oligomeric silsesquioxanes: a variable temperature multidisciplinary study* Phys. Chem. Chem. Phys., **11**, 10087 - 10094, 2009

2009-19. **Cunha-Silva, L., Ananias, D., Carlos, L.D., Almeida Paz, F.A., Rocha, J.** *Synchrotron powder structure of a new layered lanthanide-organic network* Zeitschrift für Kristallographie, **224**, 05-06, 261-272, 2009

2009-20. **Cunha-Silva, L., Lima, S., Ananias, D., Silva, P., Mafra, L., Carlos, L., Pillinger, M., Valente, A., Paz, F.A., Rocha, J.** *Multi-functional rare-earth hybrid layered networks: photoluminescence and catalysis studies* J. Mater. Chem., **19**, 2618 - 2632, 2009

2009-21. **Degtyareva, V.** *The fcc–bcc Bain path in In–Sn and related alloys at ambient and high pressure* J. Phys.: Condens. Matter, **21**, 095702-095707, 2009

2009-22. **Deledda, S. Hauback, B.C.** *The formation mechanism and structural characterization of the mixed transition-metal complex hydride $Mg_2(FeH_6)_{0.5}(CoH_5)_{0.5}$ obtained by reactive milling* Nanotechnology, **20**, 204010-204017, 2009

2009-23. **Del Río, M.S., Boccaleri, E., Milanesio, M., Croce, G., Van Beek, W., Tsiantos, C., Chyssikos, G.D., Gionis, V. et al.** *A combined synchrotron powder diffraction and vibrational study of the thermal treatment of palygorskite–indigo to produce Maya blue* J. Materials Science, **44**, 20, 5524-5536, 2009

2009-24. **Denys, R.V., Riabov, A.B., Maehlen, J.P., Lototsky, M.V., Solberg, J.K., Yartys, V.A.** *In situ synchrotron X-ray diffraction studies of hydrogen desorption and absorption properties of Mg and Mg–Mm–Ni after reactive ball milling in hydrogen* Acta Materialia, **57**, 3989-4000, 2009

2009-25. **Dzevenko, M., Miliyanchuk, K., Filinchuk, Y., Stelmakhovych, O., Akselrud, L.** *Large hydrogen capacity in hydrides R_2Ni_2In-H (R=La, Ce, Pr, Nd) with new structure type* J. Alloys & Compounds, **477**, 1-2, 182-187, 2009

2009-26. **Eibl, S., Fitch, A., Brunelli, M., Evans, A. D., Pattison, P., Plazanet, M., Johnson, M. R., Alba-Simionesco, C., Schober, H.** *Trans-Decahydronaphthalene (decalin) from powder diffraction data* Acta Cryst. , C**65**, o278-o280, 2009

2009-27. **Filinchuk, Y., Cerny, R., Hagemann, H.** *Insight into $Mg(BH_4)_2$ with Synchrotron X-ray Diffraction: Structure Revision, Crystal Chemistry, and Anomalous Thermal Expansion* Chem. Mater., **21**, 5, 925–933, 2009

2009-28. **Filinchuk, Y., Nevidomskyy, A. N., Chernyshov, D., Dmitriev, V.** *High-pressure phase and transition phenomena in ammonia borane NH3BH3 from x-ray diffraction, Landau theory, and ab initio calculations* Phys. Rev. B **79**, 21, 214111-214122, 2009

2009-29. **Filinchuk, Y., Rönnebro, E., Chandra, D.** *Crystal structures and phase transformation in $Ca(BH_4)_2$* Acta Materialia, **57**, 3, 732-738, 2009

2009-30. **Førde, T., Næss, E., Yartys, V.A.** *Modelling and experimental results of heat transfer in a metal hydride store during hydrogen charge and discharge* Int. J. Hydrogen Energy, **34**, 12, 5121-5130, 2009

2009-31. **Gao, T., Fjeld, H., Fjellvåg, H., Norby, T., Norby, P.** *In situ studies of structural stability and proton conductivity of titanate nanotubes* Energy Environ. Sci., **2**, 517 - 523, 2009

2009-32. **Gao, T., Fjellvåg, H., Norby, P.** *Defect Chemistry of a Zinc-Doped Lepidocrocite Titanate $Cs_xTi_{2-x/2}Zn_{x/2}O_4$ (x = 0.7) and its Protonic Form* Chem. Mater., **21,**15, 3503–3513, 2009

2009-33. **Gao, T., Fjellvåg, H., Norby, P.** *Protonic titanate derived from $Cs_xTi_{2-x/2}Mg_{x/2}O_4$ (x = 0.7) with lepidocrocite-type layered structure* J. Mater. Chem., **19**, 787 - 794, 2009

2009-34. **Gao, T., Fjellvåg, H., Norby, P.** *Structural and morphological evolution of ß-MnO_2 nanorods during hydrothermal synthesis* Nanotechnology, **20**, 055610-055617, 2009

2009-35. **Gao, T., Krumeich, F., Nesper, R., Fjellvg, H., Norby, P.** *Microstructures, Surface Properties, and Topotactic Transitions of Manganite Nanorods* Inorg. Chem., **48**, 13, 6242–6250, 2009

2009-36. **Gao, T., Norby, P., Okamoto, H., Fjellvåg, H.** *Syntheses, Structures, and Magnetic Properties of Nickel-Doped Lepidocrocite Titanates* Inorg. Chem., **48**, 19, 9409–9418, 2009

2009-37. **Goossens, K., Lava, K., Nockemann, P., Van Hecke, K., Van Meervelt, L., Pattison, Ph., Binnemans, K., Cardinaels, Th.** *Pyrrolidinium Ionic Liquid Crystals with Pendant Mesogenic Groups* Langmuir, **25**, 10, 5881–5897, 2009

2009-38. **Grigoriev, S.V. , Chernyshov, D., Dyadkin, V.A., Dmitriev, V. et al.** *Crystal handedness and spin helix chirality in Fe_{1-x} Co_x Si* Phys. Rev. Letters, **102**, 0372204-0372208, 2009

2009-39. **Grigoriev, S., Napolskii, K., Grigoryeva, N., Vasilieva, A., Mistonov, A., Chernyshov, D., Petukhov, A. et al.** *Structural and magnetic properties of inverse opal photonic crystals studied by x-ray diffraction, scanning electron microscopy, and small-angle neutron scattering* Phys. Rev. B **79**, 045123-045131, 2009

2009-40. **Grunwaldt, J-D.** *Shining X-rays on catalysts at work* J. Phys.: Conf. Ser. **190**, 012151-012163, 2009

2009-41. **Grunwaldt, J-D., Van Vegten, N., Baiker, A., Van Beek, W.** *Insight into the structure of Pd/ZrO2 during the total oxidation of methane using combined in situ XRD, X-ray absorption and Raman spectroscopy* J. Phys.: Conf. Ser. **190**, 012160-012164, 2009

2009-42. **Hagemann, H., Filinchuk, Y., Chernyshov, D., Van Beek, W.** *Lattice anharmonicity and structural evolution of LiBH4: an insight from Raman and X-ray diffraction experiments* Phase Transitions A, **82**, 4, 344 – 355, 2009

2009-43. **Hamon, L., Llewellyn, Ph., Devic, Th., Ghoufi, A., Clet, G., Guillerm, V., Pirngruber, G. et al.** *Co-adsorption and Separation of CO_2 - CH_4 Mixtures in the Highly Flexible MIL-53(Cr) MOF* J. Am. Chem. Soc., **131**, 47, 17490–17499, 2009

2009-44. **Harvey, A., Litterst, F.J., Yang, Z., Ruppa, J.L.M., Infortuna, A., Gauckler, L.J.** *Oxidation states of Co and Fe in $Ba_{1-x}Sr_xCo_{1-y}Fe_yO_{3-\delta}$ (x, y = 0.2–0.8) and oxygen desorption in the temperature range 300–1273 K* Phys. Chem. Chem. Phys., **11**, 3090 - 3098, 2009

2009-45. **Helland, R., Larsen, R.L., Finstad, S., Kyomuhendo, P., Larsen, A.N.** *Crystal structures of g-type lysozyme from Atlantic cod shed new light on substrate binding and the catalytic mechanism* Cellular & Molec. Life Sci., **66**, 15, 2585-2598, 2009

2009-46. **Hemmen, H., Ringdal, N., De Azevedo, E., Engelsberg, M., Hansen, E. et al.** *The Isotropic-Nematic Interface in Suspensions of Na-Fluorohectorite Synthetic Clay* Langmuir, **25**, 21, 12507–12515, 2009

2009-47. **Hesske, H., Urakawa, A., Baiker, A.** *Ab Initio Assignments of FIR, MIR, and Raman Bands of Bulk Ba Species Relevant in NOx Storage-Reduction* J. Phys. Chem. C, **113,** 28, 12286–12292, 2009

2009-48. **Hoesch, M., Bosak, A., Chernyshov, D., Berger, H., Krisch, M.** *Giant Kohn Anomaly and the Phase Transition in Charge Density Wave $ZrTe_3$* Phys. Rev. Lett. **102**, 086402-086406, 2009

2009-49. **Horcajada, P., Serre, Ch., Grosso, D., Boissière, C., Perruchas, S., Sanchez, C., Férey, G.** *Colloidal Route for Preparing Optical Thin Films of Nanoporous Metal-Organic Frameworks* Advanced Materials, **21**, 19, 1931-1935, 2009

2009-50. **Horeglad, P., Nocton, G., Filinchuk, Y., Pécaut, J., Mazzanti, M.** *Pentavalent uranyl stabilized by a dianionic bulky tetradentate ligand* Chem. Commun., 1843 - 1845, 2009

2009-51. **Isci, Ü., Afanasiev, P., Millet, J.-M., Kudrik, E. V., Ahsen, V., Sorokin, A.** *Preparation and characterization of -nitrido diiron phthalocyanines with electron-withdrawing substituents: application for catalytic aromatic oxidation* Dalton Trans., 7410 - 7420, 2009

2009-52. **Jacquat, O., Voegelin, A., Juillot, F., Kretzschmar, R.** *Changes in Zn speciation during soil formation from Zn-rich limestones* Geochim. & Cosmochim. Acta, **73**, 19, 5554-5571, 2009

2009-53. **Jacquat, O., Voegelin, A., Kretzschmar, R.** *Soil properties controlling Zn speciation and fractionation in contaminated soils* Geochim. & Cosmochim. Acta, **73**, 18, 5256-5272, 2009

2009-54. **Jalarvo, N., Haavik, C., Kongshaug, C., Norby, P., Norby, T.** *Conductivity and water uptake of $Sr_4(Sr_2Nb_2)O_{11}{\cdot}nH_2O$ and $Sr_4(Sr_2Ta_2)O_{11}{\cdot}nH_2O$* Solid State Ionics, **180**, 20-22,1151-1156, 2009

2009-55. **Jantsky, L., Norby, P., Rosseinsky, M.J., Fjellvåg, H.** *Temperature dependant X-ray diffraction study of $PrSr_3Co_{1.5}Fe_{1.5}O_{10-d}$; n = 3 Ruddlesden-Popper phase* Z.Kristallogr., **224**, 5-6, 295-301, 2009

2009-56. **Johnsen, R.E., Norby, P.** *A Structural Study of Stacking Disorder in the Decomposition Oxide of MgAl Layered Double Hydroxide: A DIFFaX+ Analysis* J. Phys. Chem. C, **113**, 44, 19061–19066, 2009

2009-57. **Jorgensen, S.W., Chanine, R., Meyers, J. P., Parks, G. D., Pundt, A. A., Filinchuk, Y.** *Panel summary* Material issues in a Hydrogen Economy, 325-333, 2009

2009-58. **Joubert, J.-M., Tokaychuk, Ya., Cerný, R.** *Crystal structures of three intermetallic phases in the Mo-Pt-Si system* J. Solid State Chemistry, **183**, 1, 173-179, 2009

2009-59. **Kleist, W., Jutz, F., Maciejewski, M., Baiker, A.** *Mixed-Linker Metal-Organic Frameworks as Catalysts for the Synthesis of Propylene Carbonate from Propylene Oxide and CO_2* Eur. J. Inorganic Chem., **24**, 3552 - 3561, 2009

2009-60. **Kongmark, Ch., Martis, V., Rubbens, A., Pirovano, C., Löfberg, A., Sankar, G., Bordes-Richard, E., Vannier, R.-N., Van Beek, W.** *Elucidating the genesis of Bi_2MoO_6 catalyst by combination of synchrotron radiation experiments and Raman scattering* Chem. Commun., 4850 - 4852, 2009

2009-61. **Kristiansen, M., Smith, P., Chanzy, H., Baerlocher, Ch., Gramlich, V., McCusker, L., Weber, Th., Pattison, Ph. et al.** *Structural Aspects of 1,3,5-Benzenetrisamides-A New Family of Nucleating Agents* Cryst. Growth Des., **9**, 6, 2556–2558, 2009

2009-62. **Kumar, S., Carniato, F., Arrais, A., Croce, G., Boccaleri, E., Palin, L., Van Beek, W., Milanesio, M.** *Investigating Surface vs Bulk Kinetics in the Formation of a Molecular Complex via Solid-State Reaction by Simultaneous Raman/X-ray Powder Diffraction* Cryst.Growth. Design, **9**, 8, 3396–3404, 2009

2009-63. **Kumar, M.S., Hammer, N., Rønning, M., Holmen, A., De Chena, Walmsley, J.S., Øye, G.** *The nature of active chromium species in Cr-catalysts for dehydrogenation of propane: New insights by a comprehensive spectroscopic study* J. Catalysis, **261**, 1, 116-128, 2009

2009-64. **Kumar, S., Milanesio, M., Marchese, L., Boccaleri, E.** *Synthesis and characterization of host-guest materials obtained by inserting coumarin into hydrotalcite layers for LED applications* Physica status solidi (a), **206**, 9, 2171 - 2176, 2009

2009-65. **Le Bail, A., Cranswick, L. M. D., Adil, K.** *Third structure determination by powder diffractometry round robin (SDPDRR-3)* Powder Diffr., **24**, 3, 254-262, 2009

2009-66. **Leontyev, I., Chernyshov, D., Guterman, V., Pakhomova, E., Guterman, A.** *Particle size effect in carbon supported Pt–Co alloy electrocatalysts prepared by the borohydride method: XRD characterization* Applied Catalysis A: General , **357,** 1, 1-4, 2009

2009-67. **Leont'ev, I.N., Guterman, V. E., Pakhomova, E. B., Guterman, A. V., Mikheikin, A. S.** *Particle size effect in nanoscale Pt3Co/C electrocatalysts for low-temperature fuel cells* Nanotechnologies in Russia, **4**, 3-4, 170-175, 2009

2009-68. **Lethbridge, Z., Walton, R., Bosak, A., Krisch, M.** *Single crystal elastic constants of the zeolite analcime measured by inelastic X-ray scattering* Chemical Physics Letters, **471**, 4-6, 286-289, 2009

2009-69. **Livage, C., Guillou, N., Rabu, P., Pattison, Ph., Marrot, J., Ferey, G.** *Bulk homochirality of a 3-D inorganic framework: ligand control of inorganic network chirality* Chem. Commun., 4551 - 4553, 2009

2009-70. **Lima, F. A., Guarnieri, A. A., Pinheiro, C. B., Speziali, N. L.** *Modulated phase of $K_2Mo_xW_{1-x}O_4$ mixed compounds using orthorhombic symmetry: A powder diffraction study* Phys. Rev. B **79**, 174103-174109, 2009

2009-71. **Liu, L., Li, J., Dong, J., Sisak, D., Baerlocher, Ch., McCusker, L.B.** *Synthesis, Structure, and Characterization of Two Photoluminescent Zirconium Phosphate-Quinoline Compounds* Inorg. Chem., **48,** 18, 8947–8954, 2009

2009-72. **Llewellyn, P. L. , Horcajada, P., Maurin, G., Devic, T., Rosenbach, N., Bourrelly, S., Serre, C. et al.** *Complex Adsorption of Short Linear Alkanes in the Flexible Metal-Organic-Framework MIL-53(Fe)* J. Am. Chem. Soc., **131**, 36, 13002–13008, 2009

2009-73. **Lototsky, M.V., Denys, R.V., Yartys, V.A.** *Combustion-Type Hydrogenation of Nanostructured Mg-Based Composites* Int. J. Energy Rerearch, **33**, 13, 1099-1250, 2009

2009-74. **McCusker, L., Baerlocher, Ch.** *Using electron microscopy to complement X-ray powder diffraction data to solve complex crystal structures* Chem. Commun., 1439 - 1451, 2009

2009-75. **Makowski, S., Rodgers, J., Henry, P., Attfield, J., Bos, J.-W.** *Coupled Spin Ordering in the Ln_2LiRuO_6 Double Perovskites* Chem. Mater., **21**, 2, 264–272, 2009

2009-76. **Marchal, C., Filinchuk, Y., Chen, X.-Y., Imbert, D., Mazzanti, M.** *Lanthanide-Based Coordination Polymers Assembled by a Flexible Multidentate Linker: Design, Structure, Photophysical Properties, and Dynamic Solid-State Behavior* Chemistry - A European J., **15**, 21, 5273-5288, 2009

2009-77. **Marques, J., Braga, T.M., Almeida Paz, F.A.A., Santos, T.M., Lopes, M.F.S., Braga, S.S.** *Cyclodextrins improve the antimicrobial activity of the chloride salt of Ruthenium(II) chloro-phenanthroline-trithiacyclononane* BioMetals, **22**, 3, 541-556, 2009

2009-78. **Martinelli, A., Palenzona, A., Ferdeghini, C., Putti, M., Emerich, H.** *Tetragonal to orthorhombic phase transition in SmFeAsO: A synchrotron powder diffraction investigation* J. Alloys & Compounds, **477**, 1-2, L21-L23, 2009

2009-79. **Martinez-Garcia, J., Arakcheeva, A., Pattison, P., Morozov, V., Chapuis, G.** *Validating the model of a (3 + 1)-dimensional incommensurately modulated structure as generator of a family of compounds for the $Eu_2(MoO_4)_3$ scheelite structure* Philosophical Mag. Letters, **89**, 4, 257 - 266, 2009

2009-80. **Mathisen, K., Stockenhuber, M., Nicholson, D.** *In situ XAS and IR studies on Cu:SAPO-5 and Cu:SAPO-11: the contributory role of monomeric linear copper(I) species in the selective catalytic reduction of NO_x by propene* Phys. Chem. Chem. Phys., **11**, 5476 - 5488, 2009

2009-81. **Maurin, I., Chernyshov, D., Varret, F., Bleuzen, A., Tokoro, H., Hashimoto, K., Ohkoshi, Sh.** *Evidence for complex multistability in photomagnetic cobalt hexacyanoferrates from combined magnetic and synchrotron x-ray diffraction measurements* Phys. Rev. B **79**, 064420- 064429, 2009

2009-82. **Meersman, F., Cabrera, R., McMillan, P., Dmitriev, V.** *Compressibility of insulin amyloid fibrils determined by X-ray diffraction in a diamond anvil cell* High Pressure Research, **29**, 4, 665 - 670, 2009

2009-83. **Miller, S., Wright, P., Devic, Th., Serre, Ch., Frey, G., Llewellyn, Ph., Denoyel, R., Gaberova, L., Filinchuk, Y.** *Single Crystal X-ray Diffraction Studies of Carbon Dioxide and Fuel-Related Gases Adsorbed on the Small Pore Scandium Terephthalate Metal Organic Framework, $Sc_2(O_2CC_6H_4CO_2)_3$* Langmuir, **25**, 6, 3618–3626, 2009

2009-84. **Mo, F., Ramsøskar, K.** *A sample cell for diffraction studies with control of temperature, relative humidity and applied electric field* J. Appl. Cryst., **42**, 531-534, 2009

2009-85. **Moreno-Calvo, E., Gbabode, G., Cordobilla, R., Calvet, T., Cuevas-Diarte, M.-A.,Negrier, Ph., Mondieig, D.** *Competing Intermolecular Interactions in the High-Temperature Solid Phases of Even Saturated Carboxylic Acids ($C_{10}H_{19}O_2H$ to $C_{20}H_{39}O_2H$)* Chemistry – A Europ. J., **15**, 47, 13141-13149, 2009

2009-86. **Muller, J. , Skjeltorp, A. T., Helgesen, G., Knudsen, K. D., Heiberg-Andersen, H.** *Carbon discs and carbon cones - new high risk materials for nano-sensors with*

low detection limit and fast kinetics NATO Science for Peace and security series B:Physics and Biophysics, 285-292, 2009

2009-87. **Naess, S.N., Elgsaeter, A., Helgesen, G., Knudsen, K.D.** *Carbon nanocones: wall structure and morphology* Sci. Technol. Adv. Mater., **10**, 065002-065008, 2009

2009-88. **Narkhede, V.V., Gies, H.** *Crystal Structure of MCM-22 (MWW) and Its Delaminated Zeolite ITQ-2 from High-Resolution Powder X-Ray Diffraction Data: An Analysis Using Rietveld Technique and Atomic Pair Distribution Function* Chem. Mater., **21**, 18, 4339–4346, 2009

2009-89. **Nordhei, C., Mathisen, K., Safonova, O., Van Beek, W., Nicholson, D.** *Decomposition of Carbon Dioxide at 500 °C over Reduced Iron, Cobalt, Nickel, and Zinc Ferrites: A Combined XANES-XRD Study* J. Phys. Chem. C, **113,** 45, 19568–19577, 2009

2009-90. **Okamoto, H., Karppinen, M., Yamauchi, H., Fjellvåg, H.** *High-temperature synchrotron X-ray diffraction study of $LaMn_7O_{12}$* Solid State Sciences, **11**, 7, 1211-1215, 2009

2009-91. **Pedersen, H., Willassen, N., Leiros, I.** *The first structure of a cold-adapted superoxide dismutase (SOD): biochemical and structural characterization of iron SOD from Aliivibrio salmonicida* Acta Cryst., F, **65**, 2, 84-92, 2009

2009-92. **Peters, T.A., Tucho, W.M., Ramachandran, A., Stange, M., Walmsley, J.C., Holmestad, R. , Borg, A. , Bredesen, R.** *Thin Pd–23%Ag/stainless steel composite membranes: Long-term stability, life-time estimation and post-process characterisation* J. Membrane Science, **326**, 572-581, 2009

2009-93. **Pirngruber, G.D., Frunz, L., Lüchinger, M.** *The characterisation and catalytic properties of biomimetic metal–peptide complexes immobilised on mesoporous silica* Phys. Chem. Chem. Phys., **11**, 2928 - 2938, 2009

2009-94. **Pregelj, M., Zaharko, O. , Zorko, A., Kutnjak, Z., Jeglic, P., Brown, P. J., Jagodic, M. et al.** *Spin Amplitude Modulation Driven Magnetoelectric Coupling in the New Multiferroic $FeTe_2O_5Br$* Phys. Rev. Lett. **103**, 147202-147206, 2009

2009-95. **Ravnsbaek, D., Filinchuk, Y., Cerenius, Y., Jakobsen, H.J., Besenbacher, F., Skibsted, J., Jensen, T.R.** *A Series of Mixed-Metal Borohydrides* Angewandte Chem. Int. Ed., **48**, 36, 6659 - 6663, 2009

2009-96. **Riis-Johannessen, Th., Bernardinelli, G., Filinchuk, Y., Clifford, S., Favera, N.D., Piguet, C.** *Self-Assembly of the First Discrete 3d-4f-4f Triple-Stranded Helicate* Inorg. Chem., **48,** 12, 5512–5525, 2009

2009-97. **Riktor, M. D., Sørby, M. H., Chopek, K., Fichtner, M., Hauback, B. C.** *The identification of a hitherto unknown intermediate phase CaB_2H_x from decomposition of Ca $(BH_4)_2$* J. Mater. Chem., **19**, 2754 - 2759, 2009

2009-98. **Riktor, M., Deledda, S., Herrich, M., Gutfleisch, M., Fjellvåg, H., Hauback, B.** *Hydride formation in ball-milled and cryomilled Mg–Fe powder mixtures* Mater. Science and Engineering: B, **158**, 1-3, 19-25, 2009

2009-99. **Rohlícek, J., Husák, M., Kratochvíl, B., Jegorov, A.** Methylergometrine maleate from synchrotron powder diffraction data Acta Cryst., E**65**, o3252-o3253, 2009

2009-100. **Ropka, J., Cerny, R., Paul-Boncour, V., Proffen, Th.** *Deuterium ordering in laves-phase deuteride $YFe_2D_{4.2}$* J. Solid State Chemistry,**182**, 7, 1907-1912, 2009

2009-101. **Roslyakov, I., Napol'skii, K., Eliseev, A., Lukashin, A., Chernyshov, D., Grigor'ev, S.** *Preparing magnetic nanoparticles with controllable anisotropy of functional properties within a porous matrix of alumina* Nanotechnologies in Russia, **4**, 3-4, 2009

2009-102. **Rozynek, Z., Wang, B., Zhou, M., Fossum, J. O.** *Dynamic column formation in Na-FLHC clay particles: Wide angle X-ray scattering and rheological studies* J. Phys.: Conf. Ser. **149**, 012026-012031, 2009

2009-103. **Salles, F., Kolokolov, D., Jobic, H., Maurin, G., Llewellyn, Ph., Devic, Th., Serre, Ch., Ferey, G.** *Adsorption and Diffusion of H_2 in the MOF Type Systems MIL-47(V) and MIL-53(Cr): A Combination of Microcalorimetry and QENS Experiments with Molecular Simulations* J. Phys. Chem. C, **113**, 18, 7802–7812, 2009

2009-104. **Salvadó, N., Butí, S., Nicholson, J., Emerich, H., Labrador, A., Pradell, T.** *Identification of reaction compounds in micrometric layers from gothic paintings using combined SR-XRD and SR-FTIR* Talanta, **79**, 419-428, 200

2009-105. **Sato, T., Sorby, M.H., Ikeda, K., Sato, S., Hauback, B.C., Orimo, S.** *Syntheses, Crystal Structures, and Thermal Analyses of Solvent-free $Ca(AlD_4)_2$ and $CaAlD_5$* J. Alloys & Compounds, **487**, 472-478, 2009

2009-106. **Sartori, S., Istad-Lem, A., Brinks, H.W., Hauback, B.C.** *Mechanochemical synthesis of alane* Int. J. Hydrogen Energy, **34,** 15, 6350-6356, 2009

2009-107. **Sartori, S., Knudsen, K., Zhao-Karger, Z., Bardaij, E., Fichtner, M., Hauback, B. C.** Small-angle scattering investigations of Mg-borohydride infiltrated in activated carbon Nanotechnology, **20**, 505702-505702, 2009

2009-108. **Sereda, O., Stoeckli, F., Stoeckli-Evans, H., Dolomanov, O., Filinchuk, Y., Pattison, Ph.** *A New Family of Bimetallic Framework Materials Showing Reversible Structural Transformations* Cryst. Growth Des., **79**, 419-428, 2009

2009-109. **Sereda, O., Stoeckli-Evans, H., Dolomanov, O., Filinchuk, Y., Pattison, Ph.** *Transformation of a Chiral Nanoporous Bimetallic Cyano-Bridged Framework Triggered by Dehydration/Rehydration* Cryst. Growth Des., **9**, 7, 3168–3176, 2009

2009-110. **Sharova, N., Fjellvåg, H., Norby, T.** *Structure, defect chemistry, and proton conductivity in nominally Sr-doped $Ba_3La(PO_4)_3$* Solid State Ionics, **180**, 4-5, 338-342, 2009

2009-111. **Smrcok, L., Bitschnau, B., Filinchuk, Y.** *Low temperature powder diffraction and DFT solid state computational study of hydrogen bonding in NH_4VO_3* Crystal Research and Technology, **44**, 9, 978-984, 2009

2009-112. **Snellings, R., Mertens, G., Hertsens, S., Elsen, J.** *The zeolite-lime pozzolanic reaction: reaction kinetics and products by in-situ synchrotron x-ray powder diffraction* Microp.& Mesop. Mat., **126**,1-2, 40-49, 2009

2009-113. **Steurer, W., Deloudi, S.** *Crystallography of Quasicrystals Concepts, Methods and Structures* Springer, 2009

2009-114. **Struis, R.P.W.J., Bachelin, D., Ludwig, Ch., Wokaun, A.** *Studying the Formation of Ni_3C from CO and Metallic Ni at T = 265 °C in Situ Using Ni K-Edge X-ray Absorption Spectroscopy* J. Phys. Chem. C, **113**, 6, 2443–2451, 2009

2009-115. **Struis, R.P.W.J., Schildhauer, T., Czekaj, I., Janousch, M., Biollaz, S., Ludwig, Ch.** *Sulphur poisoning of Ni catalysts in the SNG production from biomass: A TPO/XPS/XAS study* Applied Catalysis A: Gen., **362**,1-2, 2009

2009-116. **Strutz, A., Yamamoto, A., Steurer, W.** *Basic Co-rich decagonal Al-Co-Ni: Average structure* Phys. Rev. B **80**, 184102-184111, 2009

2009-117. **Sulzer-Mossé, S., Alexakis, A., Mareda, J., Bollot, G., Bernardinelli, G., Filinchuk, Y.** *Enantioselective Organocatalytic Conjugate Addition of Aldehydes to Vinyl Sulfones and Vinyl Phosphonates as Challenging Michael Acceptors* Chemistry - A European J., **15**, 13, 3204 - 3220, 2009

2009-118. **Szlachcic, A., Zakrzewska, M., Krowarsch, D., Os, V., Helland, R., Smalås, A. O., Otlewski, J.** *Structure of a highly stable mutant of human fibroblast growth factor 1* Acta Cryst., D**65**, 67-73, 2009

2009-119. **Takabayashi, Y., Ganin, A., Jeglic, P., Arcon, D., Takano, T., Iwasa, Y., Ohishi, Y. et al.** *The Disorder-Free Non-BCS Superconductor Cs3C60 Emerges from an Antiferromagnetic Insulator Parent State* Science, **323**, 5921, 1585 - 1590, 2009

2009-120. **Talyzin, A., Sundqvist, B., Szab, T., Dekany, I., Dmitriev, V.** *Pressure-Induced Insertion of Liquid Alcohols into Graphite Oxide Structure* J. Am. Chem. Soc., **131**, 51, 18445-18449, 2010

2009-121. **Tucho, W. M., Venvik, H. J., Walmsley, J. C., Stange, M., Ramachandran, A., Mathiesen, R. H. et al.** *Microstructural studies of self-supported (1.5–10 $m*10^{-6}$) Pd/23 wt%Ag hydrogen separation membranes subjected to different heat treatments* J. Materials Science, **44,** 16, 4429-4442, 2009

2009-122. **Van Beek, W., Carniato, F., Kumar, S., Croce, G., Boccaleri, E., Milanesio, M.** *Studying modifications and reactions in materials by simultaneous Raman and X-ray powder diffraction at non-ambient conditions: methods and applications* Phase Transitions A, **82,** 4, 293 – 302, 2009

2009-123. **Van Mechelen, J. B., Peschar, R., Schenk, H.** *Structure and polymorphism of trans mono-unsaturated triacylglycerols* Zeitschrift für Kristallographie Suppl., **30**, 491-495, 2009

2009-124. **Van Vegten, N., Maciejewski, M., Krumeich, F., Baiker, A.** *Structural properties, redox behaviour and methane combustion activity of differently supported flame-made Pd catalysts* Applied Catalysis B: Environmental, **93**, 1-2, 38-49, 2009

2009-125. **Wang, B., Rozynek, Z., Zhou, M., Fossum, J. O.** *Wide angle scattering study of nanolayered clay/gelatin electrorheological elastomer* J. Phys.: Conf. Ser. **149**, 012032-012038, 2009

2009-126. **Weber, T., Dshemuchadse, J., Kobas, M., Conrad, M., Harbrecht, B., Steurer, W.** *Large, larger, largest - a family of cluster-based tantalum copper aluminides with giant unit cells*. I. Structure solution and refinement Acta Cryst., B**65**, 308-317, 2009

2009-127. **Williams, M. , Nechaev, A.N., Lototsky, M.V. , Yartys, V.A. , Solberg, J.K., Denys, R.V. et al.** *Influence of aminosilane surface functionalization of rare earth hydride-forming alloys on palladium treatment by electroless deposition and hydrogen sorption kinetics of composite materials* Materials Chem. & Physics, **115**, 1, 136-141, 2009

2009-128. **Wragg, D.S., Johnsen, R. E., Balasundaram, M., Norby, P., Fjellvåg, H., Grønvold, A. et al.** *SAPO-34 methanol-to-olefin catalysts under working conditions: A combined in situ powder X-ray diffraction, mass spectrometry and Raman study* J. Catalysis, **268**, 290-296, 2009

2009-129. **Xie, D., McCusker, L.B., Baerlocher, Ch., Gibson, L., Burton, A.W., Hwang, S.-J.** *Optimized Synthesis and Structural Characterization of the Borosilicate MCM-70* J. Phys. Chem. C, **113**, 22, 9845–9850, 2009

2009-130. **Xu, H., Weeks, Ch. M., Blessing, R. H.** *Powder Shake-and-Bake Method* Zeitschrift für Kristallographie Suppl., **30**, 221-226, 2009

2009-131. **Yáng, Z. , Harvey, A. S., Infortuna, A., Gauckler, L. J.** *Phase relations in the Ba-Sr-Co-Fe-O system at 1273 K in air* J. Appl. Cryst., **42**, 153-160, 2009

2009-132. **Zanardi, S., Dalconi, M.C., Gambaro, C., Bellussi, G., Millini, R. et al.** *Investigation on the hydrated and dehydrated forms of the ion-exchanged microporous stannosilicate EMS-2* Microp. & Mesop. Mat., **117**, 1-2, 414-422, 2009

2009-133. **Zarechnaya, E. Yu., Dubrovinsky, L., Dubrovinskaia, N., Filinchuk, Y., Chernyshov, D., Dmitriev, V. et al.** *Superhard Semiconducting Optically Transparent High Pressure Phase of Boron* Phys. Rev. Lett. **102**, 185501- 185505, 2009

2010

2010-1. **Arakcheeva, A., Bindi, L., Pattison, Ph., Meisser, N., Chapuis, G., Pekov, I.** *The incommensurately modulated structures of natural natrite at 120 and 293 K from synchrotron X-ray data* American Mineralogist, **95**, 4, 574-581, 2010

2010-2. **Arletti, R., Quartieri, S., Vezzalini, G.** *Elastic behavior of zeolite boggsite in silicon oil and aqueous medium: A case of high-pressure-induced over-hydration* American Mineralogist, **95**, 8-9, 1247-1256, 2010

2010-3. **Babanova, O. A., Soloninin, A.V., Stepanov, A.P., Skripov, A.V., Filinchuk, Y.** *Structural and Dynamical Properties of $NaBH_4$ and KBH_4: NMR and Synchrotron X-ray Diffraction Studies* J. Phys. Chem. C, **114**, 8, 3712-3718, 2010

2010-4. **Bailey, E., McMillan, P. F.** *High pressure synthesis of superconducting nitrides in the MoN–NbN system* J. Mater. Chem., **20**, 4176-4182, 2010

2010-5. **Basso, S., Besnard, C., Wright, J. P., Margiolaki, I., Fitch, A., Pattison, P., Schiltz, M.** *Features of the secondary structure of a protein molecule from powder diffraction data* Acta Cryst., D**66**, 756-761, 2010

2010-6. **Behrnd, N.-R., Labat, G., Venugopalan, P., Hulliger, J., Bürgi, H.-B.** *Influence of the solvent of crystallization on the orientational disorder of (trans)-4-chloro-4'-nitrostilbene* CrystEngComm, **12**, 4101-4108, 2010

2010-7. **Behrnd, N.-R., Labat, G., Venugopalan, P., Hulliger, J., Bürgi, H.-B.** *Orientational Disorder of (trans)-4-Chloro-4'-nitrostilbene: A Detailed Analysis by Single Crystal X-ray Diffraction* Cryst. Growth Des., **10**, 1, 52– 59, 2010

2010-8. **Bell, A. M. T., Knight, K. S. , Henderson, C. M. B., Fitch, A. N.** *Revision of the structure of $Cs_2CuSi_5O_{12}$ leucite as orthorhombic Pbca* Acta Cryst., B**66**, 51-59, 2010

2010-9. **Bosak, A. , Chernyshov, D., Krisch, M., Dubrovinsky, L.** *Symmetry of platelet defects in diamond: new insights with synchrotron light* Acta Cryst., B**66**, 493-496, 2010

2010-10. **Bösenberg, Ul., Ravnsbæk, D.B., Hagemann, H., D'Anna, V., Minella, Ch. B., Pistidda, C., Van Beek, W. et al**. *Pressure and Temperature Influence on the Desorption Pathway of the $LiBH_4$-MgH_2 Composite* System J. Phys. Chem. C, **114**, 35, 15212–15217, 2010

2010-11. **Bourrelly, S., Moulin, B., Rivera, A., Maurin, G., Devautour-Vinot, S., Serre, Ch. et al.** *Explanation of the Adsorption of Polar Vapors in the Highly Flexible Metal Organic Framework MIL-53(Cr)* J. Am. Chem. Soc., **132**, 27, 9488–9498, 2010

2010-12. **Cerny, R., Kim, K.Ch., Penin, N., D'Anna, V., Hagemann, V., Sholl, D. S.** *$AZn_2(BH_4)_5$ (A = Li, Na) and $NaZn(BH_4)_3$: Structural Studies* J. Phys. Chem. C, **114**, 44, 19127–19133, 2010

2010-13. **Cerny, R., Ravnsbæk, D.B., Severa, G., Filinchuk, Y., D' Anna, V., Hagemann, H., Haase, D. et al.** *Structure and Characterization of $KSc(BH_4)_4$* J. Phys. Chem. C, **114**, 45, 19540–19549, 2010

2010-14. **Cerny, R., Severa, G., Ravnsbæk, D.B., Filinchuk, Y., D'Anna, V. et al.** $NaSc(BH_4)_4$: A Novel Scandium-Based Borohydride J. Phys. Chem. C, **114,** 2, 1357–1364, 2010

2010-15. **Chernyshov, D., Bosak, A.** *Diffuse scattering and correlated disorder in manganese analogue of Prussian blue* Phase Transitions, **83,** 2, 115 - 122, 2010

2010-16. **Denys, R.V., Poletaev, A. A., Solberg, J. K., Tarasov, B. P., Yartys, V. A.** *$LaMg_{11}$ with a giant unit cell synthesized by hydrogen metallurgy: Crystal structure and hydrogenation behavior* Acta Materialia, **58,** 7, 2510-2519, 2010

2010-17. **Devic, Th., Horcajada, P., Serre, Ch., Salles, F., Maurin, G., Moulin, B. et al.** *Functionalization in Flexible Porous Solids: Effects on the Pore Opening and the Host-Guest Interactions* J. Am. Chem. Soc., **132,** 3,1127–1136, 2010

2010-18. **De Smit, E., Cinquini, F., Beale, A.M., Safonova, O., Van Beek, W., Sautet, Ph., Weckhuysen, B. M.** *Stability and Reactivity of $\epsilon-\chi-\theta$ Iron Carbide Catalyst Phases in Fischer-Tropsch Synthesis: Controlling μ_C* J. Am. Chem. Soc., **132**, 42, 14928–14941, 2010

2010-19. **Eyssler, A., Mandaliev, P., Winkler, A., Hug, P., Safonova, O., Figi, R., Weidenkaff, A., Ferri, D.** *The Effect of the State of Pd on Methane Combustion in Pd-Doped $LaFeO_3$* J. Phys. Chem. C, **114**, 4584-4594, 2010

2010-20. **Filinchuk, Y.** *Light Metal Hydrides Under Non-Ambient Conditions: Probing Chemistry by Diffraction?* High-Pressure Crystallography, Series B: Physics and Biophysics, **0**, 281-291, 2010

2010-21. **Filinchuk, Y., Talyzin, A., Hagemann, H., Dmitriev, V., Chernyshov, D., Sundqvist, B.** *Cation Size and Anion Anisotropy in Structural Chemistry of Metal Borohydrides. The Peculiar Pressure Evolution of $RbBH_4$* Inorg. Chem., **49**, 11, 5285–5292, 2010

2010-22. **Fleischer, F., Weber, T., Jung, D.Y., Steurer, W.** *o'-$Al_{13}Co_4$, a new quasicrystal approximant* J. Alloys & Compounds, **500**, 2, 153-160, 2010

2010-23. **Fleischer, F., Weber, T., Steurer, W.** *Ab initio structure solution of decagonal quasicrystals by iterative dual space methods: Performance tests on synthetic and experimental data* J. Phys.: Conf. Ser., **226**, 012002-012009, 2010

2010-24. **Frommen, Ch., Aliouane, N., Deledda, S., Fonneløp, J. E., Grove, H., Lieutenant, K., Llamas-Jansa, I. et al.** *Crystal structure, polymorphism, and thermal properties of Yttrium borohydride $Y(BH_4)_3$* J. Alloys & Compounds, **496**, 1-2, 710-716, 2010

2010-25. **Gao, T. Norby, P., Krumeich, F., Okamoto, H., Nesper, R., Fjellvåg, H.** *Synthesis and Properties of Layered-Structured Mn_5O_8 Nanorods* J. Phys. Chem. C, **114**, 2, 922–928, 2010

2010-26. **Gorfman, S., Schmidt, O., Ziolkowski, M., Von Kozierowski, M., Pietsch, U.** *Time-resolved x-ray diffraction study of the piezoelectric crystal response to a fast change of an applied electric field* J. Appl. Phys., **108**, 064911- 064917, 2010

2010-27. **Grigoriev, S. V., Chernyshov, D., Dyadkin, V. A., Dmitriev, V., Moskvin, E. V., Lamago, D., Wolf, Th. et al.** *Interplay between crystalline chirality and magnetic structure in $Mn_{1-x}Fe_xSi$* Phys. Rev. B **81**, 1, 012408-012412, 2010

2010-28. **Hagemann, H., Cerný, R.** *Synthetic approaches to inorganic borohydrides* Dalton Trans., **39**, 6006 - 6012, 2010

2010-29. **Hong, J., Chu, W., Chernavskii, P.A., Khodakov, A.Y.** *Cobalt species and cobalt-support interaction in glow discharge plasma-assisted Fischer–Tropsch catalysts* J. Catalysis, **273**, 1, 9-17, 2010

2010-30. **Howard, J. A. K., Yufit, D. S., Chetina, O. V., Teat, S. J., Capelli, S. C., Pattison, Ph.** *Crystal structure of the insect neuropeptide proctolin* Org. Biomol. Chem., **8**, 5110-5112, 2010

2010-31. **Hušák, M., Kratochvíl, B., Jegorov, A., Brus, J., Maixner, J., Rohlícek, R.** *Simvastatin: structure solution of two new low-temperature phases from synchrotron powder diffraction and ss-NMR* Structural Chemistry, **21**, 3, 511-518, 2010

2010-32. **Huys, D., Van Deun, R., Pattison, P., Van Meervelt, L., Van Hecke, K.** *Redetermination of di-[mu]-hydroxido-bis[diaquachloridodioxidouranium(VI)] from single-crystal synchrotron data* Acta Cryst., E**66**, 2, 11, 2010

2010-33. **Jensen, T. R., Nielsen, T. K., Filinchuk, Y., Jørgensen, J.-E., Cerenius, Y., Gray, E. M., Webb, C. J.** *Versatile in situ powder X-ray diffraction cells for solid-gas investigations* J. Appl. Cryst., **43**, 6, 2010

2010-34. **Johnsen, R. E., Krumeich, F., Norby, P.** *Structural and microstructural changes during anion exchange of CoAl layered double hydroxides: an in situ X-ray powder diffraction study* J. Appl. Cryst., **43**, 434-447, 2010

2010-35. **Karaca, H., Hong, J., Fongarland, P., Roussel, P., Griboval-Constant, A., Lacroix, M., Hortmann, K., Safonova, O., Khodakov, A.** *In situ XRD investigation of the evolution of alumina-supported cobalt catalysts under realistic conditions of Fischer-Tropsch synthesis* Chem. Commun., **46**, 788 - 790, 2010

2010-36. **Kleist, W., Maciejewski, M., Baiker, A.** *MOF-5 Based Mixed-Linker Metal-Organic Frameworks: Synthesis, Thermal Stability and Catalytic Application* Thermochimica Acta, **499**, 1-2, 71-78, 2010

2010-37. **Kohlmann, H.** *Solid-State Structures and Properties of Europium and Samarium Hydrides* Eur. J. Inorganic Chemistry, **18**, 2582 - 2593, 2010

2010-38. **Kongmark, C., Martis, V., Pirovano, C., Löfberg, A., Van Beek, W., Sankar, G., Rubbens, A., Cristol, S. et al.** *Synthesis of γ-Bi_2MoO_6 catalyst studied by combined high-resolution powder diffraction, XANES and Raman spectroscopy* Catalysis Today, **157**, 1-4, 257-262, 2010

2010-39. **Kyomuhendo, P., Myrnes, B., Brandsdal, B.-O., Smalås, A.O., Nilsen, I.W. Helland, R.** *Thermodynamics and structure of a salmon cold active goose-type lysozyme* Comparative Biochem. & Physiology, Part B: Biochem. & Molec. Biology, **156,** 4, 254-263 , 2010

2010-40. **Leardini, L., Quartieri, S., Vezzalin, G.** *Compressibility of microporous materials with CHA topology: 1. Natural chabazite and SAPO-34* Microp. & Mesop. Materials, **127**, 3, 219-227, 2010

2010-41. **Leontyev, I.N., Guterman, V.E., Pakhomova, E.B., Timoshenko, P.E., Guterman, A.V. et al.** *XRD and electrochemical investigation of particle size effects in platinum–cobalt cathode electrocatalysts for oxygen reduction* J. Alloys & Compounds, **500**, 2, 241-246, 2010

2010-42. **Liarokapis, E., Lampakis, D., Siranidi, E., Calamiotou, M.** *Pressure induced lattice instability and phase separation in the cuprates* J. Phys.& Chem. Solids, **71**, 8, 1084-1087, 2010

2010-43. **Lindemann, I., Ferrer, R.D., Dunsch, L., Filinchuk, Y., Cerný, R. et al.** *$Al_3Li_4(BH_4)_{13}$: A Complex Double-Cation Borohydride with a New Structure* Chemistry - A Eur. J., **16**, 29, 8707-8712, 2010

2010-44. **Logvinovich, D., Arakcheeva, A.., Pattison, P., Eliseeva, S., Tome, P., Marozau, I., Chapuis, G.** *Crystal Structure and Optical and Magnetic Properties of $Pr_2(MoO_4)_3$* Inorg. Chem., **49**, 4, 1587-1594, 2010

2010-45. **Machon, D., Pinheiro, C. B., Bouvier, P., Dmitriev, V. P., Crichton, W. A.** *Absence of pressure-induced amorphization in $LiKSO_4$* J. Phys.: Condens. Matter, **22**, 31,5401-5408, 2010

2010-46. **McMillan, P. F., Daisenberger, D., Cabrera, R. Q., Meersman, F.** *Amorphous X-Ray Diffraction at High Pressure: Polyamorphic Silicon and Amyloid Fibrils* High-Pressure Cryst., NATO Science for Peace and Security Series B: Phys. & Biophys., **0**, 469-479, 2010

2010-47. **Meersman, F., Geukens, B., Wbbenhorst, M., Leys, Ja., Napolitano, S., Filinchuk, Y. et al.** *Dynamics of the Crystal to Plastic Crystal Transition in the Hydrogen Bonded N-Isopropylpropionamide* J. Phys. Chem. B, **114**, 44, 13944–13949, 2010

2010-48. **Mikutta, Ch., Frommer, J., Voegelin, A., Kaegi, R., Kretzschmar, R.** *Effect of citrate on the local Fe coordination in ferrihydrite, arsenate binding, and ternary arsenate complex formation* Geochimica et Cosmochimica Acta, **74,** 19, 5574-5592, 2010

2010-49. **Minkov, V., Tumanov, N., Cabrera, R., Boldyreva, E.** *Low temperature/high pressure polymorphism in DL-cysteine*CrystEngComm, **12**, 2551 - 2560, 2010

2010-50. **Moreira, J. A., Almeida, A., Ferreira, W. S., Araújo, J. P., Pereira, A. M., Chaves, M. R., Costa, M. M. R., Khomchenko, V. A., Kreisel, J., Chernyshov, D. et al.** *Strong magnetoelastic coupling in orthorhombic $Eu_{1-x}Y_xMnO_3$ manganite* Phys. Rev. B **82**, 094418-094427, 2010

2010-51. **Morozov. V., Arakcheeva, A., Konovalova, V., Pattison, Ph., Chapuis, G., Lebedev, O., Fomichevd, V., Van Tendeloo, G.** *$LiZnNb_4O_{11.5}$: A novel oxygen deficient compound in the Nb-rich part of the Li_2O-ZnO-Nb_2O_5 system* J. Solid State Chemistry, **183**, 2, 408-418, 2010

2010-52. **Mudu, F., Arstad, B., Bakken, E., Fjellvåg, H., Olsbye, U.** *Perovskite-type oxide catalysts for low temperature, anaerobic catalytic partial oxidation of methane to syngas* J. Catalysis, **275**, 1, 25-33, 2010

2010-53. **Napolskii, K., Sapoletova, N., Gorozhankin, D., Eliseev, A., Chernyshov, D., Byelov, D. et al.** *Fabrication of Artificial Opals by Electric-Field-Assisted Vertical Deposition* Langmuir, **26,** 4, 2346-2351, 2010

2010-54. **Newton, M. A., Van Beek, W.** *Combining synchrotron-based X-ray techniques with vibrational spectroscopies for the in situ study of heterogeneous catalysts: a view from a bridge* Chem. Soc. Rev., **39**, 4845-4863, 2010

2010-55. **Nguyen, Th. L. A., Demir-Cakan, R., Devic, Th., Morcrette, M., Ahnfeldt, T., Auban-Senzier, P., Stock, N., Goncalves, A.-M., Filinchuk, Y. et al.** *3-D Coordination Polymers Based on the Tetrathiafulvalenetetracarboxylate (TTF-TC) Derivative: Synthesis, Characterization, and Oxidation Issues* Inorg. Chem., **49**, 15, 7135–7143, 2010

2010-56. **Nguyen, Th. L. A., Devic, Th., Mialane, P., Rivire, E., Sonnauer, A. Stock, N. et al.** *Reinvestigation of the M^{II} (M = Ni, Co)/TetraThiafulvaleneTetraCarboxylate System Using High-Throughput Methods: Isolation of a Molecular Complex and Its Single-Crystal-to-Single-Crystal Transformation to a Two-Dimensional Coordination Polymer* Inorg. Chem., **49,** 22, 10710–10717, 2010

2010-57. **Nocton, G., Pécaut, J., Filinchuk, Y., Mazzanti, M.** *Ligand assisted cleavage of uranium oxo-clusters* Chem. Commun., **46**, 2757-2759, 2010

2010-58. **Okamoto, H., Imamura, N.., Karppinen, M., Yamauchi, H., Fjellvåg, H.** *Crystal structure of the monoclinic and cubic polymorphs of $BiMn_7O_{12}$* J. Solid State Chemistry, **83**, 1, 186-191, 2010

2010-59. **Okamoto, H., Imamura, N., Karppinen, M., Yamauchi, H., Fjellvag, H.** Square Coordinated MnO_2-Units in $BiMn_7O_{12}$ Inorg. Chem., **49**, 19, 8709–8712, 2010

2010-60. **Papoular, R.J., Dmitriev, V., Davydov, V.A. et al.** *Study of the Orthorhombic Polymeric Phase of C_{60} Under High Pressure Using Synchrotron X-Ray Powder*

Diffraction Fullerenes, Nanotubes & Carbon Nanostructures, **18**, 4-6, 392-395, 1, 2010

2010-61. **Papoular, R. J., Le Parc, R., Dmitriev, V., Davydov, V. A., Rakhmanina, A. V., Agafonov, V.** *First Observation of the FCC to Trigonal/Rhombohedral Transition of Pure Dimerized C_{60} Under High Pressure* Fullerenes, Nanotubes & Carbon Nanostructures, **18**, 4-6, 386-391, 1, 2010

2010-62. **Pekov I. V., Zubkova N. V., Filinchuk Ya. E., Chukanov N. V., Zadov A. E., Pushcharovsky D. Yu., Gobechia E. R.** *Shlykovite $KCa[Si_4O_9(OH)]\cdot 3H_2O$ and cryptophyllite $K_2Ca[Si_4O_{10}]\cdot 5H_2O$-new minerals from Khibiny alkaline massif (Kola Peninsula, Russia)* Zapiski RMO (Proc. Russian Mineralogical Soc.), **139**, 1,37-50, 2010

2010-63. **Phanon, D., Yvon, K.** *Synthesis, crystal structure and hydrogenation properties of rhenium-substituted YMn_2 and $ErMn_2$* J. Alloys and Compounds, **490**, 1-2, 412-421, 2010

2010-64. **Quesada Cabrera, R., Long, D.-L., Cronin, L., McMillan, P. F.** *In situ investigations of the polyoxometalate Trojan Horse compound $K_7Na[W^{VI}_{18}O_{56}(SO_3)_2(H_2O)_2]\cdot 20H_2O$ under high temperature and high pressure conditions* CrystEngComm, **12**, 2568 - 2572, 2010

2010-65. **Ravnsbæk, D. B., Filinchuk, Y., Cerný, R., Jensen, T.R.** *Powder diffraction methods for studies of borohydride-based energy storage materials* Z. Kristallographie, **225**, 557-569, 2010

2010-66. **Ravnsbæk, D. B., Filinchuk, Y., Cerny, R., Ley, M. B., Haase, D., Jakobsen, H. J. et al.** *Thermal Polymorphism and Decomposition of $Y(BH_4)_3$* Inorg. Chem., **49,** 8, 3801–3809, 2010

2010-67. **Ravnsbæk, D., Sørensen, L., Filinchuk, Y., Reed, D., Book, D., Jakobsen, H., Besenbacher, F. et al.** *Mixed-Anion and Mixed-Cation Borohydride $KZn(BH_4)Cl_2$: Synthesis, Structure and Thermal Decomposition* Eur. J. Inorganic Chemistry, **11**, 1608-1612, 2010

2010-68. **Renaudin, G., Dieudonn, B., Avignan, D., Mapemba, E., El-Ghozzi, M., Fleutot, S. et al.** *Pseudotetragonal Structure of $Li_{2+x}Ce_x^{3+}Ce_{12-x}^{4+}F_{50}$: The First Mixed Valence Cerium Fluoride* Inorg. Chem., **49**, 2, 686–694, 2010

2010-69. **Renaudin, G., Filinchuk, Y., Neubauer, J., Goetz-Neunhoeffer, F.** *A comparative structural study of wet and dried ettringite* Cement and Concrete Res., **40**, 3, 370-375, 2010

2010-70. **Røhr, Å., Hersleth, H.-P., Andersson, K.** *Tracking Flavin Conformations in Protein Crystal Structures with Raman Spectroscopy and QM/MM Calculations* Angewandte Chemie Int. Ed., **49**, 13, 2324-2327, 2010

2010-71. **Rønning, M., Tsakoumis, N., Voronov, A., Johnsen, R., Norby, P., Van Beek, W., Borg, Ø., Rytter, E., Holmen, A.** *Combined XRD and XANES studies of a Re-promoted Co/y-Al_2O_3 catalyst at Fischer–Tropsch synthesis conditions* Catalysis Today, **155**, 3-4, 289-295, 2010

2010-72. **Rosenbach, N., Ghoufi, Jr. A., Déroche, I., Llewellyn, P. L., Devic, T., Bourrelly, S. et al.** *Adsorption of light hydrocarbons in the flexible MIL-53(Cr) and rigid MIL-47(V) metal–organic frameworks: a combination of molecular simulations and microcalorimetry/gravimetry measurements* Phys. Chem. Chem. Phys., **12**, 6428-6437, 2010

2010-73. **Rozynek, Z., Knudsen, K. D., Fossum, J. O., Méheust, Y., Wang, B., Zhou, M.** *Electric field induced structuring in clay–oil suspensions: new insights from WAXS, SEM, leak current, dielectric permittivity, and rheometry* J. Phys.: Condens. Matter, **22**, 324104-324112, 2010

2010-74. **Safonova, O. V., Vykhodtseva, L. N., Fishgoit, L. A., Kononkova, N. N., Glatzel, P. , Safonov, V. A.** *Elucidation of the chemical state of phosphorus and boron in crystallographically amorphous* nickel electroplates Russian J. Electrochemistry, **46**, 11, 1223-1229, 2010

2010-75. **Safonova, O. V., Vykhodtseva, L. N., Polyakov, N. A., Swarbrick, J. C., Sikora, M., Glatzel, P., Safonov, V.A.** *Chemical composition and structural transformations of amorphous chromium coatings electrodeposited from Cr(III) electrolytes* Electrochimica Acta, **56**, 1, 145-153, 2010

2010-76. **Salles, F., Jobic, H., Devic, Th., Llewellyn, Ph., Serre, Ch., Frey, G., Maurin, G.** *Self and Transport Diffusivity of CO_2 in the Metal-Organic Framework MIL-47(V) Explored by Quasi-elastic Neutron Scattering Experiments and Molecular Dynamics Simulations* ACS Nano, **4,** 1, 143–152, 2010

2010-77. **Salles, F., Maurin, G., Serre, Ch., Llewellyn, Ph., Knfel, Ch., Choi, H. J., Filinchuk, Y. et al.** *Multistep N_2 Breathing in the Metal-Organic Framework Co(1,4-benzenedipyrazolate)* J. Am. Chem. Soc., **132,** 39, 13782–13788, 2010

2010-78. **Sarp, H., Cerny, R., Babalik, H., Hatipoglu, M., Mari, G.** *Lapeyreite, $Cu_3O[AsO_3(OH)]_2{\cdot}0.75H_2O$, a new mineral: Its description and crystal structure* American Mineralogist, **95**, 71-176, 2010

2010-79. **Schiltz, M., Bricogne, G.** *`Broken symmetries' in macromolecular crystallography: phasing from unmerged data* Acta Cryst., D**66**, 447-457, 2010

2010-80. **Serre, Ch., Haouas, M., Taulelle, F., Van Beek, W., Férey, G.** *Synthesis, structure and solid state NMR analysis of a new templated titanium(III/IV) fluorophosphate* Comptes Rendus Chimie, **13**, 3, 336-342 , 2010

2010-81. **Simmance, K., Sankar, G., Bell, R., Prestipino, C., Van Beek, W.** *Tracking the formation of cobalt substituted ALPO-5 using simultaneous in situ X-ray diffraction and X-ray absorption spectroscopy techniques* Phys. Chem. Chem. Phys., **12**, 559 - 562, 2010

2010-82. **Šišak, D., McCusker, L.B., Buckl, A., Wuitschik, G., Wu, Yi-Lin, Schweizer, W.B., Dunitz, J.D.** *The Search for Tricyanomethane (Cyanoform)* Chemistry – A Europ. J., **16,** 24, 7224-7230, 2010

2010-83. **Smrcok, L., Petrik, I., Langer, V., Filinchuk, Y., Beran, P.** *X-ray, synchrotron, and neutron diffraction analysis of Roman cavalry parade helmet fragment* Cryst. Res. Technol., **45**, 1025-1032, 2010

2010-84. **Snellings, R., Machiels, L., Mertens, G., Elsen, J.** *Rietveld refinement strategy for quantitative phase analysis of partially amorphous zeolitized tuffaceous rocks* Geologica Belgica, **13**, 3, 183-196, 2010

2010-85. **Snellings, R., Mertens, G., Cizer, Ö., Elsen, J.** *Early age hydration and pozzolanic reaction in natural zeolite blended cements: Reaction kinetics and products by in situ synchrotron X-ray powder diffraction* Cement and Concrete Research, **40**, 12, 1704-1713, 2010

2010-86. **Strutz, A., Yamamoto, A., Steurer, W.** *Basic Co-rich decagonal Al-Co-Ni: Superstructure* Phys. Rev. B **82**, 064107-064112, 2010

2010-87. **Tedesco, C., Erra, L., Immediata, I., Gaeta, C., Brunelli, M., Merlini, M., Meneghini, C., Pattison, Ph., Neri, P.** *Solvent Induced Pseudopolymorphism in a Calixarene-Based Porous Host Framework* Cryst. Growth Des., **10,** 4, 1527–1533, 2010

2010-88. **Tsakoumis, N.E., Rønning, M., Borg, Ø., Rytter, E., Holmen, A.** *Deactivation of cobalt based Fischer–Tropsch catalysts: A review* Catalysis Today, **154**, 3–4, 162–182, 2010

2010-89. **Tumanov, N. A., Boldyreva, E. V., Kolesov, B. A., Kurnosov, A. V., Quesada Cabrera, R.** *Pressure-induced phase transitions in L-alanine, revisited* Acta Cryst., B**66**, 458-471, 2010

2010-90. **Walspurger, S., Cobden, P.D., Haije, W.G., Westerwaal, R., Elzinga, G.D., Safonova, O.** *In Situ XRD Detection of Reversible Dawsonite Formation on Alkali Promoted Alumina: A Cheap Sorbent for CO_2 Capture* Eur. J. Inorganic Chemistry, **17**, 2461-2464, 2010

2010-91. **Walspurger, S., Cobden, P.D., Safonova, O., Wu, Y., Anthony, E. J.** *High CO_2 Storage Capacity in Alkali-Promoted Hydrotalcite-Based Material: In Situ Detection of Reversible Formation of Magnesium Carbonate* Chemistry – A Eur. J., **16**, 42, 12694–12700, 2010

2010-92. **Wei, X., Hug, P., Figi, R., Trottmann, M., Weidenkaff, A., Ferri, D.** *Catalytic combustion of methane on nano-structured perovskite-type oxides fabricated by ultrasonic spray combustion* Applied Catalysis B: Environmental, **94**, 1-2, 27-37, 2010

2010-93. **Williams, M., Lototsky, M., Nechaev, A., Yartys, V., Solberg, J. K. et al.** *Palladium mixed-metal surface-modified AB5-type intermetallides enhance hydrogen sorption kinetics* South African J. Science**, 106**, 9/10, 2010

2010-94. **Wragg, D. S., Johnsen, R. E., Norby, P., Fjellvåg, H.** *The Adsorption of Methanol and Water on SAPO-34: In Situ and Ex Situ X-ray Diffraction Studies* Microp. &Mesop. Materials, **134**, 1-3, 210-215, 2010

2010-95. **Yartys, V. A., Denys, R.V., Maehlen, J.P., Webb, C.J., Gray, E.M., Blach, T.et al.** *Nanostructured Metal Hydrides for Hydrogen Storage Studied by In Situ Synchrotron and Neutron Diffraction* Mater. Res. Soc. Symp. Proc., **12**, 62, 2010

2010-96. **Zaharko, O., Pregelj, M., Arcon, D., Brown, P.J., Chernyshov, D., Stuhr, U., Berger, H.** *$FeTe_2O_5Br$ system: New ferroelectric with an incommensurate spin modulation* J. Phys.: Conf. Ser., **211**, 012002-012008, 2010

2010-97. **Zanardi, S., Bellussi, G., Carati, A., Cruciani, G., Millini, R., Rizzo, C.** *EMS-6, a novel microporous gadoliniumsilicate with monteregianite structure: Synthesis, crystal structure and thermal behavior* Microp. & Mesop.Mat., **134**, 1-3, 115-123, 2010

2010-98. **Zarechnaya, E.Yu., Dubrovinskaia, N., Caracas, R., Merlini, M., Hanfland, M., Filinchuk, Y., Chernyshov, D., Dmitriev, V., Dubrovinsky, L.** *Pressure-induced isostructural phase transformation in* Y-*B28* Phys. Rev. B **82**, 184111-184122, 2010

2010-99. **Zarechnaya, E.Yu., Dubrovinskaia, N., Dubrovinsky, L., Filinchuk, Y., Chernyshov, D., Dmitriev, V.** *Growth of single crystals of B_{28} at high pressures and high temperatures* J. Crystal Growth, **312**, 22, 3388-3394, 2010

2010-100. **Zhigadlo, N. D., Katrych, S., Weyeneth, S., Puzniak, R., Moll, P. J. W., Bukowski, Z. et al.** T*h-substituted SmFeAsO: Structural details and superconductivity with T_c above 50 K* Phys. Rev. B **82**, 064517-064528, 2010

2010-101. **Zubkova, N. V., Filinchuk, Y. E., Pekov, I. V., Pushcharovsky, D. Yu., Gobechiya, E. R.** *Crystal structures of shlykovite and cryptophyllite: comparative crystal chemistry of phyllosilicate minerals of the mountainite family* Eur. J. Mineralogy, **22**, 4, 547-555, 2010

2011

2011-1 **Aboshyan-Sorgho, L., Besnard, C., Pattison, Ph., Kittilstved, K.R., Aebischer, A. et al.** *Near-Infrared ->Visible Light Upconversion in a Molecular Trinuclear d–f–d Complex* Angewandte Chem. Int. Ed., **50**, 18, 4108-4112, 2011

2011-2 **Amieiro-Fonseca, A., Ellis, S. R., Nuttall, C. J., Hayden, B. E., Guerin, S., Purdy, G. et al.** *A multidisciplinary combinatorial approach for tuning promising hydrogen storage materials towards automotive applications* Faraday Discuss., **151**, 369-384, 2011

2011-3 **Andersson, O., Filinchuk, Y., Dmitriev, V., Quwar, I., Talyzin, A., Sundqvist, B.** *Phase coexistence and hysteresis effects in the pressure-temperature phase diagram of NH_3BH_3* Phys. Rev. B **84**, 024115-024126, 2011

2011-4 **Arletti, R., Vezzalini, G., Morsli, A., Di Renzo, F., Dmitriev, V., Quartieri, S.** *Elastic behaviour of MFI-type zeolites: 1- Compressibility of Na-ZSM-5 in penetrating and non-penetrating media* Microp. & Mesop. Mat., **142**, 2-3, 696-707 , 2011

2011-5 **Babanova, O. A., Soloninin, A.V., Skripov, A.V., Ravnsbæk, D.V., Jensen, T.R., Filinchuk, Y.** *Reorientational Motion in Alkali-Metal Borohydrides: NMR Data for $RbBH_4$ and $CsBH_4$ and Systematics of the Activation Energy Variations* J. Phys. Chem. C, **115**, 20, 10305–10309, 2011

2011-6 **Barpanda, P., Ati, M., Melot, B. C., Rousse, G., Chotard, J-N., Doublet, M-L. et al.** *A 3.90 V iron-based fluorosulphate material for lithium-ion batteries crystallizing in the triplite structure* Nature Materials, **10**, 772-779, 2011

2011-7 **Barpanda, P., Chotard, J.-N., Delacourt, Ch., Reynaud, M., Filinchuk, Y. et al.** *$LiZnSO_4F$ Made in an Ionic Liquid: A Ceramic Electrolyte Composite for Solid-State Lithium Batteries* Angewandte Chem. Int. Ed., **50**, 11, 2526-2531, 2011

2011-8 **Borgschulte, A., Jain, A., Ramirez-Cuesta, A. J., Martelli, P., Remhof, A., Friedrichs, O. et al.** *Mobility and dynamics in the complex hydrides $LiAlH_4$ and $LiBH_4$* Faraday Discuss., **151**, 213-230, 2011

2011-9 **Bortolotti, M., Lonardelli, I., Pepponi, G.** *Determination of the crystal structure of nifedipine form C by synchrotron powder diffraction* Acta Cryst., B**67**, 357-364, 2011

2011-10 **Boyesen, K. L., Meneau, F., Mathisen, K.** *A combined in situ XAS/Raman and WAXS study on nanoparticulate V_2O_5 in zeolites ZSM-5 and Y* Phase Transitions, **84**, 8, 675-686, 2011

2011-11 **Buchter, F., Lodziana, Z., Remhof, A., Mauron, Ph., Friedrichs, O. et al.** *Experimental charge density of $LiBD_4$ from maximum entropy method* Phys. Rev. B **83**, 064107- 064116, 2011

2011-12 **Budhysutanto, W.N., Hendrikx, R.W.A., Kramer, H.J.M.** *Towards solving the crystal structure of polytype $3R_2$ Mg–Al layered double hydroxides* Applied Clay Science, **54**, 1, 77-82, 2011

2011-13 **Cerný, R., Filinchuk, Y.** *Complex inorganic structures from powder diffraction:case of tetrahydroborates of light metals* Zeitschrift für Kristallographie, **226**, 12, 882-891, 2011

2011-14 **Cervellino, A., Gvasaliya, S. N., Zaharko, O., Roessli, B., Rotaru, G. M., Cowley, R. A. et al.** *Diffuse scattering from the lead-based relaxor ferroelectric $PbMg_{1/3}Ta_{2/3}O_3$* J. Appl. Cryst., **44**, 603-609, 2011

2011-15 **Chernyshov, D., Van Beek, W., Emerich, H., Milanesio, M., Urakawa, A. et al.** *Kinematic diffraction on a structure with periodically varying scattering function* Acta Cryst., A**67**, 4, 327-335, 2011

2011-16 **Chong, Ch., Itoi, M., Boukheddaden, K., Codjovi, E., Rotaru, A., Varret, F., Frye, F.A. et al.** *Talham Metastable state of the photomagnetic Prussian blue analog $K_{0.3}Co[Fe(CN)_6]_{0.77}{\cdot}3.6H_2O$ investigated by various techniques* Phys. Rev. B **84**, 144102-144114, 2011

2011-17 **Chukanov, N. V., Pekov, I. V., Jonsson, E., Zubkova, N., V., Filinchuk, Y. et al.** *Langbanshyttanite, a new low-temperature arsenate mineral with a novel structure from Langban, Sweden* Eur. J. Mineralogy, **23**, 4, 675-681, 2011

2011-18 **Degryse, F., Voegelin, A., Jacquat, O., Kretzschmar, R., Smolders, E.** *Characterization of zinc in contaminated soils: complementary insights from isotopic exchange, batch extractions and XAFS spectroscopy* Eur. J. Soil Science, **62**, 2, 318-330, 2011

2011-19 **Deledda, S., Hauback, B. C.** *Hydride formation in Mg-based systems processed by reactive milling* Faraday Discuss., **151**, 315-326, 2011

2011-20 **Deloudi, S., Fleischer, F., Steurer, W.** *Unifying cluster-based structure models of decagonal Al-Co-Ni, Al-Co-Cu and Al-Fe-Ni* Acta Cryst., B**67**, 1-17, 2011

2011-21 **Denys, R.V., Yartys, V.A.** *Effect of magnesium on the crystal structure and thermodynamics of the $La_{3-x}Mg_xNi_9$ hydrides* J. Alloys & Compounds, **509**, 2, S540-S548, 2011

2011-22 **Dyadkin, V. A., Grigoriev, S. V., Menzel, D., Chernyshov, D., Dmitriev, V., Schoenes, J. et al.** *Control of chirality of transition-metal monosilicides by the Czochralski method* Phys. Rev. B **84**, 014435-014440, 2011

2011-23 **Dilnesa, B.Z., Lothenbach, B., Le Saout, G., Renaudin, G., Mesbah, A., Filinchuk, Y. et al.** *Iron in carbonate containing AFm phases* Cement & Concrete Research, **41**, 3, 311-323 , 2011

2011-24 **Fijalkowski, K. J., Genova, R. V., Filinchuk, Y., Budzianowski, A., Derzsi, M. et al.** *$Na[Li(NH_2BH_3)_2]$ – the first mixed-cation amidoborane with unusual crystal structure* Dalton Trans., **40**, 4407-4413 , 2011

2011-25 **Filinchuk, Y., Richter, B., Jensen, T.R., Dmitriev, V., Chernyshov, D., Hagemann, H.** *Porous and Dense Magnesium Borohydride Frameworks: Synthesis, Stability, and Reversible Absorption of Guest Species* Angewandte Chem. Int. Ed.,**50**, 47, 11162–11166, 2011

2011-26 **Fonneløp, J. E., Corno, M., Grove, H., Pinatel, E., Sørby, M. H., Ugliengo, P., Baricco, M., Hauback, B. C.** *Experimental and computational investigations on the AlH_3/AlF_3 system* J. Alloys & Compounds, **509**, 1, 10-14, 2011

2011-27 **Fonneløp, J. E., Løvvik, O. M., Sørby, M.H., Brinks, H.W., Hauback, B.C.** *Adjustment of the decomposition path for Na_2LiAlH_6 by TiF_3 addition* Int. J. Hydrogen Energy, **36**, 19, 12279-12285, 2011

2011-28 **Frommen, Ch., Sørby, M. H., Ravindran, P., Vajeeston, P., Fjellvåg, H., Hauback, B.C.** *Synthesis, Crystal Structure and Thermal Properties of the First Mixed-Metal and Anion-Substituted Rare Earth Borohydride $LiCe(BH_4)_3Cl$* J. Phys. Chem. C, **115,** 47, 23591–23602, 2011

2011-29 **Frommer, J., Voegelin, A., Dittmar, J., Marcus, M. A., Kretzschmar, R.** *Biogeochemical processes and arsenic enrichment around rice roots in paddy soil: results from micro-focused X-ray spectroscopy* Eur. J. Soil Science, **62**, 2, 305-317, 2011

2011-30 **Grigoryeva, N. A., Mistonov, A. A., Napolskii, K. S., Sapoletova, N. A., Eliseev, A. A. et al.** *Magnetic topology of Co-based inverse opal-like structures* Phys. Rev. B **84**, 064405-064418, 2011

2011-31 **Grove, H., Løvvik, O.M., Huang, W., Opalka, S.M., Heyn, R. H., Hauback, B.C.** *Decomposition of lithium magnesium aluminum hydride* Int. J. Hydrogen Energy, **36**, 13, 7602-7611, 2011

2011-32 **Hagemann, H., D'Anna, V., Rapin, J.-Ph., Cerný, R., Filinchuk, Y., Kimd, K. Ch. et al.** *New fundamental Experimental Studies on α-$Mg(BH_4)_2$ and other borohydrides* J. Alloys & Compounds, **509**, 2, S688-S690, 2011

2011-33 **Hersleth, H.-P., Andersson, K. K.** *How different oxidation states of crystalline myoglobin are influenced by X-rays* Bioch. & Bioph. Acta (BBA) - Proteins & Proteomics, **1814**, 6, 785-796, 2011

2011-34 **Horcajada, P., Salles, F., Wuttke, S., Devic, Th., Heurtaux, D., Maurin, G., Vimont, A. et al.** *How Linker's Modification Controls Swelling Properties of Highly Flexible Iron(III) Dicarboxylates MIL-88* J. Am. Chem. Soc., **133,** 44, 17839–17847, 2011

2011-35 **Hutanu, V., Sazonov, A., Murakawa, H., Tokura, Y., Náfrádi, B., Chernyshov, D.** *Symmetry and structure of multiferroic $Ba_2CoGe_2O_7$* Phys. Rev. B **84**, 212101-212105, 2011

2011-36 **Icli, B., Sheepwash, E., Riis-Johannessen, Th., Schenk, K., Filinchuk, Y., Scopelliti, R., Severin, K.** *Dative boron–nitrogen bonds in structural supramolecular chemistry: multicomponent assembly of prismatic organic cages* Chem. Sci., **2**, 1719-1721, 2011

2011-37 **Jacob, I., Deledda, S., Bereznitsky, M., Yeheskel, O., Filipek, S.M., Mogilyanski, D., Kimmel, G., Hauback, B.C.** *Can reduced size of metals induce hydrogen absorption: $ZrAl_2$ case* J. Alloys & Compounds, **509**, 2, S794-S796, 2011

2011-38 **Jørgensen, M. R. V., Clausen, H. F., Christensen, M., Poulsen, R. D., Overgaard, J., Iversen, B. B.** *Crystal Structures and Physical Properties of Three New Manganese-Based Coordination Polymers with p-Biphenyldicarboxylic Acid Linkers* Eur. J. Inorganic Chem., **4**, 549–555, 2011

2011-39 **Kaegi, R., Voegelin, A., Sinnet, B., Zuleeg, S., Hagendorfer, H., Burkhardt, M., Siegrist, H.** *Behavior of Metallic Silver Nanoparticles in a Pilot Wastewater Treatment Plant* Environ. Sci. Technol., **45**, 9, 3902–3908, 2011

2011-40 **Karaca, H., Safonova, O., Chambrey, S., Fongarland, P., Roussel, P., Griboval-Constant, A. et al.** Structure and catalytic performance of Pt-promoted alumina-supported cobalt catalysts under realistic conditions of Fischer–Tropsch synthesis J. Catalysis, **277**, 14-26, 2011

2011-41 **Kristiansen, T., Mathisen, K., Einarsrud, M.-A., Bjoergen, M., Nicholson, D. G.** *Single-Site Copper by Incorporation in Ambient Pressure Dried Silica Aerogel and Xerogel Systems: An XAS study* J. Phys. Chem. C, **115**, 39, 19260–19268, 2011

2011-42 **Kruk, I., Zajdel, P., Van Beek,W., Bakaimi, I., Lappas, A., Stock, Ch., Green, M. A.** *Coupled Commensurate Cation and Charge Modulation in the Tunneled Structure, $Na_{0.40(2)}MnO_2$* J. Am. Chem. Soc., **133**, 35, 13950–13956, 2011

2011-43 **Krzton-Maziopa, A., Pomjakushina, E., Pomjakushin, V., Sheptyakov, D., Chernyshov, D., Svitlyk, V. et al.** *The synthesis, and crystal and magnetic structure of the iron selenide $BaFe_2Se_3$ with possible superconductivity at T_c = 11 K* J. Phys.: Condens. Matter, **23**, 40, 2201-2208, 2011

2011-44 **Kuczera, P., Wolny, J., Fleischer, F., Steurer, W.** *Structure refinement of decagonal Al-Ni-Co, superstructure type I* Philosophical Magazine, **91**, 19-21, 2500-2509, 2011

2011-45 **Kverneland, A., Hansen, V., Thorkildsen, G., Larsen, H.B., Pattison P. et al.** *Transformations and structures in the Al-Zn-Mg alloy system. A diffraction study using synchrotron radiation and electron precession* Materials Science and Engineering: A, **528**, 880-887, 2011

2011-46 **Leclerc, H., Devic, Th., Devautour-Vinot, S., Bazin, Ph., Audebrand, N. et al.** *Influence of the Oxidation State of the Metal Center on the Flexibility and Adsorption Properties of a Porous MOF: MIL-47 (V)* J. Phys. Chem. C, **115,** 40, 19828–19840, 2011

2011-47 **Lejeune, M., Grosshans, Ph., Berclaz, Th., Sidorenkova, H., Besnard, C., Pattison, Ph., Geoffroy, M.** *Role of the aromatic bridge on radical ions formation during reduction of diphosphaalkenes* New J. Chem., **35**, 2510-2520, 2011

2011-48 **Leininger, Ph., Chernyshov, D., Bosak, A., Berger, H., Inosov, D. S.** *Competing charge density waves and temperature-dependent nesting in 2H-$TaSe_2$* Phys. Rev. B **83**, 233101-233105, 2011

2011-49 **Leontyev, I. N. ., Belenov, S. V., Guterman, V. E., Haghi-Ashtiani, P., Shaganov, A. P., Dkhil, B.** *Catalytic Activity of Carbon-Supported Pt Nanoelectrocatalysts. Why Reducing the Size of Pt Nanoparticles is Not Always Beneficial* J. Phys. Chem. C, **115,** 13, 5429–5434, 2011

2011-50 **Leontyev, I., Yuzyuk, Y., Janolin, P-E., El-Marssi, M., Chernyshov, D., Dmitriev, V. et al.** *Orthorhombic polar Nd-doped $BiFeO_3$ thin film on MgO substrate* J. Phys.: Condens. Matter, **23**, 33, 2201-2206, 2011

2011-51 **Lindemann, I., Ferrer, R. D., Dunsch, L., Cerný, R., Hagemann, H., D'Anna, V., Filinchuk, Y. et al**. *Novel sodium aluminium borohydride containing the complex anion $[Al(BH_4,Cl)_4]$* Faraday Discuss., **151**, 231-242, 2011

2011-52 **Liu, L., Yang, J., Li, J., Dong, J., Šišak, D., Luzzatto, M., McCusker, L. B.** *Ionothermal Synthesis and Structure Analysis of an Open-Framework Zirconium Phosphate with a High CO2/CH4 Adsorption Ratio* Angewandte Chem. Int. Ed., **50**, 35, 8139-8142, 2011

2011-53 **Lototsky, M.V., Williams, M., Yartys, V.A., Klochko, Ye.V., Linkov, V.M.** *Surface-Modified Advanced Hydrogen Storage Alloys for Hydrogen Separation and Purification* J. Alloys & Compounds, **509**, 2, S555-S561, 2011

2011-54 **Martinelli, A., Palenzona, A., Tropeano, M.., Putti, M., Ferdeghini, C., Profeta, G., Emerich, H.** *Retention of the Tetragonal to Orthorhombic Structural Transition in F-Substituted SmFeAsO: A New Phase Diagram for $SmFeAs(O_{1-x}F_x)$* Phys. Rev. Lett. **106**, 227001-227005, 2011

2011-55 **Martis, V., Nikitenko, S., Sen, S., Sankar, G., Van Beek, W., Filinchuk, Y., Snigireva, I., Bras, W.** *Effects of X-rays on crystal nucleation in lithium disilicate* Cryst. Growth Des., **11,** 7, 2858–2865, 2011

2011-56 **McCusker, L., Baerlocher, Ch., Burton, A., Zones, S.** *A re-examination of the structure of the germanosilicate zeolite SSZ-77* Solid State Sciences, **13**, 4, 800-805, 2011

2011-57 **Meersman, F., Quesada Cabrera, R., McMillan, P. F., Dmitriev, V.** *Structural and Mechanical Properties of TTR105-115 Amyloid Fibrils from Compression Experiments* Biophysical J., **100**, 1, 193-197, 2011

2011-58 **Mesbah, A., François, M., Cau-dit-Coumes, C., Frizon, F., Filinchuk, Y., Leroux, F. et al.** *Crystal structure of Kuzel's salt $3CaO{\cdot}Al_2O_3{\cdot}1/2CaSO_4{\cdot}1/2CaCl_2{\cdot}11H_2O$ determined by synchrotron powder diffraction* Cement & Concrete Res., **41**, 5, 504-509, 2011

2011-59 **Mondal, S., Van Smaalen, S., Schönleber, A., Filinchuk, Y., Chernyshov, D. et al.** *Electron-Deficient and Polycenter Bonds in the High-Pressure y-B_{28} Phase of Boron* Phys. Rev. Lett. **106**, 215502- 215506, 2011

2011-60 **Nagalakshmi, R., Kulkarni, R., Dhar, S.K., Thamizhavel, A., Krishnakumars, V. et al.** *Crystal growth and structure determination of the novel tetragonal compound Ce2RhGa12* Chem. Met. Alloys, **4**, 2011

2011-61 **Napolskii, K. S., Roslyakov, I.V., Eliseev, A. A., Petukhov, D. I., Lukashin, A.V., Chen, Sh.-F., Liu, Ch.-P., Tsirlina, G.A.** *Tuning the microstructure and*

functional properties of metal nanowire arrays via deposition potential Electrochimica Acta, **56**, 5, 1, 2378-2384 , 2011

2011-62 **Narygina, O., Dubrovinsky, L. S., Miyajima, N., McCammon, C. A., Kantor, I. Yu., Mezouar, M., Prakapenka, V. B., Dubrovinskaia, N. A., Dmitriev, V.** *Phase relations in Fe–Ni–C system at high pressures and temperatures* Phys. Chem. Minerals., **38**, 3, 203-214, 2011

2011-63 **Neuhausen, Ch., Pattison, Ph., Schiltz, M.** *A new polymorph of dicesium tetracyanoplatinate monohydrate with unusual platinum stacking* CrystEngComm, **13**, 430-432 , 2011

2011-64 **Olsen, J.E., Sørby, M.H., Hauback, B.C.** *Chloride-substitution in sodium borohydride* J. Alloys & Compounds, **509**, 24, L228-L231, 2011

2011-65 **Palatinus, L., Fleischer, F., Pattison, P., Weber, T., Steurer, W.** *Ab initio reconstruction of difference densities by charge flipping* Acta Cryst., A**67**, 9-20, 2011

2011-66 **Palin, L., Croce, G., Viterbo, D., Milanesio, M.** *Monitoring the Formation of H-MCM-22 by a Combined XRPD and Computational Study of the Decomposition of the Structure Directing Agent* Chem. Mater., **23,** 22, 4900–4909, 2011

2011-67 **Paul-Boncour, V., Filipek, S.M., Sato, R., Wierzbicki, R., André, G., Porcher, F., Reissner, M., Wiesingerd, G.** *Structural and magnetic properties of $RMn_{2-x}Fe_xD_6$ compounds (R=Y, Er; x≤0.2) synthesized under high deuterium pressure* J. Solid State Chemistry, **184**, 2, 463-469 , 2011

2011-68 **Podder, A. S., Lonardelli, I., Molinari, A., Bhadeshia, H. K. D. H.** *Thermal stability of retained austenite in bainitic steel: an in situ study* Proc. R. Soc. A, **15**, 2011

2011-69 **Poletaev, A.A., Denys, R.V., Solberg, J.K., Tarasov, B.P., Yartys, V.A.** *Microstructural optimization of $LaMg_{12}$ alloy for hydrogen storage* J. Alloys & Compounds, **509**, 2, S633-S639, 2010

2011-70 **Pomjakushin, V. Yu., Sheptyakov, D. V., Pomjakushina, E. V., Krzton-Maziopa, A., Conder, K., Chernyshov, D., Svitlyk, V. et al.** *Iron-vacancy superstructure and possible room-temperature antiferromagnetic order in superconducting $Cs_yFe_{2-x}Se_2$* Phys. Rev. B, **83**, 14, 144410-144415, 2011

2011-71 **Prigent, J., Joubert, J.-M.** *The phase diagrams of the ternary systems La–Ni–M (M = Re, Ru, Os, Rh, Ir, Pd, Ag, Au) in the La-poor region* Intermetallics, **19**, 295-301, 2011

2011-72 **Quartieri, S., Montagna, G., Arletti, R., Vezzalini, G.** *Elastic behavior of MFI-type zeolites: Compressibility of H-ZSM-5 in penetrating and non-penetrating media* J. Solid State Chem., **184**, 6, 1505-1516, 2011

2011-73 **Quesada Cabrera, R., Meersman, F., McMillan, P.F., Dmitriev, V.** *Nanomechanical and Structural Properties of Native Cellulose Under Compressive Stress* Biomacromolecules, **2,** 6, 2178–2183, 2011

2011-74 **Quesada Cabrera, R., Sella, A., Bailey, E., Leynaud, O., McMillan, P.F.** *High-pressure synthesis and structural behavior of sodium orthonitrate Na_3NO_4* J. Solid State Chem., **184**, 4, 915-920, 2011

2011-75 **Ramsahye, N.A., Trung, T.K., Bourrelly, S., Yang, Q., Devic, Th., Maurin, G. et al.** *Influence of the Organic Ligand Functionalization on the Breathing of the Porous Iron Terephthalate Metal Organic Framework Type Material upon Hydrocarbon Adsorption* J. Phys. Chem. C, **115,** 38, 18683–18695, 2011

2011-76 **Riabov, A.B., Denys, R.V., Maehlen, J.P., Yartys, V.A.** *Synchrotron diffraction studies and thermodynamics of hydrogen absorption–desorption processes in $La_{0.5}Ce_{0.5}Ni_4Co$* J. Alloys & Compounds, **509**, 2, S844-S848, 2011

2011-77 **Riktor, M. D., Filinchuk, Y., Vajeeston, P., Bardají, E. G., Fichtner, M., Fjellvåg, H., Sørby, M. H., Hauback, B. C.** *The crystal structure of the first borohydride borate, $Ca_3(BD_4)_3(BO_3)$* J. Mater. Chem., **21**, 7188-7193, 2011

2011-78 **Rude, L. H., Filinchuk, Y., Sørby, M.H., Hauback, B.C., Besenbacher, F., Jensen, T.R.** *Anion Substitution in $Ca(BH_4)_2$-CaI_2: Synthesis, Structure and Stability of Three New Compounds* J. Phys. Chem. C, **115**, 15, 7768–7777, 2011

2011-79 **Rude, L. H., Groppo, E., Arnbjerg, L. M., Ravnsbæk, D. B., Malmkjæras, R. A., Filinchuk, Y. et al.** *Iodide substitution in lithium borohydride, $LiBH_4$-LiI* J. Alloys & Compounds, **509**, 33, 8299-8305, 2011

2011-80 **Rude, L.H., Zavorotynska, O., Arnbjerg, L.M., Ravnsbæk, D.B., Malmkjær, R.A. et al.** *Bromide substitution in lithium borohydride, $LiBH_4$–LiBr* Int. J. Hydrogen Energy, **36**, 24, 15664-15672, 2011

2011-81 **Sadeqzadeh, M., Karaca, H., Safonova, O.V., Fongarland, P., Chambrey, S., Roussel, P.,A., Griboval-Constant, P., Lacroix, M. et al.** *Identification of the active species in the working alumina-supported cobalt catalyst under various conditions of Fischer–Tropsch synthesis* Catalysis Today, **164**, 1, 62-67, 2011

2011-82 **Salvadó, N., Butí, S., Labrador, A., Cinque, G., Emerich, H., Pradell,T.** *SR-XRD and SR-FTIR study of the alteration of silver foils in medieval paintings* Anal. Bioanal. Chem., **399**, 9, 3041-3052, 2011

2011-83 **Schärer, M. A., Eliot, A.C., Grütter, M. G., Capitani, G.** *Structural basis for reduced activity of 1-aminocyclopropane-1-carboxylate synthase affected by a mutation linked to andromonoecy* FEBS Letters, **585**, 111-114, 2011

2011-84 **Schaub, P. Weber, T., Steurer, W.** *Analysis and modelling of structural disorder by the use of the three-dimensional pair distribution function method exemplified by the disordered twofold superstructure of decagonal Al-Cu-Co* J. Appl. Cryst., **44**, 1, 134–149, 2011

2011-85 **Serra-Crespo, P., Ramos-Fernandez, E. V., Gascon, J., Kapteijn, F.** *Synthesis and Characterization of an Amino Functionalized MIL-101(Al): Separation and Catalytic Properties* Chem. Mater., **23,** 10, 2565–2572, 2011

2011-86 **Skorpa, R., Bordiga, S., Bleken, F., Olsbye, U., Arstad, B., Tolchard, J., Mathisen, K. et al.** *Assessing the surface sites of the large pore 3-dimensional microporous material H-ITQ-7 using FT-IR spectroscopy and molecular probes* Microp. & Mesop. Mater., **141**, 1-3, 146-156, 2011

2011-87 **Skrzypski, J., Bezverkhyy, I., Safonova, O., Bellat, J.-P.** *2.8NiO-$H_{1.8}Ni_{0.6}(OH)MoO_4$ - novel nanocomposite material for the reactive adsorption of sulfur-containing molecules at moderate temperature* Applied Catalysis B: Environmental, **106**, 3-4, 460-468, 2011

2011-88 **Song, H., Sjåstad, A. O., Fjellvåg, H., Okamoto, H., Vistad, Ø. B., Arstad, B., Norby, P.** *Exfoliation and thermal transformations of Nb-substituted layered titanates* J. Solid State Chemistry, **184**, 12, 4900–4909, 2011

2011-89 **Stare, K., Cerný, R., Skapin, S.D., Suvorov, D., Meden, A.** *Crystal Structures of $CaLa_8Ti_9O_{31}$ and $Ca_2La_4Ti_6O_{20}$ Determined from Powder Diffraction Data* Acta Chim. Slov., **58**, 465–470, 2011

2011-90 **Suwarno, S., Solberg, J.K., Yartys, V.A., Krogh, B.** *Hydrogenation and Microstructural Study of Melt-Spun $Ti_{0.8}V_{0.2}$* J. Alloys & Compounds, **509,** 2, S775-S778, 2011

2011-91 **Svitlyk, V., Chernyshov, D., Pomjakushina, E., Krzton-Maziopa, A., Conder, K., Pomjakushin, V., Dmitriev, V.** *Temperature and Pressure Evolution of the Crystal Structure of $A_x(Fe_{1-y}Se)_2$ (A = Cs, Rb, K) Studied by Synchrotron Powder Diffraction* Inorg. Chem., **50**, 21, 10703–10708, 2011

2011-92 **Talyzin, A. V., Luzan, S. M., Leifer, K., Akhtar, S., Fetzer, J., Cataldo, F. et al.** *Coronene Fusion by Heat Treatment: Road to Nanographenes* J. Phys. Chem. C, **115,** 27, 13207–1321, 2011

2011-93 **Talyzin, A.V., Luzan, S.M., Szabó, T., Chernyshev, D., Dmitriev, V.** *Temperature dependent structural breathing of hydrated graphite oxide in H_2O* Carbon, **49**, 6, 1894-1899, 2011

2011-94 **Talyzin, A. V. , Sundqvist, B., Szab, T., Dmitriev, V.** *Structural Breathing of Graphite Oxide Pressurized in Basic and Acidic Solutions* J. Phys. Chem. Lett., 2, 4, 309–313, 2011

2011-95 **Tew, M. W., Emerich, H., van Bokhoven, J.A.** *Formation and Characterization of PdZn Alloy: A Very Selective Catalyst for Alkyne Semihydrogenation* J. Phys. Chem. C, **115**, 17, 8457–8465, 2011

2011-96 **Tong, L. H., Gune, L., Williams, A.F.** *Pentasubstituted Ferrocene and Dirhodium(II) Tetracarboxylate as Building Blocks for Discrete Fullerene-Like and Extended Supramolecular Structures* Inorg. Chem., **50**, 6, 2450–2457, 2011

2011-97 **Trung, Th. Kh., Déroche, I., Rivera, A., Yang, Q., Yot, P., Ramsahye, N. et al.** *Hydrocarbon adsorption in the isostructural Metal Organic Frameworks MIL-53 (Cr) and MIL-47 (V)* Microp. & Mesop. Materials, **140**, 1-3, 114-119, 2011

2011-98 **Urakawa, A., Van Beek, W., Monrabal-Capilla, M., Galn-Mascars, J.R., Palin, L., Milanesio, M.** *Combined, Modulation Enhanced X-ray Powder Diffraction and Raman Spectroscopic Study of Structural Transitions in the Spin Crossover Material [Fe(Htrz)2(trz)](BF4)* J. Phys. Chem. C, **115,** 4, 1323–1329, 2011

2011-99 **Vakhrushev, S. B., Shaganov, A.P., Dkhil, B., Lebolock, D., Ouvada, K.** *Study of the formation processes of a domain nanostructure in relaxor ferroelectrics* Physics of Particles and Nuclei Letters, **8**, 10, 1061-1062, 2011

2011-100 **Van Beek, W., Safonova, O.V., Wiker, G., Emerich, H.** *SNBL, a dedicated beamline for combined in situ X-ray diffraction, X-ray absorption and Raman scattering experiments* Phase Transitions, **84**, 8, 726-732, 2011

2011-101 **Voegelin, A., Jacquat, O., Pfister, S., Barmettler, K., Scheinost, A.S., Kretzschmar, R.** *Time-Dependent Changes of Zinc Speciation in Four Soils Contaminated with Zincite or Sphalerite* Environ. Sci. Technol., **45**, 1, 255–261, 2011

2011-102 **Vullum, P. E., Pitt, M., Walmsley, J., Hauback, B., Holmestad, R.** *Equation TEM characterization of pure and transition metal enhanced $NaAlH_4$* J. Alloys & Compounds, **509**, 2, 281-289, 2011

2011-103 **Walspurger, S., de Munck, S., Cobden, P.D., Haije, W.G., van den Brink, R.W., Safonova, O.V.** *Correlation between structural rearrangement of hydrotalcite-type materials and CO_2 sorption processes under pre-combustion decarbonisation conditions* Energy Procedia, **4**, 1162-1167, 2011

2011-104 **Wang, J., Schenk, K., Carvalho, A., Wylie-van Eerd, B. et al.** *Structure Determination and Compositional Modification of Body-Centered Tetragonal PX-Phase Lead Titanate* Chem. Mater., **23,** 10, 2529–2535, 2011

2011-105 **Wiersum, A. D., Soubeyrand-Lenoir, E., Yang, Q., Moulin, B., Guillerm, V. et al.** *An Evaluation of UiO-66 for Gas-Based Applications* Chemistry – An Asian J., **6**, 12, 3270–3280, 2011

2011-106 **Wragg, D.S., Akporiaye, D., Fjellvåg, H.** *Direct observation of catalyst behaviour under real working conditions with X-ray diffraction: Comparing SAPO-18 and SAPO-34 methanol to olefin catalysts* J. Catalysis, **279**, 2, 397-402, 2011

2011-107 **Xie, D., Baerlocher, Ch., McCusker, L.B.** *Using phases retrieved from two-dimensional projections to facilitate structure solution from X-ray powder diffraction data* J. Appl. Cryst., **44**, 5, 2011

2011-108 **Xie, D., McCusker, L.B., Baerlocher, Ch.** *Structure of the borosilicate zeolite catalyst SSZ-82 solved using 2D-XPD charge flipping* J. Am. Chem. Soc.,**133,** 50, 20604–20610, 2011

2011-109 **Yartys, V.A., Denys, R.V., Webb, C.J., Mæhlen, J.P., Gray, MacA., Blach, T. et al.** *High pressure in situ diffraction studies of metal-hydrogen systems* J. Alloys & Compounds, **509**, 2, S817-S822, 2011

2011-110 **Zhang, J., Cerný, R., Villeroy, B., Godart, C., Chandra, D., Latroche, M.** *$Li_{3-x}M_xN$ (M = Co, Ni) synthesized by Spark Plasma Sintering for hydrogen storage* J. Alloys & Compounds, **509**, 2, S732-S735, 2011

2012

2012-1 **Abdala, P., Safonova, O., Wiker, G., Van Beek, W., Emerich, H., Van Bokhoven, J. et al.** Scientific Opportunities for Heterogeneous Catalysis Research at the SuperXAS and SNBL Beam Lines CHIMIA Int. J. Chemistry, **66**, 9, 699-705, 2012

2012-2 **Afanasiev, P.** *Snapshots of ZnO Formation in Molten Salt: Hollow Microtubules Generated by Oriented Attachment and Kirkendall Effect* J. Phys. Chem. C, **116**, 3, 2371-2381, 2012

2012-3 **Aimoz, L., Taviot-Gueho, Ch., Churakov, S.V., Chukalina, M., Daehn, R. et al.** *Anion and Cation Order in Iodide-Bearing Zn/Mg-Al Layered Double Hydroxides* J. Phys. Chem. C, **116,** 9, 5460-5475, 2012

2012-4 **Aimoz, L., Wieland, E., Taviot-Gueho, Ch., Daehn, R., Vespa, M., Churakov, S.V.** *Structural insight into iodide uptake by AFm phases* Environ. Sci. Technol., **46**, 7, 3874–3881, 2012

2012-5 **Alcantara, K.S., Lopez, J.R., Bösenberg, U., Saldan, I., Pistidda, C., Requejo, F. et al.** *3CaH2+4MgB2+CaF2 Reactive Hydride Composite as a Potential Hydrogen Storage Material: Hydrogenation and Dehydrogenation Pathway* J. Phys. Chem. C, **116**, 12, 7207–7212, 2012

2012-6 **Arakcheeva, A., Logvinovich, D., Chapuis, G., Morozov, V., Eliseeva, S., Bünzli, J.-C., Pattison, P.** *The luminescence of $Na_xEu^{3+}_{(2-x)/3}MoO_4$ scheelites depends on the number of Eu-clusters occurring in their incommensurately modulated structure* Chem. Sci., **3**, 384-390, 2012

2012-7 **Arnbjerg, L. M., Jensen, T. R.** *New compounds in the potassium-aluminium-hydrogen system observed during release and uptake of hydrogen* Int. J. Hydrogen Energy, **37**, 1, 345-356, 2012

2012-8 **Bellussi, G., Montanari, E., Di Paola, E., Millini, R., Carati, A., Rizzo, C., O'Neil Parker Jr., W. et al.** *ECS-3: A Crystalline Hybrid Organic–Inorganic Aluminosilicate with Open Porosity* Angewandte Chem. Int. Ed., **51**, 3, 666-669, 2012

2012-9 **Bezverkhyy, I., Skrzypski, J., Safonova, O., Bellat, J.-P.** *Sulfidation Mechanism of Pure and Cu-Doped ZnO Nanoparticles at Moderate Temperature: TEM and In Situ XRD Studies* J. Phys. Chem. C, **116,** 27, 14423-14430, 2012

2012-10 **Bora, D.K., Braun, A., Erat, S., Safonova, O., Graule, Th., Constable, E.C.** *Evolution of structural properties of iron oxide nano particles during temperature treatment from 250°C – 900°C: X-ray diffraction and Fe K-shell pre-edge X-ray absorption study* Current Applied Physics, **12**, 3, 817-825, 2012

2012-11 **Bosak, A., Chernyshov, D., Vakhrushev, S.** *Glass-like structure of a lead-based relaxor ferroelectric* J. Appl. Cryst., **45**, 6, 2012

2012-12 **Bosak, A., Chernyshov, D., Vakhrushev, S., Krisch, M.** *Diffuse scattering in relaxor ferroelectrics: true three-dimensional mapping, experimental artefacts and modelling* Acta Cryst., A**68**, 1, 117-123, 2012

2012-13 **Bosak, A., Krisch, M., Chernyshov, D., Winkler, B., Milman, V., Refson, K., Schulze-Briese, C.** *New insights into the lattice dynamics of α-quartz* Z. Kristallographie - Crystalline Mat., **227**, 2, 84-91, 2012

2012-14 **Bozoklu, G., Gateau, Ch., Imbert, D., Pécaut, J., Robeyns, K., Filinchuk, Y. et al.** *Controlled Diastereoselective Self-Assembly and Circularly Polarized Luminescence of a Chiral Heptanuclear Europium Wheel* J. Am. Chem. Soc., **134**, 20, 8372–8375, 2012

2012-15 **Burkovsky, R. G., Bronwald, Yu. A., Filimonov, A. V., Rudskoy, A. I., Chernyshov, D., Bosak, A. et al.** *Structural Heterogeneity and Diffuse Scattering in Morphotropic Lead Zirconate-Titanate Single Crystals* Phys. Rev. Lett., **109**, 097603-097607, 2012

2012-16 **Bykova, E., Parakhonskiy, G., Dubrovinskaia, N., Chernyshov, D., Dubrovinsky, L.** *The crystal structure of aluminum doped β-rhombohedral boron* J. Solid State Chemistry, **194**, 188-193, 2012

2012-17 **Caliandro, R., Chernyshov, D., Emerich, H., Milanesio, M., Palin, L., et al.** *Patterson selectivity by modulation-enhanced diffraction* J. Appl. Cryst., **45**, 3, 458-470, 2012

2012-18 **Ceotto, M., Lo Presti, L., Cappelletti, G., Meroni, D., Spadavecchia, F., Zecca. R. et al.** *About the Nitrogen Location in Nanocrystalline N-Doped TiO_2: Combined DFT and EXAFS Approach* J. Phys. Chem. C, **116**, 2, 1764–1771, 2012

2012-19 **Cerný, R., Ravnsbæk, D.B., Schouwink, P., Filinchuk, Y., Penin, N., Teyssier, J. et al**. *Potassium zinc borohydrides containing triangular $[Zn(BH4)3]^-$ and tetrahedral $[Zn(BH4)xCl4-x]2^-$ anions* J. Phys. Chem. C, **116**, 1, 1563-1571, 2012

2012-20 **Cervellino, A., Gvasaliya, S. N., Roessli, B., Rotaru, G. M., Cowley, R. A. et al.** *Cube-shaped diffuse scattering and the ground state of $BaMg_{1/3}Ta_{2/3}O_3$* Phys. Rev. B **86**, 104107-104129, 2012 (Kaleidoscope Image)

2012-21 **Chakraborty, P., Bronisz, R., Besnard, C., Guénée, L., Pattison, P., Hauser, A.** Persistent Bidirectional Optical Switching in the 2D High-Spin Polymer $\{[Fe(bbtr)_3](BF_4)_2\}_\infty$ J. Am. Chem. Soc., **134**, 9, 4049–4052, 2012

2012-22 **Chavan, S., Vitillo, J.G., Gianolio, D., Zavorotynska, O., Civalleri, B., Jakobsen, S. et al.** H_2 storage in isostructural UiO-67 and UiO-66 MOFs Phys. Chem. Chem. Phys., **14**, 1614-1626, 2012

2012-23 **Christensen, A.N., Lebech, B.** *Investigation of the crystal structure of a basic bismuth(III) nitrate with the composition* $[Bi_6O_4(OH)_4]_{0.54(1)}[Bi_6O_5(OH)_3]_{0.46(1)}(NO_3)_{5.54(1)}$ Dalton Trans., **41**, 1971-1980, 2012

2012-24 **Conradi, M.S., Eagles, M., Sun, B., Richter, B., Jensen, T.R., Filinchuk, Y.** *NMR Investigation of Nanoporous y-*$Mg(BH_4)_2$ *and its Thermally-Induced Phase Changes* J. Phys. Chem. C, **116**, 24, 13033-13037, 2012

2012-25 **Conterosito, E., Croce, G., Palin, L., Boccaleri, E., Van Beek, W., Milanesio, M.** *Crystal structure and solid-state transformations of Zn–triethanolamine–acetate complexes to ZnO* CrystEngComm, **14**, 4472-4477, 2012

2012-26 **Couck, S., Gobechiya, E., Kirschhock, C.E.A., Serra-Crespo, P., Juan-Alcañiz, J., Joaristi, A.M. et al.** *Adsorption and Separation of Light Gases on an Amino-Functionalized Metal–Organic Framework: An Adsorption and In Situ XRD Study* ChemSusChem., **5**, 4, 740-750, 2012

2012-27 **Deka, U., Lezcano-Gonzalez, I., Warrender, S.J., Picone, A.L., Wright, P.A., Weckhuysen, B.M. et al.** *Changing active sites in Cu-CHA catalysts: deNOx selectivity as a function of the preparation method* Microporous & Mesoporous Mat., **166**, 144-152, 2012

2012-28 **Deka, U., Juhin, A., Eilertsen, E.A., Emerich, H., Green, M.A., Korhonen, S.T. et al.** *Confirmation of Isolated* Cu^{2+} *ions in SSZ-13 Zeolite as Active Sites in* NH_3 *- Selective Catalytic Reduction* J. Phys. Chem. C,**116**, 7, 4809–4818, 2012

2012-29 **Denys, R.V., Poletaev, A. A., Maehlen, J.P., Solberg, J.K., Tarasov, B.P., Yartys, V.A.** *Nanostructured rapidly solidified* $LaMg_{11}Ni$ *alloy. II. In situ synchrotron X-ray diffraction studies of hydrogen absorption–desorption behaviours* Int. J. Hydrogen Energy, **37**, 7, 5710-5722, 2012

2012-30 **Denys, R.V., Yartys, V.A., Webb, C.J.** *Hydrogen in* $La_2MgNi_9D_{13}$*: The Role of Magnesium* Inorg. Chem., **51**, 7, 4231-4238, 2012

2012-31 **Devic, Th., Salles, F., Bourrelly, S., Moulin, B., Maurin, G., Horcajada, P. et al.** *Effect of the organic functionalization of flexible MOFs on the adsorption of* CO_2 J. Mater. Chem., **22**, 10266-10273, 2012

2012-32 **Diana, E., Chierotti, M.R., Marchese, E.M.C., Croce, G., Milanesio, M., Luigi, P.** Stanghellini Blue and red shift hydrogen bonds in crystalline cobaltocinium complexes New J. Chem., **36**, 1099-1107, 2012

2012-33 **Di Bartolomeo, E., D'Epifanio, A., Pugnalini, P., Giannici, F., Longo, A., Martorana, A. et al.** *Structural analysis, phase stability and electrochemical characterization of Nb doped* $BaCe_{0.9}Y_{0.1}O_{3-x}$ *electrolyte for IT-SOFCs* J. Power Sources, **199**, 201–206, 2012

2012-34 **Djerdj, I., Škapin, S.D., Ceh, M., Jaglicic, Z., Pajic, D., Kozlevcar, B., Orel, B., Orel, Z.C.** *Interplay between the structural and magnetic probes in the elucidation of the structure of a novel 2D layered* $[V_4O_4(OH)_2(O_2CC_6H_4CO_2)_4]\cdot DMF$ Dalton Trans., **41**, 581-589, 2012

2012-35 **Dmitriev, V., Chernyshov, D., Grigoriev, S., Dyadkin, V.** *A chiral link between structure and magnetism in MnSi* J. Phys.: Condens. Matter, **24,** 36, 6005-6012, 2012

2012-36 **Eagles, M., Sun, B., Richter, B., Jensen, T.R., Filinchuk, Y., Conradi, M.S.** *NMR Investigation of Nanoporous* γ*-*$Mg(BH_4)_2$ *and Its Thermally Induced Phase Changes* J. Phys. Chem. C, **116**, 24, 13033-13037, 2012

2012-37 **Fonneløp, J. E., Sartori, S., Sørby, M.H., Hauback, B.C.** *Polymorphic composition of alane after cryomilling with fluorides* J. Alloys & Compounds, **540**, 241-247, 2012

2012-38 **Gvasaliya, S. N., Cervellino, A., Roessli, B., Rotaru, G. M., Cowley, R. A., Lushnikov, S. G. et al.** *The structure and low-energy phonons of the nonferroelectric mixed perovskite:* $BaMg_{1/3}Ta_{2/3}O_3$ J. Phys.: Condens. Matter, **24**, 45, 5401-5408, 2012

2012-39 **Guzik, M.N., Hauback, B.C., Yvon, K.** *Hydrogen atom distribution and hydrogen induced site depopulation for the* $La_{2-x}Mg_xNi_7$ *– H system* J. Solid State Chemistry, **186**, 9-16, 2012

2012-40 **Hamacek, J., Besnard, C., Mehanna, N., Lacour, J.** *Tripodal europium complex with triangulenium dye: a model bifunctional metallo-organic system* Dalton Trans., **41**, 6777-6782, 2012

2012-41 **Hansen, E. L., Hemmen, H., Fonseca, D. M., Coutant, C., Knudsen, K. D. et al.** *Swelling transition of a clay induced by heating* Scientific Reports, **2**, 618, 2012

2012-42 **Hino, S., Fonneløp, J.E., Corno, M., Zavorotynska, O., Damin, A., Richter, B. et al.** *Halide Substitution in Magnesium Borohydride* J. Phys. Chem. C, **116**, 23, 12482-12488, 2012

2012-43 **Jakobsen, S., Gianolio, D., Wragg, D.S., Nilsen, M.H., Emerich, H., Bordiga, S., Lamberti, C. et al.** *Structural determination of a highly stable metal-organic framework with possible application to interim radioactive waste scavenging: Hf-UiO-66* Phys. Rev. B **86**, 125429-125440, 2012

2012-44 **Jansa, I.L., Friedrichs, O., Fichtner, M., Bardaji, E.G., Zuettel, A., Hauback, B.C.** *The Role of $Ca(BH_4)_2$ Polymorphs* J. Phys. Chem. C, **116**, 25, 13472-13479, 2012

2012-45 **Jantsky, L., Okamoto, H., Demont, A., Fjellvåg, H.** *Tuning of Water and Hydroxide Content of Intercalated Ruddlesden–Popper-type Oxides in the $PrSr_3Co_{1.5}Fe_{1.5}O_{10-\delta}$ System* Inorg. Chem., **51**,17, 9181-9191, 2012

2012-46 **Kongmark, Ch., Coulter, R., Cristol, S., Rubbens, A., Pirovano, C., Löfberg, A., Sankar, G., Van Beek, W. et al.** *A Comprehensive Scenario of the Crystal Growth of γ-Bi_2MoO_6 Catalyst during Hydrothermal Synthesis* Cryst. Growth Des., **12**, 12, 5994-6003, 2012

2012-47 **Kristiansen, T., Støvneng, J.A., Einarsrud, M.-A., Nicholson, D.G., Mathisen, K.** *There and Back Again: The Unique Nature of Copper in Ambient Pressure Dried-Silica Aerogels* J. Phys. Chem. C, **116**, 38, 20368-20379, 2012

2012-48 **Kuczera, P., Wolny, J., Steurer, W.** *Comparative structural study of decagonal quasicrystals in the systems Al-Cu-Me (Me = Co, Rh, Ir)* Acta Cryst., B**68**, 578-589, 2012

2012-49 **Lang, J., Gerhauser, A., Filinchuk, Y., Klassen, T., Huot, J.** *Differential Scanning Calorimetry (DSC) and Synchrotron X-ray Diffraction Study of Unmilled and Milled $LiBH_4$: A Partial Release of Hydrogen at Moderate Temperatures* Crystals., **2**, 1, 1-21, 2012

2012-50 **Leardini, L., Quartieri, S., Martucci, A., Vezzalini, M.G., Dmitriev, V.** *Compressibility of microporous materials with CHA topology: 2. ALPO-34* Z. Kristallogr., **227**, 2012

2012-51 **Leiros, H.-K.S., Fedøy, A.E., Leiros, I., Steen, I.H.** *The complex structures of isocitrate dehydrogenase from Clostridium thermocellum and Desulfotalea psychrophila suggest a new active site locking mechanism* FEBS Open Bio, **2**, 159-172, 2012

2012-52 **Leontyev, I., Kuriganova, A., Kudryavtsev, Y., Dkhil, B., Smirnova, N.** *New Life of a Forgotten method: Electrochemical Route toward Highly Efficient Pt/C Catalysts for Low-Temperature Fuel Cells* Applied Catalysis A: General, **431-432**, 120-125, 2012

2012-53 **Ley, M.B., Boulineau, S., Janot, R., Filinchuk, Y., Jensen, T.R.** *New Li Ion Conductors and Solid State Hydrogen Storage Materials: $LiM(BH_4)_3Cl$, M = La, Gd* J. Phys. Chem. C, **116**, 40, 21267-21266, 2012

2012-54 **Ley, M.B., Ravnsbæk, D.B., Filinchuk, Y., Lee, Y.-S., Janot, R., Cho, Y.W. et al.** *$LiCe(BH_4)3Cl$, a new lithium-ion conductor and hydrogen storage material with isolated tetranuclear anionic clusters* Chem. Mater., **24**,1654-1663, 2012

2012-55 **Llamas-Jansa, I., Aliouane, N., Deledda, S., Fonneløp, J.E., Frommen, Ch., Humphries, T. et al.** *Chloride substitution induced by mechano-chemical reactions between $NaBH_4$ and transition metal chlorides* J. Alloys and Compounds, **530**, 186-192, 2012

2012-56 **Lonardelli, I., Bortolotti, M., Van Beek, W., Girardini, L., Zadra, M., Bhadeshia, H.K.D.H.** *Powder metallurgical nanostructured medium carbon bainitic steel: Kinetics, structure, and in situ thermal stability studies* Mat. Science and Engineering: A, **565**, 139-147, 2012

2012-57 **Maegli, A.E., Hisatomi, T., Otal, E.H., Yoon, S., Pokrant, S., Grätzel, M., Weidenkaff, A.** *Structural and photocatalytic properties of perovskite-type (La, Ca) Ti (O, N)$_3$ prepared from A-site deficient precursors* J. Mater. Chem., **22**, 17906-17913, 2012

2012-58 **Maercz, M., Johnsen, R.E., Dietzel, P.D.C., Fjellvåg, H.** *The iron member of the CPO-27 coordination polymer series: Synthesis, characterization, and intriguing redox properties* Microp.& Mesop. Mat., **157**, 62-74, 2012

2012-59 **Martinelli, A., Palenzona, A., Putti, M., Ferdeghini, C.** *Microstructural evolution throughout the structural transition in 1111 oxypnictides* Phys. Rev. B **85**, 224534-224546, 2012

2012-60 **Matam, S.K., Otal, E.H., Aguirre, M.H., Winkler, A., Ulrich, A., Rentsch, D., Weidenkaff, A., Ferr, D.** *Thermal and chemical aging of model three-way catalyst Pd/Al_2O_3 and its impact on the conversion of CNG vehicle exhaust* Catalysis Today, **184**, 1, 237-244, 2012

2012-61 **Mathisen, K., Nilsen, M.H., Nordhei, C., Nicholson, D.G.** *Irreversible Silver(I) Interconversion in Ag:ZSM-5 and Ag:SAPO-5 by Propene and Hydrogen* J. Phys. Chem. C, **116**, 1, 171-184, 2012

2012-62 **Mikheykin, A. S., Dmitriev, V. P, Chagovets, S. V., Kuriganova, A. B., Smirnova, N. V., Leontyev, I. N.** *The compressibility of nanocrystalline Pt* Appl. Phys. Lett. **101**, 173111-173115, 2012

2012-63 **Minkov, V.S., Boldyreva, E., Drebushchak, T.N., Gorbitz, C.H.** *Stabilizing structures of cysteine-containing crystals with respect to variations of temperature and pressure by immobilizing amino acid side chains* CrystEngComm, **14**, 5943-5954, 2012

2012-64 **Moliner, M., Willhammar, T., Wan, W., González, J., Rey, F., Jorda, J.L. et al.** *Synthesis Design and Structure of a Multipore Zeolite with Interconnected 12- and 10-MR Channels* J. Am. Chem. Soc., **134**, 14, 6473–6478, 2012

2012-65 **Nielsen, Th.K., Jensen, T.R.** *MgH_2–Nb_2O_5 investigated by in situ synchrotron X-ray diffraction* Int. J. Hydrogen Energy, **37**, 18, 13405-13416, 2012

2012-66 **Nielsen, R.B., Norby, P., Kongshaug. K.O., Fejellvag, H.** *Synthesis, crystal structure and thermal properties of $Ca_6(C_{12}H_{14}O_4)_4(CO_3)(OH)_2(H2O)_x$ – a 3D inorganic hybrid material* Dalton Trans., **41**, 12082-12089, 2012

2012-67 **Østreng, E., Nilsen, O., Fjellvåg. H.** *Optical Properties of Vanadium Pentoxide Deposited by ALD* J. Phys. Chem. C, **116**, 36, 19444-19450, 2012

2012-68 **Ovsyannikov, S.V., Wu, X., Karkin, A.E., Shchennikov, V.V., Manthilake, G.M.** *Pressure-temperature phase diagram of Ti_2O_3 and physical properties in the golden Th_2S_3-type phase* Phys. Rev. B **86**, 024106-024120, 2012

2012-69 **Phan, H. V., Chakraborty, P., Chen, M., Calm, Y.M., Kovnir, K. et al.** *Heteroleptic Fe^{II} Complexes of 2,2' - Biimidazole and Its Alkylated Derivatives: Spin-Crossover and Photomagnetic Behavior* Chemistry - A European J., **18**, 49, 15805-15815, 2012

2012-70 **Parsons, S., Pattison, P., Flack, H. D.** *Analysing Friedel averages and differences* Acta Cryst., A**68**, 736-749, 2012

2012-71 **Paun, C., Safonova, O., Szlachetko, J., Abdala, P., Nachtegaal, M., De Paiva Sa, J. et al.** *Polyhedral CeO_2 Nanoparticles: Size-Dependant Geometrical and Electronic Structure* J. Phys. Chem. C, **116**, 13, 7312-7317, 2012

2012-72 **Pekov, I.V., Zubkova, N.V., Chukanov, N.V., Turchkova, A.G., Filinchuk, Y.E., Pushcharovsky, D.Y**. *Delhayelite and Mountainite Mineral Families: Crystal Chemical Relationship, Microporous Character and Genetic Features* Minerals as Adv. Mater. **II,** 213-219, 2012

2012-73 **Petukhov, D. I., Eliseev, A. A., Kolesnik, I.V., Napolskii, K.S., Lukashin, A.V., Garshev, A.V. et al.** *Mechanically stable flat anodic titania membranes for gas transport applications* J. Porous Materials, **19**,1, 71-77, 2012

2012-74 **Pinatel, U.R., Rude, L.H., Corno, M., Kragelund, M., Ugliengo, P., Jensen, T.R., Baricco, M.** *Thermodynamic Tuning of Calcium Hydride by Fluorine Substitution* Mater. Res. Soc. Symp. Proc., **1441**, 2012

2012-75 **Pitt, M.P., Vullum, P.E., Sørby, M.H., Blanchard, D., Sulic, M.P., Emerich, H. et al.** *The location of Ti containing phases after the completion of the $NaAlH_4$ + $xTiCl_3$ milling process* J. Alloys & Compounds, **513**, 597-605, 2012

2012-76 **Pitt, M.P., Vullum, P.E., Sørby, M.H., Emerich, H., Paskevicius, M., Buckley, C.E. et al.** *Amorphous $Al_{1-x}Ti_x$, $Al_{1-x}V_x$, and $Al_{1-x}Fe_x$ phases in the hydrogen cycled $TiCl_3$, VCl_3 and $FeCl_3$ enhanced $NaAlH_4$ systems* J. Alloys & Compounds, **521**, 112-120, 2012

2012-77 **Pitt, M.P., Vullum, P.E., Sørby, M.H., Emerich, H., Paskevicius, M., Buckley, C.E. et al.** *Absorption Kinetics of the Transition-Metal-Chloride Enhanced $NaAlH_4$ System* J. Phys. Chem. C, **116**, 27, 14205-14217, 2012

2012-78 **Pitt, M.P., Vullum, P.E., Sørby, M.H., Emerich, H., Paskevicius, M., Buckley, C.E. et al.** *A structural review of nanoscopic $Al_{1-x}TM_x$ phase formation in the $TMCl_n$ enhanced $NaAlH_4$ system* J. Alloys & Compounds, **527**, 16-24, 2012

2012-79 **Pitt, M.P., Vullum, P.E., Sørby, M.H., Sulic, M.P., Emerich, H., Paskevicius, M., Buckley, C.E., Walmsley, J.C. et al.** *Functionality of the nanoscopic crystalline Al/amorphous $Al_{50}Ti_{50}$ surface embedded composite observed in the $NaAlH_4$ + $xTiCl_3$ system after milling* J. Alloys & Compounds, **514**,163-169, 2012

2012-80 **Pitt, M.P., Vullum, E., Sørby, M.H., Emerich, H., Paskevicius, M., Webb, C.J. et al.** *Hydrogen absorption kinetics and structural features of $NaAlH_4$ enhanced with transition-metal and Ti-based nanoparticles* Int. J. Hydrogen Energy, **37**, 20, 15175-15186, 2012

2012-81 **Poletaev, A.A., Denys, R.V., Maehlen, J.P., Solberg, J.K., Tarasov, B.R., Yartys, V.A.** *Nanostructured rapidly solidified LaMg11Ni alloy: Microstructure, crystal structure and hydrogenation properties* Int. J. Hydrogen Energy, **37**, 4, 3548-3557, 2012

2012-82 **Pomjakushin, V. Y., Krzton-Maziopa, A., Pomjakushina, E. V., Conder, K., Chernyshov, D., Svitlyk, V., Bosak, A.** *Intrinsic crystal phase separation in the antiferromagnetic superconductor RbyFe2-xSe2: a diffraction study* J. Phys.: Condens. Matter, **24,** 435701-435710, 2012

2012-83 **Pregelj, M., Jeschke, H.O., Feldner, H., Valentí, R., Honecker, A., Saha-Dasgupta, T., Das, H. et al.** *Multiferroic $FeTe_2O_5Br$: Alternating spin chains with frustrated interchain interactions* Phys. Rev. B **86**, 054402-054408, 2012

2012-84 **Quartieri, S., Arletti, R., Vezzalini, G., Di Renzo, F., Dmitriev, V.** *Elastic behavior of MFI-type zeolites: 3 – Compressibility of silicalite and mutinaite* J. Solid State Chemistry, **191**, 201-212, 2012

2012-85 **Ravnsbæk, D.B., Ley, M.B., Lee, Y.-S., Hagemann, H., D'Anna, V., Cho, Y.W., Filinchuk, Y., Jensen, T.R.** *A mixed-cation mixed-anion borohydride $NaY(BH_4)_2Cl_2$* Int. J. Hydrogen Energy, **37**,10, 8428-8438, 2012

2012-86 **Ravnsbæk, D.B., Sørensen, L.H., Filinchuk, Y., Besenbacher, F., Jensen, T.R.** *Screening of Metal Borohydrides by Mechanochemistry and Diffraction* Angewandte Chem. Int. Ed., **51**,15, 3582-3586, 2012

2012-87 **Rozynek, Z., Wang, B., Fossum, J. O., Knudsen, K. D.** *Dipolar structuring of organically modified fluorohectorite clay particles* Europ. Phys. J. E: Soft Matter and Biological Physics, **35**, 1, 9, 2012

2012-88 **Schouwink, P., D'Anna, V., Ley, M.B., Daku, L.M.L., Richter, B., Jensen, T.R. et al.** *Bimetallic Borohydrides in the System $M(BH_4)_2$- KBH_4 (M=Mg, Mn): On the Structural Diversity* J. Phys. Chem. C, **116**, 20, 10829-10840, 2012

2012-89 **Serra-Crespo, P., Gobechiya, E., Ramos-Fernandez, E.V., Juan-Alcañiz, J., Martinez-Joaristi, A. et al.** *Interplay of metal node and amine functionality in NH2-MIL-53: modulating breathing behaviour through intra-framework interactions* Langmuir, **28**, 35, 12916-12922, 2012

2012-90 **Serra-Crespo, P., Van der Veen, M.A., Gobechiya, E., Houthoofd, K., Filinchuk, Y., Kirschhock, Ch.E.A. et al.** *NH_2-MIL-53(Al): A High-Contrast Reversible Solid-State Nonlinear Optical Switch* J. Am. Chem. Soc., **134**, 20, 8314–8317, 2012

2012-91 **Sisak, D., Baerlocher, Ch., McCusker, L.B., Gilmore, Ch.J.** *Optimizing the input parameters for powder charge flipping* J. Appl. Cryst., **45**, 1125-1135, 2012

2012-92 **Suwarno, S., Gosselin, Y., Solberg, J.K., Maehlen, J.P., Williams, M., Krogh, B., Børresen, B.T., Rytter, E. et al.** *Selective hydrogen absorption from gaseous mixtures by BCC Ti-V alloys* Int. J. Hydrogen Energy, **37**, 5, 4127-4138, 2012

2012-93 **Suwarno, S., Solberg, J. K., Maehlen, J.P., Krogh, B., Borresen, B. T., Ochoa-Fernandez, E. et al**. *Microstructure and hydrogen storage properties of as-cast and rapidly solidified Ti-rich Ti–V alloys* Transactions of Nonferrous Met. Soc. China, **22**, 8, 1831–1838, 2012

2012-94 **Suwarno, S., Solberg, J.K., Maehlen, J.P., Krogh, B, Yartys, V.A.** *Influence of Cr on the hydrogen storage properties of Ti-rich Ti–V–Cr alloys* Int. J. Hydrogen Energy, **37**, 9, 7624-7628, 2012

2012-95 **Tchougréeff, A.L., Liu, X., Müller, P., Van Beek, W., Ruschewitz, U., Dronskowski, R.** *Structural Study of CuNCN and Its Theoretical Implications: A Case of a Resonating-Valence-Bond State?* J. Phys. Chem. Lett., **3**, 22, 3360–3366, 2012

2012-96 **Texier, Y., Deisenhofer, J., Tsurkan, V., Loidl, A., Inosov, D. S., Friemel, G., Bobroff, J.** *NMR Study in the Iron-Selenide $Rb_{0.74}Fe_{1.6}Se_2$: Determination of the Superconducting Phase as Iron Vacancy-Free $Rb_{0.3}Fe_2Se_2$* Phys. Rev. Lett. **108**, 237002-237007, 2012

2012-97 **Tsakoumis, N.E., Voronov, A., Rønning, M., Van Beek, W., Borg, Ø., Rytter, E., Holmen, A.** *Fischer–Tropsch synthesis: An XAS/XRPD combined in situ study from catalyst activation to deactivation* J. Catalysis, **291**, 138-148, 2012

2012-98 **Tumanov, N. A., Boldyreva, E. V.** *X-ray diffraction and Raman study of DL-alanine at high pressure: revision of phase transitions* Acta Cryst., B**68**, 412-423, 2012

2012-99 **Valenzano, L., Vitillo, J.G., Chavan, S., Civalleri, B., Bonino, F., Bordiga, S. et al.** *Structure–activity relationships of simple molecules adsorbed on CPO-27-Ni metal–organic framework: In situ experiments vs. theory* Catalysis Today, **182**,1, 67-79, 2012

2012-100 **Van Beek, W., Emerich, H., Urakawa, A., Palin, L., Milanesio, M., Caliandro, R., Viterbo, D., Chernyshov, D.** *Untangling diffraction intensity: modulation enhanced diffraction on ZrO_2 powder* J. Appl. Cryst., **45**, 4, 738-747, 2012

2012-101 **Varin, R.A., Zbroniec, L., Polanski, M., Filinchuk, Y., Cerný, R.** *Mechano-chemical synthesis of manganese borohydride ($Mn(BH_4)_2$) and inverse cubic spinel (Li_2MnCl_4) in the ($nLiBH_4 + MnCl_2$) (n = 1, 2, 3, 5, 9 and 23) mixtures and their dehydrogenation behavior* Int. J. Hydrogen Energy, **37**, 21, 16056-16069, 2012

2012-102 **Ve, Th., Mathisen, K., Helland, R., Karlsen, O.A., Fjellbirkeland, A., Røhr, Å.K., Andersson, K.K. et al.** *The Methylococcus capsulatus (Bath) Secreted Protein, MopE*, Binds Both Reduced and Oxidized Copper* PLoS ONE, **7**, 8, e43146, 2012

2012-103 **Verheyen, E., Joos, L., Havenbergh, K. V., Breynaert, E., Kasian, N., Gobechiya, E. et al.** *Design of zeolite by inverse sigma transformation* Nature Materials, **11**, 1059-1064, 2012

2012-104 **Vichery, Ch., Maurin, I., Bonville, P., Boilot, J.-P., Gacoin, Th.** *Influence of Protected Annealing on the Magnetic Properties of ?-Fe2O3 Nanoparticles* J. Phys. Chem. C, **116**, 30, 16311-16318, 2012

2012-105 **Wang, J., Chernavskii, P. A., Khodakov, A. Y., Wang, Y.** *Structure and catalytic performance of alumina-supported copper–cobalt catalysts for carbon monoxide hydrogenation* J. Catalysis, **286**, 51-61, 2012

2012-106 **Wragg, D.S., Akporiaye, D., Fjellvåg, H.** *Direct observation of catalyst behaviour under real working conditions with X-ray diffraction: Comparing SAPO-18 and SAPO-34 methanol to olefin catalysts* J. Catalysis, **279**, 2, 397-402, 2012

2012-107 **Yot, P.G., Ma, Q., Haines, J., Yang, Q., Ghoufi, A., Devic, Th., Serre, Ch., Dmitriev, V. et al.** *Large breathing of the MOF MIL-47(V^{IV}) under mechanical pressure: a joint experimental–modelling exploration* Chem. Sci., **3**, 1100-1104, 2012

2012-108 **Živkovic, I., Djokic, D. M., Herak, M., Pajic, D., Prša, K., Pattison, P. et al.** *Site-selective quantum correlations revealed by magnetic anisotropy in the tetramer system $SeCuO_3$* Phys. Rev. B **86**, 054405-054414, 2012

2013

2013-1 **Arakcheeva, A., Ashokkumar, S., Leela, S., Ramamurthi, K., Stoeckli-Evans, H. et al.** *Synthesis, growth and characterization of 4-bromo-4'nitrobenzylidene aniline (BNBA): A novel nonlinear optical material with a (3+1)-dimensional incommensurately modulated structure* CrystEngComm, **15**, 2474-2481, 2013

2013-2 **Arakcheeva, A., Pattison, P., Bauer-Brandl, A., Birkedal, H., Chapuis, G.** *Cimetidine, $C_{10}H_{16}N_6S$, form C: crystal structure and modelling of polytypes using the superspace approach* J. Appl. Cryst., **46**, 99-107, 2013

2013-3 **Aree, Th., Buergi, H.-B., Minkov, B.S., Boldyreva, E.V., Chernyshov, D., Tornroos, K.W.** *Dynamics and Thermodynamics of Crystalline Polymorphs. Part 2:* β *- Glycine, Analysis of Variable-Temperature Atomic Displacement Parameters* J. Phys. Chem. A, **113**, 33, 8001-8009, 2013

2013-4 **Barpanda, P., Ati, M., Melot, B., Chotard, J.-N., Rousse, G., Tarascon, J.-M**. *Effect of Both Mn and Zn Partial Substitution on the Electrochemical Performance of $LiFeSO_4F$* ECS Trans., **45**, 29, 227-233, 2013

2013-5 **Cairns, A.B., Catafesta, J., Levelut, C., Rouquette, J., Van der Lee, A., Peters, L., Thompson, A.L., Dmitriev, V. et al.** *Giant negative linear compressibility in zinc dicyanoaurate* Nature Materials, **12**, 212-216, 2013

2013-6 **Can, M., Krucinska, J., Zoppellaro, G., Andersen, N.H., Wedekind, J.E., Hersleth, H.-P. et al.** *Structural Characterization of Nitrosomonas europaea Cytochrome c-552 Variants with Marked Differences in Electronic Structure* ChemBioChem., in press, 2013

2013-7 **Cerny, R., Schouwink, P., Sadikin, Y., Stare, K., Smrcok, L., Richter, B., Jensen, T.R.** *Trimetallic Borohydride $Li_3MZn_5(BH_4)_{15}$ (M = Mg, Mn) Containing Two Weakly Interconnected Frameworks* Inorg. Chem., in press, 2013

2013-8 **Chakraborty, P., Tissot, A., Peterhans, L., Guénée, L., Besnard, C., Pattison, Ph., Hauser, A.** *Determination of the molecular structure of the short-lived light-induced high-spin state in the spin-crossover compound [Fe(6-mepy)3tren](PF6)2* Phys. Rev. B **87**, 214306-214315, 2013

2013-9 **Chevreau, H., Devic, Th., Salles, F., Maurin, G., Stock, N., Serre, Ch**. *Mixed-Linker Hybrid Superpolyhedra for the Production of a Series of Large-Pore Iron(III) Carboxylate Metal–Organic Frameworks* Angewandte Chemie Int. Ed., **52**, 19, 5056-5060, 2013

2013-10 **Collings, I.M., Cairns, A.B., Thompson, A.L., Parker, J.E., Tang, C.C., Tucker, M.G., Catafesta, J. et al.** *Homologous critical behaviour in the molecular frameworks $Zn(CN)_2$ and $Cd(imidazolate)_2$* J. Am. Chem. Soc., **135**,20, 7610-7620, 2013

2013-11 **Conterosito, E., Van Beek, W., Palin, L., Croce, G., Perioli, L. et al.** *Development of a fast and clean intercalation method for organic molecules into Layered Double Hydroxides* Cryst. Growth Des., **13**, 3, 1162-1169, 2013

2013-12 **Deka, U., Lezcano-Gonzalez, I., Warrender, S.J., Picone, A.L., Wright, P.A. et al**. *Changing active sites in Cu–CHA catalysts: deNOx selectivity as a function of the preparation method* Microp. & Mesop. Mater., **166**, 144-152, 2013

2013-13 **Gianolio, D., Vitillo, J G., Civalleri, B., Bordiga, S., Olsbye, U., Lillerud, K. P., Valenzano, L., Lamberti, C.** *Combined study of structural properties on metal-organic frameworks with same topology but different linkers or metal* J. Phys.: Conf. Ser. **430**, 012134-012140, 2013

2013-14 **Gorfman, S., Schmidt, O., Tsirelson, V., Ziolkowski, M., Pietsch, U.** *Crystallography under External Electric Field* Zeitschrift für anorganische und allgemeine Chemie, in press, 2013

2013-15 **Grigoriev, S. V., Potapova, N.M., Siegfried, S.-A., Dyadkin, V. A., Moskvin, E. V., Dmitriev, V., Menzel, D. et al.** *Chiral Properties of Structure and Magnetism in Mn1-xFexGe Compounds: When the Left and the Right are Fighting, Who Wins?* Phys. Rev. Lett. **110**, 207201-207206, 2013

2013-16 **Hammer, N., Mathisen, K., Rønning, M**. *CO Oxidation over Au/TiO_2–Carbon Catalysts: The Effect of Thermal Treatment, Stability and TiO_2 Support Structure* Topics in Catalysis, **56**, 9-10, 637-649, 2013

2013-17 **Hermann, D., Emerich, H., Lepski, R., Schaniel, D., Ruschewitz, U.** *Metal–Organic Frameworks as Hosts for Photochromic Guest Molecules* Inorg. Chem., **52**, 5, 2744-2749, 2013

2013-18 **Kaegi, R., Voegelin, A., Ort, Ch., Sinnet, B., Thalmann, B., Krismer, J., Hagendorfer, H. et al.** *Fate and Transformation of Silver Nanoparticles in Urban Wastewater Systems* Water Research, **47**, 12, 3866-3877, 2013

2013-19 **Korablov, D., Ravnsbæk, D.B., Ban, V., Filinchuk, Y., Besenbacher, F., Jensen, T.R.** *Investigation of MBH4–VCl2, M = Li, Na or K* Int. J. Hydrogen Energy, **38**, 20, 8376–8383, 2013

2013-20 **Korthout, K., Parmentier, A.B., Smet, Ph.F., Dirk, P.** *A XAS study of the luminescent Eu centers in thiosilicate phosphors* Phys. Chem. Chem. Phys., **15**, 8678-8683, 2013

2013-21 **Leardini, L., Quartieri, S., Vezzalini, G., Martucci, A., Dmitriev, V.,** *Elastic behavior and high pressure-induced phase transition in chabazite: new data from a natural sample from nova scotia* Microp. & Mesop. Mater., **170**, 52-61, 2013

2013-22 **Liu, Y.-Y., Couck, S., Vandichel, M., Grzywa, M., Leus, K., Biswas, Sh., Volkmer, D. et al.** *New VIV-Based Metal–Organic Framework Having Framework Flexibility and High CO2 Adsorption Capacity* Inorg. Chem., **52**, 1, 113–120, 2013

2013-23 **Lototskyy, M., Sibanyoni, J.M., Denys, R.V., Williams, M., Pollet B.G., Yartys, V.A.** *Magnesium-Carbon Hydrogen Storage Hybrid Materials Produced by Reactive Ball Milling in Hydrogen* Carbon, **57**, 146-160, 2013

2013-24 **Lu, Y., Eyssler, A., Otal, E. H., Matam, S.K., Brunko, O., Weidenkaff, A., Ferri, D.** *Influence of the synthesis method on the structure of Pd-substituted perovskite catalysts for methane oxidation* Catalysis Today, **208**, 42-47, 2013

2013-25 **Maehlen, J.P., Mongstad, T.T., You, Ch. Ch., Karazhanov S.** *Lattice contraction in photochromic yttrium hydride* J. Alloys and Compounds, in press, 2013

2013-26 **Makarova, I. P., Grebenev, V. V., Chernaya, T. S., Verin, I. A. et al.** *Temperature-induced changes in the single-crystal structure of K9H7(SO4)8 · H2O* Crystallography Reports, **58**, 3, 393-400, 2013

2013-27 **Michalow, K.A., Otal, E.H., Burnat, D., Fortunato, G., Emerich, H., Ferri, D., Heel, A. et al.** *Flame-made visible light active TiO2:Cr photocatalysts: Correlation between structural, optical and photocatalytic properties* Catalysis Today, **209**, 47-53, 2013

2013-28 **Mondal, S., Van Smaalen, S., Parakhonskiy, G., Prathapa, S. J., Noohinejad, L., Bykova, E., Dubrovinskaia, N. et al.** *Experimental evidence of orbital order in* α *-B_{12} and* γ*-B_{28} polymorphs of elemental boron* Phys. Rev. B **88**, 024118-024126, 2013

2013-29 **Moury, R., Demirci, U.B., Ichikawa, T., Filinchuk, Y., Chiriac, R., Van der Lee, A., Miele, Ph.** *Sodium Hydrazinidoborane: A Chemical Hydrogen-Storage Material* ChemSusChem, **6**, 4, 667-673, 2013

2013-30 **Niehaus, O., Abdala, P.M., Riecken, J.F., Winter, F., Chevalier, B., Pöttgen, R.** *Cerium Valence Change in the Solid Solutions Ce($Rh_{1-x}Ru_x$)Sn* Z. Naturforsch., **68b**, 960 – 970, 2013

2013-31 **Nielsen, Th., Karkamkar, A., Bowden, M., Besenbacher, F., JensenT.R., Autrey, T.** *Methods to stabilize and destabilize ammonium borohydride* Dalton Trans., **42**, 680-687, 2013

2013-32 **Nwakwuo, Ch. C., Holm, Th., Denys, R. V., Hu, W., Maehlen, J. P., Solberg, J. K., Yartys, V. A.** *Effect of magnesium content and quenching rate on the phase structure and composition of rapidly solidified La_2MgNi_9 metal hydride battery electrode alloy* J. Alloys & Compounds, **555**, 201–208, 2013

2013-33 **Olsen, J.E., Frommen, Ch., Sørby, M.H., Hauback, B.C.** *Crystal structures and properties of solvent-free LiYb(BH_4)$_{4-x}Cl_x$, Yb(BH_4)$_3$ and Yb(BH_4)$_{2-x}Cl_x$* RSC Adv., **3**, 27, 10764-10774, 2013

2013-34 **Ovsyannikov, S. V., Abakumov, A.M., Tsirlin, A.A., Schnelle, W., Egoavil, R., Verbeeck, J., Tendeloo, J.V. et al.** *Perovskite-like Mn2O3: A Path to New Manganites* Angewandte Chemie Int. Ed., **52**, 5, 1494-1498, 2013

2013-35 **Parakhonskiy, G., Dubrovinskai, N., Bykova, E., Wirth, R., Dubrovinsky, L.** *High pressure synthesis and investigation of single crystals of metastable boron phases* High Pressure Research: Int. J., in press, 2013

2013-36 **Paul, A.K., Jansen, M., Yan, B., Felser, C., Reehuis, M., Abdala, P.M.** *Synthesis, Crystal Structure, and Physical Properties of Sr_2FeOsO_6* Inorg. Chem., **52**, 11, 6713–6719, 2013

2013-37 **Pekov, I. V., Zubkova, N. V., Chernyshov, D. Yu., Zelenski, M. E., Yapaskurt, V. O., Pushcharovskii, D. Yu.** *A new Cu-rich variety of lyonsite from fumarolic sublimates of the Tolbachik volcano (Kamchatka, Russia) and its crystal structure* Doklady Earth Sciences, **448**, 1, 112-116, 2013

2013-38 **Peña, D., Griboval-Constant, A., Diehl, F., Lecocq, V., Khodakov, A.Y.** *Agglomeration at the Micrometer Length Scale of Cobalt Nanoparticles in Alumina-Supported Fischer–Tropsch Catalysts in a Slurry Reactor* ChemCatChem, **5**, 3, 728-731, 2013

2013-39 **Pitt,M.P., Vullum, P.E., Sørby, M.H., Emerich, H., Paskevicius, M., Buckley, C.E. et al.** *Crystalline Al1 - x Ti x phases in the hydrogen cycled NaAlH4 + 0.02TiCl3 system* Philosophical Magazine, **93**, 9, 2013

2013-40 **Popoff, N., Espinas, J., Pelletier, J., Macqueron, B., Szeto, K.C., Boyron, O. et al.** *Small Changes Have Consequences: Lessons from Tetrabenzyltitanium and -zirconium Surface Organometallic Chemistry* Chemistry - A European J., **19**, 3, 964–973, 2013

2013-41 **Røhr, A.K., Hammerstad, M., Andersson, K.K.** *Tuning of Thioredoxin Redox Properties by Intramolecular Hydrogen Bonds* PLOS ONE, in press, 2013

2013-42 **Rozynek, Z., Zacher, T., Janek, M., Caplovicová, M., Fossum, O.J.** *Electric-field-induced structuring and rheological properties of kaolinite and halloysite* Applied Clay Science, **77-78**, 1-9, 2013

2013-43 **Salamat, A., Hector, A.L., Gray, B.M.,Kimber, S.A.J., Bouvier, P., McMillan, P.F**. *Synthesis of Tetragonal and Orthorhombic Polymorphs of Hf3N4 by High-Pressure Annealing of a Prestructured Nanocrystalline Precursor* J. Am. Chem. Soc., **135**, 25, 9503–9511, 2013

2013-44 **Sene, S., Reinholdt, M., Renaudin, G., Berthomieu, D., Zicovich-Wilson, C.M., Gervais, Ch., Gaveau, Ph**. *Boronate Ligands in Materials: Determining Their Local Environment by Using a Combination of IR/Solid-State NMR Spectroscopies and DFT Calculations* Chemistry - A European J., **19**, 3, 880–891, 2013

2013-45 **Seryotkin, Y. V., Drebushchak, T.N., Boldyreva, E.V.** *A high-pressure polymorph of chlorpropamide formed on hydrostatic compression of the* α-form in saturated ethanol solution Acta Crystall., B, **69**, 1, 77–85, 2013

2013-46 **Šimuneková, M., Schwendt, P., Chrappová, J., Smrcok, L., Cerný, R., Van Beek, W.** *The first transition metal iodato peroxido complex: the synthesis, vibrational spectra and crystal structure from powder diffraction data of K3[V2O2(O2)4(IO3)]·H2O* Central Eur. J. Chemistry, **11**, 8, 1352-1359, 2013

2013-47 **Smirnova, N. V., Kuriganova, A. B., Leont'eva, D. V., Leont'ev, I. N., Mikheikin, A. S**. *Structural and electrocatalytic properties of Pt/C and Pt-Ni/C catalysts prepared by electrochemical dispersion* Kinetics and Catalysis, **54**, 2, 255-262, 2013

2013-48 **Sønsteby, H. H., Chernyshov, D., Getz, M., Nilsen, O., Fjellvåg, H.** *On the application of a single-crystal [kappa]-diffractometer and a CCD area detector for studies of thin films* J. Synchrotron Rad., **20**, 4, 2013

2013-49 **Subashini, A., Leela, S., Ramamurthi, K., Arakcheeva, A., Stoeckli-Evans, H., Petricek, V. et al.** *Synthesis, growth and characterization of 4-bromo-4'-nitrobenzylidene aniline (BNBA): a novel nonlinear optical material with a (3+1)-dimensional incommensurately modulated structure* CrystEngComm, **15**, 2474-2481, 2013

2013-50 **Suwarno, S., Solberg, J.K., Maehlen, J.P., Krogh, B. Yartys, V.A.** *The Effects of Rapid Solidification on Microstructure and Hydrogen Sorption Properties of Binary Bcc Ti-V* Alloys J. Alloys & Compounds, in press, 2013

2013-51 **Svitlyk, V., Hermes, W., Chevalier, B., Matar, S.F., Gaudin, E., Voßwinkel, D., Chernyshov, D. et al.** *Change of the cerium valence with temperature – structure and chemical bonding of HT-CeRhGe* Solid State Sciences, **21**, 6-10, 2013

2013-52 **Tagantsev, A. K. , Vaideeswaran, K., Vakhrushev, S. B., Filimonov, A. V., .Burkovsky, R. G., Shaganov, A. et al.** *The origin of antiferroelectricity in $PbZrO_3$* Nature Communications, **4**, in press, 2013

2013-53 **Tsakoumis, N.E., Dehghan, R., Johnsen, R.E., Voronov, A., Van Beek, W., Walmsley, J.S. et al.** *A combined in situ XAS-XRPD-Raman study of Fischer–Tropsch synthesis over a carbon supported Co catalyst* Catalysis Today, **205**, 86-93, 2013

2013-54 **Tsypkin, M., Goméz de la Fuente, J.L., Rodríguez, S.G., Yua, Y., Ochal, P., Seland, F., Safonova, O. et al.** *Effect of heat treatment on the electrocatalytic properties of nano-structured Ru cores with Pt shells* J. Electroanalytical Chem., **704**, 57–66, 2013

2013-55 **Wragg, D.S., Grønvold, A., Voronov, A., Norby, P., Fjellvåg, H.** *Combined XRD and Raman studies of coke types found in SAPO-34 after methanol and propene conversion* Microp.& Mesop. Mat., **173**, 166–174, 2013

2013-56 **Wragg, D., O'Brien, M.G., Bleken, F., Fjellvåg, H., Di Michiel, M., Olsbye, U.** *The fast Z-scan method for studying working catalytic reactors with high energy X-ray diffraction: ZSM-5 in the methanol to gasoline process* Phys. Chem. Chem. Phys., **15**, 8662-8671, 2013

APPENDIX B

PhD Theses: 2009-2012
(based in part on data from SNBL)

PhD THESIS (based in part on data from SNBL)

Bösenberg U. GKSS, Geesthacht, 2009	$LiBh_4$-MgH_2 Composites for Hydrogen Storage.
Buchter F. Empa Dübendorf, 2009	Insights into the structure and dynamics of tetrahydroborates
Budhysutanto W.N. Technische Universiteit Delft, 2010	Hydrothermal synthesis and characterization of 3R polytypes of Mg-Al Layered Double Hydroxides.
Dilnesa B.Z. École polytechnique frderale de Lausanne, 2011	Fe-containing hydrates and their fate during cement hydration: thermodynamic data and experimental study.
Guzik M. University of Geneva, 2010	Studies of Hydrogen Atom Configurations in Selected Metal Hydrides in View of Repulsive Interactions.
Sjølyst-Kverneland A. University of Stavanger, 2009	Precipitation in AL-Zn-Mg Alloys Structure Analysis by Electron Microscopy and Synchrotron Radiation.
Tsakoumis N.E. NTNU, 2011	Deactivation of cobalt based Fischer-Tropsch synthesis catalysts.
Van Beek W. Universita` del Piemonte Orientale ‘‘A. Avogadro’’, Alessandria, 2011	Development of Modulation Enhanced Diffraction.
Veen S.D. University of Utrecht, 2009	Assemblies of Polyoxometalaten.
Xie Dan ETH Zurich, 2010	Structure Elucidation of Polycrystalline materials using X-ray Powder Diffraction and Electron Microscopy Techniques.

Master thesis work (based in part on data from SNBL)

Getz M. University of Oslo, 2012	Growth and modeling of ZnO and the characterization of epitaxial thin films by means of synchrotron radiation : a comprehensive study of synthesis, characterization and modeling of selected model structures.

Sønsteby H. University of Oslo, 2012	Structural Investigation of Crystalline Systems Utilizing Synchrotron X-ray Radiation : A Complete Study of Synthesis and Characterization of Selected Model Structures / Henrik Sønsteby.
Holm Th. NTNU Trondheim, 2012	Synthesis and characterisation of the nanostructured magnesium-lanthanum-nickel alloys for Ni-metal hydride battery applications.

APPENDIX C

List of Abbreviations

ASNG	Association Swiss-Norwegian Grenoble (Grenoble, France)
BL	Beam Line
DUBBLE	Dutch-Belgium Beam Lines at ESRF (Grenoble, France)
EMPA	Swiss Federal Laboratories for Materials Testing and Research (Dübendorf, Switzerland)
EPFL	Ecole Polytechnique Fédérale de Lausanne (Switzerland)
ETHZ	Eidgenössische Technische Hochschule Zürich (Switzerland)
EXAFS	Extended X-ray Absorption Fine Structure
HRPD	High-Resolution Powder Diffraction
IFE	Institute for Energy Technology (Kjeller, Norway)
NSR	Research Council of Norway
NTNU	Norwegian University of Science and Technology (Trondheim, Norway)
PSI	Paul Scherrer Institute (Villigen, Switzerland)
SER	State Secretariat for Education and Research (Bern, Switzerland)
SERI	State Secretariat for Education, Research and Innovations (Bern, Switzerland)
SLS	Swiss Light Source (Villigen, Switzerland)
SN	Swiss-Norwegian
SNBL	Swiss-Norwegian Beam Lines at ESRF
SNX	Swiss-Norwegian Foundation for Research with X-rays
SR	Synchrotron Radiation
UiB	University of Bergen (Norway)
UiO	University of Oslo (Norway)
UiS	University of Stavanger (Norway)
UiT	University of Tromsø (Norway)
UniB	University of Bern (Switzerland)
UniGE	University of Geneva (Switzerland)
UniNE	University of Neuchatel (Switzerland)
XAFS	X-ray Absorption Fine Structure